



NEW FRONTIERS OF ULTRAFAST THIN-DISK LASER OSCILLATORS FOR APPLICATIONS IN METROLOGY AND THE GENERATION OF THZ AND XUV RADIATION

A dissertation submitted to

UNIVERSITÉ DE NEUCHÂTEL

FACULTÉ DES SCIENCES

for the degree of

DOCTOR OF SCIENCES

presented by

NORBERT PAUL MODSCHING

Master of Science in Photonics

born on 17. December 1986

citizen of Germany

accepted on the recommendation of

Prof. Dr. Thomas Südmeyer, Supervisor

Prof. Dr. Jens Limpert, Co-Examiner

Dr. Valentin J. Wittwer, Co-Examiner

17. May 2019

IMPRIMATUR POUR THESE DE DOCTORAT

La Faculté des sciences de l'Université de Neuchâtel
autorise l'impression de la présente thèse soutenue par

Monsieur Norbert Paul MODSCHING

Titre:

**“New Frontiers of Ultrafast Thin-Disk Laser
Oscillators for Applications in Metrology and
the Generation of THz and XUV radiation”**

sur le rapport des membres du jury composé comme suit:

- Prof. Thomas Südmeyer, directeur de thèse, Université de Neuchâtel, Suisse
- Dr Valentin J. Wittwer, Université de Neuchâtel, Suisse
- Prof. Jens Limpert, Friedrich-Schiller-Universität Jena, Germany

Neuchâtel, le 29 juillet 2019

Le Doyen, Prof. P. Felber



Das Erreichen eines Zieles beendet die Erfahrung.

The achievement of an aim ends the experience.

Abstract

Ultrafast laser systems find application as versatile tool in industry and science. Ultrafast laser systems based on Ti:sapphire – the workhorse in ultrafast science – operate typically at kHz repetition rates and benefit from the available broad gain bandwidth for the direct generation of sub-100-fs pulse durations. However, thermal effects in the gain medium due to a high quantum defect limit their average power to several watt. Many applications would benefit to be driven at MHz repetition rates by simple and powerful laser systems. Ultrafast laser systems based Yb-doped gain materials have experienced an unprecedented scaling of the average power over the last decades. Nowadays, these systems reach the kilowatt level of average power while operating at MHz repetition rates. The tremendous progress was achieved by laser operation at a reduced quantum defect in combination with novel concepts utilizing optimized geometries of the laser gain medium for efficient heat extraction (fiber, slab, thin disk). In general, two basic design approaches for high-power ultrafast laser systems can be distinguished. Either they are based on a low-power master oscillator as seed source followed by multiple amplification stages, or they are directly based on high-power laser oscillators. However, the limited gain bandwidth of Yb-doped gain materials results typically in the generation of pulses with several hundred femtoseconds of duration. Additional nonlinear pulse compression becomes necessary in order to reach the required sub-100-fs pulse durations for many applications. This adds, on the one hand, complexity into the driving laser systems and can, on the other hand, degrade the temporal and spatial quality of the generated pulse train.

This thesis investigates the potential of ultrafast thin-disk laser (TDL) oscillators for laser operation directly in the sub-100-fs pulse duration regime at high average powers. The thin-disk geometry has already proven to be suitable to operate at the highest average power of any ultrafast laser oscillator technology. The development of powerful sub-100-fs TDL oscillators can ultimately overcome the need for amplification and nonlinear pulse compression. By that, these sources are highly attractive as simple single-stage driving laser systems for many applications, featuring

transform-limited soliton pulses at excellent beam quality without pre- or post-pulses and potential for further power-scaling.

The key ingredient of the presented sub-100-fs TDL oscillators is the combination of the Kerr lens mode-locking scheme with Yb-doped gain materials of broader gain bandwidth than Yb:YAG. Laser operation of a Kerr lens mode-locked (KLM) Yb:Lu₂O₃ TDL oscillator in the regime of strong intracavity self-phase modulation (SPM) enabled the generation of shorter pulse durations than directly supported by the corresponding gain bandwidth. The expansion of the optical spectrum up to three times beyond the gain bandwidth resulted in the generation of 35-fs pulses at 1.6 W of average power. In a modified laser configuration slightly longer pulse duration of 49 fs were generated at 4.5 W. Increased round-trip gain by folding the laser cavity a second time on the disk resulted in laser operation with 95-fs pulses at 21 W. These are the highest average powers so far achieved by a sub-50-fs and sub-100-fs laser oscillator, respectively. Compared to the results achieved prior to this thesis, the average power of sub-100-fs TDL oscillators has been increased by a factor of 4. By utilizing the very broad gain bandwidth of Yb:CALGO even shorter pulse durations of 30 fs are generated by the first KLM Yb:CALGO TDL oscillator. This is the shortest pulse duration so far achieved by a TDL oscillator and 40% shorter compared to the pulse durations of TDL oscillators achieved prior to this thesis. At that time, this pulse duration was equal to the shortest one achieved by Yb-based bulk oscillators. The presented results demonstrate that the thin-disk geometry is as well suitable for the generation of shortest pulse durations.

The suitability of laser operation in the strongly SPM-broadened regime for applications in metrology as optical frequency comb is investigated by detecting and stabilizing the carrier envelope offset frequency (f_{CEO}). In the presented configuration the KLM Yb:Lu₂O₃ TDL oscillator generated 50-fs pulses at 4.4 W of average power. For f_{CEO} detection in a standard f -to- $2f$ interferometer, the short pulse duration enabled the required coherent super continuum generation in a photonic crystal fiber without the need for adjacent nonlinear pulse compression. Only a minor fraction of the available average power was required for f_{CEO} detection while the major part remained available for application. In the presented experiment the f_{CEO} was stabilized to an external radio-frequency reference up to a bandwidth of 10 kHz by applying an active feedback to the current of the pump diode. A tight phase lock was achieved with a

residual in-loop integrated phase noise of 197 mrad (integrated from 1 Hz to 1 MHz). This is the shortest pulse duration and the highest average power of an Yb-based laser oscillator that has been so far f_{CEO} stabilized without the need for additional amplification or nonlinear pulse compression. Additionally, a preliminary study presents investigations for full frequency comb stabilization by parallel stabilization of the repetition rate (f_{rep}). Stabilization of the f_{rep} to an external radio-frequency reference was enabled by mounting one folding cavity mirror onto a controlled piezoelectric transducer. Simultaneous stabilization of f_{CEO} and f_{rep} was achieved in the range of minutes. Cross-talking between both stabilization loops required to limit the f_{rep} stabilization to a bandwidth of 35 Hz while the integrated residual f_{CEO} phase noise increased to 745 mrad.

Another application of the developed sub-100-fs KLM TDL oscillators as single-stage driving laser system is presented by driving directly the generation and detection of broadband THz radiation. In an initial configuration broadband THz radiation was generated via optical rectification in GaP utilizing the output of a KLM Yb:Lu₂O₃ TDL oscillator operating with 50-fs pulses at 4 W of average power. The generated THz spectrum was centered around 3.4 THz and extended from below 1 THz to nearly 7 THz. A spectroscopic characterization of a GaP crystal enabled phase matching calculation which are in good agreement with the observed features in the THz spectrum. As benchmark for applications in linear THz time-domain spectroscopy the absorption spectrum of water vapor was measured with a sub-50-GHz resolution. A presented second study investigates in more detail the impact of the GaP crystal thickness and the driving pulse duration on the generated THz spectrum. Modification of the driving TDL oscillator enabled high-fidelity measurements at discrete pulse durations ranging from 50 fs to 220 fs. Based on the experimental results a procedure is presented allowing to estimate the THz spectrum via multiplicative factors in the frequency domain. Driving THz generation with 95-fs pulses at 20 W of average power enabled the generation of 0.3 mW of THz average power with a spectrum extending up to 5 THz.

Additionally, the first experimental realization of high harmonic generation (HHG) inside the cavity of a mode-locked TDL oscillator is presented. In this proof-of-principle experiment HHG is driven by launching a high-pressure xenon gas jet into the 12 μm radius intracavity focus of a SESAM mode-locked TDL oscillator. The laser

operated with a pulse duration of 255 fs at 64 MW of intracavity peak power and 320 W of intracavity average power. At an intracavity peak intensity of $\sim 2.8 \times 10^{13}$ W/cm² up to the 17th harmonic (61 nm, 20 eV) has been detected. A generated photon flux of 2.6×10^8 photons/s was estimated for the 11th harmonic (94 nm, 13.2 eV). Launching the gas jet into the laser cavity did not disturb the mode-locked operation and noise performance. Further improvement can be expected by utilizing the Kerr lens mode-locking scheme with laser operation in the strongly SPM-broadened regime to reach shorter pulse durations in combination with cavity optimization towards higher intracavity peak powers. The prior presented investigations of f_{CEO} and f_{rep} stabilization anticipate that full frequency comb stabilization is feasible. As such, TDL driven intra-oscillator HHG is a promising approach for the development of single-stage extreme ultraviolet frequency combs.

Keywords:

Mode-locked lasers; ultrafast lasers; ytterbium; Yb-doped gain materials; Kerr lens mode-locking; thin-disk laser oscillators; optical frequency combs; carrier envelope offset frequency; terahertz radiation; optical rectification; high-harmonic generation; extreme-ultraviolet frequency combs.

Résumé

Les systèmes laser ultra brefs sont des outils versatiles ayant des applications dans l'industrie et la recherche scientifique. Ceux basés sur le Ti:saphire fonctionnent généralement à des taux de répétition autour du kHz et bénéficient de la large bande spectrale d'amplification disponible pour la génération directe de durée d'impulsions inférieure à 100 fs. Cependant, les effets thermiques délétères dans le milieu amplificateur limitent leur puissance moyenne à quelques watts. De nombreuses applications bénéficieraient d'être pilotées à des taux de répétition de l'ordre du MHz en utilisant des systèmes laser simples et puissants. Les systèmes laser ultra brefs basés sur des milieux amplificateurs dopés aux ions ytterbium ont vu une augmentation drastique sans précédent de leur puissance moyenne au cours des dernières décennies. Ces immenses progrès ont été obtenus grâce au faible défaut quantique de ces milieux, combiné à des concepts novateurs utilisant des géométries de milieu amplificateur optimisées pour une extraction de chaleur efficace (fibres optiques, slab, disques minces). Ces systèmes sont habituellement basés sur des architectures présentant plusieurs étages d'amplification et atteignent aujourd'hui des puissances moyennes de l'ordre du kilowatt à des taux de répétition autour du MHz. Cependant, la bande spectrale d'amplification limitée des milieux amplificateurs dopés aux ions ytterbium entraîne la génération d'impulsion ayant des durées de plusieurs centaines de femtosecondes. De plus, la post-compression nonlinéaire de ces impulsions devient nécessaire afin d'obtenir des durées d'impulsions inférieures à 100 fs requises par un grand nombre d'applications.

Les études présentées dans cette thèse portent sur le potentiel des oscillateurs lasers à base de disque mince (TDL) puissants et ultra brefs pour la génération d'impulsions de durée inférieure à 100 fs. La géométrie des disques minces a déjà prouvé qu'elle était adaptée à ces besoins en délivrant la plus grande puissance moyenne de toutes les technologies d'oscillateurs laser ultra brefs. À terme, le développement de puissants oscillateurs TDL délivrant des durées d'impulsions inférieures à 100 fs peut surmonter la nécessité d'amplifications et de post-compression nonlinéaire additionnelles. De ce fait, en tant que système laser simple et

mono étage délivrant des impulsions solitoniques limitées par transformée de Fourier sans piédestal pré ou post impulsions avec une excellente qualité de faisceau et un potentiel d'augmentation de puissance, ces sources sont extrêmement attractives pour un grand nombre d'applications

L'ingrédient clé des oscillateurs TDL délivrant des impulsions inférieures à 100 fs présentés dans cette thèse réside dans le blocage de mode par effet Kerr combiné à l'utilisation de milieux amplificateurs dopés aux ions ytterbium présentant des bandes spectrales d'amplification plus large que l'Yb:YAG. Un oscillateur laser en de blocage de mode par effet Kerr (KLM) fonctionnant en régime de forte automodulation de phase intra-cavité basé sur l'Yb:Lu₂O₃ a permis la génération de durées d'impulsions plus courtes que celles supportées par la bande spectrale d'amplification correspondante. Différentes configurations ont permis la génération d'impulsions d'une durée de 49 fs avec une puissance moyenne de 4.5 W d'une part et de 95 fs avec 21 W d'autre part. Ces performances représentent les plus importantes puissances moyennes obtenues jusqu'ici par des oscillateurs laser délivrant respectivement des impulsions de durée inférieure à 50 fs et 100 fs. Comparé aux résultats publiés avant cette thèse, la puissance moyenne des oscillateurs TDL a été multipliée par un facteur 4. En utilisant la bande spectrale d'amplification très large de l'Yb:CALGO, des impulsions de 30 fs ont été générées par le premier oscillateur TDL en régime de blocage de mode par effet Kerr basé sur ce milieu amplificateur. À ce jour, ce résultat représente la plus courte durée d'impulsions obtenue par un oscillateur TDL et est 40% plus courte que les durées d'impulsions générées par des oscillateurs TDL avant cette thèse.

La capacité des oscillateurs TDL développés à être utilisés dans des applications en métrologie comme peigne de fréquence optique est démontrée. Le décalage de la fréquence enveloppe-porteuse est détecté et stabilisé avec un asservissement tight de la phase. Une étude préliminaire étudie la stabilisation complète du peigne de fréquence grâce à une stabilisation parallèle du taux de répétition.

Les sources laser développées ont également permis la génération de radiation THz de large bande spectrale, pour la première fois par un oscillateur TDL ultra bref. En utilisant le processus de rectification électro-optique in GaP, un spectre optique s'étendant jusqu'à 7 THz a été généré. La génération de THz avec des impulsions de 95 fs à 20 W de puissance moyenne a produit 0.3 mW de puissance moyenne THz avec

un spectre optique allant jusqu'à 5 THz. Le spectre d'absorption de la vapeur d'eau a été mesuré avec une résolution inférieure à 20 GHz comme référence pour les applications de spectroscopie linéaire dans le domaine temporel en THz. En outre, une procédure est présentée permettant d'estimer le spectre THz à l'aide de facteurs multiplicatifs dans le domaine de Fourier. Moreover, a procedure is presented allowing to estimate the THz spectrum via multiplicative factors in the frequency domain.

De plus, la première réalisation expérimentale de génération d'harmoniques d'ordres élevés à l'intérieur de la cavité d'un oscillateur TDL à blocage de mode par SESAM est présentée. Ce ouvre la voie à une nouvelle classe de sources de lumière dans l'extrême ultraviolet à un étage fonctionnant à des taux de répétition de l'ordre du MHz.

Mots clés :

Laser à blocage de mode; laser ultra brefs; ytterbium; matériaux amplificateurs dopés aux ions ytterbium; blocage de mode par effet Kerr; oscillateur laser à disque mince; peignes de fréquences optiques; décalage de la fréquence enveloppe-porteuse; radiation terahertz; rectification electro-optique; génération d'harmoniques d'ordres élevés; peignes de fréquences dans l'extrême ultraviolet.

Table of Contents

ABSTRACT	I
RÉSUMÉ	VII
TABLE OF CONTENTS	XI
PUBLICATIONS	XV
JOURNAL PAPERS.....	XV
SELECTION OF CONFERENCE SUBMISSIONS.....	XVI
CHAPTER 1 INTRODUCTION	1
1.1 MOTIVATION AND OVERVIEW.....	1
1.2 GEOMETRIES FOR HIGH-POWER ULTRAFAST LASERS	4
1.3 THIN-DISK CONCEPT.....	5
1.4 SUMMARY OF INCLUDED PAPERS AND AUTHORS CONTRIBUTION	7
CHAPTER 2 CUTTING-EDGE SUB-100-FS THIN-DISK LASER OSCILLATORS	13
2.1 GENERATION OF SUB-100-FS PULSE DURATIONS FROM THIN-DISK LASER OSCILLATORS.....	13
2.1.1 <i>Mode-locking of TDL oscillators via the Kerr effect</i>	15
2.1.2 <i>Yb-doped gain materials</i>	18
2.2 GENERATION OF 35-FS PULSES FROM A KERR LENS MODE-LOCKED YB:LU ₂ O ₃ THIN-DISK LASER.....	23
2.2.1 <i>Introduction</i>	23
2.2.2 <i>Laser characterization in continuous-wave operation</i>	26
2.2.3 <i>Results of the laser experiments in mode-locked operation</i>	28
2.2.4 <i>Conclusion and outlook</i>	32
2.3 SUB-100-FS KERR LENS MODE-LOCKED YB:LU ₂ O ₃ THIN-DISK LASER OSCILLATOR OPERATING AT 21 W AVERAGE POWER.....	35
2.3.1 <i>Introduction</i>	35
2.3.2 <i>Cavity design</i>	38
2.3.3 <i>Performance in mode-locked operation</i>	41
2.3.4 <i>Conclusion and outlook</i>	45
2.4 KERR LENS MODE-LOCKED YB:CALGO THIN-DISK LASER	48
2.4.1 <i>Introduction</i>	48
2.4.2 <i>Disk characterization in continuous-wave operation</i>	51
2.4.3 <i>Setup and performance in mode-locked operation</i>	54
2.4.4 <i>Advantage of the thin-disk pumping scheme</i>	55
2.4.5 <i>Conclusion and outlook</i>	55
2.5 EXPERIMENTAL OPTIMIZATION IN THE SUB-100-FS PULSE DURATION REGIME.....	59

CHAPTER 3 CARRIER ENVELOPE OFFSET FREQUENCY STABILIZED SUB-100-FS THIN-DISK LASER OSCILLATOR.....	69
3.1 FREQUENCY COMBS	69
3.2 CARRIER-ENVELOPE OFFSET FREQUENCY STABILIZATION OF A THIN-DISK LASER OSCILLATOR OPERATING IN THE STRONGLY SELF-PHASE MODULATION BROADENED REGIME.....	74
3.2.1 <i>Introduction</i>	75
3.2.2 <i>Thin-disk laser oscillator and experimental setup</i>	76
3.2.3 <i>Transfer functions</i>	78
3.2.4 <i>CEO beat detection and stabilization</i>	80
3.2.5 <i>Conclusion and outlook</i>	82
3.3 TOWARDS TDL-BASED FREQUENCY COMBS.....	86
CHAPTER 4 THZ GENERATION DRIVEN BY SUB-100-FS THIN-DISK LASER OSCILLATORS	91
4.1 POWERFUL YB-BASED LASERS FOR THZ GENERATION	91
4.2 BROADBAND TERAHERTZ PULSE GENERATION DRIVEN BY AN ULTRAFAST THIN-DISK LASER OSCILLATOR.....	95
4.2.1 <i>Introduction</i>	95
4.2.2 <i>Broadband THz generation and detection</i>	97
4.2.3 <i>Spectroscopic characterization of GaP</i>	100
4.2.4 <i>THz spectroscopy of water vapor</i>	102
4.2.5 <i>Conclusion and outlook</i>	103
4.3 OPTICAL RECTIFICATION OF ULTRAFAST YB-LASERS: PUSHING POWER AND BANDWIDTH OF THZ GENERATION IN GAP	108
4.3.1 <i>Introduction</i>	108
4.3.2 <i>Experimental setup</i>	110
4.3.3 <i>Influence of pulse duration and crystal thickness on the THz spectrum</i>	111
4.3.4 <i>Estimation of the THz spectrum</i>	113
4.3.5 <i>Toward high THz powers</i>	116
4.3.6 <i>Conclusion</i>	118
4.3.7 <i>Appendix</i>	119
CHAPTER 5 THIN-DISK LASER DRIVEN INTRA-OSCILLATOR HIGH HARMONIC GENERATION.....	125
5.1 HIGH-HARMONIC GENERATION IN GAS JETS.....	125
5.2 EXTREME ULTRAVIOLET LIGHT SOURCE AT A MEGAHERTZ REPETITION RATE BASED ON HIGH-HARMONIC GENERATION INSIDE A MODE-LOCKED THIN-DISK LASER OSCILLATOR.....	131
5.2.1 <i>Introduction</i>	132
5.2.2 <i>Experimental setup</i>	134
5.2.3 <i>Experimental results</i>	135
5.2.4 <i>Conclusion</i>	138
CHAPTER 6 CONCLUSION AND OUTLOOK.....	143
CURRICULUM VITAE.....	155
ACKNOWLEDGEMENTS.....	159

Publications

Parts of this thesis are published in the following journal papers and conference proceedings.

Journal papers

1. J. Drs, **N. Modsching**, C. Paradis, C. Kränkel, V. J. Wittwer, O. Razskazovskaya, and T. Südmeyer, "Optical rectification of ultrafast Yb-lasers: Pushing power and bandwidth of THz generation in GaP," *JOSA B* **submitted** (2019).
2. **N. Modsching**, J. Drs, J. Fischer, C. Paradis, F. Labaye, M. Gaponenko, C. Kränkel, V. J. Wittwer, and T. Südmeyer, "Sub-100-fs Kerr lens mode-locked Yb:Lu₂O₃ thin-disk laser oscillator operating at 21 W average power," *Opt. Express* **27**(11), 16111–16120 (2019).
3. F. Labaye, M. Gaponenko, **N. Modsching**, B. Pierre, C. Paradis, S. Schilt, V. J. Wittwer, and T. Südmeyer, "XUV sources based on intra-oscillator high harmonic generation with thin-disk lasers: current status and prospects," *IEEE J. Sel. Top. Quantum Electron.* **25**(4), 8800619 (2019).
4. C. Paradis, J. Drs, **N. Modsching**, O. Razskazovskaya, F. Meyer, C. Kränkel, C. J. Saraceno, V. J. Wittwer, and T. Südmeyer, "Broadband terahertz pulse generation driven by an ultrafast thin-disk laser oscillator," *Opt. Express* **26**(20), 26377–26384 (2018).
5. **N. Modsching**, C. Paradis, P. Brochard, N. Jornod, K. Gürel, C. Kränkel, S. Schilt, V. J. Wittwer, and T. Südmeyer, "Carrier-envelope offset frequency stabilization of a thin-disk laser oscillator operating in the strongly self-phase modulation broadened regime," *Opt. Express* **26**(22), 28461–28467 (2018).
6. **N. Modsching**, C. Paradis, F. Labaye, M. Gaponenko, I. J. Graumann, A. Diebold, F. Emaury, V. J. Wittwer, and T. Südmeyer, "Kerr lens mode-locked Yb:CALGO thin-disk laser," *Opt. Lett.* **43**(4), 879–882 (2018).
7. F. Labaye, M. Gaponenko, V. J. Wittwer, A. Diebold, C. Paradis, **N. Modsching**, L. Merceron, F. Emaury, I. J. Graumann, C. R. Phillips, C. J. Saraceno, C. Kränkel, U. Keller, and T. Südmeyer, "Extreme ultraviolet light source at a megahertz repetition rate based on high-harmonic generation inside a mode-locked thin-disk laser oscillator," *Opt. Lett.* **42**(24), 5170–5173 (2017).

8. C. Paradis, **N. Modsching**, V. J. Wittwer, B. Deppe, C. Kränkel, and T. Südmeyer, "Generation of 35-fs pulses from a Kerr lens mode-locked Yb:Lu₂O₃ thin-disk laser," *Opt. Express* **25**(13), 14918–14925 (2017). (**Editor's pick**)

Selection of conference contributions

1. **N. Modsching**, J. Drs, J. Fischer, C. Paradis, F. Labaye, M. Gaponenko, C. Kränkel, V. J. Wittwer, T. Südmeyer, "95-fs Yb:Lu₂O₃ Thin-Disk Laser Operating at 21 W Average Power," accepted for oral presentation at *2019 European Conference on Lasers and Electro-Optics and European Quantum Electronics Conference*, (Optical Society of America, 2019), oral CA-5.1
2. J. Drs, **N. Modsching**, C. Paradis, C. Kränkel, V. J. Wittwer, O. Razskazovskaya and T. Südmeyer, "High-Power 0.33 mW Broadband THz Source Driven by an Ultrafast Yb-based Thin-Disk Laser Oscillator," accepted for oral presentation at *2019 European Conference on Lasers and Electro-Optics and European Quantum Electronics Conference*, (Optical Society of America, 2019), oral CC-6.6.
3. **N. Modsching**, J. Drs, J. Fischer, C. Paradis, F. Labaye, M. Gaponenko, C. Kränkel, V. J. Wittwer, and T. Südmeyer, "21 W average power sub-100-fs Yb:Lu₂O₃ thin-disk laser," accepted for oral presentation at *Conference on Lasers and Electro-Optics*, San Jose, USA, Mai 13-18, 2019, oral SF3E.4.
4. J. Drs, **N. Modsching**, C. Paradis, C. Kränkel, V. J. Wittwer, O. Razskazovskaya and T. Südmeyer, "New horizons for high power broadband THz sources driven by ultrafast Yb-based thin-disk laser oscillators," accepted for oral presentation at *Conference on Lasers and Electro-Optics*, San Jose, USA, Mai 13-18, 2019, oral STh3F.5.
5. C. Paradis, **N. Modsching**, O. Razskazovskaya, J. Drs, F. Meyer, C. Kränkel, C. J. Saraceno, V. J. Wittwer, and T. Südmeyer, "Thin-Disk Laser Oscillator Driving THz Generation Up To 6 THz," presented at *2018 43rd International Conference on Infrared, Millimeter and Terahertz Waves (IRMMW THz-2018)*, Nagoya, Japan, September 9-14, 2018, oral Tu-P1-1c-4.
6. M. Gaponenko, F. Labaye, P. Brochard, **N. Modsching**, K. Gürel, V. J. Wittwer, C. Paradis, C. Kränkel, S. Schilt, and T. Südmeyer, "CEO frequency stabilization of a thin-disk laser with intra-cavity high harmonic generation," presented at the *8th EPS-QEOD Europhoton conference*, Barcelona, Spain, September 2-7, 2018, oral FrM2.6.

7. C. Paradis, **N. Modsching**, O. Razskazovskaya, J. Drs, F. Meyer, C. Kränkel, C. J. Saraceno, V. J. Wittwer, and T. Südmeyer, "50-fs thin-disk laser oscillator generating broadband THz pulses," presented at the *8th EPS-QEOD Europhoton conference*, Barcelona, Spain, September 2-7, 2018, oral ThA1.1.
8. C. Kränkel, E. Castellano-Hernández, A. Uvarova, P. von Brunn, C. Paradis, **N. Modsching**, V. J. Wittwer, T. Südmeyer, and A. M. Heuer, "Advanced Materials for Multi-Wavelength, High Power and Short Pulse Solid State Lasers," presented at *OPTIQUE Toulouse 2018*, Toulouse, France, July 3-6, 2018. (**invited**)
9. F. Labaye, M. Gaponenko, V. J. Wittwer, A. Diebold, C. Paradis, **N. Modsching**, L. Merceron, F. Emaury, I. J. Graumann, C. R. Phillips, C. J. Saraceno, C. Kränkel, U. Keller, and T. Südmeyer, "Extreme Ultraviolet Light Source by High-Harmonic Generation Inside an Ultrafast Thin-Disk Laser," in *Advanced Photonics 2018 (BGPP, IPR, NP, NOMA, Sensors, Networks, SPPCom, SOF)*, OSA Technical Digest (online) (Optical Society of America, 2018), paper NpTh1C.8.
10. **N. Modsching**, C. Paradis, M. Gaponenko, F. Labaye, V. J. Wittwer, and T. Südmeyer, "Towards few-cycle pulses from ultrafast thin disk lasers," presented at *18th International Conference on Laser Optics (ICLO 2018)*, St. Petersburg, Russia, June 4-8, 2018. (**invited**)
11. C. Paradis, **N. Modsching**, M. Gaponenko, F. Labaye, V. J. Wittwer, and T. Südmeyer, "Frontiers in Ultrafast Thin-Disk Laser Oscillators," in *Conference on Lasers and Electro-Optics*, OSA Technical Digest (online) (Optical Society of America, 2018), paper SF2N.3. (**invited**)
12. **N. Modsching**, C. Paradis, P. Brochard, N. Jornod, K. Gürel, C. Kränkel, S. Schilt, V. J. Wittwer, and T. Südmeyer, "Frequency Comb Stabilization of a 50-fs Thin-Disk Laser Oscillator Operating in a Strongly SPM-broadened Regime," in *Conference on Lasers and Electro-Optics*, OSA Technical Digest (online) (Optical Society of America, 2018), paper SM4L.6.
13. C. Paradis, **N. Modsching**, O. Razskazovskaya, J. Drs, F. Meyer, C. J. Saraceno, C. Kränkel, V. J. Wittwer, and T. Südmeyer, "Broadband THz generation driven by a thin-disk laser oscillator," presented at *EOS Topical Meeting on Terahertz Science & Technology (TST 2018)*, Berlin, Germany, Mai 6-9, 2018, poster #165.
14. **N. Modsching**, C. Paradis, P. Brochard, N. Jornod, K. Gürel, C. Kränkel, S. Schilt, V. J. Wittwer, and T. Südmeyer, "Frequency Comb Stabilization of a 4 W, 50-fs Thin-Disk Laser Oscillator," presented at *32nd European Frequency and Time Forum 2018*, April 10-12, 2018, paper #7087. (**best student paper award**)
15. V. J. Wittwer, M. Hoffmann, C. Paradis, **N. Modsching**, M. Gaponenko, F. Labaye, T. Südmeyer, "Broadband IBS Coatings for sub-50-fs Pulse Generation from Ultrafast Thin-Disk Lasers," presented at *SPIE Photonics West 2018, LASE*,

Conference 10511, San Francisco, California, United States, Jan. 27–Feb. 1, 2018, poster 10511-82.

16. C. Paradis, **N. Modsching**, F. Labaye, M. Gaponenko, F. Emaury, A. Diebold, I. Graumann, B. Deppe, C. Kränkel, V. J. Wittwer, T. Südmeyer, "Kerr lens mode-locked thin-disk lasers delivering 30-fs pulses from Yb:CALGO and 35-fs pulses from Yb:Lu₂O₃," presented at *Ultrafast Optics (UFO) XI*, Jackson Hole, Wyoming, United States, October 8–13, 2017, talk Tu7.2.
17. F. Labaye, M. Gaponenko, V. Wittwer, C. Paradis, **N. Modsching**, L. Merceron, A. Diebold, F. Emaury, I. Graumann, C. Phillips, C. J. Saraceno, C. Kränkel, U. Keller, T. Südmeyer, "Compact megahertz repetition rate coherent XUV light source based on HHG inside a modelocked thin-disk laser," presented at *Ultrafast Optics (UFO) XI*, Jackson Hole, Wyoming, United States, October 8–13, 2017, talk Tu7.5. (**upgraded as invited**)
18. N. Modsching, C. Paradis, M. Gaponenko, F. Labaye, F. Emaury, A. Diebold, I. Graumann, B. Deppe, C. Kränkel, V. J. Wittwer, and T. Südmeyer, "Towards Few-Cycle Ultrafast Thin-Disk Lasers," in *Laser Congress 2017 (ASSL, LAC)*, OSA Technical Digest (online) (Optical Society of America, 2017), paper JM5A.41. (**awarded with "outstanding student poster presentation prize"**)
19. F. Labaye, M. Gaponenko, V. J. Wittwer, C. Paradis, **N. Modsching**, L. Merceron, A. Diebold, F. Emaury, I. J. Graumann, C. R. Phillips, C. J. Saraceno, C. Kränkel, U. Keller, and T. Südmeyer, "SESAM-Modelocked Thin-Disk Laser (TDL) with Intracavity High-Harmonic Generation (HHG)," in *Laser Congress 2017 (ASSL, LAC)*, OSA Technical Digest (online) (Optical Society of America, 2017), paper ATh5A.3.
20. M. Gaponenko, F. Labaye, V. J. Wittwer, C. Paradis, **N. Modsching**, L. Merceron, A. Diebold, F. Emaury, I. J. Graumann, C. R. Phillips, C. J. Saraceno, C. Kränkel, U. Keller, and T. Südmeyer, "High Harmonic Generation (HHG) inside a Modelocked Thin-Disk Laser," in *Frontiers in Optics 2017*, OSA Technical Digest (online) (Optical Society of America, 2017), paper FTh2B.1.
21. M. Gaponenko, F. Labaye, V. J. Wittwer, C. Paradis, **N. Modsching**, L. Merceron, A. Diebold, F. Emaury, I. J. Graumann, C. R. Phillips, C. J. Saraceno, C. Kränkel, U. Keller, and T. Südmeyer, "Compact megahertz coherent XUV generation by HHG inside an ultrafast thin-disk laser," in *Nonlinear Optics*, OSA Technical Digest (online) (Optical Society of America, 2017), paper NTh3A.1. (**postdeadline paper**)

22. C. Paradis, **N. Modsching**, M. Gaponenko, F. Labaye, F. Emaury, A. Diebold, I. Graumann, B. Deppe, C. Kränkel, V. J. Wittwer, and T. Südmeyer, "Sub-50-fs Kerr Lens Mode-Locked Thin-Disk Lasers," in *2017 European Conference on Lasers and Electro-Optics and European Quantum Electronics Conference*, (Optical Society of America, 2017), paper PD_1_4. (**postdeadline paper**)
23. **N. Modsching**, C. Paradis, V. J. Wittwer, B. Deppe, C. Kränkel, and T. Südmeyer, "64-fs Pulses from a Kerr-Lens Modelocked Yb:LuO Thin-Disk Laser," in *2017 European Conference on Lasers and Electro-Optics and European Quantum Electronics Conference*, (Optical Society of America, 2017), paper CA_7_1.
24. C. Paradis, **N. Modsching**, V. J. Wittwer, B. Deppe, C. Kränkel, and T. Südmeyer, "128-fs Pulses from a Kerr-Lens Modelocked Yb:LuO Thin-Disk Laser," in *Conference on Lasers and Electro-Optics*, OSA Technical Digest (online) (Optical Society of America, 2017), paper SM1I.3.

Chapter 1

Introduction

1.1 Motivation and overview

The development of novel laser sources over the last decades strongly impacted industry, science and our daily life. Smartphones, internet and even the bar-code scanners in the supermarket are examples of their manifold application. In science lasers have become cutting-edge tools leading to fundamental breakthroughs in physics, chemistry and biology. The Nobel prize in physics 2017 was awarded for the detection of gravitational waves, enabled by a large-scale laser interferometer [1]. Recently, the physics Nobel prize 2018 honored the invention of the chirped pulse amplification technique [2]. This technology marks a breakthrough in the development of powerful ultrafast laser systems and illustrates the high impact of ultrafast laser sources on science and technology.

Ultrafast lasers generate optical pulses (Fig. 1), intensive flashes of light, at a certain repetition rate (f_{rep}) with pulse durations (τ_{pulse}) typically in the order of picoseconds down to femtoseconds (10^{-12} s to 10^{-15} s). The compression of the pulse energy (E_{pulse}) in a short temporal duration results in the creation of a high peak power ($P_{\text{peak}} \sim E_{\text{pulse}} / \tau_{\text{pulse}}$). As such, table-top laser systems operating at high repetition rates are capable of generating up to several GW of peak power, a value comparable to the electrical power generated in nuclear power plants. Focused into a small spot diameter, extreme intensities can be reached that enable accessing and investigating the nonlinear optical properties of matter. Nonlinear optical effects like optical rectification or high harmonic generation enable the wavelength conversion of the

driving laser light from the low-energetic THz range up to the high-energetic extreme ultraviolet, respectively.

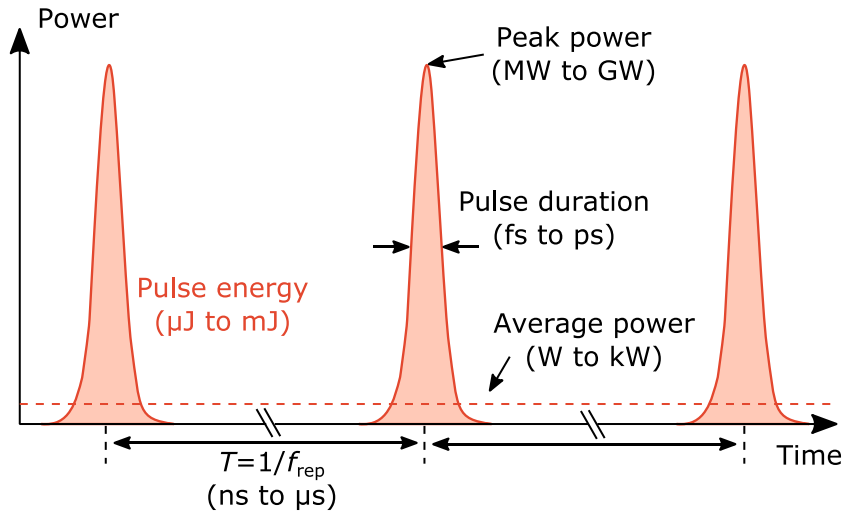


Fig. 1. Schematic of an optical pulse train generated by an ultrafast laser operating at high repetition rate. The compression of the pulse energy (area under the pulse envelope) in a short pulse duration results in the creation of a high peak power. The temporal spacing (T) between two successive pulses is the inverse of the repetition rate.

Driving nonlinear frequency conversion with even more extreme performance requires the continuous improvement of ultrafast lasers in following key parameters:

- **Shorter pulse durations** are beneficial for increasing the peak power. But more important, many nonlinear experiments rely on sub-100-fs pulse durations. In order to reach such short pulse durations, ultrafast lasers typically rely on gain materials with broad gain bandwidth or nonlinear pulse compression.
- **Higher average powers** result from the demand for higher pulse energy and laser operation at increased repetition rate ($P_{\text{ave}} = E_{\text{pulse}} \cdot f_{\text{rep}}$)
 - **Higher pulse energies** are required for the generation of higher peak powers. They can be achieved by propagating the optical pulses through several amplifier stages or developing powerful laser oscillators. In case that the average power is the limiting factor higher pulse energies can be achieved by decreasing the repetition rate.

- **Increased repetition rates** can improve the signal-to-noise ratio, result in reduced measurement times, and enable new types of nonlinear experiments. As such, targeted experiments require typically a faster recovery time than the temporal spacing between two consecutive pulses. Here, current research effort aims for increasing the repetition rate from several kHz up to the MHz and even the GHz range.

The main technological challenges for power-scaling arise from two factors. First, laser operation at high average power leads to an excessive heat load generated in the laser gain medium and applied to the cavity components. Second, high peak powers result in too much accumulation of nonlinearities during pulse propagation and can cause damage on the laser components. Overcoming those two limiting factors lead to different laser geometries and concepts for further average power and peak power scaling (section 1.2). One direction is based on the amplifier scheme using a low-power seed laser oscillator followed by several amplifier stages. The other direction is based on the development of high-power laser oscillators.

This thesis follows the approach of developing powerful thin-disk laser (TDL) oscillators that operate at MHz repetition rates (section 1.3). It aims for pushing the average power and minimal achievable pulse duration of high-power TDL oscillators in the sub-100-fs pulse duration regime. Prior to this work sub-100-fs TDL oscillators were limited to 5 W average power [3,4] and the minimal achieved pulse duration was 49 fs [5,6]. The combination of the Kerr lens mode-locking scheme and laser materials with broader gain bandwidth enabled the development of sub-100-fs TDL oscillators operating at 4 times higher average power and generating 40% shorter pulse durations than demonstrated before (chapter 2).

The potential of the developed sub-100-fs TDL oscillator for applications in metrology as powerful single-stage frequency comb is demonstrated by stabilizing its carrier-envelope offset frequency (chapter 3). Their suitability to perform nonlinear frequency conversions without additional nonlinear pulse compression is presented by the first THz generation and detection directly driven by the output of a thin-disk laser oscillator. Further scaling of the average power of the driving sub-100-fs TDL oscillator even enabled the generation of broadband THz radiation approaching the

mW-level of THz average power by optical rectification in gallium phosphide (chapter 4).

In a proof-of-principle experiment the extreme nonlinear process of high harmonic generation is driven directly inside the laser cavity of a TDL oscillator (chapter 5). While operating at longer pulse durations of 250 fs, this approach demonstrates the potential of the TDL oscillator technology as single-stage coherent extreme-ultraviolet light source operating at enhanced intracavity average powers and MHz repetition rates.

Finally, the experimental results will be concluded and an overview about future steps for further performance improvement of sub-100-fs Kerr lens mode-locked TDL oscillators and their applications is given (chapter 6).

1.2 Geometries for high-power ultrafast lasers

Heat load in the gain medium during laser operation challenges further scaling of the average power of ultrafast laser systems. The energy difference between pump and laser photon, referred to as quantum defect, is besides non-radiative decays the main heat load generating mechanism during laser operation. An excessive heat load generated in the gain medium or induced into other cavity components can change their optical and material properties. Effects like thermal lensing influence the beam quality and propagation. Induced mechanical stress can ultimately result in damage of the laser gain medium.

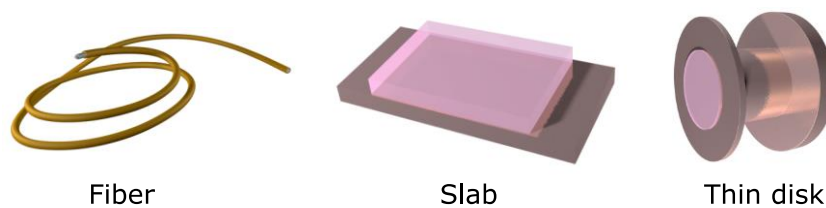


Fig. 1. Geometries of the gain medium enabling high-power laser operation. Efficient extraction of the generated heat load is achieved by optimizing the surface-to-volume ratio. Figure are courtesy of Martin Saraceno [7]

Fiber [8], slab [9] and thin disk [10] are different geometrical approaches of the gain medium (Fig. 1). They aim for optimizing the heat extraction by maximizing the surface-to-volume ratio. In the fiber geometry the laser beam is guided in a waveguide structure. Heat load is efficiently extracted in radial direction over the large surface.

The long interaction length in fibers is advantageous for a high gain. However, guiding of optical pulses with high peak power in small fiber-core diameters leads to a strong accumulation of nonlinearities. Temporal stretching techniques, like the chirped pulse amplification, have to be applied to the pulse in order to decrease its peak power and minimize the accumulation of nonlinearities. The fiber geometry finds therefore typically application in high-power amplifier systems. In the slab geometry the gain medium has the form of a thin bar, short in one direction and extended in the other two. The laser beam is propagated along the extended lengths of the slab. Efficient cooling is achieved by extracting the heat load over both larger surfaces. However, the directional cooling induces a thermal gradient in perpendicular direction. This results in the formation of an asymmetric thermal lens. Designing the laser cavity with an elliptical mode or passing the gain material in a zig-zag geometry can compensate partially the thermal lensing. The third approach is the thin-disk geometry. Here the gain medium has the shape of a disk with a thickness in the order of 100 μm . Laser operation with increased beam diameters on the gain medium reduces nonlinearities and makes this approach attractive for operation at high peak powers. As such, the thin-disk concept finds application in high-power laser oscillator and as well in multi-pass and regenerative amplifiers. This thesis applies the thin-disk concept for the development of powerful ultrafast laser oscillators.

1.3 Thin-disk concept

The thin disk is a power-scalable concept for high-power laser sources [10]. For a more detailed overview about the current status of thin-disk lasers the reader is referred to [11]. In the following, the basic concept of the thin-disk geometry will be recapitulated.

The disk features typically a thickness in the range of 100 μm to 300 μm with diameters in the cm-range and is mounted with its backside onto a heat sink [Fig. 2(a)]. Efficient heat extraction is achieved by cooling the backside of the disk with water in turbulent flow [Fig. 2(b)]. The large ratio between cooling surface to disk thickness results in a one-dimensional heat flow in propagation direction of the beam [Fig. 2(c)]. This suppresses thermal lensing and is suitable for laser operation at high average powers.

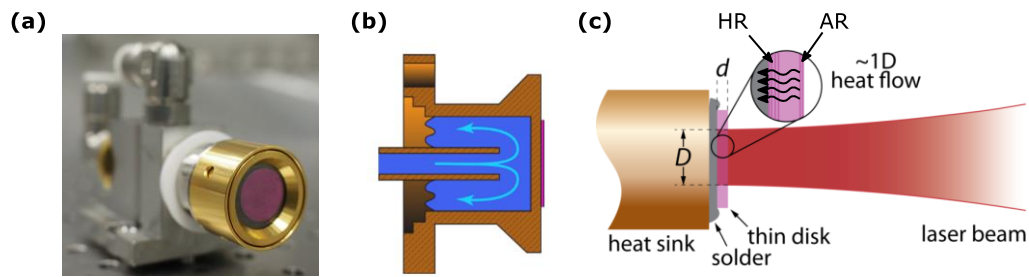


Fig. 2. (a) A thin disk contacted onto an industrial cooling finger (Trumpf GmbH). Mounting of the disk onto diamond enables efficient heat transport to the coolant. (b) Schematic of the cooling finger. Heat is extracted from the disk by turbulent water flow on the backside. (c) The large ratio between cooling surface to disk thickness features a one-dimensional (1D) heat flow. This suppresses thermal lensing and enables laser operation at high average powers. The disk is coated to be highly-reflective (HR) on the back side and anti-reflective (AR) on the front for pump and laser wavelength.

The backside of the disk is coated to be highly reflective (HR) and the front-side to be anti-reflective (AR) for the pump and laser wavelength [Fig. 2(c)]. The thin thickness limits the single-pass pump absorption and gain. Efficient pump absorption of more than 90% is achieved via a multi-pass pumping scheme allowing for more than 48 passes through the laser gain medium (Fig. 3). Higher cavity round-trip gain can be achieved in a similar manner by folding the laser cavity multiple times over the disk or by implementing several disks into the laser cavity.

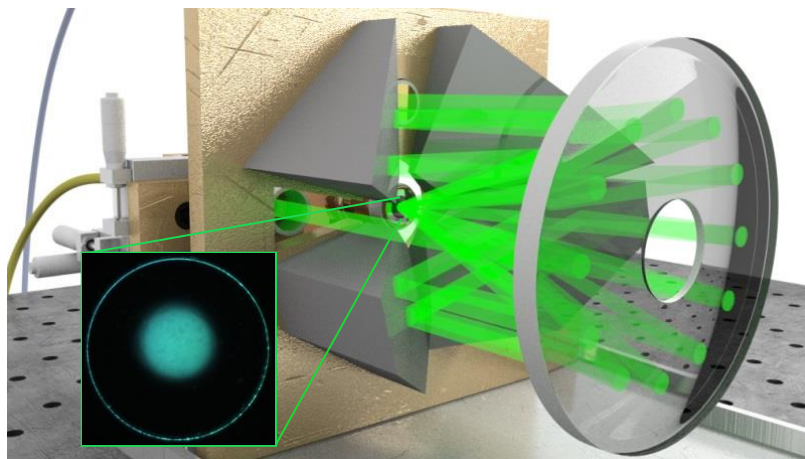


Fig. 3. Illustration on the multi-pass pumping scheme enabling efficient absorption of the pump light. In this image the pump is folded 24 times over the disk (after folding the pump light 12 times on the disk it is reflected back by an end mirror) resulting in 48 passes through the gain medium. The inset shows the pump spot on the disk after alignment of all passes. The illustration is courtesy of Martin Saraceno [7].

Geometrical power-scaling can be achieved by increasing the pump spot diameter on the disk (inset Fig. 3) in combination with an according increase of the laser beam diameter on it. Large beam diameters in the order of millimeters reduce the accumulation of nonlinearities in the disk due to a reduced peak intensity. This is beneficial for laser operation at high peak powers in pulsed laser operation. Nonlinearities can be instead adjusted by means of other cavity components which results in more freedom of the design parameters.

1.4 Summary of included papers and authors contribution

This thesis concludes the achieved results in a cumulative collection of published papers. Each chapter contains an individual introduction that focusses on giving the reader a basic background about the discussed topic and summarizes the key results of the experimental investigation. Section 2.5 and section 3.3 contain additional experimental results that have not be included into the published papers.

Included papers have been published or are currently submitted to the corresponding journal. The originals are available on OSA Publishing (<https://www.osapublishing.org/>). Texts and figures contain identical content as published but have been replotted and formatted to match in appearance a corporate thesis style. All papers are reprinted with permission from the corresponding publishers. The copyright of the original publications is retained by the respective copyright holders.

The thesis was realized in the research group of Prof. Dr. Thomas Südmeyer. Each project was carried out in collaboration with other doctoral students, post-docs, senior scientists and external collaborators. The included papers are listed in their appearance in this thesis and the authors contribution to the published result is stated.

- **Paper 1:** C. Paradis, N. Modsching, V. J. Wittwer, B. Deppe, C. Kränkel, and T. Südmeyer, "Generation of 35-fs pulses from a Kerr lens mode-locked Yb:Lu₂O₃ thin-disk laser," *Opt. Express* **25**(13), 14918–14925 (2017).

Contribution in discussions and the development of the script for the simulation of the Kerr lens mode-locking. Contribution in the experimental

optimization of the ultrafast TDL oscillator for shortest pulse duration and highest average power in the sub-100-fs pulse duration regime.

- **Paper 2:** N. Modsching, J. Drs, J. Fischer, C. Paradis, F. Labaye, M. Gaponenko, C. Kränkel, V. J. Wittwer, and T. Südmeyer, "Sub-100-fs Kerr lens mode-locked Yb:Lu₂O₃ thin-disk laser oscillator operating at 21 W average power," *Opt. Express* **27**(11), 16111–16120 (2019).

Project leader, development of the cavity design, setup of the TDL oscillator, full experimental characterization and optimization of the mode-locked laser performance.

- **Paper 3:** N. Modsching, C. Paradis, F. Labaye, M. Gaponenko, I. J. Graumann, A. Diebold, F. Emaury, V. J. Wittwer, and T. Südmeyer, "Kerr lens mode-locked Yb:CALGO thin-disk laser," *Opt. Lett.* **43**(4), 879–882 (2018).

Project leader, development of the cavity design, setup of the TDL oscillator, full experimental characterization and optimization of the mode-locked laser performance.

- **Paper 4:** N. Modsching, C. Paradis, P. Brochard, N. Jornod, K. Gürel, C. Kränkel, S. Schilt, V. J. Wittwer, and T. Südmeyer, "Carrier-envelope offset frequency stabilization of a thin-disk laser oscillator operating in the strongly self-phase modulation broadened regime," *Opt. Express* **26**(22), 28461 (2018).

Project leader, contribution in developing the driving laser system (paper 1), implementation of the stabilization electronics in the experimental setup, detection of the carrier-envelope offset frequency (f_{CEO}) with a provided f -to- $2f$ interferometer, experimental characterization and stabilization of the f_{CEO} , optimization of the active feedback loop.

- **Paper 5:** C. Paradis, J. Drs, N. Modsching, O. Razskazovskaya, F. Meyer, C. Kränkel, C. J. Saraceno, V. J. Wittwer, and T. Südmeyer, "Broadband terahertz pulse generation driven by an ultrafast thin-disk laser oscillator," *Opt. Express* **26**(20), 26377–26384 (2018).

Contribution in developing the driving laser system (paper 1), participation in preliminary experimental investigations for THz generation,

participation in measurement campaigns and optimization of the experimental setup.

- **Paper 6:** J. Drs, **N. Modsching**, C. Paradis, C. Kränkel, V. J. Wittwer, O. Razskazovskaya, and T. Südmeyer, "Optical rectification of ultrafast Yb-lasers: Pushing power and bandwidth of THz generation in GaP," *JOSA B submitted* (2019).

Experimental modification of the driving TDL oscillator to different pulse durations (paper 1), power-scaling of the TDL laser oscillator for achieving the high THz average power result (paper 2), participation in all THz measurement campaigns.

- **Paper 7:** F. Labaye, M. Gaponenko, V. J. Wittwer, A. Diebold, C. Paradis, **N. Modsching**, L. Merceron, F. Emaury, I. J. Graumann, C. R. Phillips, C. J. Saraceno, C. Kränkel, U. Keller, and T. Südmeyer, "Extreme ultraviolet light source at a megahertz repetition rate based on high-harmonic generation inside a mode-locked thin-disk laser oscillator," *Opt. Lett.* **42**(24), 5170–5173 (2017).

Initial experimental investigation demonstrating the suitability of the used Yb:Lu₂O₃ disk for the generation of sub-300-fs pulses durations at high average powers by SESAM mode-locking. Contribution in the discussion about cavity design.

References

1. R. Weiss, "Nobel Lecture: LIGO and the discovery of gravitational waves I," *Rev. Mod. Phys.* **90**(4)(2018).
2. Royal Swedish Academy of Sciences, "Press release of the Nobel Prize in Physics 2018," www.nobelprize.org (October 2, 2018).
3. A. Diebold, F. Emaury, C. Schriber, M. Golling, C. J. Saraceno, T. Südmeyer, and U. Keller, "SESAM mode-locked Yb:CaGdAlO₄ thin disk laser with 62 fs pulse generation," *Opt. Lett.* **38**(19), 3842–3845 (2013).
4. C. J. Saraceno, O. H. Heckl, C. R. E. Baer, C. Schriber, M. Golling, K. Beil, C. Kränkel, T. Südmeyer, G. Huber, and U. Keller, "Sub-100 femtosecond pulses from a SESAM modelocked thin disk laser," *Appl. Phys. B* **106**(3), 559–562 (2012).
5. C. Schriber, L. Merceron, A. Diebold, F. Emaury, M. Golling, K. Beil, C. Kränkel, C. J. Saraceno, T. Südmeyer, and U. Keller, "Pushing SESAM modelocked thin-disk lasers to shortest pulse durations," in *Advanced Solid State Lasers* (Optical Society of America, 2014), paper AF1A.4.
6. J. Zhang, J. Brons, M. Seidel, V. Pervak, V. Kalashnikov, Z. Wei, A. Apolonski, F. Krausz, and O. Pronin, "49-fs Yb:YAG thin-disk oscillator with distributed Kerr-lens mode-locking," in *European Quantum Electronics Conference* (Optical Society of America, 2015), paper PD_A_1.

7. M. Saraceno, martin@saraceno.info.
8. E. Snitzer, "Proposed Fiber Cavities for Optical Masers," J. Appl. Phys. **32**(1), 36–39 (1961).
9. K. Du, P. Loosen, and R. Poprawe, "Optical amplifier arrangement for a solid state laser," U.S. patent 6,654,163 (2003).
10. A. Giesen, H. Hügel, A. Voss, K. Wittig, U. Brauch, and H. Opower, "Scalable concept for diode-pumped high-power solid-state lasers," Appl. Phys. B Lasers Opt. **58**(5), 365–372 (1994).
11. C. J. Saraceno, "Mode-locked thin-disk lasers and their potential application for high-power terahertz generation," J. Opt. **20**(4), 044010 (2018).

Chapter 2

Cutting-edge sub-100-fs thin-disk laser oscillators

This chapter presents the development of Kerr lens mode-locked (KLM) thin-disk laser (TDL) oscillators operating in the sub-100-fs pulse duration regime. Section 2.1 summarizes in an overview the achieved results in the framework of this thesis. Subsection 2.1.1 and 2.1.2 introduce the Kerr lens mode-locking technique and discuss the physical properties of the chosen Yb-doped gain materials, respectively. Section 2.2 to 2.4 present the developed KLM TDL oscillators. Section 2.5 discusses in more detail the experimental optimization for laser operation in the sub-100-fs pulse duration regime. Applications of the developed KLM TDL oscillators will be presented ongoing in chapter 3 and chapter 4.

2.1 Generation of sub-100-fs pulse durations from thin-disk laser oscillators

In the framework of this thesis ultrafast TDL oscillators were developed with improved performance for laser operation the sub-100-fs pulse duration regime. Key ingredient was the combination of the Kerr lens mode-locking scheme for TDL oscillators [1] with the gain materials Yb:Lu₂O₃ [2] and Yb:CALGO [3]. This combination enabled the development of sub-100-fs TDL oscillators operating at a 4 times higher average power compared to previous results [Fig. 1(a)]. Additionally,

unprecedented pulse durations of ultrafast TDL oscillators have been achieved, 40% shorter compared to previous results [Fig. 1(b)]. This resulted in a change of paradigm showing that the thin-disk geometry can generate pulse durations from Yb-doped gain materials as short as the one achievable with Yb-doped bulk oscillators.

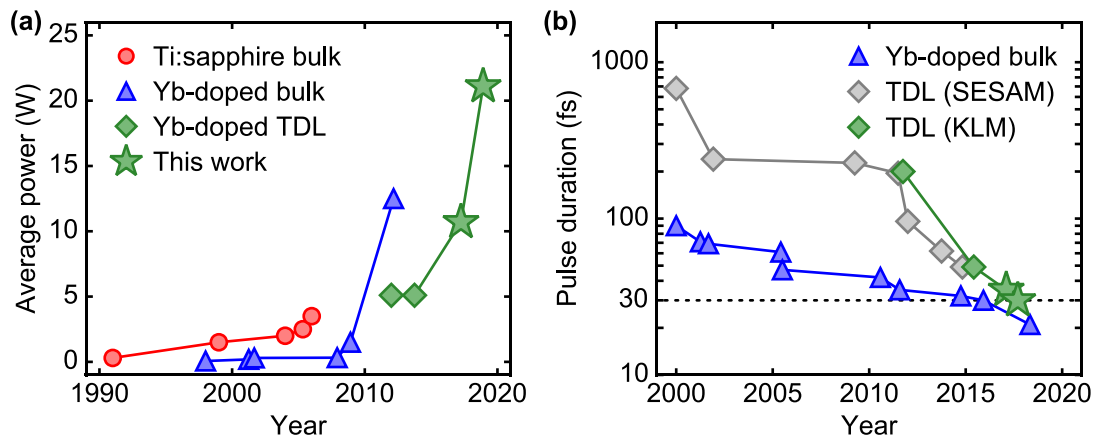


Fig. 1. (a) Progress in average power of sub-100-fs oscillators based on Ti:sapphire and Yb-doped gain materials for bulk and thin-disk laser (TDL) geometry. (b) Evolution of the shortest pulse duration generated by ultrafast Yb-doped bulk and TDL oscillators. Ultrafast TDL oscillators are distinguished into the applied mode-locking technique (SESAM: saturable absorber mirror; KLM: Kerr lens mode-locking). Presented results in this thesis are highlighted with a green star, references can be found in [4,5].

Subsection 2.1.1 introduces the Kerr lens mode-locking scheme of TDL oscillators and subsection 2.1.2 summarizes the physical key properties of the applied gain materials Yb:Lu₂O₃ and Yb:CALGO in comparison to Yb:YAG, the standard gain material for nowadays TDL. Section 2.2 to 2.4 contain the experimental results of the developed Kerr lens mode-locked (KLM) TDL oscillators that are following concluded with their experimental results and key messages.

Section 2.2 presents the development of a KLM TDL oscillator based on the gain material Yb:Lu₂O₃. Different combinations of output-coupler transmission, introduced group delay dispersion and hard aperture diameter have been realized to study the impact of those laser parameter on the pulse duration and average power.

- Laser operation at 10.7 W of average power in 88-fs pulses, 4.5 W in 49-fs pulses, and 1.6 W in 35-fs pulses
- First demonstration of a sub-100-fs TDL oscillator operating at more than 10 W of average power

- At that time the shortest pulse duration generated by a TDL oscillator
- Demonstration that Yb:Lu₂O₃ is a promising gain material for power-scaling of sub-100-fs TDL oscillators

Section 2.3 presents the performance improvement of the KLM TDL oscillator developed in section 2.2. Based on the same Yb:Lu₂O₃ disk a modified cavity design has been developed folding the laser cavity a second time on the disk. The impact of higher round-trip gain onto the laser performance in the sub-100-fs pulse duration regime was investigated.

- Laser operation at 21 W of average power in 95-fs pulses
- Highest average power demonstrated by a sub-100-fs oscillator
- Highest optical-to-optical efficiency achieved by a sub-100-fs TDL oscillator
- Demonstration that TDL oscillators operating in the self-phase modulation broadened regime can generate sub-100-fs pulses at high average powers with optical-to-optical efficiencies that are comparable to sub-100-fs Yb-based bulk oscillators

Section 2.4 presents the development of a KLM TDL oscillator based on the broadband gain material Yb:CALGO.

- First demonstration of a KLM Yb:CALGO TDL oscillator.
- Generation of 30-fs pulses which is the shortest pulse duration so far achieved by an ultrafast TDL oscillator
- Advantage of the thin-disk pumping scheme for the generation of even shorter pulse duration in comparison to standard end-pumped bulk oscillators.

Section 2.5 concludes this chapter by explaining in more detail the underlying experimental optimization for laser operation in the sub-100-fs pulse duration regime. The impact of various optimization parameters onto the laser performance is determined.

2.1.1 Mode-locking of TDL oscillators via the Kerr effect

Passive mode-locking enables the formation of a pulse inside a laser oscillator with durations in the femtosecond regime [6–8]. The fundamental principle of mode-locking has been intensively discussed in various text books [9–11]. In the thin-disk

geometry several mode-locking techniques have been applied, e.g. by saturable absorber mirrors (SESAMs) [12], Kerr lens mode-locking [13], nonlinear polarization rotation [14] and, more recently, non-linear mirror mode-locking [15]. Among those techniques the shortest pulse durations were generated via Kerr lens mode-locking as will be presented in this thesis.

The Kerr effect describes the change of the refractive index of a material (n) in the presence of light with high intensity (I). Its strength depends on the nonlinear material refractive index n_2 and the intensity of the light as follows

$$n(I) = n + n_2 I.$$

In a transverse Gaussian profile, the highest intensity appears in the center of the laser beam. In case that $n_2 > 0$ the Kerr effect creates a corresponding refractive index profile with the maximum in the center. The increased refractive index retards the central laser beam components compared to the outer ones. This results in the formation of an intensity dependent focusing lens. The focal length of the so created Kerr lens (f_{Kerr}) can be approximated by

$$f_{\text{Kerr}}^{-1} = \frac{8n_2 d_{\text{KM}}}{\pi w^2} \cdot I,$$

where d_{KM} is the thickness of the Kerr medium (KM) and w the beam radius in the KM [16].

Mode-locking via the Kerr effect is based on the formation of a Kerr lens in a bulk material, referred to as Kerr medium [inset Fig. 2(left)]. The KM is usually an undoped YAG, sapphire or fused silica plate of several millimeter thickness. It is typically placed under Brewster's angle into the cavity to avoid Fresnel reflection losses. In the standard Kerr lens mode-locking scheme of TDL oscillators the KM is placed in the vicinity of an intracavity focus that is created between two curved mirrors [13]. The Kerr lens can promote two types of passive loss modulation for the generation of ultrashort pulses. In case of "hard aperture mode-locking" the required loss modulation is achieved by placing a pinhole into the laser cavity [inset Fig. 2(right)]. The Kerr lens focusses the laser beam at the position of the hard aperture [Fig. 2(bottom)]. Reduced round-trip losses make the mode-locked operation more

favourable than the continuous-wave operation. In case of “soft aperture mode-locking” the Kerr lens improves in mode-locked operation the overlap of the laser beam with the pumped area in the gain material.

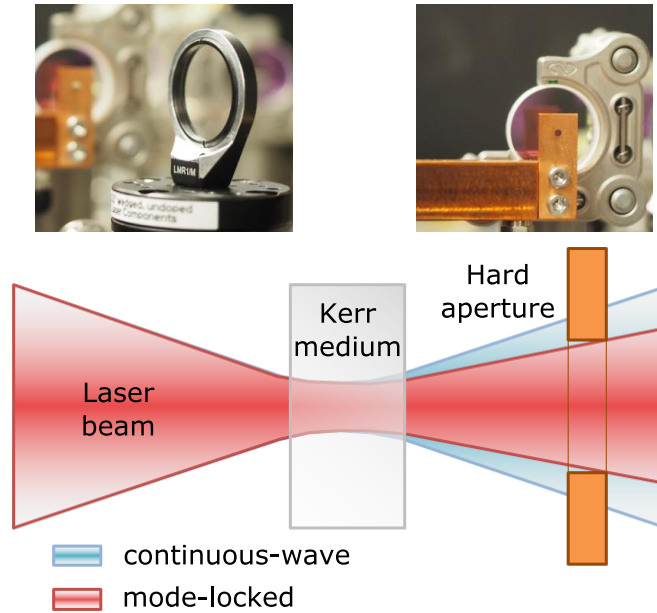


Fig. 2. (left) Kerr medium and (right) pinhole placed in front of a cavity end mirror for hard aperture mode-locking. (bottom) Schematic of the beam propagation in continuous-wave and in mode-locked operation. The Kerr lens in mode-locked operation reduces the losses by focusing the laser beam through the hard aperture.

Kerr lens mode-locking features a spectrally broadband passive loss modulation at high modulation depths. The nearly instantaneous response and relaxation is beneficial for the formation of ultrashort pulse durations. Without real absorption taking place, this technique is as well suitable for laser operation at high intracavity average powers and peak powers. However, the challenge for Kerr lens mode-locking relies in the cavity design. Usually a continuous-wave operation close to the edge of the stability zone is required [13].

Focussing of the pulse into the KM generates besides the Kerr lens also self-phase modulation (SPM). The amount of SPM created per cavity roundtrip (γ_{SPM}) along the propagation length z can be estimated for a Gaussian beam by

$$\gamma_{\text{SPM}} = \frac{2\pi}{\lambda} \int_0^L n_2 \frac{2}{\pi \cdot w^2(z)} \cdot dz,$$

where λ is the wavelength [10]. SPM generates new frequency components for a corresponding up-chirp. The created amount of SPM in the KM is usually much larger than the one accumulated during free space propagation. For soliton pulse formation the SPM has to be accordingly compensated by negative group delay dispersion (GDD). The fundamental soliton equation relates the resulting pulse energy E_{pulse} , to the amount of total GDD, the SPM-coefficient γ_{SPM} , and the full width at half maximum (FWHM) pulse duration τ_{FWHM} as follows:

$$E_{\text{pulse}} = \frac{2 \cdot 1.76 \cdot |\text{GDD}|}{|\gamma_{\text{SPM}}| \cdot \tau_{\text{FWHM}}}$$

A large amount of SPM can result in the generation of frequency components beyond the gain bandwidth. This enables the generation of shorter pulse duration than actually supported by the gain material [17]. By operating in the strongly SPM-broadened regime a KLM Yb:YAG TDL oscillator generated pulses durations as short as 49 fs [18]. Section 2.2 presents the development of a KLM Yb:Lu₂O₃ TDL oscillator operating in the same regime generating even a shorter pulse duration of 35 fs. In both cases enabled the large amount of SPM the expansion of the optical spectrum three times beyond the corresponding FWHM gain bandwidth.

2.1.2 *Yb-doped gain materials*

The development of novel gain materials and the continuous improvement of the crystal quality from existing ones is crucial for further progress of powerful ultrafast lasers. Besides the manifold of laser active ions (Cr³⁺, Er³⁺, Ti³⁺, Tm³⁺, Ho³⁺, Yb³⁺, ...), Yb-doped gain materials feature the most suitable properties for laser operation at high average power [19]. Main advantages are a reduced heat load due to the low quantum defect, high doping concentration up to 10% and optical pumping with diode laser systems that are commercially available at kW power levels. The choice of the Yb-doped host [19–23] (e.g. garnets like YAG or LuAG; sesquioxides like Lu₂O₃, Sc₂O₃ or LuScO₃; tungstates like KYW, KGW or KLuW; vanadates like LuVO, YVO, GdVO; CALGO or CALYO) is crucial for the thermo-mechanical and spectral properties of the gain material. An extensive overview about Yb-doped gain materials and their suitability for the development of sub-100-fs TDL oscillators is given in [21]. Most favourable properties of a gain material for application in the thin-disk configuration

are: High thermal conductivity, large gain cross-sections, broad spectral gain bandwidth, high doping concentrations, high crystal quality, homogenous crystal properties, reproducible manufacturing of large crystal diameters. However, the ideal gain material fulfilling all required properties does not exist yet and a trade-off has to be found.

In the framework of this thesis the gain materials Yb:Lu₂O₃ and Yb:CALGO have been selected as most promising for the development of sub-100-fs TDL oscillators. Their gain cross-sections at an inversion level β of 0.3 are shown in Fig. 1 in comparison to Yb:YAG, the standard gain material of TDLs nowadays. Selected physical properties of the three gain materials are summarized in Tab. 1.

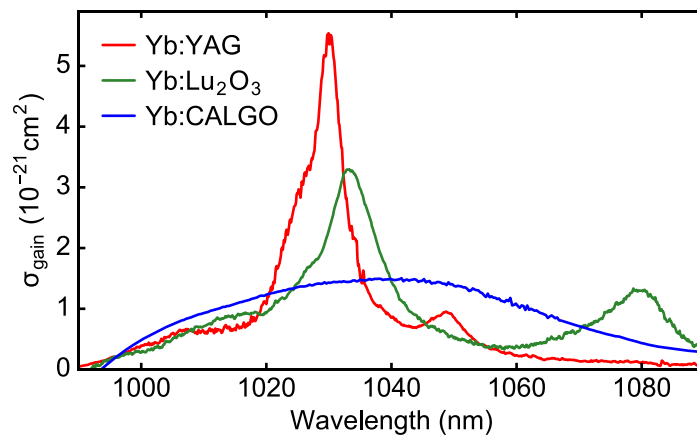


Fig. 3. Gain cross sections (inversion level $\beta = 0.3$) of the gain materials Yb:Lu₂O₃ and Yb:CALGO (σ -polarization) are shown in comparison to Yb:YAG, the standard gain material of nowadays high-power TDL. The figure has been taken from [5] and modified.

The physical properties of Yb:Lu₂O₃ are promising for the development of powerful sub-100-fs TDL oscillators (Tab. 1). Its thermal conductivity drops only slightly with increasing doping concentration [20]. In comparison to Yb:YAG this results in a 50% higher thermal conductivity at a doping concentration of 3 at.%. The 40% smaller gain cross section could thus be compensated with an increased doping concentration and a larger disk thickness. The 60% larger FWHM gain bandwidth at an inversion level of $\beta = 0.3$ is beneficial for the generation of sub-100-fs pulse durations. However, the extremely high melting temperature of 2500 °C makes the fabrication of single crystal Yb:Lu₂O₃ challenging [19]. Highest single crystal quality was so far achieved by the heat-exchanger method [24]. The potential of single crystal Yb:Lu₂O₃ TDL oscillators was demonstrated with 670 W of average power in multi-

mode operation [25]. In mode-locked operation 141 W of average power were achieved at a somewhat longer pulse duration of 738 fs [26]. Recently, the fabrication of ceramic Yb:Lu₂O₃ via the sintering method has become another promising approach to fabricate Yb:Lu₂O₃ disks at lower temperatures [27]. Ceramic Yb:Lu₂O₃ TDL oscillators achieved already 174 W of average power in multi-mode operation [28]. In mode-locked operation 3.7 W were demonstrated with 98-fs pulses [29].

The potential of KLM TDL oscillators based on crystalline Yb:Lu₂O₃ disks for high-power laser operation in the sub-100-fs pulse duration regime is presented in section 2.2. Section 2.3 demonstrates laser operation of a sub-100-fs Yb:Lu₂O₃ KLM TDL oscillators at 21 W of average power.

Tab. 1. Selected physical properties of the gain materials Yb:YAG, Yb:Lu₂O₃ and Yb:CALGO (FWHM, full width at half maximum) [3,30,31].

	Yb:YAG	Yb:Lu ₂ O ₃	Yb:CALGO (c-cut)
Chemical formula	Yb:Y ₃ Al ₅ O ₁₂	Yb:Lu ₂ O ₃	Yb:CaGdAlO ₄
Melting point (undoped)	1930 °C	2500 °C	< 1700 °C
Thermal conductivity (undoped)	9.8 W/m · K	12.2 W/m · K	11.4 W/m · K
Thermal conductivity (Yb-doped)	7.1 W/m · K (3 at.%)	10.8 W/m · K (3 at.%)	6.3 W/m · K (2 at.%)
Gain properties at inversion level of $\beta = 0.3$ (values retrieved from Fig. 1)			
Central wavelength	1030 nm	1033 nm	1042 nm
Gain cross section	$5.5 \cdot 10^{-21}$ cm ²	$3.3 \cdot 10^{-21}$ cm ²	$1.5 \cdot 10^{-21}$ cm ²
FWHM bandwidth	8 nm	13 nm	> 60 nm
Bandwidth corresponding Fourier limited pulse duration	140 fs	90 fs	< 20 fs

Yb:CALGO features the broadest gain bandwidth of Yb-doped gain materials that have been so far applied in the thin-disk configuration (Fig. 1). It supports theoretically the generation of sub-20-fs pulse durations (Tab. 1). However, the disordered crystalline structure results in a strongly reduced gain cross section and restricts the available single pass gain. Although the thermal conductivity drops for higher doping concentrations, it remains good compared to other broadband gain materials [21]. The strongest limitation in the development of more powerful ultrafast Yb:CALGO TDL oscillators is the available disk quality which still suffers from inhomogeneities [5,32]. In the thin-disk configuration already 190 W of average power were reported in multi-

mode operation [32]. In mode-locked operation 28 W of average power were achieved in 300-fs pulses [33] and pulses as short as 49 fs were generated at 2 W of average power [34]. Exploiting the gain bandwidth of Yb:CALGO further by generating 30-fs pulses from a KLM TDL oscillator is presented in section 2.4.

References

1. O. Pronin, J. Brons, C. Grasse, V. Pervak, G. Boehm, M.-C. Amann, V. L. Kalashnikov, A. Apolonski, and F. Krausz, "High-power 200 fs Kerr-lens mode-locked Yb:YAG thin-disk oscillator," *Opt. Lett.* **36**(24), 4746–4748 (2011).
2. C. Kränkel, "Rare-earth-doped sesquioxides for diode-pumped high-power lasers in the 1-, 2-, and 3- μ m spectral range," *IEEE J. Sel. Top. Quantum Electron.* **21**(1), 250–262 (2015).
3. J. Petit, P. Goldner, and B. Viana, "Laser emission with low quantum defect in Yb:CaGdAlO₄," *Opt. Lett.* **30**(11), 1345–1347 (2005).
4. N. Modsching, J. Drs, J. Fischer, C. Paradis, F. Labaye, M. Gaponenko, C. Kränkel, V. J. Wittwer, and T. Südmeyer, "Sub-100-fs Kerr lens mode-locked Yb:Lu₂O₃ thin-disk laser oscillator operating at 21 W average power," *Opt. Express* **submitted** (2019).
5. N. Modsching, C. Paradis, F. Labaye, M. Gaponenko, I. J. Graumann, A. Diebold, F. Emaury, V. J. Wittwer, and T. Südmeyer, "Kerr lens mode-locked Yb:CALGO thin-disk laser," *Opt. Lett.* **43**(4), 879–882 (2018).
6. D. E. Spence, P. N. Kean, and W. Sibbett, "60-fsec pulse generation from a self-mode-locked Ti:sapphire laser," *Opt. Lett.* **16**(1), 42–44 (1991).
7. D. E. Spence, J. M. Evans, W. E. Sleat, and W. Sibbett, "Regeneratively initiated self-mode-locked Ti:sapphire laser," *Opt Lett* **16**(22), 1762–1764 (1991).
8. W. Sibbett, A. A. Lagatsky, and C. T. A. Brown, "The development and application of femtosecond laser systems," *Opt. Express* **20**(7), 6989–7001 (2012).
9. U. Keller, *Ultrafast Solid-State Lasers*, Landolt-Börnstein. Laser Physics and Applications. Subvolume B: Laser Systems. Part I (Springer, 2007).
10. G. Agrawal, *Nonlinear Fiber Optics* (Academic press, 2001).
11. A. M. Weiner, *Ultrafast Optics* (John Wiley & Sons, Inc., Hoboken, New Jersey, 2009).
12. J. A. der Au, G. J. Spühler, T. Südmeyer, R. Paschotta, R. Hövel, M. Moser, S. Erhard, M. Karszewski, A. Giesen, and U. Keller, "16.2-W average power from a diode-pumped femtosecond Yb:YAG thin disk laser," *Opt. Lett.* **25**(11), 859–861 (2000).
13. O. Pronin, J. Brons, M. Seidel, J. Zhang, M. Trubetskov, D. Bauer, D. Sutter, V. Kalashnikov, A. Apolonski, V. Pervak, and others, "High-power femtosecond thin-disk oscillators," in *The European Conference on Lasers and Electro-Optics (Optical Society of America, 2015)*, paper CA_10_5.
14. B. Borchers, C. Schäfer, C. Fries, M. Larionov, and R. Knappe, "Nonlinear polarization rotation mode-locking via phase-mismatched type I SHG of a thin disk femtosecond laser," in *Advanced Solid State Lasers (Optical Society of America, 2015)*, paper AT4A.9.
15. F. Saltarelli, A. Diebold, I. J. Graumann, C. R. Phillips, and U. Keller, "Modelocking of a thin-disk laser with the frequency-doubling nonlinear-mirror technique," *Opt. Express* **25**(19), 23254 (2017).
16. S. Yefet and A. Pe'er, "A Review of Cavity Design for Kerr Lens Mode-Locked Solid-State Lasers," *Appl. Sci.* **3**(4), 1–31 (2015).
17. M. Tokurakawa, A. Shirakawa, K. Ueda, H. Yagi, S. Hosokawa, T. Yanagitani, and A. A. Kaminskii, "Diode-pumped 65 fs Kerr-lens mode-locked Yb³⁺:Lu₂O₃ and nondoped Y₂O₃ combined ceramic laser," *Opt. Lett.* **33**(12), 1380–1382 (2008).

18. J. Zhang, J. Brons, M. Seidel, V. Pervak, V. Kalashnikov, Z. Wei, A. Apolonski, F. Krausz, and O. Pronin, "49-fs Yb:YAG thin-disk oscillator with distributed Kerr-lens mode-locking," in European Quantum Electronics Conference (Optical Society of America, 2015), paper PD_A_1.
19. C. Kränkel, "Rare-Earth-Doped Sesquioxides for Diode-Pumped High-Power Lasers in the 1-, 2-, and 3- μm Spectral Range," *IEEE J. Sel. Top. Quantum Electron.* **21**(1), 250–262 (2015).
20. R. Peters, C. Kränkel, S. T. Fredrich-Thornton, K. Beil, K. Petermann, G. Huber, O. H. Heckl, C. R. E. Baer, C. J. Saraceno, T. Südmeyer, and U. Keller, "Thermal analysis and efficient high power continuous-wave and mode-locked thin disk laser operation of Yb-doped sesquioxides," *Appl. Phys. B* **102**(3), 509–514 (2011).
21. T. Südmeyer, C. Kränkel, C. R. E. Baer, O. H. Heckl, C. J. Saraceno, M. Golling, R. Peters, K. Petermann, G. Huber, and U. Keller, "High-power ultrafast thin disk laser oscillators and their potential for sub-100-femtosecond pulse generation," *Appl. Phys. B* **97**(2), 281–295 (2009).
22. P. Loiko, F. Druon, P. Georges, B. Viana, and K. Yumashev, "Thermo-optic characterization of Yb:CaGdAlO₄ laser crystal," *Opt. Mater. Express* **4**(11), 2241–2249 (2014).
23. D. Li, X. Xu, H. Zhu, X. Chen, W. D. Tan, J. Zhang, D. Tang, J. Ma, F. Wu, C. Xia, and J. Xu, "Characterization of laser crystal Yb:CaYAlO₄," *J. Opt. Soc. Am. B* **28**(7), 1650–1654 (2011).
24. R. Peters, C. Kränkel, K. Petermann, and G. Huber, "Crystal growth by the heat exchanger method, spectroscopic characterization and laser operation of high-purity Yb:Lu₂O₃," *J. Cryst. Growth* **310**(7–9), 1934–1938 (2008).
25. B. Weichelt, K. S. Wentsch, A. Voss, M. A. Ahmed, and T. Graf, "A 670 W Yb:Lu₂O₃ thin-disk laser," *Laser Phys. Lett.* **9**(2), 110–115 (2012).
26. C. R. E. Baer, C. Kränkel, C. J. Saraceno, O. H. Heckl, M. Golling, R. Peters, K. Petermann, T. Südmeyer, G. Huber, and U. Keller, "Femtosecond thin-disk laser with 141 W of average power," *Opt. Lett.* **35**(13), 2302–2304 (2010).
27. M. Tokurakawa, K. Takaichi, A. Shirakawa, K. Ueda, H. Yagi, S. Hosokawa, T. Yanagitani, and A. A. Kaminskii, "Diode-pumped mode-locked Yb³⁺:Lu₂O₃ ceramic laser," *Opt. Express* **14**(26), 12832 (2006).
28. S. Kitajima, H. Nakao, A. Shirakawa, H. Yagi, and T. Yanagitani, "CW Performance and Temperature Observation of Yb:Lu₂O₃ Ceramic Thin-Disk Laser," in Laser Congress 2017 (ASSL, LAC) (Optical Society of America, 2017), paper JM5A.32.
29. S. Kitajima, A. Shirakawa, H. Yagi, and T. Yanagitani, "Sub-100 fs pulse generation from a Kerr-lens mode-locked Yb:Lu₂O₃ ceramic thin-disk laser," *Opt. Lett.* **43**(21), 5451 (2018).
30. R. Peters, C. Kränkel, K. Petermann, and G. Huber, "Broadly tunable high-power Yb:Lu₂O₃ thin disk laser with 80% slope efficiency," *Opt. Express* **15**(11), 7075 (2007).
31. J. Boudeile, F. Druon, M. Hanna, P. Georges, Y. Zaouter, E. Cormier, J. Petit, P. Goldner, and B. Viana, "Continuous-wave and femtosecond laser operation of Yb:CaGdAlO₄ under high-power diode pumping," *Opt. Lett.* **32**(14), 1962–1964 (2007).
32. J. Brons, V. Pervak, E. Fedulova, M. Seidel, D. Bauer, D. Sutter, V. Kalashnikov, A. Apolonskiy, O. Pronin, and F. Krausz, "High power Kerr-lens mode-locking of Yb:YAG and Yb:CALGO thin-disk oscillators," in Advanced Solid State Lasers (Optical Society of America, 2014), paper AF1A-5.
33. S. Ricaud, A. Jaffres, K. Wentsch, A. Suganuma, B. Viana, P. Loiseau, B. Weichelt, M. Abdou-Ahmed, A. Voss, T. Graf, D. Rytz, C. Hönninger, E. Mottay, P. Georges, and F. Druon, "Femtosecond Yb:CaGdAlO₄ thin-disk oscillator," *Opt. Lett.* **37**(19), 3984–3986 (2012).
34. C. Schriber, L. Merceron, A. Diebold, F. Emaury, M. Golling, K. Beil, C. Kränkel, C. J. Saraceno, T. Südmeyer, and U. Keller, "Pushing SESAM modelocked thin-disk lasers to shortest pulse durations," in Advanced Solid State Lasers (Optical Society of America, 2014), paper AF1A.4.

2.2 Generation of 35-fs pulses from a Kerr lens mode-locked Yb:Lu₂O₃ thin-disk laser

Clément Paradis,^{1,*} Norbert Modsching,¹ Valentin J. Wittwer,¹ Bastian Deppe,^{2,3} Christian Kränkel,^{2,3,4} and Thomas Südmeyer¹

¹Laboratoire Temps-Fréquence, Institut de Physique, Université de Neuchâtel, Avenue de Bellevaux 51, 2000 Neuchâtel, Switzerland

²Institut für Laser-Physik, Universität Hamburg, Luruper Chaussee 149, 22761 Hamburg, Germany

³The Hamburg Centre for Ultrafast Imaging, Universität Hamburg, Luruper Chaussee 149, 22761 Hamburg, Germany

⁴Center for Laser Materials, Leibniz Institute for Crystal Growth, Max-Born-Str. 2, 12489 Berlin, Germany

We investigate Kerr lens mode locking of Yb:Lu₂O₃ thin-disk laser oscillators operating in the sub-100-fs regime. Pulses as short as 35 fs were generated at an average output power of 1.6 W. These are the shortest pulses directly emitted from a thin-disk laser oscillator. The optical spectrum of the 35-fs pulses is almost 3 times broader than the corresponding emission band of the gain crystal. At slightly longer pulse duration of 49 fs, we achieve an average power of 4.5 W. In addition, 10.7 W are obtained in 88-fs pulses, which is twice higher than the previous power record for ultrafast thin-disk lasers generating pulses shorter than 100 fs. Our results prove that Kerr lens mode-locked Yb:Lu₂O₃ thin-disk lasers are a promising technology for further average power and pulse energy scaling of ultrafast high-power oscillators operating in the sub-100-fs regime.

2.2.1 Introduction

Following the demonstration of the first mode-locked thin-disk laser (TDL) oscillator more than fifteen years ago [1], tremendous progress in the area of power scaling has been achieved [2]. In this period, the field of mode-locked TDLs has evolved into being the leading technology for high power and high pulse energy ultrafast laser oscillators. State-of-the-art ultrafast TDLs emit up to 275 W of output power [3,4] and 80 μ J of pulse energy [5] with several hundred femtoseconds pulse durations. Such

performance has enabled TDLs to directly drive applications which previously required the use of complex amplifier systems [6–8]. However, reducing the pulse duration of high-power oscillators is a major challenge. The first TDL emitting sub-100-fs pulses has been demonstrated only in 2012 [9] and even today, the power levels in this regime are limited to 5 W [9,10] (see Fig. 1). Therefore, external nonlinear pulse compression is applied for many applications in areas such as high field science and frequency comb generation. This introduces an additional stage of complexity to the system which may reduce the beam quality, power level and temporal pulse profile. Overcoming the trade-off between output power and pulse duration by providing compact and simple laser oscillators delivering hundreds of watts and tens of micro-joules in sub-100-fs pulses will simplify many existing experiments and open new application areas.

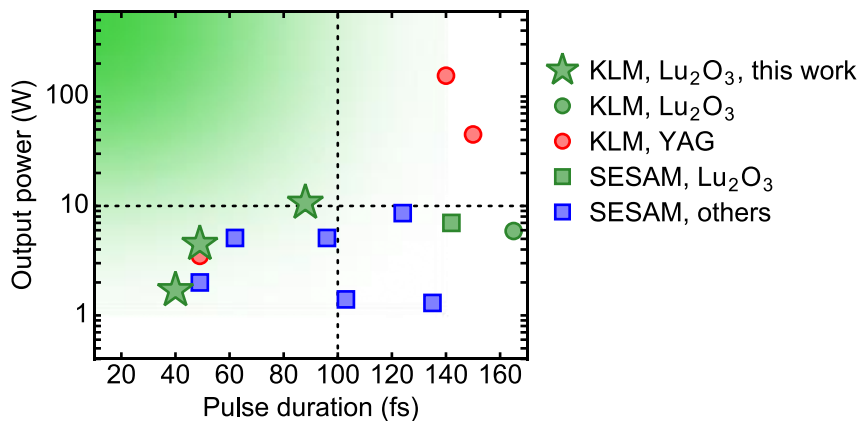


Fig. 1. Overview of sub-170-fs mode-locked thin-disk lasers based on Yb-doped materials [9–17]. The results presented in this article are highlighted with star symbols. The green area spotlights the desired performance of ultrafast oscillators to directly drive applications such as high field science and frequency comb generation.

Initially, all ultrafast TDLs were passively mode-locked using a semiconductor saturable absorber mirror (SESAM, [18]). Besides self-starting pulsed operation and simplicity of the cavity design, the combination of TDLs and SESAMs enables power scalability of the modelocked performance of the laser [2]. Following the demonstration of the first Kerr lens modelocked (KLM) TDL [19], similar scaling laws were demonstrated for this alternative mode locking technique resulting in average output powers up to 270 W in 330-fs pulses utilizing Yb:Y₃Al₅O₁₂ (Yb:YAG) [4]. Recently, 140-fs pulses were generated directly from a KLM Yb:YAG thin-disk

oscillator at an average output power of 155 W and an optical-to-optical efficiency of 29% [17]. This pulse duration is more than three times shorter than any Yb:YAG SESAM mode-locked TDL [2]. Mode locking of TDLs via the Kerr lensing mechanism enables high modulation depth as well as instantaneous response time of the self-amplitude modulation. While Yb:YAG may be the best choice for high (average) output power, its gain bandwidth of 9 nm (FWHM) does not support pulses shorter than 120 fs. In order to achieve mode-locked operation with pulse durations shorter than 100 fs, numerous TDL using Yb-doped laser materials with broader gain bandwidths have been developed [20]. In this way, the minimum pulse duration was successfully reduced from initially hundreds of femtoseconds to 49 fs, which were obtained from a SESAM mode-locked Yb:CaGdAlO₄ (Yb:CALGO) TDL [10,14]. Most of the recently demonstrated Yb-based broadband gain materials are still in an early phase of thin-disk development, suffering from growth defects and non-optimized disk processing technologies. Moreover, many of them exhibit comparably low thermal conductivity due to their disordered nature. All of these factors hinder further power scaling at the moment. Until recently, all TDLs generating record-short pulses were based on SESAM mode locking. In 2015, pulses as short as 49 fs with 33 nm optical bandwidth have been obtained from a KLM Yb:YAG TDL [15]. This result relied on spectral broadening of the pulses utilizing additional spectral components generated due to SPM well beyond the gain limitation [21]. Although the output power of 3.5 W was moderate, this result clearly indicates that KLM is a promising approach for achieving even shorter pulses from TDLs based on Yb-gain materials with broader emission bands than Yb:YAG.

Yb:Lu₂O₃ is an excellent candidate to push the performance of ultrafast TDLs towards high-power and short pulses. The cubic host lutetia (Lu₂O₃) features a high thermal conductivity of 12 Wm⁻¹K⁻¹, which is nearly independent on the doping concentration, while the thermal conductivity of Yb:YAG drops by nearly a factor of two to 7 Wm⁻¹K⁻¹ at the Yb³⁺-doping concentrations required in the TDL configuration. When doped with Yb³⁺, Lu₂O₃ exhibits a 30 % broader gain bandwidth than Yb:YAG, amounting to 12 nm (FWHM) and directly supporting sub-100-fs pulse formation. The absorption cross sections at the zero-phonon line around 976 nm are more than a factor of 3 higher than those of Yb:YAG. Pumping at this wavelength brings also the advantage of an increased Stokes efficiency and thus a lower amount of generated heat

compared to Yb:YAG, which is typically pumped at 940 nm or 969 nm [22]. The high melting point exceeding 2400 °C makes the growth of lutetia very challenging, but the heat exchanger method has proven to be a viable technique for growing high quality crystals [23]. The beneficial properties of this gain material supported very high optical-to-optical efficiencies exceeding 70 % in continuous wave operation. In the bulk geometry, an Yb:Lu₂O₃ oscillator emitted 71 fs pulses [24] while in SESAM-mode-locked TDL operation, it generated more than 140 W of average output power with sub-ps pulses [25] and supported pulses as short as 142 fs [11]. Recently, the first KLM Yb:Lu₂O₃ TDL was presented delivering 5.9 W with 165-fs pulses [16]. Figure 2 presents a timeline of the minimum achieved pulse duration from ultrafast Yb:Lu₂O₃ bulk and thin-disk lasers.

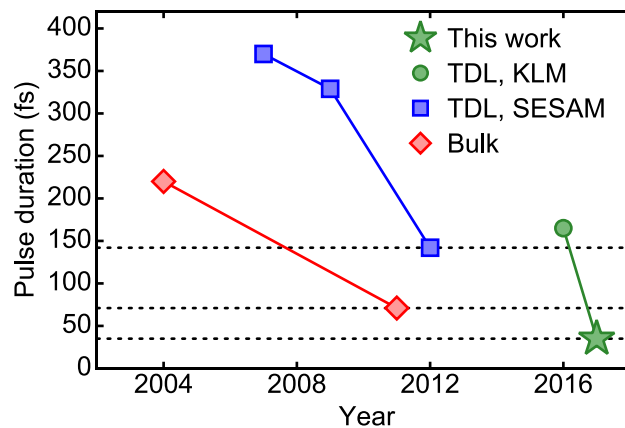


Fig. 2. Overview of the minimum achieved pulse duration from ultrafast oscillators based on the Yb:Lu₂O₃ gain material in bulk and thin-disk geometries [11,16,24,26–28]. The presented work is highlighted with a star symbol.

Here we demonstrate that the use of the broadband gain material Yb:Lu₂O₃ in the TDL configuration in combination with KLM technique is well-suited for the generation of pulses shorter than 100 fs. We achieved the shortest pulses as well as two times higher average power in the sub-100-fs domain than from any TDL.

2.2.2 Laser characterization in continuous-wave operation

The laser experiments were performed with a 12-mm-diameter Yb(3%):Lu₂O₃ disk. The crystal boule has been grown at the Institut für Laser-Physik (Universität Hamburg) and was afterwards cut and polished to a thickness of 160 μm. The disk

exhibits a wedge of 0.1° in order to avoid interaction between the residual reflections and the main beam. The front surface is anti-reflection (AR) coated while the back surface is coated to be highly reflective (HR) for laser and pump wavelengths. The disk is contacted onto a diamond heat sink and has a concave radius of curvature (RoC) of 2.1 m. Water-cooling of the diamond from the backside allows for efficient removal of the heat generated in the active material. A fiber-coupled volume-Bragg-grating (VBG) stabilized 400-W diode laser system pumps the gain material at the zero-phonon line at a wavelength of 976 nm with a spectral width below 0.5 nm. The disk is placed in a TDL head designed for 36 passes of the pump through the gain material in order to achieve high pump absorption. The pump spot is set to a diameter of 2.8 mm.

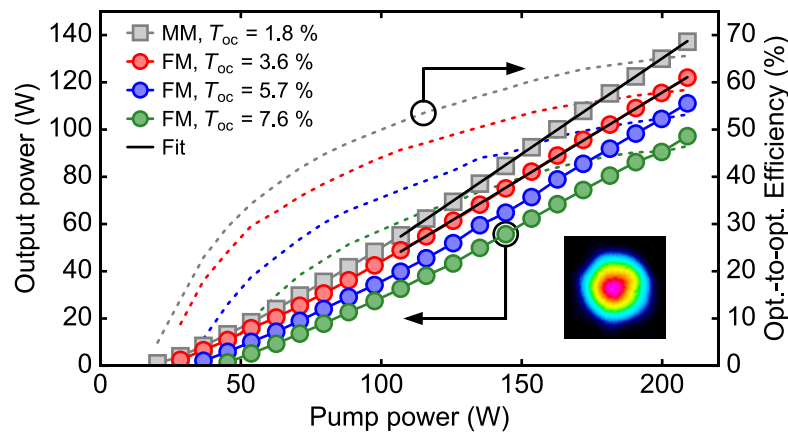


Fig. 3. Output power (solid) and optical-to-optical efficiency (dashed) as a function of the pump power for a multi-mode linear cavity (MM, output coupler transmission $T_{OC} = 1.8\%$) and a fundamental transverse mode cavity folded over the disk (FM, $T_{OC} = 3.6 - 7.6\%$), thus experiencing two times higher gain; The black solid lines show the linear fits used for the calculation of the slope efficiencies. Inset: near-field mode profile of the laser at 122 W of output power at a T_{OC} of 3.6 %.

The disk was initially tested in continuous-wave (cw) operation in a linear multimode (MM) cavity consisting of a flat output coupler (OC) with a transmission T_{OC} of 1.8% and the HR coated backside of the disk, separated by ≈ 7 cm. The beam radius of the fundamental mode on the gain crystal was estimated to be $360\ \mu\text{m}$, thus the laser operation was highly multi-mode given the pump spot diameter of 2.8 mm. In such a configuration, highest efficiencies can be expected due to an improved overlap of the top-head pump profile and the laser beam compared to a diffraction limited Gaussian beam. As shown in Fig. 3, a cw output power of 137 W was obtained under 209 W of incident pump power. The optical-to-optical efficiency amounted to

66% and the slope efficiency was 81%. These values are close to the best reported results with this gain material in the thin-disk configuration [22]. In order to avoid damage, we limited the pump intensity on the disk to $\approx 3.5 \text{ kW/cm}^2$ even though no hints for degradation of the laser efficiency were observed even at highest pump powers.

In the next step, we built a 3 m long linear cavity supporting fundamental transverse mode (FM) operation following a similar design as the one reported in [25]. The disk and a concave curved mirror (CM) (RoC = 3 m) are placed between two flat end mirrors, of which one is partially transmissive and used as an OC. In this configuration where the disk is used as a folding mirror, the laser beam passes four times per roundtrip (RT) through the gain crystal which leads to a twice higher gain and consequently a twice larger optimal output coupling rate compared to the multi-mode cavity. The lasing performance in cw operation was evaluated for different output coupling rates (see Fig. 3). The estimated laser mode to pump diameter ratio was around 80% and the beam quality factor M_2 was measured to be below 1.2 in all experiments, confirming fundamental mode operation of the laser. At $T_{OC} = 3.6\%$, 122 W were emitted with an optical-to-optical efficiency approaching 60% and a high slope efficiency of 70%. The near field mode profile of the laser at this output power is depicted in the inset of Fig. 3. These results reveal that this particular disk exhibits high growth and manufacturing quality and is well suited for further mode-locking experiments.

2.2.3 Results of the laser experiments in mode-locked operation

For mode-locked operation, we modified the cavity similar to [19] in order to favor pulsed operation by applying the Kerr effect as depicted in Fig. 4. A 2-mm-thick undoped YAG plate is placed under Brewster's angle in the focal region between the two concave mirrors (CM2 and CM3), which have both a RoC of 400 mm. This Brewster plate (BP) ensures linear polarization of the laser beam and serves as the Kerr medium for the mode-locking mechanism. The beam spot radius inside the BP is estimated to be $90 \text{ }\mu\text{m} \times 150 \text{ }\mu\text{m}$ in sagittal and tangential planes. A water-cooled pinhole placed in front of an end mirror serves as a hard aperture for KLM. The intracavity group delay dispersion (GDD) is adjusted by several dispersive mirrors for the soliton formation. The pulsed operation is generally initiated by a gentle knock on the

laser table. The cavity length of the resonator is 2.5 m, which results in a 61 MHz repetition rate of the generated pulses. The resonator is operated in ambient air and has a footprint of only 80 cm \times 40 cm.

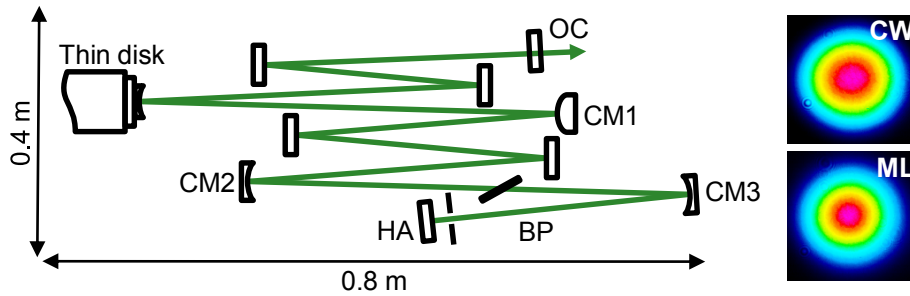


Fig. 4. Schematic of the cavity used for mode locking operation. CM1, convex RoC of 2 m; CM2, CM3 concave RoC of 400 mm; BP, Brewster plate; HA, hard aperture; OC, output coupler. All other mirrors are highly reflective or dispersive depending on the configuration. A difference in the size of the beam profile was between cw and ML operation (data shown for the 35-fs operation).

In our work, we focused on optimizing the laser for shortest pulse duration and highest average output power in the sub-100-fs regime. For this purpose, we studied the influence of critical laser parameters in one general cavity configuration, keeping the cavity design and the concave mirrors around the Kerr element constant. We investigated the mode locking performance for varying output coupling rate, intra-cavity dispersion, and hard aperture diameter. For each configuration, the pump power was set to the level delivering the minimum pulse duration in stable fundamental mode locking. At slightly higher pump power, a cw breakthrough was typically observed in the optical spectrum. In this way, stable mode locking was obtained for a large variety of laser parameters. The transverse beam quality M^2 was measured in several mode-locked configurations and was always below 1.05. Table 1 summarizes the mode-locked performance and laser parameters for a few representative configurations.

Table 1. Mode locking performance and laser parameters for the presented configurations with pulse durations of 35 fs, 49 fs and 88 fs.

Configuration	35 fs	49 fs	88 fs	Configuration	35 fs	49 fs	88 fs
Output power (W)	1.6	4.5	10.7	GDD per RT (fs ²)	-1000	-1100	-2200
Peak power (MW)	0.7	1.3	1.8	Hard aperture diameter (mm)	1.9	2.0	2.0
Pulse energy (μJ)	0.03	0.07	0.18	Repetition rate (MHz)	61	61	61
Central wavelength (nm)	1028.8	1031.5	1037.6	Output coupling rate (%)	0.9	2.7	4.6
FWHM bandwidth (nm)	33.9	24.1	14.4	Pump power (W)	76	96	186
Time bandwidth product	0.332	0.330	0.353	Opt.-to-opt. efficiency (%)	2.1	4.7	5.8

Figures 5(a) and 5(b) show the optical spectra and the gain at an inversion level of 0.3 for reference, as well as the intensity autocorrelation traces with the corresponding fit to the autocorrelation of a sech^2 function for the three configurations. The side peaks observed in the spectra of the short pulses carry only a minor fraction of the power and are associated with dispersive waves, similar to the sidebands observed in previous work [14,24]. Moreover, the output coupler transmission increases by more than a factor of two at the edges of the spectrum. The radio frequency spectrum and sampling oscilloscope trace of the shortest pulses are shown in Figs. 5(c) and 5(d). The 88-fs and 49-fs configurations achieve an average power of 10.7 and 4.5 W, respectively. The shortest pulse duration of 35 fs has been achieved at an output power of 1.6 W. For this pulse duration measurement, an extra-cavity dispersive mirror with negative group delay dispersion of -250 fs^2 was used to compensate for the material dispersion of the output coupler mirror and for the propagation in air. For all configurations, we confirmed fundamental single pulse mode-locked operation of the laser with a 180-ps long-range autocorrelation and a fast 18.5-ps photodiode in combination with a 40-GHz sampling oscilloscope as shown in Fig. 5(c).

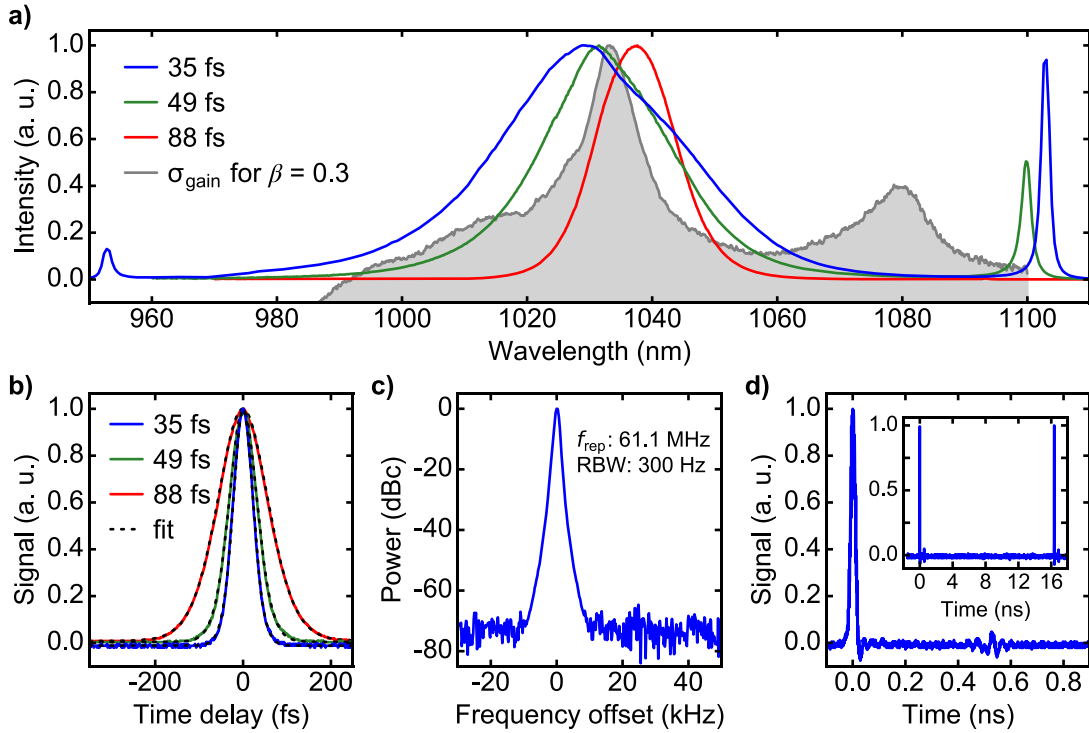


Fig. 5. (a) Optical spectra of the 35-fs, 49-fs and 88-fs laser configurations. The normalized gain cross section σ_{gain} of Yb:Lu₂O₃ for an inversion level β of 0.3 is shown for reference (data taken from [20]). (b) Intensity autocorrelation traces with fit to the autocorrelation of a sech². (c) Radio frequency spectrum of the 35-fs pulses measured with a resolution bandwidth RBW of 300 Hz. (d) Sampling oscilloscope trace in 1 ns and (inset) 20 ns for the 35-fs pulse train confirming the single pulse operation of the mode-locked laser. The weak ringing in the signal trace at 0.5 ns is an artefact due to the electronics of the detection setup.

This result demonstrates pulses 4 times shorter than previously achieved from a SESAM mode-locked Yb:Lu₂O₃ TDL [11] and 50% shorter than obtained in bulk geometry with the same gain material [24]. For reaching shorter pulse durations, we observed general trends in agreement with previous reported studies on mode-locking with fast saturable absorbers [17,29,30]. Operating at a moderate level of introduced negative dispersion of -1000 fs^2 up to -2000 fs^2 per roundtrip enabled shortest pulse durations. Pulses became unstable at lower GDD values, while for higher values, the minimum achievable pulse duration increased. Other critical parameters are output coupling rate and hard aperture diameter. To optimize pulse durations, it was important to reduce the output coupling rate while at the same time decreasing the aperture size. This allows maximizing the modulation depth of the self-amplitude

modulation, enabling stable mode-locking operation even in a regime with strong gain narrowing of the pulses. In this context, it should be noted that the optical bandwidth of the 35-fs pulses is almost 3 times broader than the FWHM of the emission cross section of the gain crystal.

2.2.4 Conclusion and outlook

We studied the minimum pulse durations achievable in soliton mode-locking with a TDL based on the broadband gain material Yb:Lu₂O₃ and KLM for various configurations of output coupling rate, intra-cavity dispersion, and hard aperture diameter. This work presents the shortest pulses and the highest power with sub-100-fs pulses directly emitted from a thin-disk laser oscillator. In order to reach shortest pulse durations, the total negative intra-cavity dispersion needs to be minimized and the modulation depth of the saturable absorber has to be maximized by selecting a low degree of output coupling and adapting the hard aperture diameter. The efficiency in mode-locked operation is currently below 10% but we expect that further optimization of the cavity design in combination with mode-locking parameters for lower non-saturable losses should enable higher values. Furthermore, in 2014, Brons *et al.* showed that scaling the intra-cavity peak power is feasible by enlarging the spot size on the Kerr medium [4], eventually leading to a significant increase of the output power of the laser. As a next step towards power scaling of sub-100-fs lasers, we will perform a similar study on an Yb:Lu₂O₃-based KLM oscillator. We expect that an increase of the spot size in the Kerr medium in combination with a larger pump area on the disk and multi-pass on the laser crystal will enable significantly higher output powers and pulse energies, making this source even more attractive for numerous experiments. Our work shows that Yb:Lu₂O₃ is one of the most promising gain materials for power-scaling of sub-100-fs TDL oscillators towards several hundred watts of output power.

Fundings

European Research Council (ERC) (starting grant 2001 #279545); National Center of Competence in Research for Molecular Ultrafast Science and Technology (NCCR-MUST); Swiss National Science Foundation (SNF) (200021-159931/1); Deutsche Forschungsgemeinschaft (DFG) (EXC 1074); German Federal Ministry of Education and Research (BMBF) (13N14192).

Acknowledgments

We thank Clara Saraceno (Ruhr-Universität Bochum, Germany), Florian Emaury, Andreas Diebold and Ursula Keller (ETH Zürich, Switzerland) for helpful discussions on ultrafast thin-disk laser technology.

References

1. J. A. der Au, G. J. Spühler, T. Südmeyer, R. Paschotta, R. Hövel, M. Moser, S. Erhard, M. Karszewski, A. Giesen, and U. Keller, "16.2-W average power from a diode-pumped femtosecond Yb:YAG thin disk laser," *Opt. Lett.* **25**(11), 859–861 (2000).
2. C. J. Saraceno, F. Emaury, C. Schriber, A. Diebold, M. Hoffmann, M. Golling, T. Südmeyer, and U. Keller, "Toward Millijoule-Level High-Power Ultrafast Thin-Disk Oscillators," *IEEE J. Sel. Top. Quantum Electron.* **21**(1), 106–123 (2015).
3. C. J. Saraceno, F. Emaury, O. H. Heckl, C. R. E. Baer, M. Hoffmann, C. Schriber, M. Golling, T. Südmeyer, and U. Keller, "275 W average output power from a femtosecond thin disk oscillator operated in a vacuum environment," *Opt. Express* **20**(21), 23535–23541 (2012).
4. J. Brons, V. Pervak, E. Fedulova, D. Bauer, D. Sutter, V. Kalashnikov, A. Apolonskiy, O. Pronin, and F. Krausz, "Energy scaling of Kerr-lens mode-locked thin-disk oscillators," *Opt. Lett.* **39**(22), 6442–6445 (2014).
5. C. J. Saraceno, F. Emaury, C. Schriber, M. Hoffmann, M. Golling, T. Südmeyer, and U. Keller, "Ultrafast thin-disk laser with 80 μ J pulse energy and 242 W of average power," *Opt. Lett.* **39**(1), 9–12 (2014).
6. T. Südmeyer, S. V. Marchese, S. Hashimoto, C. R. E. Baer, G. Gingras, B. Witzel, and U. Keller, "Femtosecond laser oscillators for high-field science," *Nat. Photonics* **2**(10), 599–604 (2008).
7. I. Pupeza, D. Sánchez, J. Zhang, N. Lilienfein, M. Seidel, N. Karpowicz, T. Paasch-Colberg, I. Znakovskaya, M. Pescher, W. Schweinberger, V. Pervak, E. Fill, O. Pronin, Z. Wei, F. Krausz, A. Apolonski, and J. Biegert, "High-power sub-two-cycle mid-infrared pulses at 100 MHz repetition rate," *Nat. Photonics* **9**(11), 721–724 (2015).
8. F. Emaury, A. Diebold, C. J. Saraceno, and U. Keller, "Compact extreme ultraviolet source at megahertz pulse repetition rate with a low-noise ultrafast thin-disk laser oscillator," *Optica* **2**(11), 980–984 (2015).
9. C. J. Saraceno, O. H. Heckl, C. R. E. Baer, C. Schriber, M. Golling, K. Beil, C. Kränkel, T. Südmeyer, G. Huber, and U. Keller, "Sub-100 femtosecond pulses from a SESAM modelocked thin disk laser," *Appl. Phys. B* **106**(3), 559–562 (2012).
10. A. Diebold, F. Emaury, C. Schriber, M. Golling, C. J. Saraceno, T. Südmeyer, and U. Keller, "SESAM mode-locked Yb:CaGdAlO₄ thin disk laser with 62 fs pulse generation," *Opt. Lett.* **38**(19), 3842–3845 (2013).
11. C. J. Saraceno, S. Pekarek, O. H. Heckl, C. R. E. Baer, C. Schriber, M. Golling, K. Beil, C. Kränkel, G. Huber, U. Keller, and T. Südmeyer, "Self-referenceable frequency comb from an ultrafast thin disk laser," *Opt. Express* **20**(9), 9650–9656 (2012).
12. S. Ricaud, A. Jaffres, K. Wentsch, A. Sukanuma, B. Viana, P. Loiseau, B. Weichelt, M. Abdou-Ahmed, A. Voss, T. Graf, D. Rytz, C. Hönninger, E. Mottay, P. Georges, and F. Druon, "Femtosecond Yb:CaGdAlO₄ thin-disk oscillator," *Opt. Lett.* **37**(19), 3984–3986 (2012).
13. C. Schriber, F. Emaury, A. Diebold, S. Link, M. Golling, K. Beil, C. Kränkel, C. J. Saraceno, T. Südmeyer, and U. Keller, "Dual-gain SESAM modelocked thin disk laser based on Yb:Lu₂O₃ and Yb:Sc₂O₃," *Opt. Express* **22**(16), 18979 (2014).

14. C. Schriber, L. Merceron, A. Diebold, F. Emaury, M. Golling, K. Beil, C. Kränkel, C. J. Saraceno, T. Südmeyer, and U. Keller, "Pushing SESAM modelocked thin-disk lasers to shortest pulse durations," in *Advanced Solid State Lasers* (Optical Society of America, 2014), paper AF1A.4.
15. J. Zhang, J. Brons, M. Seidel, V. Pervak, V. Kalashnikov, Z. Wei, A. Apolonski, F. Krausz, and O. Pronin, "49-fs Yb:YAG thin-disk oscillator with distributed Kerr-lens mode-locking," in *2015 European Conference on Lasers and Electro-Optics - European Quantum Electronics Conference* (Optical Society of America, 2015), paper PD_A_1.
16. B. Kreipe, J. Andrade, B. Deppe, C. Kränkel, and U. Morgner, "Kerr-lens mode-locked Yb³⁺:Lu₂O₃ thin-disk laser," in *Conference on Lasers and Electro-Optics* (Optical Society of America, 2016), paper SM1I.4.
17. J. Brons, V. Pervak, D. Bauer, D. Sutter, O. Pronin, and F. Krausz, "Powerful 100-fs-scale Kerr-lens mode-locked thin-disk oscillator," *Opt. Lett.* **41**(15), 3567 (2016).
18. U. Keller, K. J. Weingarten, F. X. Kärtner, D. Kopf, B. Braun, I. D. Jung, R. Fluck, C. Honninger, N. Matuschek, and J. Aus der Au, "Semiconductor saturable absorber mirrors (SESAM's) for femtosecond to nanosecond pulse generation in solid-state lasers," *IEEE J. Sel. Top. Quantum Electron.* **2**(3), 435–453 (1996).
19. O. Pronin, J. Brons, C. Grasse, V. Pervak, G. Boehm, M.-C. Amann, V. L. Kalashnikov, A. Apolonski, and F. Krausz, "High-power 200 fs Kerr-lens mode-locked Yb:YAG thin-disk oscillator," *Opt. Lett.* **36**(24), 4746–4748 (2011).
20. T. Südmeyer, C. Kränkel, C. R. E. Baer, O. H. Heckl, C. J. Saraceno, M. Golling, R. Peters, K. Petermann, G. Huber, and U. Keller, "High-power ultrafast thin disk laser oscillators and their potential for sub-100-femtosecond pulse generation," *Appl. Phys. B* **97**(2), 281–295 (2009).
21. M. Tokurakawa and A. Shirakawa, "Numerical analysis of fast saturable absorber mode-locked Yb³⁺ lasers under large modulation depth," *Opt. Express* **23**(20), 26288 (2015).
22. C. Kränkel, "Rare-Earth-Doped Sesquioxides for Diode-Pumped High-Power Lasers in the 1-, 2-, and 3- μm Spectral Range," *IEEE J. Sel. Top. Quantum Electron.* **21**(1), 250–262 (2015).
23. R. Peters, C. Kränkel, K. Petermann, and G. Huber, "Crystal growth by the heat exchanger method, spectroscopic characterization and laser operation of high-purity Yb:Lu₂O₃," *J. Cryst. Growth* **310**(7–9), 1934–1938 (2008).
24. M. Tokurakawa, A. Shirakawa, K. Ueda, R. Peters, S. T. Fredrich-Thornton, K. Petermann, and G. Huber, "Ultrashort pulse generation from diode pumped mode-locked Yb³⁺:sesquioxide single crystal lasers," *Opt. Express* **19**(4), 2904–2909 (2011).
25. C. R. E. Baer, C. Kränkel, C. J. Saraceno, O. H. Heckl, M. Golling, R. Peters, K. Petermann, T. Südmeyer, G. Huber, and U. Keller, "Femtosecond thin-disk laser with 141 W of average power," *Opt. Lett.* **35**(13), 2302 (2010).
26. U. Griebner, V. Petrov, K. Petermann, and V. Peters, "Passively mode-locked Yb:Lu₂O₃ laser," *Opt. Express* **12**(14), 3125 (2004).
27. S. V. Marchese, C. R. E. Baer, R. Peters, C. Kränkel, A. G. Engqvist, M. Golling, D. J. H. C. Maas, K. Petermann, T. Südmeyer, G. Huber, and U. Keller, "Efficient femtosecond high power Yb:Lu₂O₃ thin disk laser," *Opt. Express* **15**(25), 16966 (2007).
28. C. R. Baer, C. Kränkel, C. J. Saraceno, O. H. Heckl, M. Golling, T. Südmeyer, R. Peters, K. Petermann, G. Huber, and U. Keller, "Femtosecond Yb:Lu₂O₃ thin disk laser with 63 W of average power," *Opt. Lett.* **34**(18), 2823 (2009).
29. F. X. Kärtner, J. A. Der Au, and U. Keller, "Mode-locking with slow and fast saturable absorbers—what's the difference?," *IEEE J. Sel. Top. Quantum Electron.* **4**(2), 159–168 (1998).
30. H. A. Haus, "Mode-locking of lasers," *IEEE J. Sel. Top. Quantum Electron.* **6**(6), 1173–1185 (2000).

2.3 Sub-100-fs Kerr lens mode-locked Yb:Lu₂O₃ thin-disk laser oscillator operating at 21 W average power

Norbert Modsching,^{1,*} Jakub Drs, Julian Fischer, Clément Paradis,¹
François Labaye,¹ Maxim Gaponenko,¹ Christian Kränkel,² Valentin J. Wittwer,¹
and Thomas Südmeyer¹

¹Laboratoire Temps-Fréquence (LTF), Institut de Physique, Université de Neuchâtel, Avenue de Bellevaux 51, 2000 Neuchâtel, Switzerland

²Center for Laser Materials, Leibniz-Institut für Kristallzüchtung, Max-Born-Str. 2, 12489 Berlin, Germany

We investigate power-scaling of a Kerr lens mode-locked (KLM) Yb:Lu₂O₃ thin-disk laser (TDL) oscillator operating in the sub-100-fs pulse duration regime. Employing a scheme with higher round-trip gain by increasing the number of passes through the thin-disk gain element, we increase the average power by a factor of two and the optical-to-optical efficiency by a factor of almost three compared to our previous sub-100-fs mode-locking results. The oscillator generates pulses with a duration of 95 fs at 21.1 W average power and 47.9 MHz repetition rate. We discuss the cavity design for continuous-wave and mode-locked operation and the estimation of the focal length of the Kerr lens. Unlike to usual KLM TDL oscillators, an operation at the edge of the stability zone in continuous-wave operation is not required. This work shows that KLM TDL oscillators based on the gain material Yb:Lu₂O₃ are an excellent choice for power-scaling of laser oscillators in the sub-100-fs regime, and we expect that such lasers will soon operate at power levels in excess of hundred watts.

2.3.1 Introduction

High-power ultrafast laser systems operating at MHz repetition rates are a versatile tool for numerous applications in science and industry [1]. Compared to amplifiers, oscillators generate usually close to transform-limited pulses in fundamental TEM₀₀ mode operation without pre- or post-pulses and feature low noise levels, suitable for

carrier-envelope-offset frequency stabilization. However, the currently achieved power levels decrease strongly as function of the minimum achieved pulse duration. In the last decade, numerous studies have been targeting to increase the achievable power levels of ultrafast laser oscillators operating in the sub-100-fs regime [2–4]. Sub-100-fs bulk oscillators based on Ti:sapphire are currently limited to 3.5 W of average power [5] (Fig. 1). In comparison, sub-100-fs oscillators based on Yb-doped bulk gain materials operate at a reduced quantum defect, enabling up to 12.5 W of average power [6]. However, even in this case thermal effects in the bulk gain material are the most severe challenge for further increase of the average power.

The thin-disk geometry is advantageous for further power increase of sub-100-fs laser oscillators, because it reduces the thermal effects in the gain material during laser operation [7]. Various techniques have been applied for efficient mode-locking of thin-disk laser (TDL) oscillators, e.g. by saturable absorber mirrors (SESAMs) [8], nonlinear polarization rotation [9], nonlinear mirror mode-locking [10] and Kerr lens mode-locking [11]. Among those techniques, the shortest pulse duration of a TDL oscillator was achieved by Kerr lens mode-locking [12].

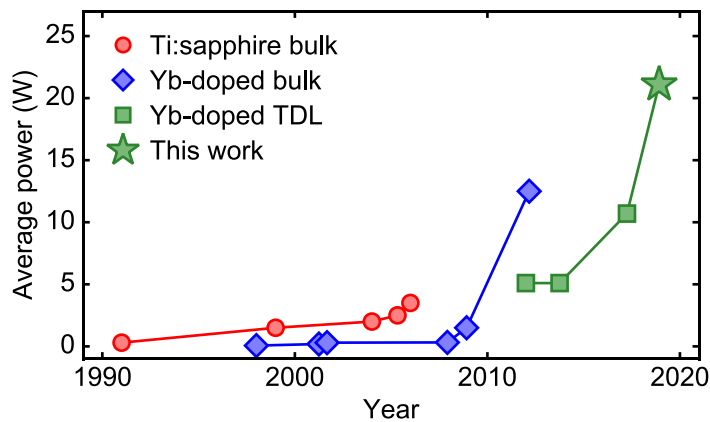


Fig. 1. Progress of the average power of ultrafast solid-state laser oscillators operating in the sub-100-fs pulse duration regime (Ti:sapphire [5,13], Yb-doped bulk [6,13–15], Yb-doped thin-disk laser (TDL) [16–18]).

In order to expand high-power operation of ultrafast TDL oscillators into the sub-100-fs regime [2], mode-locking of various broadband Yb-doped gain materials was investigated by several research groups [19–24]. The first TDL oscillators achieving sub-100-fs pulse durations were based on the broadband gain materials Yb:LuScO₃ and Yb:CALGO. Up to 5.1 W average power were demonstrated with an optical-to-

optical efficiency amounting to 11% [16,17] (Table 1). Although their distorted crystalline structure is beneficial for a broad gain bandwidth, the resulting reduced thermal conductivity as well as the crystal quality of the available disks are limiting factors for achieving higher average powers. Currently, the highest average power of any ultrafast TDL oscillator based on disordered gain materials is limited to 28 W with 300-fs pulses [24].

Table 1. Selection of state-of-the-art Yb-based sub-100-fs oscillators.^a

Type	Gain material	P_{ave}	τ_{pulse}	η_{eff}	Reference
Bulk	Yb:CALGO	12.5 W	94 fs	20%	[9]
Bulk	Yb:CALGO	3.3 W	45 fs	16%	[25]
TDL	Yb:LuScO ₃	5.1 W	96 fs	11%	[16]
TDL	Yb:CALGO	5.1 W	62 fs	7%	[17]
TDL	Yb:YAG	155 W	140 fs	29%	[26]
TDL	Yb:YAG	3.5 W	49 fs	3.5%	[27,28]
TDL	Yb:Lu ₂ O ₃	10.7 W	88 fs	5.8%	[18]
TDL	Yb:Lu ₂ O ₃	21.1 W	95 fs	16.2%	This work

^a P_{ave} : average power; τ_{pulse} : pulse duration; η_{eff} : optical-to-optical efficiency; TDL, thin-disk laser.

Ultrafast TDL oscillators based on the most mature gain material Yb:YAG have already reached average powers of 275 W, but operating at several hundred femtoseconds of pulse duration [29,30]. Kerr lens mode-locked (KLM) TDL oscillators demonstrated laser operation with 140-fs pulses at 155 W of average power and an optical-to-optical efficiency of 29% by fully exploiting the emission bandwidth of Yb:YAG [26]. Even shorter pulse durations of 49 fs were achieved by inserting nonlinear crystals for the generation of additional spectral components by self-phase modulation (SPM) in the cavity of a KLM Yb:YAG TDL oscillators. However, in this case the laser performance was limited to 3.5 W of average power at an optical-to-optical efficiency of 3.5% [27,28]. A gain material for high-power laser operation, which directly supports sub-100-fs pulse durations is Yb:Lu₂O₃. Yb:Lu₂O₃ provides a 60% broader emission bandwidth than Yb:YAG supporting the generation of 86-fs pulses at an even better thermal conductivity [2]. Although the gain material is still at an early stage of development, its suitability for high-power laser operation was already demonstrated by an ultrafast SESAM mode-locked TDL oscillator reaching 141 W of average power, albeit at pulse durations of several hundred femtoseconds [31]. In

2017, we demonstrated a KLM TDL oscillator fully exploiting the emission bandwidth of Yb:Lu₂O₃. The laser operated at 10.7 W of average power in 88-fs pulses with a modest optical-to-optical efficiency of 5.8% [18].

In this work, we investigate the impact of higher round-trip gain on the average power and the optical-to-optical efficiency of a sub-100-fs KLM Yb:Lu₂O₃ TDL oscillator. Folding the standing-wave cavity two times on the disk enabled an increase of the average output power by a factor of two and the optical-to-optical efficiency by a factor of three compared to our previous result [18]. We demonstrate that using this approach TDL oscillators based on the gain material Yb:Lu₂O₃ are suitable for the generation of sub-100-fs pulses at high average power with optical-to-optical efficiencies that are comparable to Yb-doped bulk oscillators (Table 1).

2.3.2 Cavity design

The performance of the Yb:Lu₂O₃ disk in continuous-wave (CW) operation and previous mode-locking results are published in [18]. Compared to these results, the presented cavity is modified by folding the standing-wave cavity a second time on the disk (Fig. 2). A second folding of the cavity on the disk is commonly used in high-power KLM TDL oscillators [26,30]. In this configuration, the gain propagation length of the laser beam per cavity round-trip amounts to the eightfold of the gain crystal thickness, resulting in a higher round-trip gain.

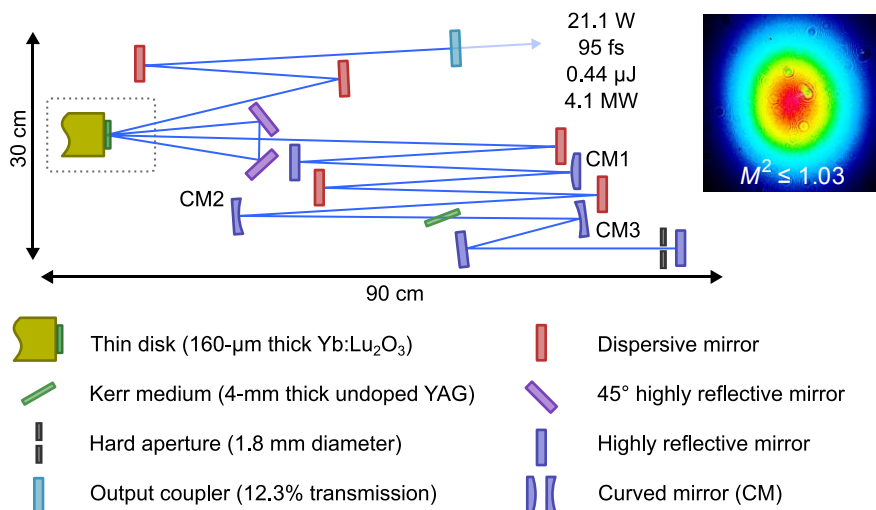


Fig. 2. Schematic of the Kerr lens mode-locked Yb:Lu₂O₃ thin-disk laser oscillator. (inset) Beam profile in mode-locked operation and M² beam quality factor. CM1, convex radius of curvature (ROC) of 2 m; CM2 and CM3, concave ROC of 250 mm.

Higher round-trip gain in the oscillator cavity enables laser operation at higher total cavity losses and, thus, the operation at a higher output coupler transmission (TOC). Considering a constant intracavity performance, an increase in the TOC should result in an increase of the output performance. However, higher round-trip gain also causes stronger gain narrowing which can reduce the spectral bandwidth and might prevent an exploitation of the gain bandwidth. The gain spectrum of Yb:Lu2O3 features a peak at a central wavelength of around 1033 nm with a full width at half maximum (FWHM) bandwidth of around 13 nm [Fig. 5(a)] [2,32]. Both parameters are nearly constant with the inversion level. Therefore, effects on the spectral gain properties for laser operation at a different inversion level can be neglected.

The mode radius in the cavity is calculated based on a formalism of ray transfer matrices for Gaussian beams (Fig. 3). We restrict the discussion to the sagittal plane which experiences a stronger Kerr lens due to the smaller beam radius in the Kerr medium (KM). The different mode radii in tangential and sagittal plane originate from the Brewster's angle under which the KM is placed. In mode-locked operation, the additional Kerr lens changes the mode radius compared to the CW operation.

The focal length of the Kerr lens (f_{KM}) is estimated for a given intracavity peak power by an iterative optimization routine. In the simplified model, f_{KM} is considered as a single lens in the center of the KM. In the routine, the cavity is calculated for an initially guessed focal length $f_{\text{KM,guess}}$. For a stable cavity, the mode radius in the KM (w_{KM}) is retrieved and a resulting averaged focal length of the lens in the Kerr medium ($f_{\text{KM,calc}}$) is calculated based on

$$f_{\text{KM,calc}}^{-1} = \frac{4n_2 d_{\text{KM,eff}}}{\pi w_{\text{KM}}^4} \cdot P_{\text{peak,IC}} \quad ,$$

where n_2 is the nonlinear refractive index of the KM, $d_{\text{KM,eff}}$ is the effective thickness of the KM under Brewster's angle, and $P_{\text{peak,IC}}$ is the intracavity peak power [33]. A stable solution for f_{KM} can be found by an iterative optimization routine minimizing the difference between $f_{\text{KM,guess}}$ and $f_{\text{KM,calc}}$ for a given intracavity peak power. Once a stable solution is found, it enables an estimation of the mode radius in mode-locked operation (Fig. 3). In the presented cavity are two design aspects considered. First, the mode radius has to decrease at the position of the hard aperture (HA) to form a fast

saturable absorber for self-amplitude modulation. Second, the mode radii at the position of the disk (DISK1, DISK2), have to increase for an optimized overlap with the pump spot. This increase affects the optical-to-optical efficiency and creates an additional soft-aperture self-amplitude modulation.

For efficient laser operation, the mode radius on the disk in mode-locked operation has to fit to the pump spot on the disk. An 80% overlap with the pump spot diameter of 2.8 mm was evaluated for highest optical-to-optical efficiency of the fundamental-mode in CW operation [18] (Fig. 3). The different mode radii on the disk originate from the concave 2.1 m radius of curvature of the disk. For improved overlap of both mode radii on the disk (DISK1, DISK2) the free space propagation distance between them (length b) was minimized, using two highly reflective mirrors optimized for 45° angle of incidence (Fig. 2). In contrast to our previous mode-locking results, a slightly elliptical beam profile is observed (inset of Fig. 2). We attributed the ellipticity to the larger angle of incidence on the disk of 9°.

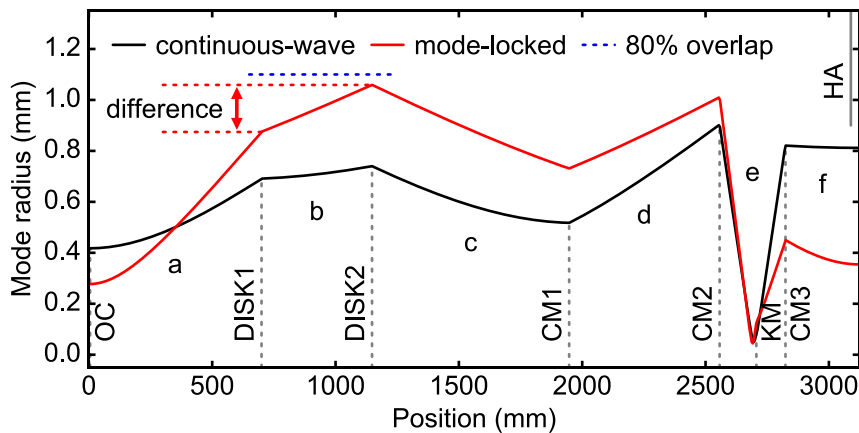


Fig. 3. Cavity design in continuous-wave and mode-locked operation shown for the sagittal plane. The mode radius is defined as the $1/e^2$ decay of the maximal intensity. In mode-locked operation the effect of the Kerr lens in the Kerr medium (KM) is estimated for an intracavity peak power of 33 MW. Gray dotted lines indicate the position of the cavity components. In mode-locked operation the mode radius on the disk (DISK1, DISK2) targets an 80% overlap with the pump spot (blue dotted). The different mode radii on the disk (red dotted) originate from the ROC of the disk. Cavity lengths in the simulation are a = 700 mm; b = 448 mm; c = 799 mm; d = 610 mm; e = 267mm; f = 300 mm. The distance between curved mirror CM2 and the KM is 149 mm. The hard aperture (HA, gray solid) is placed 30 mm before the cavity end mirror. In the experimental setup, the uncertainty of each length measurement towards the disk is ± 3 mm. The uncertainty of each length measurement between all other cavity components is ± 1 mm. OC, output coupler.

Unlike to usual KLM TDL oscillators [11,34], an operation at the edge of the stability zone in CW operation is not required. Typically, KLM TDL oscillators are first optimized for fundamental-mode CW laser operation in the center of the stability zone and adjusted mode radius on the disk. Then, a 4-f imaging section is introduced into the cavity via two curved mirrors to create an intracavity focus without influencing the behavior of the laser in CW operation. The Kerr medium is placed in the vicinity of the intracavity focus for the formation of the Kerr lens in mode-locked operation. By increasing the distance between the curved mirrors, the cavity is shifted towards the edge of the stability zone in CW operation to promote Kerr lens mode-locking. In contrast, our cavity design has not been optimized for CW operation. The curved mirrors CM2 and CM3 form an intracavity focus without serving the purpose of a 4-f imaging section leading to different cavity dynamics. This allows for tailoring the mode size on the disk by adjusting the length e between CM2 and CM3 (Fig. 4). During the experimental optimization of the mode-locking performance for highest average power at sub-100-fs pulse durations the length e , the position and thickness of the KM, the HA diameter, the TOC and the introduced group delay dispersion (GDD) were adapted.

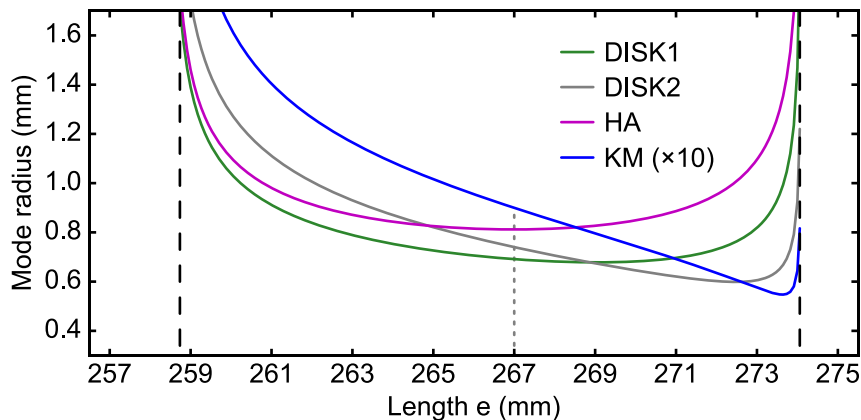


Fig. 4. Impact of the distance between the curved mirrors CM2 and CM3 in CW operation on the mode radii on the disk (DISK1; DISK2), in the Kerr medium (KM) and on the hard aperture (HA). Vertical black dashed lines indicate the edge of the stability zone for a stable cavity. The gray dotted line indicates the length e after the cavity optimization.

2.3.3 Performance in mode-locked operation

For mode-locked operation, -5400 fs^2 of GDD per cavity roundtrip are introduced by five dispersive mirrors (Fig. 2) at a TOC of 12.3%. A 4 mm thick undoped YAG plate

acts as KM and the diameter of the HA is 1.8 mm. The mode radii in the KM in CW operation were estimated by the cavity calculation to be $90 \mu\text{m} \times 165 \mu\text{m}$ in sagittal and tangential plane, respectively. The start-up of the mode-locked operation follows the same procedure utilized in our initial laser result [18]. In the presented configuration, the formation of a single soliton in the cavity is achieved by setting the pump power to 160 W and knocking on the laser table. Afterwards, the pump power is reduced to 130 W to suppress a CW breakthrough visible in the optical spectrum. As Kerr lens mode-locking features discrete stable solutions for the pulse formation, residual energy is often extracted by CW lasing.

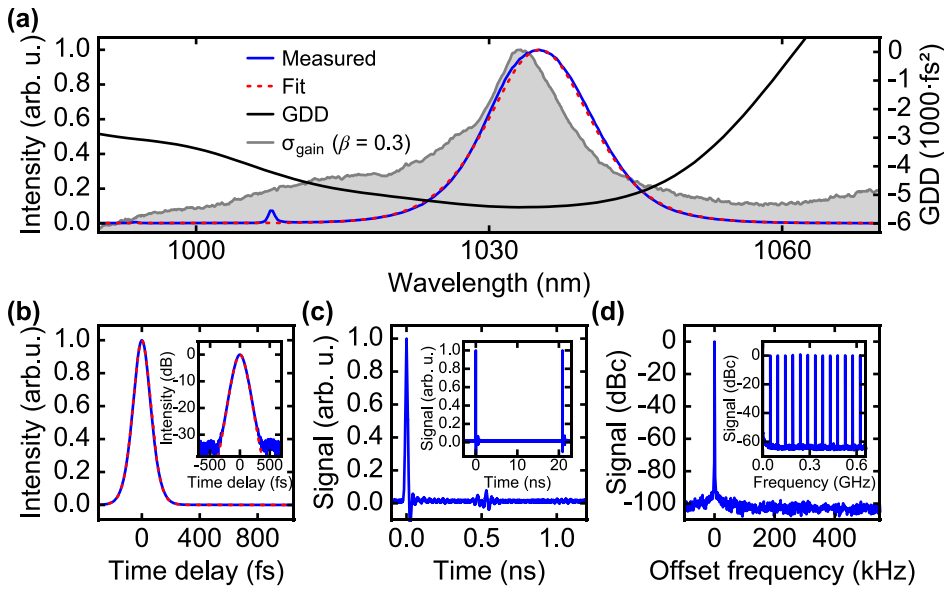


Fig. 5. (a) Optical spectrum of the laser output with sech^2 fit for soliton pulses, introduced group delay dispersion (GDD) per cavity roundtrip, and normalized gain cross-section of $\text{Yb:Lu}_2\text{O}_3$ for an inversion level β of 0.3 as reference (data taken from [2]). (b) Autocorrelation trace of the 95-fs pulses with sech^2 fit (measured in blue solid line and fit in red dotted line) in linear and (inset) logarithmic scale. (c) Sampling oscilloscope trace for 1 ns and (inset) 20 ns. (d) Radio-frequency spectrum of the fundamental repetition-rate frequency at 47.9 MHz and (inset) its harmonics at 100 Hz and 1 kHz resolution bandwidth, respectively.

In this configuration, the oscillator generates 95-fs pulses at an average output power of 21.1 W. The generated peak power is estimated to be 4.1 MW for soliton pulses at 0.44 μJ of pulse energy. The optical spectrum of the generated pulses [Fig. 5(a)] is centered at a wavelength of 1035.1 nm with a FWHM bandwidth of 12.3 nm. It is in good agreement with the sech^2 fit for soliton pulses. In comparison, the normalized spectrum of the gain cross-sections of $\text{Yb:Lu}_2\text{O}_3$ is plotted for an

inversion level β of 0.3. Compared to the gain cross-sections, the central wavelength of the optical spectrum is shifted by 2 nm towards longer wavelengths. The shift is a result of the reflectivity and dispersion of the cavity components.

The pulse duration of 95 fs is measured by intensity autocorrelation [Fig. 5(b)] and has an ideal sech² shape for soliton pulses down to the measurement noise floor of -32 dB. The time-bandwidth product of 0.325 is close to the transform limit and 1.04 times the ideal value for sech² pulses. Single pulse operation was proven by a 180-ps scan with the autocorrelator and by observing the pulse train with an 18.5-ps-rise-time photodetector on a 40-GHz sampling oscilloscope [Fig. 5(c)]. Fluctuations at 0.5 ns and 1.0 ns are electronic reflections. The radio-frequency spectrum measured at the fundamental repetition frequency of 47.9 MHz shows no side peaks down to the measurement noise floor of -100 dBc and modulation-free higher harmonics confirm clean mode-locking [Fig. 5(d)]. The beam quality factor M^2 was measured to be ≤ 1.03 . A summary of the parameters in mode-locked operation is given in Table 2.

For long-term operation, the pump power was slightly reduced to 126 W, decreasing the average power by 5% to 20.0 W. This suppressed a CW breakthrough that appeared during the warm-up of the system after several minutes. During a one-hour measurement in this condition, the average power and pulse duration showed no drift and fluctuated by less than 0.3% rms (Fig. 6).

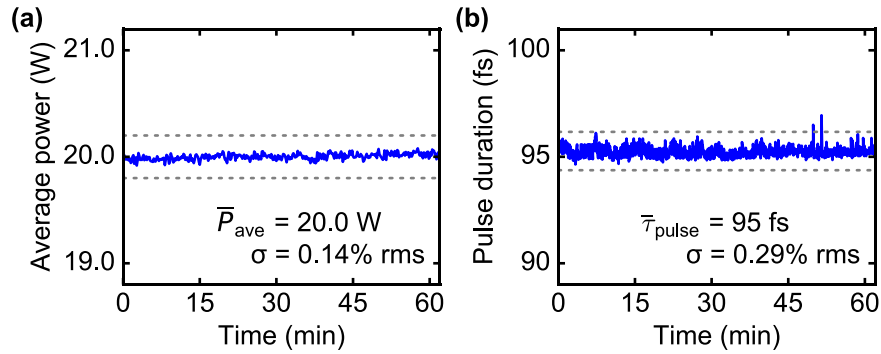


Fig. 6. (a) Average power and (b) pulse duration during a stability measurement of one hour. Corresponding averaged values are given with the root mean square (rms) error (σ). Gray dotted lines indicate the $\pm 1\%$ margins of the average value.

The performance of the oscillator is compared to previous mode-locking results achieved with folding the cavity once on the disk (Table 2) [18]. In both configurations, the mode size in the KM in CW operation and the pulse duration are similar.

Doubling the number of passes through the disk per cavity round-trip enabled an increase of the average output power by a factor of two. Optical-to-optical efficiency and output coupler transmission were increased by a factor of almost three to 16.2% and 12.3%, respectively. Although peak power and pulse energy increased, the corresponding intracavity values remained comparable. This observation agrees with the geometrical scaling law of KLM TDLs [27] which relates the achievable intracavity peak power to the mode size in the KM in CW operation. As consequence of a similar intracavity peak power ($P_{\text{peak,IC}} \approx 0.88 \cdot E_{\text{pulse,IC}} / \tau_{\text{FWHM}}$), the 26% decrease in intracavity average power can be attributed to the reduced repetition rate ($E_{\text{pulse,IC}} = P_{\text{ave}} / T_{\text{OC}} f_{\text{rep}}$). The two times larger amount of introduced GDD per round-trip compensates for the stronger SPM (γ_{SPM}) in the two times thicker YAG KM plate ($E_{\text{pulse,IC}} \approx 2 \cdot 1.76 \cdot |\text{GDD}| / \gamma_{\text{SPM}} \tau_{\text{FWHM}}$). The stronger SPM is required for the compensation of the gain narrowing caused by the increased T_{OC} to maintain the spectral bandwidth. The central wavelength is slightly shifted by 2 nm towards the gain peak in the cross sections of Yb:Lu₂O₃ at 1033 nm, which may contribute to the increased laser efficiency. We suggest that the different central wavelengths originate from the slightly different dispersion profiles of the dispersive mirrors used in both lasers.

Table 2. Summary of the mode-locking performance of the KLM Yb:Lu₂O₃ TDL oscillator for a single and double folding of the cavity on the disk.^a

	Single folding	Double folding	Comparison		Single folding	Double folding	Comparison
$w_{\text{KM,CW}}$	90 $\mu\text{m} \times$ 150 μm	90 $\mu\text{m} \times$ 165 μm	\approx	E_{pulse}	0.18 μJ	0.44 μJ	$2 \times \uparrow$
				$P_{\text{peak,IC}}$	39 MW	33 MW	\approx
τ_{FWHM}	88 fs	95 fs	\approx	$E_{\text{pulse,IC}}$	3.9 μJ	3.6 μJ	\approx
$N_{\text{Disk,RT}}$	4	8	$2 \times \uparrow$	$P_{\text{ave,IC}}$	233 W	172 W	26% \downarrow
P_{ave}	10.7 W	21.1 W	$2 \times \uparrow$	f_{rep}	61 MHz	47.9 MHz	21% \downarrow
η_{eff}	5.8%	16.2%	$3 \times \uparrow$	GDD _{RT}	-2200 fs ²	-5400 fs ²	$2 \times \uparrow$
T_{OC}	4.6%	12.3%	$3 \times \uparrow$	d_{KM}	2 mm	4 mm	$2 \times \uparrow$
P_{peak}	1.8 MW	4.1 MW	$2 \times \uparrow$	λ_{central}	1037.6 nm	1035.1 nm	

^a $w_{\text{KM,CW}}$: mode radius in the Kerr medium in continuous-wave operation; τ_{FWHM} : FWHM pulse duration;

N_{Disk} : number of passes through the disk per cavity round-trip; P_{ave} : average power; η_{eff} : optical-to-optical efficiency; T_{OC} : output coupler transmission; P_{peak} : peak power; E_{pulse} : pulse energy;

IC: intracavity; f_{rep} : repetition rate; GDD_{RT}: introduced group delay dispersion per cavity round-trip; d_{KM} : thickness of the Kerr medium; λ_{central} : central wavelength; \approx : comparable; \uparrow : increase; \downarrow : decrease.

2.3.4 Conclusion and outlook

We demonstrated a KLM Yb:Lu₂O₃ TDL oscillator generating 95-fs pulses at 21.1 W average power. By folding the cavity two times on the disk, the average power was increased by a factor of two with an almost three times higher optical-to-optical efficiency of 16.2%, compared to our previous result [18]. We showed that KLM TDL oscillators based on the gain material Yb:Lu₂O₃ are suitable for the generation of sub-100-fs pulses at high average power with optical-to-optical efficiencies that are comparable to Yb-doped bulk oscillators. The presented TDL oscillator has been used as single-stage driving laser for broadband THz generation via optical rectification in GaP [35]. In this case, high-power laser operation with sub-100-fs pulse duration was beneficial for the generated THz spectral bandwidth that expanded up to 5 THz at 0.3 mW of THz average power.

The average power of SESAM mode-locked Yb:Lu₂O₃ TDL oscillators was scaled from initially 20 W up to 141 W [31,36]. We anticipate that similar power-scaling should be feasible for sub-100-fs KLM Yb:Lu₂O₃ TDL oscillators. We expect that further power-scaling of sub-100-fs KLM Yb:Lu₂O₃ TDL oscillators can be achieved by scaling the intracavity peak power via adapting the mode size in the Kerr medium [30], enlarging the pump spot diameter on the disk [7] and by further increasing the number of passes through the disk. By this, we anticipate that sub-100-fs KLM Yb:Lu₂O₃ TDL oscillators operating at more than hundred watt of average power are within reach.

Funding

Swiss National Science Foundation (SNSF) (179146, 170772, 144970); German Ministry of Education and Research (BMBF) (13N14192).

Acknowledgements

The authors thank Olga Razskazovskaya (Université de Neuchâtel, Switzerland) for the fabrication of optical coatings and helpful discussions.

References

1. D. T. Reid, C. M. Heyl, R. R. Thomson, R. Trebino, G. Steinmeyer, H. H. Fielding, R. Holzwarth, Z. Zhang, P. Del'Haye, T. Südmeyer, G. Mourou, T. Tajima, D. Faccio, F. J. M. Harren, and G. Cerullo, "Roadmap on ultrafast optics," *J. Opt.* **18**(9), 093006 (2016).

2. T. Südmeyer, C. Kränkel, C. R. E. Baer, O. H. Heckl, C. J. Saraceno, M. Golling, R. Peters, K. Petermann, G. Huber, and U. Keller, "High-power ultrafast thin disk laser oscillators and their potential for sub-100-femtosecond pulse generation," *Appl. Phys. B* **97**(2), 281–295 (2009).
3. H. Zhao and A. Major, "Megawatt peak power level sub-100 fs Yb:KGW oscillators," *Opt. Express* **22**(25), 30425 (2014).
4. U. Keller, "Ultrafast solid-state laser oscillators: a success story for the last 20 years with no end in sight," *Appl. Phys. B* **100**(1), 15–28 (2010).
5. S. Dewald, T. Lang, C. D. Schröter, R. Moshhammer, J. Ullrich, M. Siegel, and U. Morgner, "Ionization of noble gases with pulses directly from a laser oscillator," *Opt. Lett.* **31**(13), 2072–2074 (2006).
6. A. Greborio, A. Guandalini, and J. Aus der Au, "Sub-100 fs pulses with 12.5-W from Yb:CALGO based oscillators," in *Proc. SPIE*, (2012), paper 823511.
7. A. Giesen, H. Hügel, A. Voss, K. Wittig, U. Brauch, and H. Opower, "Scalable concept for diode-pumped high-power solid-state lasers," *Appl. Phys. B Lasers Opt.* **58**(5), 365–372 (1994).
8. J. A. der Au, G. J. Spühler, T. Südmeyer, R. Paschotta, R. Hövel, M. Moser, S. Erhard, M. Karszewski, A. Giesen, and U. Keller, "16.2-W average power from a diode-pumped femtosecond Yb:YAG thin disk laser," *Opt. Lett.* **25**(11), 859–861 (2000).
9. B. Borchers, C. Schäfer, C. Fries, M. Larionov, and R. Knappe, "Nonlinear polarization rotation mode-locking via phase-mismatched type I SHG of a thin disk femtosecond laser," in *Advanced Solid State Lasers* (Optical Society of America, 2015), paper AT4A.9.
10. F. Saltarelli, A. Diebold, I. J. Graumann, C. R. Phillips, and U. Keller, "Modelocking of a thin-disk laser with the frequency-doubling nonlinear-mirror technique," *Opt. Express* **25**(19), 23254 (2017).
11. O. Pronin, J. Brons, C. Grasse, V. Pervak, G. Boehm, M.-C. Amann, V. L. Kalashnikov, A. Apolonski, and F. Krausz, "High-power 200 fs Kerr-lens mode-locked Yb:YAG thin-disk oscillator," *Opt. Lett.* **36**(24), 4746–4748 (2011).
12. N. Modsching, C. Paradis, F. Labaye, M. Gaponenko, I. J. Graumann, A. Diebold, F. Emaury, V. J. Wittwer, and T. Südmeyer, "Kerr lens mode-locked Yb:CALGO thin-disk laser," *Opt. Lett.* **43**(4), 879–882 (2018).
13. U. Keller, *Ultrafast Solid-State Lasers*, Landolt-Börnstein. Laser Physics and Applications. Subvolume B: Laser Systems. Part I (Springer, 2007).
14. M. Tokurakawa, A. Shirakawa, K. Ueda, H. Yagi, S. Hosokawa, T. Yanagitani, and A. A. Kaminskii, "Diode-pumped 65 fs Kerr-lens mode-locked Yb³⁺:Lu₂O₃ and nondoped Y₂O₃ combined ceramic laser," *Opt. Lett.* **33**(12), 1380–1382 (2008).
15. M. Tokurakawa, A. Shirakawa, K. Ueda, H. Yagi, M. Noriyuki, T. Yanagitani, and A. A. Kaminskii, "Diode-pumped ultrashort-pulse generation based on Yb³⁺:Sc₂O₃ and Yb³⁺:Y₂O₃ ceramic multi-gain-media oscillator," *Opt. Express* **17**(5), 3353–3361 (2009).
16. C. J. Saraceno, O. H. Heckl, C. R. E. Baer, C. Schriber, M. Golling, K. Beil, C. Kränkel, T. Südmeyer, G. Huber, and U. Keller, "Sub-100 femtosecond pulses from a SESAM modelocked thin disk laser," *Appl. Phys. B* **106**(3), 559–562 (2012).
17. A. Diebold, F. Emaury, C. Schriber, M. Golling, C. J. Saraceno, T. Südmeyer, and U. Keller, "SESAM mode-locked Yb:CaGdAlO₄ thin disk laser with 62 fs pulse generation," *Opt. Lett.* **38**(19), 3842–3845 (2013).
18. C. Paradis, N. Modsching, V. J. Wittwer, B. Deppe, C. Kränkel, and T. Südmeyer, "Generation of 35-fs pulses from a Kerr lens mode-locked Yb:Lu₂O₃ thin-disk laser," *Opt. Express* **25**(13), 14918–14925 (2017).
19. C. R. E. Baer, C. Kränkel, O. H. Heckl, M. Golling, T. Südmeyer, R. Peters, K. Petermann, G. Huber, and U. Keller, "227-fs pulses from a mode-locked Yb:LuScO₃ thin disk laser," *Opt. Express* **17**(13), 10725 (2009).

20. G. Palmer, M. Schultze, M. Siegel, M. Emons, U. Bunting, and U. Morgner, "Passively mode-locked Yb:KLu(WO₄)₂ thin-disk oscillator operated in the positive and negative dispersion regime," *Opt. Lett.* **33**(14), 1608 (2008).
21. F. Brunner, T. Südmeyer, E. Innerhofer, F. Morier-Genoud, R. Paschotta, V. E. Kisel, V. G. Shcherbitsky, N. V. Kuleshov, J. Gao, K. Contag, A. Giesen, and U. Keller, "240-fs pulses with 22-W average power from a mode-locked thin-disk Yb:KY(WO₄)₂ laser," *Opt. Lett.* **27**(13), 1162 (2002).
22. O. H. Heckl, C. Kränkel, C. R. E. Baer, C. J. Saraceno, T. Südmeyer, K. Petermann, G. Huber, and U. Keller, "Continuous-wave and modelocked Yb:YCOB thin disk laser: first demonstration and future prospects," *Opt. Express* **18**(18), 19201 (2010).
23. C. J. Saraceno, O. H. Heckl, C. R. E. Baer, M. Golling, T. Südmeyer, K. Beil, C. Kränkel, K. Petermann, G. Huber, and U. Keller, "CW and Modelocked Operation of an Yb:(Sc,Y,Lu)₂O₃ Thin-disk Laser," in *CLEO:2011 - Laser Applications to Photonic Applications* (Optical Society of America, 2011), paper CWP1.
24. S. Ricaud, A. Jaffres, K. Wentsch, A. Suganuma, B. Viana, P. Loiseau, B. Weichelt, M. Abdou-Ahmed, A. Voss, T. Graf, D. Rytz, C. Hönninger, E. Mottay, P. Georges, and F. Druon, "Femtosecond Yb:CaGdAlO₄ thin-disk oscillator," *Opt. Lett.* **37**(19), 3984–3986 (2012).
25. S. Manjooran and A. Major, "Diode-pumped 45 fs Yb:CALGO laser oscillator with 1.7 MW of peak power," *Opt. Lett.* **43**(10), 2324 (2018).
26. J. Brons, V. Pervak, D. Bauer, D. Sutter, O. Pronin, and F. Krausz, "Powerful 100-fs-scale Kerr-lens mode-locked thin-disk oscillator," *Opt. Lett.* **41**(15), 3567–3570 (2016).
27. J. Zhang, J. Brons, M. Seidel, V. Pervak, V. Kalashnikov, Z. Wei, A. Apolonski, F. Krausz, and O. Pronin, "49-fs Yb:YAG thin-disk oscillator with distributed Kerr-lens mode-locking," in *European Quantum Electronics Conference* (Optical Society of America, 2015), paper PD_A_1.
28. J. Brons, "High-power femtosecond laser-oscillators for applications in high-field physics," Dissertation, Ludwig-Maximilians-Universität München (2017).
29. C. J. Saraceno, F. Emaury, O. H. Heckl, C. R. E. Baer, M. Hoffmann, C. Schriber, M. Golling, T. Südmeyer, and U. Keller, "275 W average output power from a femtosecond thin disk oscillator operated in a vacuum environment," *Opt. Express* **20**(21), 23535–23541 (2012).
30. J. Brons, V. Pervak, E. Fedulova, D. Bauer, D. Sutter, V. Kalashnikov, A. Apolonskiy, O. Pronin, and F. Krausz, "Energy scaling of Kerr-lens mode-locked thin-disk oscillators," *Opt. Lett.* **39**(22), 6442–6445 (2014).
31. C. R. E. Baer, C. Kränkel, C. J. Saraceno, O. H. Heckl, M. Golling, R. Peters, K. Petermann, T. Südmeyer, G. Huber, and U. Keller, "Femtosecond thin-disk laser with 141 W of average power," *Opt. Lett.* **35**(13), 2302 (2010).
32. C. Kränkel, "Rare-earth-doped sesquioxides for diode-pumped high-power lasers in the 1-, 2-, and 3- μ m spectral range," *IEEE J. Sel. Top. Quantum Electron.* **21**(1), 250–262 (2015).
33. S. Yefet and A. Pe'er, "A Review of Cavity Design for Kerr Lens Mode-Locked Solid-State Lasers," *Appl. Sci.* **3**(4), 1–31 (2015).
34. J. Brons, O. Pronin, M. Seidel, V. Pervak, D. Bauer, D. Sutter, V. L. Kalashnikov, A. Apolonski, and F. Krausz, "120 W, 4 μ J from a purely Kerr-lens mode-locked Yb:YAG thin-disk oscillator," in *Advanced Solid-State Lasers Congress* (Advanced Solid-State Lasers Congress, G. Huber and P. Moulton, eds., OSA Technical Digest (online), 2013), paper AF3A.4.
35. J. Drs, N. Modsching, C. Paradis, C. Kränkel, V. Wittwer, O. Razskazovskaya, and T. Südmeyer, "Optical rectification of ultrafast Yb-lasers: Pushing power and bandwidth of THz generation in GaP," *JOSA B* **submitted** (2019).
36. S. V. Marchese, C. R. E. Baer, R. Peters, C. Kränkel, A. G. Engqvist, M. Golling, D. J. H. C. Maas, K. Petermann, T. Südmeyer, G. Huber, and U. Keller, "Efficient femtosecond high power Yb:Lu₂O₃ thin disk laser," *Opt. Express* **15**(25), 16966 (2007).

2.4 Kerr lens mode-locked Yb:CALGO thin-disk laser

Norbert Modsching,^{1,*} Clément Paradis,¹ François Labaye,¹ Maxim Gaponenko,¹
Ivan J. Graumann,² Andreas Diebold,² Florian Emaury,² Valentin J. Wittwer,¹ and
Thomas Südmeyer¹

¹*Laboratoire Temps-Fréquence, Institut de Physique, Université de Neuchâtel, Avenue de
Bellevoaux 51, 2000 Neuchâtel, Switzerland*

²*Ultrafast Laser Physics, Institute for Quantum Electronics, ETH Zurich, 8093 Zurich,
Switzerland*

We demonstrate the first Kerr lens mode-locked Yb:CaGdAlO₄ (Yb:CALGO) thin-disk laser oscillator. It generates pulses with a duration of 30 fs at a central wavelength of 1048 nm and a repetition rate of 124 MHz. The laser emits the shortest pulses generated by a thin-disk laser oscillator, equal to the shortest pulse duration obtained by Yb-doped bulk oscillators. The average output power is currently limited to 150 mW by the low gain and limited disk quality. We expect that more suitable Yb:CALGO disks will enable substantially higher power levels with similar pulse durations.

2.4.1 Introduction

High-harmonic generation based on Yb-doped ultrafast thin-disk laser (TDL) oscillators is a simple amplification-free approach to produce coherent extreme ultraviolet (XUV) light at megahertz repetition rates [1,2]. In the current systems, the long pulses produced by the oscillator (250–900 fs duration) either require external pulse compression or severely limit the XUV photon flux and photon energies. This motivates extending the record performance of mode-locked TDLs to the sub-100-fs regime as well as reaching new pulse duration limits.

The TDL geometry [3] enabled ultrafast oscillators to generate record-high average output powers of 275 W [4]. Mounting the thin-disk crystal onto a backside-cooled heat sink allows for an efficient heat removal. High nonlinearities and thermal effects in the gain crystal are efficiently reduced thanks to its thin thickness of 100–300 μm used with millimeter- to centimeter-size beam diameters. The total intracavity nonlinearity can thus be adjusted independently from the gain crystal. However, TDL

oscillators demonstrated longer pulses than in the bulk configuration (Fig. 1). Yb-doped bulk oscillators already generated pulses as short as 30 fs, but only at average output powers <100 mW [5,6]. Thermal effects and excessive nonlinearities in the gain crystal are severe challenges for a significant average power increase.

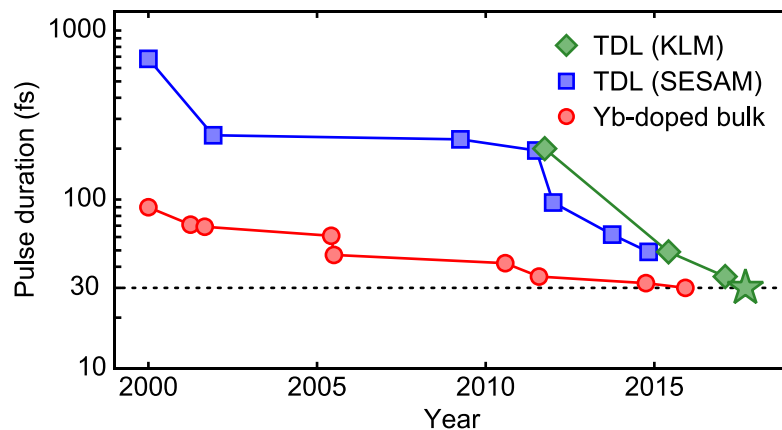


Fig. 1. Evolution of the shortest pulse duration generated by ultrafast Yb-doped bulk and thin-disk laser oscillators [4-12]. The presented result is highlighted with a green star symbol.

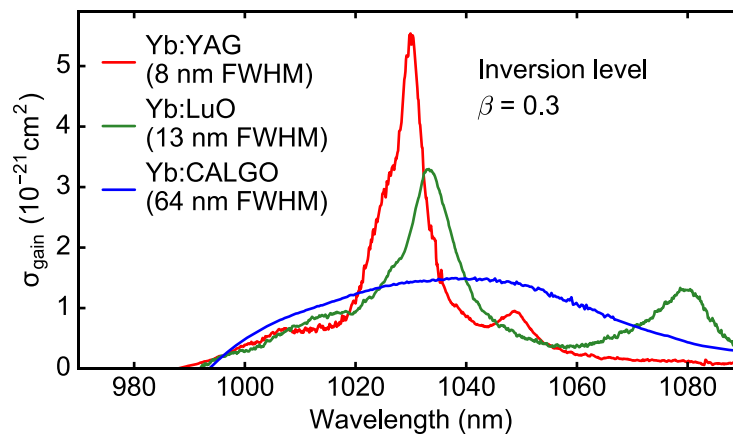


Fig. 2. Calculated gain cross sections (inversion level $\beta = 0.3$) of the Yb-doped laser crystals YAG, LuO, and CALGO (σ -polarization). The corresponding FWHM gain bandwidths are given in parentheses. Data taken from Refs. [17,18].

Initially, mode-locked TDLs relied on semiconductor saturable absorber mirrors (SESAMs, [13]). The availability of TDL crystals with broader gain emission bandwidths [14] allowed reducing the pulse duration of TDLs from initially 680 fs [4] to 49 fs, which has been delivered at 2 W average output power [9]. On the other hand,

Kerr lens mode-locking is advantageous for generating short pulses because it provides an instantaneous response and a high modulation depth [15]. However, the Kerr lens mode-locked (KLM) resonator design is challenging because it typically requires operation close to a stability edge for continuous-wave (cw) operation. Prior to this work, stable pulsed operation of KLM TDLs has only been demonstrated for the gain materials Yb:YAG [10] and Yb:Lu₂O₃ (Yb:LuO) [16]. Despite the limited gain bandwidth of Yb:YAG, 49-fs pulses have been demonstrated at 3.5 W output power [11]. Yb:LuO features a 30% broader gain bandwidth (Fig. 2), which enabled the recent demonstration 35-fs pulses at 1.6 W from a KLM TDL [12]. Combining broadband Yb-based gain materials with the Kerr lens mode-locking scheme is therefore a promising approach towards TDLs generating even shorter pulse durations.

Table 1. Overview of the State-of-the-Art Performance of Ultrafast Yb:CALGO Bulk and Thin-Disk Laser (TDL) Oscillators ^a

Geometry	ML	τ	P_{out}	Reference
Bulk	SESAM	94 fs	12.5 W	[21]
Bulk	KLM	37 fs	1.5 W	[6]
Bulk	KLM	32 fs	90 mW	[6]
TDL	SESAM	300 fs	28 W	[22]
TDL	SESAM	49 fs	2 W	[9]
TDL	KLM	30 fs	150 mW	this work

^a ML, mode-locking scheme; τ , pulse duration; P_{out} , average output power.

Yb:CALGO offers a nearly flat and broad gain profile due to its disordered crystalline structure. Its full width at half maximum (FWHM) bandwidth in the σ -polarization exceeds 60 nm at 30% inversion level, being eight times larger than that of Yb:YAG (Fig. 2). The thermal conductivity of Yb:CALGO of $6.3 \text{ Wm}^{-1} \text{ K}^{-1}$ is comparably good with respect to other broadband gain materials [19]. An overview of the state-of-the-art performance of ultrafast Yb:CALGO oscillators in the bulk and thin-disk geometry is given in Table 1. A previous attempt of Kerr lens mode-locking an Yb:CALGO TDL has been reported, but stable pulse operation was not demonstrated [22]. In this Letter, we present, to the best of our knowledge, the first Kerr lens mode-locked Yb:CALGO TDL. The laser achieves 30-fs pulses, which are the shortest pulses generated by ultrafast TDLs and equal to the shortest pulses demonstrated by Yb-doped bulk oscillators.

2.4.2 Disk characterization in continuous-wave operation

The laser is based on a wedged, 150- μm -thick Yb(~ 3.8 at. %):CALGO disk with a c-cut crystal orientation (FEE GmbH). The disk has a diameter of 9.3 mm and a concave radius of curvature of 2 m. It is contacted on a diamond heat sink (Trumpf GmbH) and pumped at 979 nm by a fiber-coupled narrow-bandwidth (<1 nm FWHM) diode-laser system. The pump light passes 36 times through the disk to achieve high pump absorption. The pump spot was set to a diameter of 2 mm. Initial tests in transverse multi-mode (MM) and fundamental-mode (FM) cw operation have been performed in a simple V-cavity [Figs. 3(a) and 3(b)].

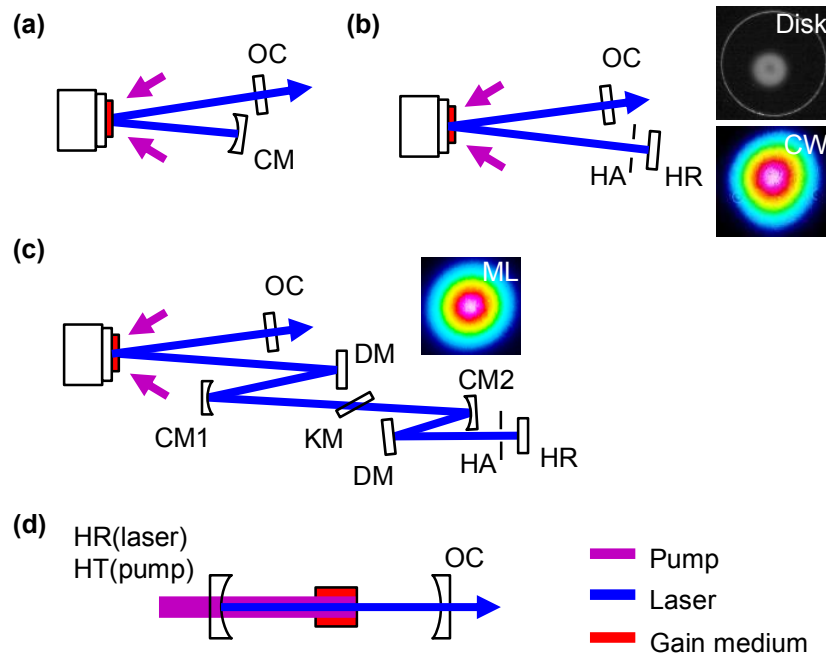


Fig. 3. Schematics of the Yb:CALGO thin-disk laser (TDL) in (a) continuous-wave (cw) transverse multi-mode and (b) fundamental-mode (FM) operation. Inset: pictures of the disk with pump spot (top) and corresponding output beam profile (bottom) in FM operation. The darker area in the center of the pump spot is depleted by the laser. (c) Yb:CALGO TDL cavity with inset of the beam profile in mode-locked (ML) operation. (d) Schematic of a standard endpumping configuration of bulk oscillators. CM, curved mirror; DM, dispersive mirror; HA, hard aperture; HR, highly reflective; HT, highly transmissive; KM, Kerr medium; OC, output coupler.

The overlap ratio between the FM size on the disk and the pump spot size has been set to 0.4 for highly MM behavior. The extracted power depended strongly on the position on the disk, which indicates inhomogeneities in the crystalline structure. An

average output power of 60 W was emitted with 30% optical-to-optical and 37% slope efficiency at 0.8% output coupler transmission (Fig. 4). Increasing the output coupler transmission to 2.7% decreased the optical-to-optical efficiency, which dropped to 6.1% with a slope efficiency of 11%. This indicates a strong limitation of the tolerable total cavity losses for efficient laser operation, which results from the combination of low doping concentration and thin disk thickness.

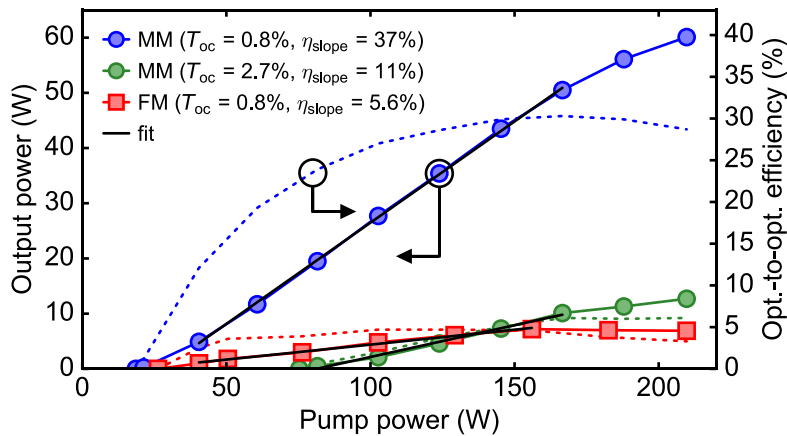


Fig. 4. Continuous-wave performance. Average output power (markers) and corresponding optical-to-optical efficiency (dashed line) of the disk in multi-mode (MM) and fundamental-mode (FM) operation for different output coupler transmissions (T_{oc}). Black solid lines are the linear fits for the calculation of the slope efficiencies (η_{slope}).

Increasing the overlap ratio between the fundamental laser mode and the pump spot to $\geq 80\%$ did not lead to FM operation as it is usually expected for TDLs. Transverse FM operation ($M^2 < 1.05$) was only achieved when inserting a hard aperture in the cavity to suppress the onset of higher-order modes. Only a small area of the pump spot gets efficiently extracted, as shown in Fig. 3(b). For an overlap ratio of 60% and a 1.8-mm hard-aperture diameter, the laser delivered up to 7 W average power with 4.6% optical-to-optical efficiency and 5.6% slope efficiency at an output coupler transmission of 0.8%. The cw performance of this particular disk is comparably poor in terms of average output power [22,23], efficiency [24], and gain [25]. The decrease of the optical-to-optical efficiency and clamping of the average output power for pump powers higher than 150 W indicates thermal effects of the disk, which was pumped up to a power density of 6.5 kW/cm². The strong drop of the laser performance from MM to FM cw operation can therefore be attributed to a low disk quality. The losses from the hard aperture and the small overlap ratio contribute largely to the low efficiency

observed in FM operation. Due to the difficulties to operate the laser in the FM, multiple bounces on the disk were not considered.

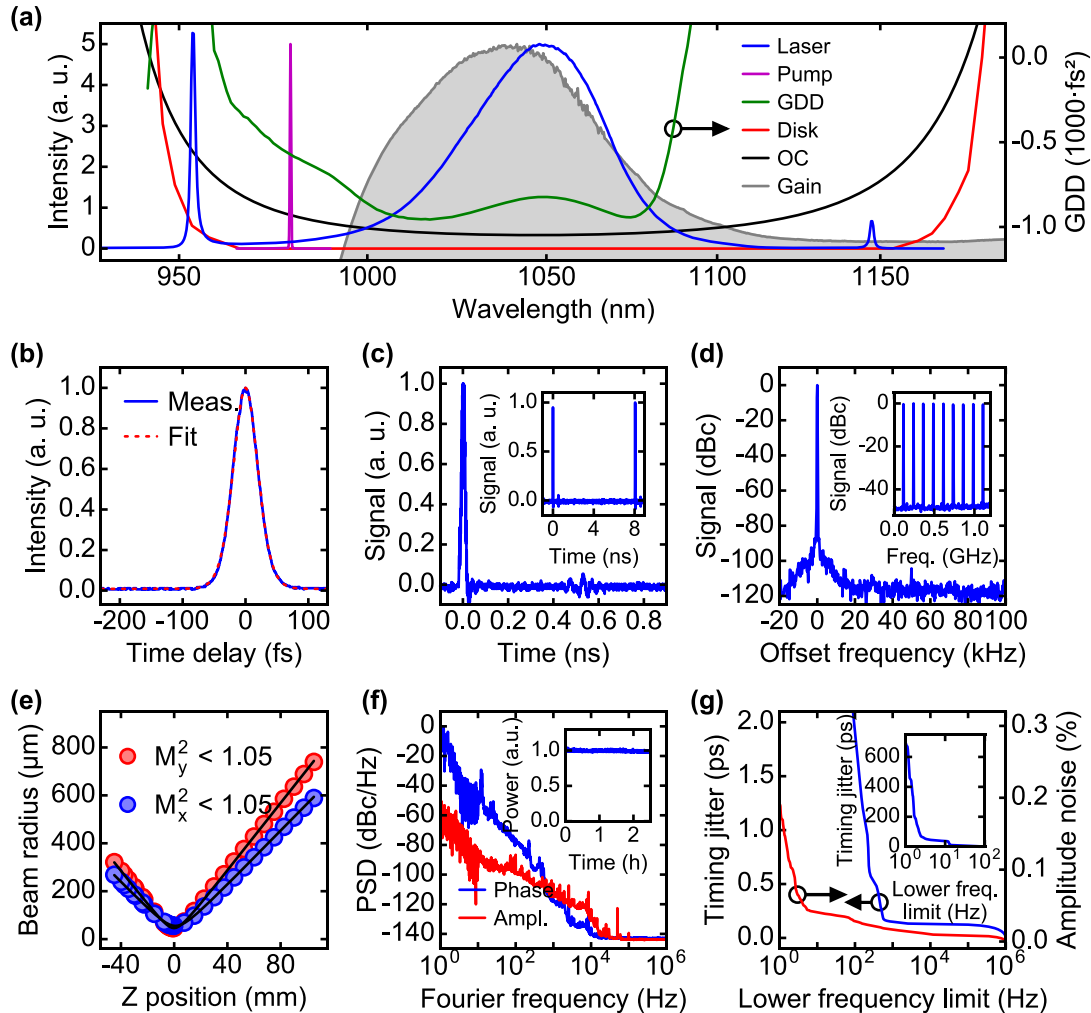


Fig. 5. Characterization of the KLM Yb:CALGO TDL. (a) Normalized optical spectrum of the pump and laser output, gain cross section for an inversion level of $\beta = 0.3$ chosen for reference, transmission (left y-axis, $5.0 \pm 5.0\%$) of the highly reflective disk coating and of the output coupler (OC), introduced group delay dispersion (GDD) of the dispersive mirrors per cavity round trip (right y-axis); (b) autocorrelation trace of the 30-fs pulses and sech^2 fit; (c) 1-ns and (inset) 10-ns sampling oscilloscope trace; (d) radio-frequency (RF) spectrum of the laser fundamental repetition-rate frequency measured with a 300-Hz resolution bandwidth (RBW); inset: RF spectrum of the higher harmonics with a 100-kHz RBW; (e) beam quality factor M^2 ; (f) phase and amplitude noise power spectral densities measured at the fundamental repetition frequency of 124 MHz; inset: normalized average output power logged over 2.5 h; (g) rms timing jitter and rms amplitude noise integrated up to 1 MHz as a function of the lower cut-off frequency; inset: rms timing jitter in different scales.

2.4.3 Setup and performance in mode-locked operation

For mode-locking experiments, the FM cavity was extended with two curved mirrors (CM1 and CM2) with a concave radius of curvature of 250 mm [Fig. 3(c)]. A 4 mm-thick undoped YAG plate placed under Brewster's angle between CM1 and CM2 serves as Kerr medium (KM) for the mode-locking mechanism. The beam radii inside the KM are estimated to be $80\ \mu\text{m} \times 140\ \mu\text{m}$ in the tangential and sagittal planes, respectively, during cw operation. The plate induces self-phase modulation (SPM) and forces the laser to operate in linear polarization. A water-cooled intracavity pinhole with an aperture diameter of 1.6 mm placed in front of an end mirror serves as hard aperture for Kerr lens mode-locking, while the second end mirror is an output coupler with a transmission of 0.3%. Two dispersive mirrors introduce a group delay dispersion (GDD) of $-900\ \text{fs}^2$ per round trip. The corresponding spectral profile is shown in Fig. 5(a). They have been designed to support a broad spectral bandwidth and were grown using our ion-beam-sputtering coating machine. Mode-locking is initiated by shifting the position of CM2. Then, the pump power is adjusted to suppress parasitic cw lasing. The oscillator footprint is $90\ \text{cm} \times 30\ \text{cm}$.

The laser generates pulses with a temporal width of 30 fs FWHM as shown by the autocorrelation trace in Fig. 5(b). We introduced $-440\ \text{fs}^2$ of GDD in front of the autocorrelator (obtained by two dispersive mirrors and a 3-mm-thick fused silica plate). Single pulse operation is proven by a 180-ps scan in the autocorrelator and by observing the pulse train with an 18.5-ps-rise-time photodetector on a 40-GHz sampling oscilloscope [Fig. 5(c)]. The small fluctuations appearing at 0.5 ns are an artifact from the detection electronics. An average output power of 150 mW is achieved with an optical-to-optical efficiency of 0.1% and an excellent beam quality [$M^2 < 1.05$, Fig. 5(e)]. The laser optical spectrum shown in Fig. 5(a) has a central wavelength of 1048 nm and a bandwidth of 45 nm FWHM, which leads to a time-bandwidth product of 0.37 (1.17 times the ideal value for sech^2 pulses). The observed chirp can be attributed to uncompensated higher-order dispersion originating from the non-flat profile introduced by the dispersive mirrors [26]. Improved dispersion management should result in transform-limited pulses as demonstrated in a SESAM mode-locked Yb:CALGO TDL [9]. The peaks around 950 nm and 1150 nm are associated with dispersive waves as already observed in various oscillators, e.g., [5,6,12]. While the disk coating supports the entire laser optical spectrum, the transmission of the output

coupler increases from 0.3% at the central wavelength to $\sim 2\%$ at the wings. Additionally, the dispersive mirrors operate at the limit of their spectral bandwidth. The radio-frequency spectrum at the repetition rate of 124 MHz shows no side peaks and the modulation-free higher harmonics confirm a clean mode-locking [Fig. 5(d)]. While the laser operates over hours, the short-term stability is confirmed by the amplitude and phase noise measurement [Figs. 5(f) and 5(g)]. We measured a root-mean-square (rms) amplitude noise of $<0.2\%$ (integrated from 1 Hz to 1 MHz), which is lower compared to previous ultrafast TDLs [1,2,27]. The rms timing jitter is <2 ps (from 100 Hz to 1 MHz, corresponding to an integrated phase noise of 1.49 mrad) and <150 fs (from 1 kHz to 1 MHz, integrated phase noise of 116.7 μ rad). The phase noise in the lower Fourier frequency range is comparably high for a TDL, which operates at an order of magnitude higher repetition rate. Moreover, it is directly mounted onto a laser without mechanically stable laser housing and not actively stabilized. We expect that the rather high phase noise at Fourier frequencies <1 kHz can be strongly reduced by active stabilization of the repetition rate.

2.4.4 *Advantage of the thin-disk pumping scheme*

The optical spectrum extends to shorter wavelengths below the pump wavelength [Fig. 5(a)]. The short-wavelength part of the spectrum is generated via SPM in the KM and not amplified by the gain medium. However, reabsorption in the gain medium causes additional losses that decrease the optical-to-optical efficiency. This broad spectral width is enabled by the TDL pumping geometry [Figs. 3(a)–3(c)], where the pump delivery and the laser cavity share no optics except of the disk. The spectral properties of intracavity components can be optimized for shorter pulses independently from the pumping wavelength. In contrast, standard end-pumped bulk oscillators [Fig. 3(d)] use intracavity dichroic mirrors with high transmission for the pump wavelength and high reflectivity for the laser wavelength, which would prevent such a mode of operation. Although similar broad spectra have been obtained in bulk configuration, the lasers operated at longer central wavelengths of ~ 1060 nm [5,6].

2.4.5 *Conclusion and outlook*

In conclusion, we presented the first KLM Yb:CALGO TDL. It generates the shortest pulses of any TDL, being equal to the shortest pulses demonstrated by Yb-doped bulk oscillators. Our work confirms the benefits of the thin-disk pumping scheme for the

generation of ultrashort pulses. KLM TDLs already produced pulses with an optical spectrum three times larger than the gain bandwidth [11,12]. The presented 30-fs laser does not fully exploit the ultra-broad bandwidth of Yb:CALGO. Therefore, we believe that further decrease of the pulse duration towards the direct generation of few-cycle pulses from Yb-based diode-pumped solid-state lasers is feasible. Next steps require the optimization of the disk parameters (doping concentration, thickness, crystal quality) as well as the optimization of the optical properties of all intracavity components for a broad reflectivity and flat dispersion profile. This should also enable substantially higher power levels with better optical-to-optical efficiencies at similar pulse durations.

Fundings

H2020 European Research Council (ERC) (2001 #279505); National Center of Competence in Research for Molecular Ultrafast Science and Technology (NCCR MUST); Schweizerischer Nationalfonds zur Förderung der Wissenschaftlichen Forschung (SNF) (200021-159931/1).

Acknowledgements

We thank Christian Kränkel (IKZ Berlin), Christoph Liebald, and Daniel Rytz (FEE GmbH) for helpful discussions on Yb:CALGO disk development.

References

1. F. Emaury, A. Diebold, C. J. Saraceno, and U. Keller, "Compact extreme ultraviolet source at megahertz pulse repetition rate with a low-noise ultrafast thin-disk laser oscillator," *Optica* **2**(11), 980–984 (2015).
2. F. Labaye, M. Gaponenko, V. J. Wittwer, A. Diebold, C. Paradis, N. Modsching, L. Merceron, F. Emaury, I. J. Graumann, C. R. Phillips, C. J. Saraceno, C. Kränkel, U. Keller, and T. Südmeyer, "Extreme ultraviolet light source at a megahertz repetition rate based on high-harmonic generation inside a mode-locked thin-disk laser oscillator," *Opt. Lett.* **42**(24), 5170–5173 (2017).
3. A. Giesen, H. Hügel, A. Voss, K. Wittig, U. Brauch, and H. Opower, "Scalable concept for diode-pumped high-power solid-state lasers," *Appl. Phys. B Lasers Opt.* **58**(5), 365–372 (1994).
4. C. J. Saraceno, C. Schriber, F. Emaury, O. H. Heckl, C. R. E. Baer, M. Hoffmann, K. Beil, C. Kränkel, M. Golling, T. Südmeyer, and U. Keller, "Cutting-Edge High-Power Ultrafast Thin Disk Oscillators," *Appl. Sci.* **3**(2), 355–395 (2013).
5. J. Ma, H. Huang, K. Ning, X. Xu, G. Xie, L. Qian, K. P. Loh, and D. Tang, "Generation of 30 fs pulses from a diode-pumped graphene mode-locked Yb:CaYAlO₄ laser," *Opt. Lett.* **41**(5), 890 (2016).
6. P. Sévillano, P. Georges, F. Druon, D. Descamps, and E. Cormier, "32-fs Kerr-lens mode-locked Yb:CaGdAlO₄ oscillator optically pumped by a bright fiber laser," *Opt. Lett.* **39**(20), 6001 (2014).

7. U. Keller, *Ultrafast Solid-State Lasers*, Landolt-Börnstein. Laser Physics and Applications. Subvolume B: Laser Systems. Part I (Springer, 2007).
8. A. Yoshida, A. Schmidt, V. Petrov, C. Fiebig, G. Erbert, J. Liu, H. Zhang, J. Wang, and U. Griebner, "Diode-pumped mode-locked Yb:YCOB laser generating 35 fs pulses," *Opt. Lett.* **36**(22), 4425–4427 (2011).
9. C. Schriber, L. Merceron, A. Diebold, F. Emaury, M. Golling, K. Beil, C. Kränkel, C. J. Saraceno, T. Südmeyer, and U. Keller, "Pushing SESAM modelocked thin-disk lasers to shortest pulse durations," in *Advanced Solid State Lasers* (Optical Society of America, 2014), paper AF1A.4.
10. O. Pronin, J. Brons, C. Grasse, V. Pervak, G. Boehm, M.-C. Amann, V. L. Kalashnikov, A. Apolonski, and F. Krausz, "High-power 200 fs Kerr-lens mode-locked Yb:YAG thin-disk oscillator," *Opt. Lett.* **36**(24), 4746–4748 (2011).
11. J. Zhang, J. Brons, M. Seidel, V. Pervak, V. Kalashnikov, Z. Wei, A. Apolonski, F. Krausz, and O. Pronin, "49-fs Yb:YAG thin-disk oscillator with distributed Kerr-lens mode-locking," in *European Quantum Electronics Conference* (Optical Society of America, 2015), paper PD_A_1.
12. C. Paradis, N. Modsching, V. J. Wittwer, B. Deppe, C. Kränkel, and T. Südmeyer, "Generation of 35-fs pulses from a Kerr lens mode-locked Yb:Lu₂O₃ thin-disk laser," *Opt. Express* **25**(13), 14918–14925 (2017).
13. U. Keller, K. J. Weingarten, F. X. Kärtner, D. Kopf, B. Braun, I. D. Jung, R. Fluck, C. Hönninger, N. Matuschek, and J. Aus der Au, "Semiconductor Saturable Absorber Mirrors (SESAM's) for Femtosecond to Nanosecond Pulse Generation in Solid-State Lasers," *IEEE J. Sel. Top. Quantum Electron.* **2**(3), 435–453 (1996).
14. T. Südmeyer, C. Kränkel, C. R. E. Baer, O. H. Heckl, C. J. Saraceno, M. Golling, R. Peters, K. Petermann, G. Huber, and U. Keller, "High-power ultrafast thin disk laser oscillators and their potential for sub-100-femtosecond pulse generation," *Appl. Phys. B* **97**(2), 281–295 (2009).
15. T. Brabec, C. Spielmann, P. F. Curley, and F. Krausz, "Kerr lens mode locking," *Opt. Lett.* **17**(18), 1292–1294 (1992).
16. B. Kreipe, J. Andrade, B. Deppe, C. Kränkel, and U. Morgner, "Kerr-lens mode-locked Yb³⁺:Lu₂O₃ thin-disk laser," in *Conference on Lasers and Electro-Optics* (Optical Society of America, 2016), paper SM1I.4.
17. C. Kränkel, "Rare-Earth-Doped Sesquioxides for Diode-Pumped High-Power Lasers in the 1-, 2-, and 3- μm Spectral Range," *IEEE J. Sel. Top. Quantum Electron.* **21**(1), 250–262 (2015).
18. K. Hasse, T. Calmano, B. Deppe, C. Liebold, and C. Kränkel, "Efficient Yb³⁺:CaGdAlO₄ bulk and femtosecond-laser-written waveguide lasers," *Opt. Lett.* **40**(15), 3552–3555 (2015).
19. A. Greborio, A. Guandalini, and J. Aus der Au, "Sub-100 fs pulses with 12.5-W from Yb:CALGO based oscillators," in *Proc. SPIE*, (2012), paper 823511.
20. S. Ricaud, A. Jaffres, K. Wentsch, A. Suganuma, B. Viana, P. Loiseau, B. Weichelt, M. Abdou-Ahmed, A. Voss, T. Graf, D. Rytz, C. Hönninger, E. Mottay, P. Georges, and F. Druon, "Femtosecond Yb:CaGdAlO₄ thin-disk oscillator," *Opt. Lett.* **37**(19), 3984–3986 (2012).
21. J. Petit, P. Goldner, and B. Viana, "Laser emission with low quantum defect in Yb:CaGdAlO₄," *Opt. Lett.* **30**(11), 1345–1347 (2005).
22. J. Brons, V. Pervak, E. Fedulova, M. Seidel, D. Bauer, D. Sutter, V. Kalashnikov, A. Apolonskiy, O. Pronin, and F. Krausz, "High power Kerr-lens mode-locking of Yb:YAG and Yb:CALGO thin-disk oscillators," in *Advanced Solid State Lasers* (Optical Society of America, 2014), paper AF1A-5.
23. F. P. Druon, S. Ricaud, A. Jaffrès, K. S. Wentsch, A. Suganuma, P. Loiseau, B. Weichelt, M. A. Ahmed, A. Voss, T. Graf, C. Hoenninger, D. Rytz, E. Mottay, B. Viana, and P. Georges, "High power cw and fs Yb:CALGO thin-disk laser using diamond heat spreader," in *Advanced Solid-State Lasers Congress* (2013), Paper AF3A.7 (Optical Society of America, 2013), paper AF3A.7.
24. K. Beil, B. Deppe, and C. Kränkel, "Yb:CaGdAlO₄ thin-disk laser with 70% slope efficiency and 90 nm wavelength tuning range," *Opt. Lett.* **38**(11), 1966–1968 (2013).

25. S. Ricaud, A. Jaffres, P. Loiseau, B. Viana, B. Weichelt, M. Abdou-Ahmed, A. Voss, T. Graf, D. Rytz, M. Delaigue, E. Mottay, P. Georges, and F. Druon, "Yb:CaGdAlO₄ thin-disk laser," *Opt. Lett.* **36**(21), 4134–4136 (2011).
26. A. Diebold, F. Emaury, C. Schriber, M. Golling, C. J. Saraceno, T. Südmeyer, and U. Keller, "SESAM mode-locked Yb:CaGdAlO₄ thin disk laser with 62 fs pulse generation," *Opt. Lett.* **38**(19), 3842–3845 (2013).
27. J. Brons, V. Pervak, D. Bauer, D. Sutter, O. Pronin, and F. Krausz, "Powerful 100-fs-scale Kerr-lens mode-locked thin-disk oscillator," *Opt. Lett.* **41**(15), 3567 (2016).

2.5 Experimental optimization in the sub-100-fs pulse duration regime

Section 2.2 to 2.4 presented cutting-edge performance of sub-100-fs KLM TDL oscillators. This section aims to explain in more detail the underlying experimental optimization. The impact of various optimization parameters onto the laser performance is determined.

The design of the laser cavity has the strongest impact onto the laser performance. It influences the round-trip gain by the number of passes through the disk. Cavity dynamics caused by the Kerr lens affect the change of the beam size on the hard aperture as well as the soft aperture effects connected to the beam overlap on the pump spot. Besides the more general cavity design exist several other parameters that have to be experimentally optimized. As such, there are the output coupler transmission (T_{OC}), the hard aperture diameter, the amount and the bandwidth of the introduced group delay dispersion (GDD), the beam radius in the Kerr medium (w_{KM}) as well as its material, thickness and position. w_{KM} is defined by the radius of curvature (ROC) of the two curved mirrors that form the intracavity focus. The distance between those two mirrors can be used to adjust the vicinity to the edge of the stability zone in continuous-wave operation. In this thesis, optimization targeted for shortest pulse duration and highest average power in the sub-100-fs regime.

In an initial study of the KLM Yb:Lu₂O₃ TDL oscillator presented in section 2.2, more than 300 different cavity configurations have been tested. The Kerr medium (KM) was placed in the vicinity of the intracavity focus between two concave mirrors of 300 mm ROC and w_{KM} was estimated to be 70 μm in continuous-wave operation. Mode-locked operation was initiated for each configuration by increasing the pump power and knocking on the laser table until a stable pulse train was observed. For detection, the leakage of a cavity mirror was sent onto a fast photodiode and observed by use of an oscilloscope. Afterwards the pump power was reduced until a typically observed continuous-wave breakthrough visible in the optical spectrum was suppressed. The experimental results are summarized in Fig. 1 and show a tradeoff between pulse duration and average power. Following trends were observed for variation of the introduced GDD, hard aperture diameter and T_{OC} while all other

cavity parameters remained constant. The pump power was adjusted in each configuration for best performance.

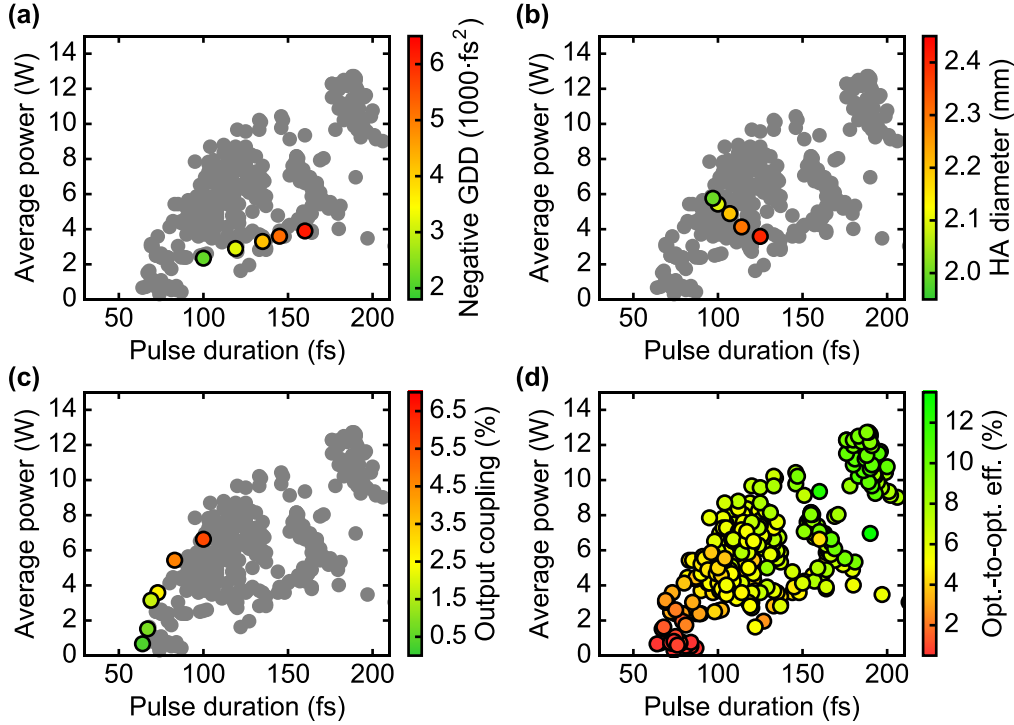


Fig. 1. Initial study of about 300 different laser configurations (gray) of the KLM Yb:Lu₂O₃ TDL oscillator presented in section 2.2. A tradeoff between pulse duration and average power is observed. (a-c) Highlighted points indicate the trends observed while varying only the corresponding cavity parameter. The pump power was in all configurations adjusted for laser operation at highest average power and shortest pulse durations. (d) The optical-to-optical efficiency over all configurations shows an drop towards shorter pulse durations. GDD: group delay dispersion; HA: hard aperture; Opt.-to-opt. eff.: optical-to-optical efficiency.

- **Negative GDD [Fig. 1(a)]:** Decreasing the introduced GDD resulted in shorter pulse durations and a decreased average power.
- **Hard aperture diameter [Fig. 1(b)]:** A decrease of the hard aperture diameter resulted in shorter pulse durations and increased average powers.
- **Output coupling [Fig. 1(c)]:** A decreased T_{OC} resulted in shorter pulse durations and decreased average power. For a T_{OC} below 2% the pulse duration remained almost constant while the average power dropped strongly. This observation is attributed to the limiting GDD bandwidth of the dispersive mirrors [Fig. 4(a)].

- The overall optical-to-optical efficiency [Fig. 1(d)] decreased towards shorter pulse durations. On the one hand, this trend is attributed to the reduced T_{OC} . On the other hand, laser operation in the strongly self-phase modulation broadened regime expands the optical spectrum beyond the supported gain bandwidth at the expense of higher losses for the passive loss modulation.

The observed trends show that the performance improvement of a KLM TDL oscillator is a multi-dimensional optimization problem of coupled parameters. For best performance a compromise between different cavity parameters has to be found. The overall tradeoff between pulse duration and average power was improved by increasing w_{KM} from 70 μm to 90 μm (Fig. 2). For that, the ROC of the concave mirrors was increased from 300 mm to 400 mm. Cavity lengths were adapted accordingly. Shorter pulse durations down to 35 fs were generated by using dispersive mirrors that supported a broader GDD bandwidth [Fig. 4(c)]. Achieved results in this configuration are discussed in more detail in section 2.2.

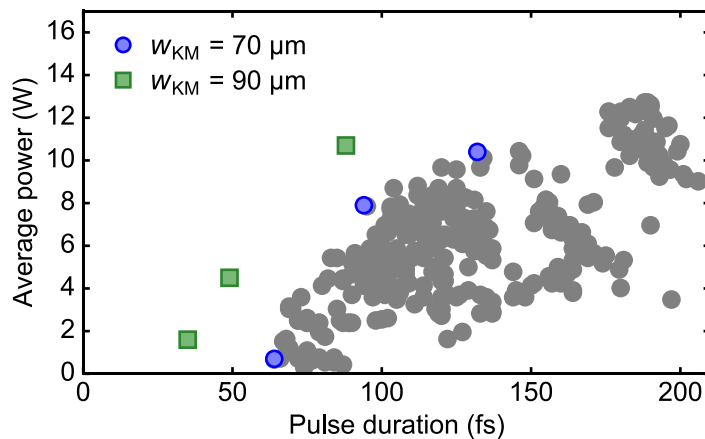


Fig. 2. Scaling of the beam radius in the Kerr medium (w_{KM}) enabled to shift the observed tradeoff towards higher average powers at shorter pulse durations. Results achieved with the w_{KM} of 90 μm are presented in more detail in section 2.2.

Despite the improved performance by increasing w_{KM} , the optical-to-optical efficiency in the sub-100-fs pulse duration regime remained below 6%. The follow up study of the KLM Yb:Lu₂O₃ TDL oscillator presented in section 2.3 investigated the impact of higher round-trip gain onto the laser performance. Higher round-trip gain was achieved by folding the cavity a second time on the disk. The intracavity focus was designed to keep w_{KM} comparable to the previous configuration.

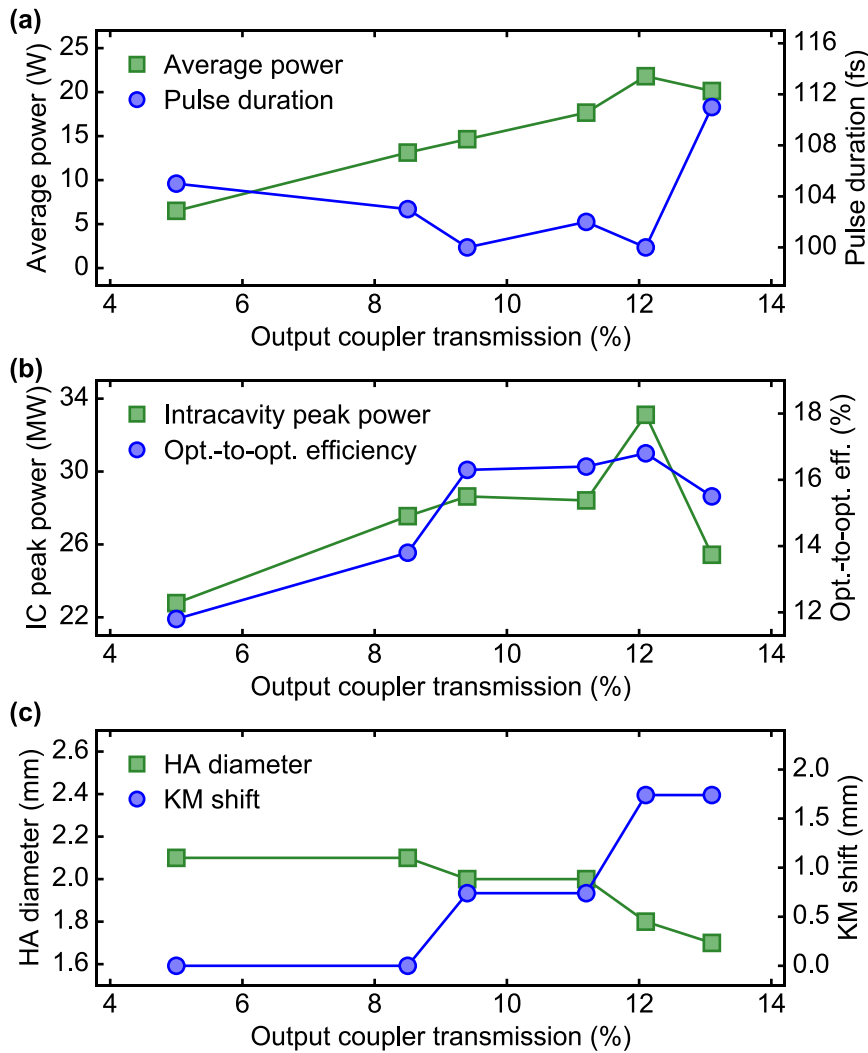


Fig. 3. (a-b) Laser performance and (c) adjusted KLM cavity parameters during the optimization of the KLM Yb:Lu₂O₃ TDL oscillator. The optimization targeted laser operation at increased T_{OC} for highest average power in the sub-100-fs pulse duration regime. The introduced negative GDD (-5400 fs^2) was optimized in an initial laser configuration for 100-fs pulses ($T_{OC} = 5\%$). Afterwards the T_{OC} was stepwise increased. For each T_{OC} the hard aperture (HA) diameter was adjusted for highest average power and shortest pulse duration. During the optimization the Kerr medium (KM) got shifted further out of the intracavity focus. T_{OC} above 10% were realized by placing a second output coupler as cavity end mirror and adding their transmission. The average power was measured separately behind each cavity end mirror and summed up. Optimal performance was achieved at a T_{OC} of 12%. For the results discussed in section 2.3 the two output couplers were replaced by a single output coupler with an adjusted T_{OC} of 12.3%. IC: intracavity; Opt.-to-opt. efficiency: optical-to-optical efficiency.

Higher round-trip gain enables laser operation at higher total cavity losses and, thus, a higher T_{OC} . Considering that the intracavity performance remains constant, an

increase in the T_{OC} should result in improved output performance. However, as observed in the initial study tends laser operation at higher T_{OC} in longer pulse durations.

Fig. 3 summarizes the laser performance and cavity parameters of the KLM Yb:Lu₂O₃ TDL oscillator with increased cavity round-trip gain during the optimization for a higher T_{OC} . The optimization targeted highest average power for around 100-fs pulses. Increasing the T_{OC} up to 12% enabled laser operation at increased average power of up to 20 W. The pulse duration at around 100 fs could be maintained by decreasing the hard aperture diameter and shifting the KM out of the intracavity focus. The resulting optical-to-optical efficiency increased and amounted to 16%. The performance drop at an T_{OC} of 13% indicates the end of the optimization range and for an T_{OC} of 15% no mode-locking was observed. The increase in the intracavity peak power is attributed to a larger amount of SPM created in the KM. This is required to compensate for the stronger gain narrowing due to higher round-trip gain in order to maintain 100-fs pulses. In the 88-fs result described in section 2.2 (folding the cavity once on the disk, utilizing a comparable w_{KM}) the laser operated at an T_{OC} of 4.6%. Compared to this result, the best performance here was achieved at an around 3 times higher T_{OC} of 12%. But, assuming a linear relationship between round-trip gain and T_{OC} only a factor of 2 would be expected. This deviation can be attributed to the ratio between the losses required for mode-locking and the T_{OC} . One can assume that in the 88-fs result the ratio between mode-locking losses and T_{OC} was about 1:1. While doubling the round-trip gain enabled to operate at twice higher total cavity losses, the losses required for mode-locking with a similar pulse duration of 95-fs should remain comparable. By this, the ratio of the total cavity losses between mode-locking losses to T_{OC} shifts towards 1:3. The same relation can be used to explain the around 3 times higher optical-to-optical efficiency (5.8% vs. 16.2%). As such, even better laser performance can be expected by increasing the number of passes further.

The optimization of the KLM Yb:Lu₂O₃ TDL oscillator towards even shorter pulse durations has been investigated. Limiting factor to decrease the pulse duration below 80 fs was the observation of very stable double pulsing. Trying to remove the second pulse by decreasing the pump power and changes in the cavity alignment resulted repeatably in the break-up of both solitons at the same time. The temporal distance between both pulses varied with changes in the cavity length. This revealed that both

pulses coincided in the Kerr medium, benefitting from a common Kerr lens once during each cavity round-trip. Further experimental investigations and better understanding of the cavity and soliton dynamics with help of simulations should enable to understand the origin of the stable double pulsing. Solving this issue should enable further performance improvement towards higher average powers in the sub-50-fs pulse duration regime.

The shortest pulse durations achieved in the framework of this thesis were 35 fs from the KLM Yb:Lu₂O₃ TDL oscillator (section 2.2) and 30 fs from the KLM Yb:CALGO TDL oscillator (section 2.4). Key parameter for reaching such short pulse durations was the optimization of the GDD bandwidth of the dispersive mirrors. The in-house design and manufacturing of optical coatings on an ion-beam sputtering coating machine (Navigator 1100, CEC GmbH) enabled the development of broadband dispersive mirrors.

Fig. 4 shows the total introduced GDD of the dispersive mirrors and the corresponding optical spectra obtained for the Yb:Lu₂O₃ and Yb:CALGO TDL oscillator. Shorter pulse durations were generated by increasing the bandwidth while decreasing the total amount of introduced GDD. For the KLM Yb:Lu₂O₃ KLM TDL oscillator the pulse duration was decreased from 64 fs to 35 fs by lowering the total introduced GDD from -2200 fs² to -1000 fs². For the KLM Yb:CALGO TDL oscillator the pulse duration was decreased from 62 fs to 30 fs by lowering the introduced GDD -1300 fs² to -900 fs². Further optimization for shorter pulse durations will converge towards a zero-net dispersion in the cavity. This requires the precise characterization and adjustment of the amount and bandwidth of the GDD that is introduced into the cavity. The generation of even shorter pulse duration can be expected by further improving of the GDD bandwidth of the dispersive mirrors. However, a broader GDD bandwidth is typically achieved in tradeoff with a lower amount of GDD (Fig. 5).

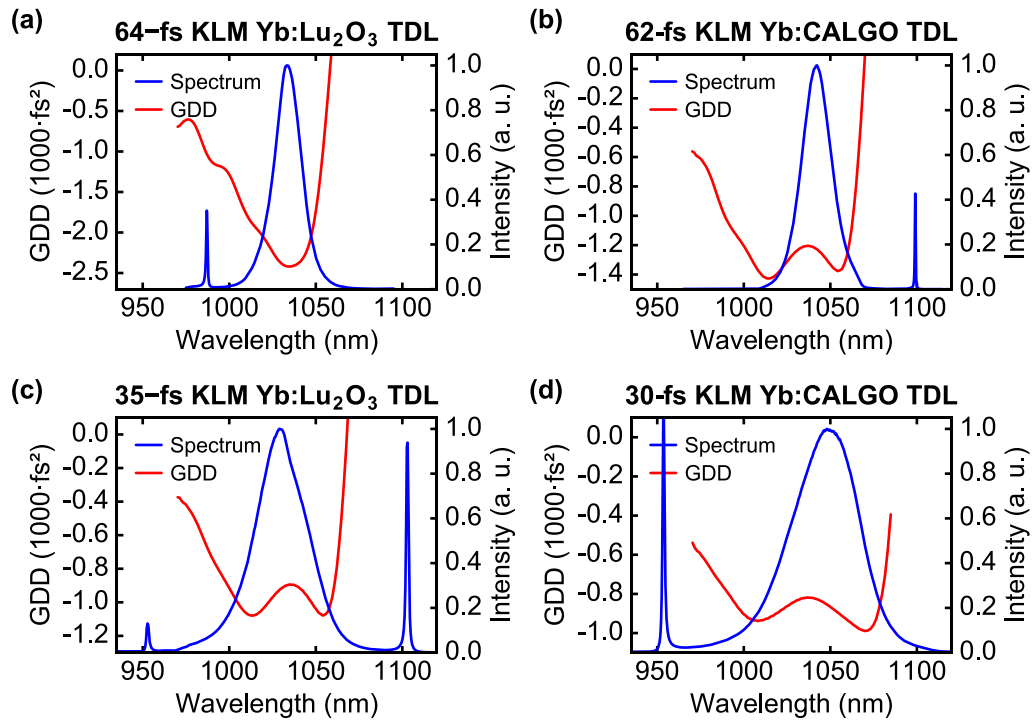


Fig. 4. Introduced group delay dispersion (GDD) and obtained optical spectra for different TDL oscillator configurations. Configuration for (a) 64-fs and (c) 35-fs pulses of the KLM Yb:Lu₂O₃ TDL oscillator (section 2.2). Configuration for (b) 62-fs and (d) 30-fs pulses of the KLM Yb:CALGO TDL oscillator (section 2.4). The bandwidth of the optical spectra are limited by the rising edges in the GDD bandwidth of the dispersive mirrors.

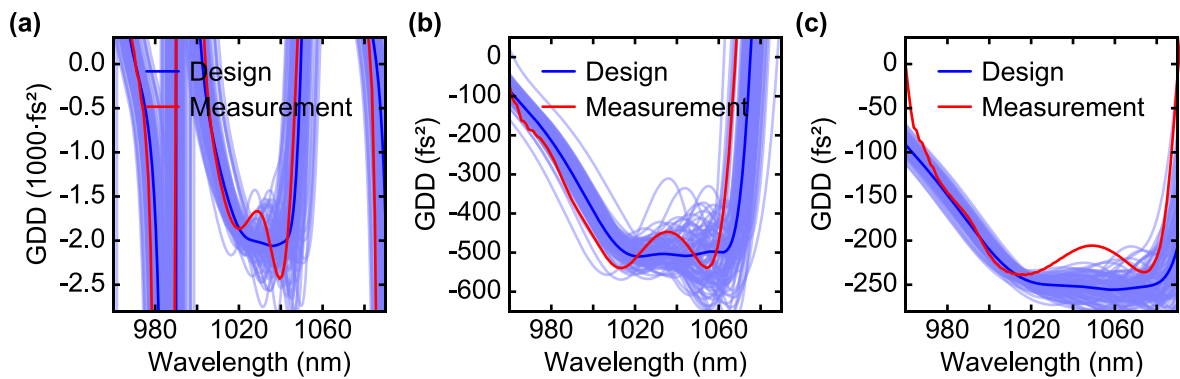


Fig. 5. Designed and measured group delay dispersion (GDD) of different dispersive mirrors targeting (a) -2000 fs^2 (b) -500 fs^2 and (c) -250 fs^2 . The impact of growth errors during the manufacturing process are estimated in light blue. In the design a tradeoff has to be found between the amount of GDD and achievable spectral bandwidth.

The time-bandwidth product of the 35-fs and 30-fs configuration was 0.332 and 0.37 after extra-cavity compensation, respectively. This corresponds to 1.05 and 1.17 times the value for ideal soliton shape pulses. Especially for the 30-fs configuration can this value be attributed to higher order dispersion that could not be characterized and compensated for at that time. Characterization of the phase with according diagnostic tools should allow a more detailed analysis. Higher order dispersion is attributed to the non-flat dispersion profile introduced by the dispersive mirrors [Fig. 4(d)]. Improving the flatness of the dispersion profile should enable shorter pulse durations. This can be achieved by improving the dispersive mirror design and the manufacturing technique. Another possibility is to average out higher order dispersion by precise characterization of the GDD and selection of the dispersive mirrors for compensation.

Improving the bandwidth of the dispersive mirrors with careful adjustment of the introduced GDD will enable further decrease in the achievable pulse durations. By that TDL oscillator operating in the sub-20-fs pulse durations regime become feasible.

Chapter 3

Carrier envelope offset frequency

stabilized sub-100-fs thin-disk laser

oscillator

This chapter investigates the suitability of the developed sub-100-fs KLM Yb:Lu₂O₃ TDL oscillator for frequency-comb applications. Section 3.1 gives a basic introduction into frequency combs and summarizes the presented results. Section 3.2 demonstrates the detection and tight-lock stabilization of the carrier envelope offset frequency of the developed sub-100-fs KLM Yb:Lu₂O₃ TDL oscillator for laser operation in the strongly self-phase modulation broadened regime (section 2.2). Section 3.3 contains a preliminary study investigating the potential for full frequency comb stabilization by simultaneous repetition rate stabilization. These investigations are of particular interest for the future development of XUV frequency combs via intra-oscillator high-harmonic generation (chapter 5).

3.1 Frequency combs

Optical frequency combs enable the phase-coherent link between optical and microwave frequencies [1]. Applied as precise ruler in the frequency domain they

revolutionized various scientific areas, as e.g. in optical-frequency metrology, high-resolution spectroscopy and optical clocks [2,3]. Increasing the average power of frequency combs is beneficial as it results in higher power per comb line. Simple yet powerful laser systems stabilized as frequency comb are as well attractive to drive nonlinear frequency conversion for expansion of the spectral range towards the mid-infrared or to extreme ultraviolet region [4-7]. Among different approaches are sub-100-fs KLM TDL oscillators of particular interest as single-stage systems with potential for further power-scaling.

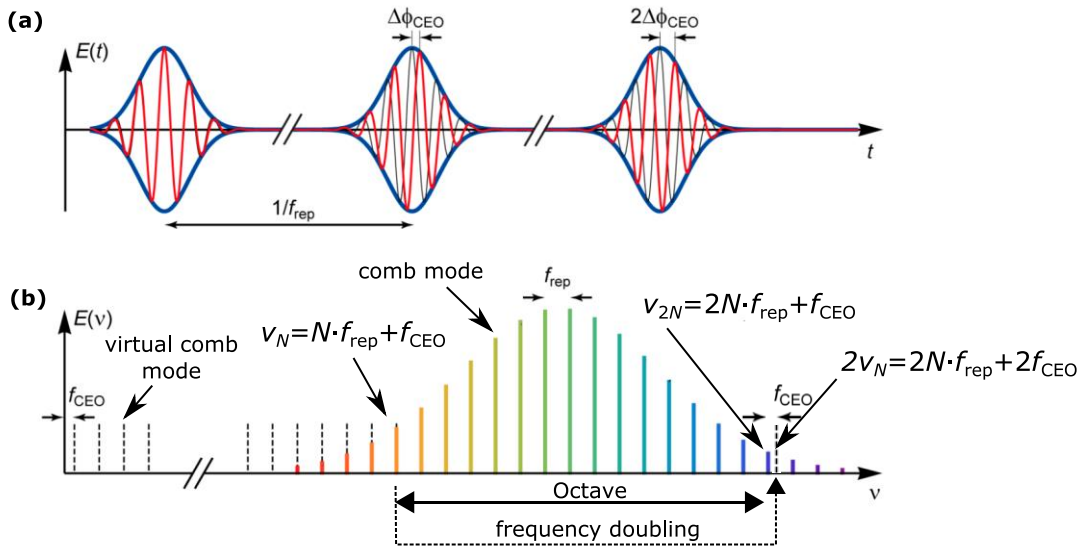


Fig. 1. (a) Pulse train generated from a mode-locked oscillator in the time domain and (b) corresponding optical spectrum in the Fourier domain. The phase offset of the electric field under the envelope from pulse to pulse in the time domain ($\Delta\phi_{\text{CEO}}$) corresponds to the shift from the zero-frequency of the first comb mode (f_{CEO}) in the Fourier domain. For f_{CEO} detection in the f -to- $2f$ interferometer the lower frequency component of a coherent octave spanning spectrum (ν_N) is frequency doubled ($2\nu_N$) and overlapped with the corresponding higher frequency component (ν_{2N}). The f_{CEO} can be detected in the beat signal of both frequencies ($f_{\text{CEO}} = 2\nu_N - \nu_{2N}$). Figure adapted from [8].

Mode-locked laser oscillators generate in the time domain a train of optical pulses [Fig. 1(a)]. Assuming that only a single pulse is circulating in the oscillator cavity, the time between two consecutive pulses is equal to the inverse of the repetition rate (f_{rep}). In the Fourier domain features this train of pulses a comb-like optical spectrum of equidistantly-spaced discrete frequencies [Fig. 1(b)]. These discrete frequencies are referred to as comb modes and separated by f_{rep} . The carrier-envelope offset frequency (f_{CEO}) is the shift of the first comb mode to the zero-frequency. In the temporal domain

the f_{CEO} corresponds to a phase offset ($\Delta\Phi_{\text{CEO}}$) of the electric field under the envelope from one pulse to the next one [Fig. 1(a)]. Based on the comb equation $\nu_N = N \cdot f_{\text{rep}} + f_{\text{CEO}}$ [1] the frequency of each individual comb mode (ν_N) can be calculated if the mode number (N), f_{rep} and the carrier envelope offset frequency f_{CEO} are known. In order to fully stabilize the pulse train of a mode-locked oscillator as frequency comb the f_{rep} and the f_{CEO} have to be detected and locked.

The detection of the f_{rep} can be realized straightforward by detecting the train of optical pulses on a fast photodiode with sufficient bandwidth [8]. A stabilization is typically achieved by mounting a cavity mirror onto a piezo-electric actuator that enables the adjustment of the cavity length while being locked to an external reference. In contrast, the f_{CEO} can be considered as a virtual comb mode without any spectral content [Fig. 1(b)]. As such, it cannot be directly measured and requires more sophisticated detection schemes. The most common approach for f_{CEO} detection is the nonlinear f -to- $2f$ interferometer [9]. This self-referenced detection scheme requires an octave-spanning coherent spectrum which can be generated by spectral broadening, e.g. in highly nonlinear photonic crystal fibers (HN-PCF) [10]. In order to maintain the coherence during the spectral broadening in HN-PCFs usually pulse durations below 150 fs are needed for 1 μm central wavelength. For longer pulse durations often a preceding nonlinear pulse compression is required. After generation of the coherent octave spanning spectrum, the lower frequency end of the spectrum (ν_N) is frequency doubled. Beating of the frequency-doubled lower spectral end ($2\nu_N$) with the corresponding higher frequency spectral end (ν_{2N}) enables then the detection of the f_{CEO} on a photodiode. Locking of the f_{CEO} to an external reference can be finally achieved by e.g. active feedback to the current of the pump-diode, dual wavelength pumping, or placing an acoustic optical modulator into the cavity [11–13].

Section 3.2 presents the f_{CEO} stabilization of the developed sub-100-fs KLM Yb:Lu₂O₃ TDL oscillator (section 2.2). By operating in the strongly self-phase modulation broadened regime, the oscillator generates 50-fs pulses at 4.4 W of average power and 61 MHz of repetition rate. The f_{CEO} was detected by use of a nonlinear f -to- $2f$ interferometer and stabilized to an external reference via pump current modulation.

Key messages of this result are:

- KLM TDL oscillator operating the strongly SPM-broadened regime can be f_{CEO} stabilized

- Tight phase-lock stabilization of the f_{CEO} is achieved with a residual in-loop integrated phase noise of 197 mrad integrated (from 1 Hz to 1 MHz)
- f_{CEO} -stable laser operation is demonstrated at the highest average power and the shortest pulse duration so far achieved by a sub-100-fs Yb-based oscillator

Section 3.3 investigates in a preliminary study simultaneous stabilization of the f_{CEO} and f_{rep} . Stabilization of the f_{rep} to an external reference was achieved by mounting one folding cavity mirror onto a controlled piezoelectric transducer. Key messages of this study are:

- Simultaneous stabilization of f_{CEO} and f_{rep} can be achieved in a KLM TDL oscillator
- Cross-talking between both stabilization loops resulted in an increased f_{CEO} noise of 745 mrad and limited the f_{rep} -stabilization bandwidth to 35 Hz with 7 ps of residual integrated timing jitter (integrated from 1 Hz to 1 MHz)

References

1. T. W. Hänsch, "Nobel Lecture: Passion for precision," *Rev. Mod. Phys.* **78**(4), 1297–1309 (2006).
2. T. Udem and F. Riehle, *Frequency Combs Applications and Optical Frequency Standards* (2007), Vol. 30.
3. N. R. Newbury, "Searching for applications with a fine-tooth comb," *Nat. Photonics* **5**(4), 186–188 (2011).
4. A. Schliesser, N. Picqué, and T. W. Hänsch, "Mid-infrared frequency combs," *Nat. Photonics* **6**(7), 440–449 (2012).
5. D. T. Reid, C. M. Heyl, R. R. Thomson, R. Trebino, G. Steinmeyer, H. H. Fielding, R. Holzwarth, Z. Zhang, P. Del'Haye, T. Südmeyer, G. Mourou, T. Tajima, D. Faccio, F. J. M. Harren, and G. Cerullo, "Roadmap on ultrafast optics," *J. Opt.* **18**(9), 093006 (2016).
6. R. J. Jones, K. D. Moll, M. J. Thorpe, and J. Ye, "Phase-Coherent Frequency Combs in the Vacuum Ultraviolet via High-Harmonic Generation inside a Femtosecond Enhancement Cavity," *Phys. Rev. Lett.* **94**(19), 193201 (2005).
7. A. K. Mills, T. J. Hammond, M. H. C. Lam, and D. J. Jones, "XUV frequency combs via femtosecond enhancement cavities," *J. Phys. B At. Mol. Opt. Phys.* **45**(14), 142001 (2012).
8. S. Schilt and T. Südmeyer, "Carrier-Envelope Offset Stabilized Ultrafast Diode-Pumped Solid-State Lasers," *Appl. Sci.* **5**(4), 787–816 (2015).
9. H. R. Telle, G. Steinmeyer, A. E. Dunlop, J. Stenger, D. H. Sutter, and U. Keller, "Carrier-envelope offset phase control: A novel concept for absolute optical frequency measurement and ultrashort pulse generation," *Appl. Phys. B* **69**(4), 327–332 (1999).
10. J. M. Dudley, G. Genty, and S. Coen, "Supercontinuum generation in photonic crystal fiber," *Rev. Mod. Phys.* **78**(4), 1135–1184 (2006).
11. A. Klenner, F. Emaury, C. Schriber, A. Diebold, C. J. Saraceno, S. Schilt, U. Keller, and T. Südmeyer, "Phase-stabilization of the carrier-envelope-offset frequency of a SESAM modelocked thin disk laser," *Opt. Express* **21**(21), 24770–24780 (2013).
12. M. Seidel, J. Brons, F. Lücking, V. Pervak, A. Apolonski, T. Udem, and O. Pronin, "Carrier-envelope-phase stabilization via dual wavelength pumping," *Opt. Lett.* **41**(8), 1853 (2016).

13. O. Pronin, M. Seidel, J. Brons, F. Lücking, V. Pervak, A. Apolonski, T. Udem, and F. Krausz, "Carrier-envelope phase stabilized thin-disk oscillator," in *Advanced Solid-State Lasers Congress (2013)*, Paper AF3A.5 (Optical Society of America, 2013), paper AF3A.5.

3.2 Carrier-envelope offset frequency stabilization of a thin-disk laser oscillator operating in the strongly self-phase modulation broadened regime

Norbert Modsching,^{1,*} Clément Paradis,¹ Pierre Brochard,¹ Nayara Jornod,¹ Kutan Gürel,¹ Christian Kränkel,² Stéphane Schilt,¹ Valentin J. Wittwer,¹ and Thomas Südmeyer¹

¹*Laboratoire Temps-Fréquence, Institut de Physique, Université de Neuchâtel, Avenue de Bellevaux 51, 2000 Neuchâtel, Switzerland*

²*Center for Laser Materials, Leibniz Institute for Crystal Growth, Max-Born-Str. 2, 12489 Berlin, Germany*

We demonstrate the carrier-envelope offset (CEO) frequency stabilization of a Kerr lens mode-locked Yb:Lu₂O₃ thin-disk laser oscillator operating in the strongly self-phase modulation (SPM) broadened regime. This novel approach allows overcoming the intrinsic gain bandwidth limit and is suited to support frequency combs from sub-100-fs pulse trains with very high output power. In this work, strong intra-oscillator SPM in the Kerr medium enables the optical spectrum of the oscillating pulse to exceed the bandwidth of the gain material Yb:Lu₂O₃ by a factor of two. This results in the direct generation of 50-fs pulses without the need for external pulse compression. The oscillator delivers an average power of 4.4 W at a repetition rate of 61 MHz. We investigated the cavity dynamics in this regime by characterizing the transfer function of the laser output power for pump power modulation, both in continuous-wave and mode-locked operations. The cavity dynamics in mode-locked operation limit the CEO modulation bandwidth to ~10 kHz. This value is sufficient to achieve a tight phase-lock of the CEO beat via active feedback to the pump current and yields a residual in-loop integrated CEO phase noise of 197 mrad integrated from 1 Hz to 1 MHz.

3.2.1 Introduction

Optical frequency combs (OFCs) based on mode-locked lasers are a key tool for numerous scientific and industrial applications [1–4]. Most commonly, they are either based on Ti:sapphire lasers that are pumped by complex frequency-doubled solid-state lasers [1,2], or more recently diode-pumped sources [5] or based on diode-pumped fiber-lasers which require several stages for amplification and pulse compression [6].

Yb-doped diode-pumped solid-state laser (Yb-DPSSL) oscillators are an alternative technology providing reliable and low noise operation [7,8]. These sources have also a high potential for power-scaling, which is especially attractive for nonlinear frequency conversion to the mid-infrared spectral region by parametric nonlinear processes [3,9] and to the extreme ultraviolet by high harmonic generation [9–11].

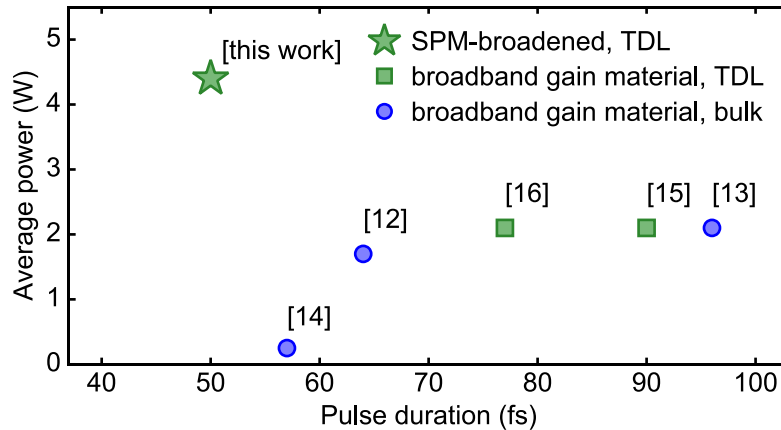


Fig. 1. Overview of f_{CEO} -stabilized Yb-DPSSL oscillators delivering sub-100-fs pulses without external pulse compression. So far, they have relied exclusively on broadband gain materials (bulk [12–14], thin-disk laser (TDL) [15,16]). Our Yb:Lu₂O₃ TDL oscillator operates in the strongly self-phase modulation (SPM) broadened regime and is highlighted with a green star symbol.

However, only a few Yb-DPSSL oscillators have been reported with a stabilization of the carrier envelope offset (CEO) frequency (f_{CEO}) operating at a watt-level average power and sub-100-fs pulses generated directly from the oscillator, i.e. without the need for external amplification or pulse compression. So far, the direct f_{CEO} stabilization of sub-100-fs Yb-DPSSL oscillators relied exclusively on broadband gain materials (Fig. 1). In the bulk geometry, f_{CEO} -stabilized Yb:CALGO oscillators delivered pulses as short as 64 fs at an average power level of 2 W [12,13]. A shorter pulse duration of 57 fs has

been achieved from a f_{CEO} -stabilized Yb:CYA oscillator but at a lower average power of 250 mW [14]. In the thin-disk geometry, f_{CEO} -stabilization has been realized with an Yb:CALGO thin-disk laser (TDL) oscillator delivering 77 fs pulses at 2.1 W average power [15,16]. The highest reported average power of an f_{CEO} -stabilized Yb-DPSSL oscillator was recently generated by an Yb:YAG TDL operating at 105 W with 190-fs pulses, but a compression stage was required before coherent supercontinuum generation [17].

In the last years, Kerr lens mode-locked (KLM) TDL oscillators based on the gain materials Yb:YAG and Yb:Lu₂O₃ [18] operating in the regime of strong self-phase modulation (SPM) have been developed [19,20]. In this regime the optical spectrum of the oscillating pulse strongly exceeds the bandwidth of the gain material. An expansion up to a factor of 3 has been achieved so far. Strong intra-oscillator SPM in the Kerr medium (usually a fused silica, sapphire, or YAG plate with a thickness of several millimeters) generates frequencies beyond the spectral range of the gain. This enables the direct generation of sub-100-fs soliton pulses from bandwidth-limiting gain materials at high average powers. More than 10 W of average power in 88-fs pulses and pulse durations as short as 35 fs at 1.6 W were demonstrated [20]. Therefore, the strongly SPM-broadened regime is promising for the generation of high power OFCs without the need for additional amplification or pulse-compression. Prior to this work, it was uncertain if oscillators operating in this regime could be f_{CEO} -stabilized. Although their output parameters appear suitable, particular cavity and f_{CEO} dynamics could prevent a stabilization [16,21].

Here, we demonstrate for the first time the f_{CEO} stabilization of an Yb-DPSSL oscillator operating in the strongly SPM-broadened regime with 50 fs pulse durations, shorter than the gain bandwidth of the active material would support. We characterize the transfer function of the output power of the oscillator in continuous-wave (cw) and mode-locked operation for a modulation of the pump power and achieve a tight f_{CEO} lock with <200 mrad of integrated phase noise in a phase-locked loop with feedback applied to the pump current.

3.2.2 Thin-disk laser oscillator and experimental setup

The experiment has been performed using a KLM Yb:Lu₂O₃ TDL oscillator generating pulses which are among the shortest of any TDL oscillators. The laser is described in

detail in [20]. It delivers 4.4 W of average output power in time-bandwidth-limited 50-fs soliton pulses [inset of Fig. 2(a)] at 61 MHz repetition rate. This results in a pulse energy of >60 nJ and a peak power of >1 MW. The optical spectrum of the mode-locked laser is centered at around 1031 nm with a full width at half maximum (FWHM) bandwidth of 24 nm that exceeds the FWHM gain bandwidth of Yb:Lu₂O₃ by a factor of 2 [Fig. 2(a)]. A schematic of the experimental setup is shown in Fig. 2(b). The oscillator is pumped by a highly transverse multimode fiber-coupled (600 μm core diameter; 0.22 numerical aperture) volume-Bragg-grating stabilized pump diode with a power of 100 W at a wavelength of 976 nm. The driver of the pump diode operates at a current of ~16 A with a compliance voltage of ~17 V.

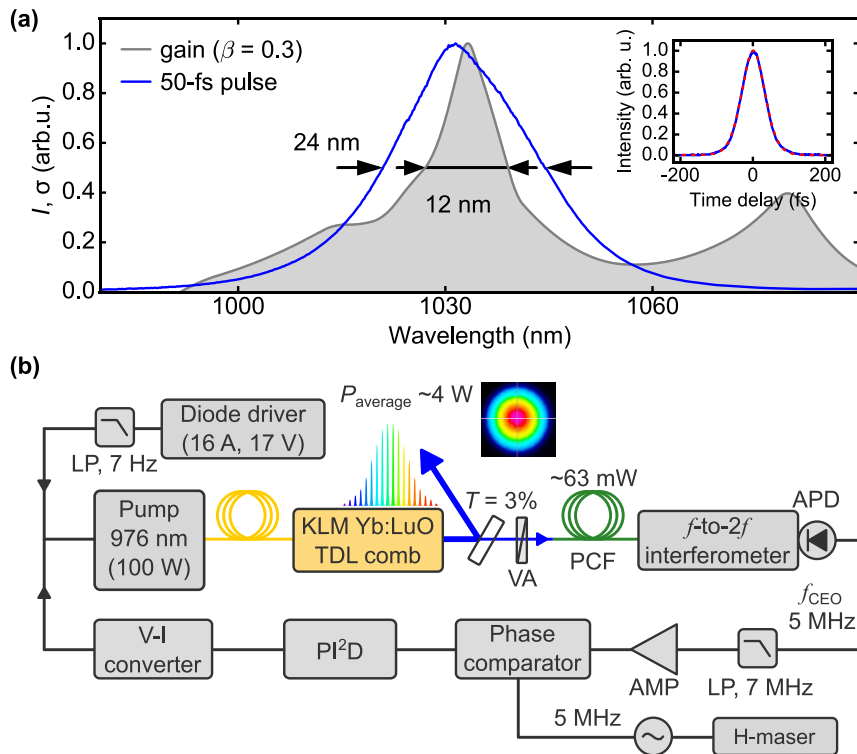


Fig. 2. (a) Optical spectrum of the mode-locked laser operating in the strongly self-phase modulation broadened regime and gain spectrum of Yb:Lu₂O₃ for an inversion level of $\beta = 0.3$ (data taken from [22]); inset: auto-correlation trace of the 50-fs pulses with a sech² fit for soliton pulses (dashed red line). (b) Schematic of the experimental setup for f_{CEO} detection and stabilization. The beam profile is shown in mode-locked operation. Electrical connections are indicated by black lines. AMP: amplifier; APD: avalanche photodiode; LP: low-pass filter; P_{average} : average power; PCF: photonic crystal fiber; T : transmission; VA, variable attenuator; V-I converter: voltage-to-current converter; PI²D: proportional-double-integral-derivative servo controller; \sim : signal generator.

A MHz-bandwidth modulation of the pump current is enabled by an in-house-developed voltage-to-current (V-I) converter that delivers up to ± 1 A of current for ± 10 V of applied voltage modulation. The transfer function of its output current was measured using a lock-in amplifier for a modulation of the input voltage (Fig. 3). The V-I converter induces a -90° phase shift at a frequency around 2 MHz. It was connected to the pump diode in parallel to the diode driver. Cross-talks between both current sources were prevented using a low-pass RC-filter with a cut-off frequency of 7 Hz (0.22Ω , 0.1 F), which attenuates at the same time the noise of the high current DC source.

3.2.3 *Transfer functions*

The transfer function of the pump power was measured at a typical operating point of the pump diode of 16 A, corresponding to an emitted power of 100 W. Around this point, the pump current was modulated by the V-I converter with a peak-to-peak amplitude of 20 mA, corresponding to a relative pump power modulation of $\pm 0.06\%$. The transfer function shows a nearly constant amplitude response up to about 10 kHz, followed by a slight decrease resulting in a 3-dB bandwidth of around 100 kHz (Fig. 3). The -90° phase shift in the phase response is reached at around 1.5 MHz.

In the subsequent step, we investigated the transfer function of the laser output power for the same cavity and the same modulation applied to the input voltage of the V-I converter, first in cw and then in mode-locked operation. In cw operation, the laser emitted only 2.3 W at a pump power of 100 W. Its efficiency was reduced, due to the increased losses caused by the hard aperture required for the Kerr lens mode-locking scheme. The peak in the relative amplitude of the transfer function at around 15 kHz [Fig. 3(a)] is attributed to the relaxation oscillation that is typical for oscillators in cw operation. This value is in good agreement with the expected theoretical value of 18 kHz (assuming an upper state lifetime of $850 \mu\text{s}$, experimentally estimated total cavity losses of 10% and a normalized pump rate of 1.9) [23]. The large phase change associated with the relaxation oscillations limits the modulation bandwidth to ~ 20 kHz in cw operation [Fig. 3(b)].

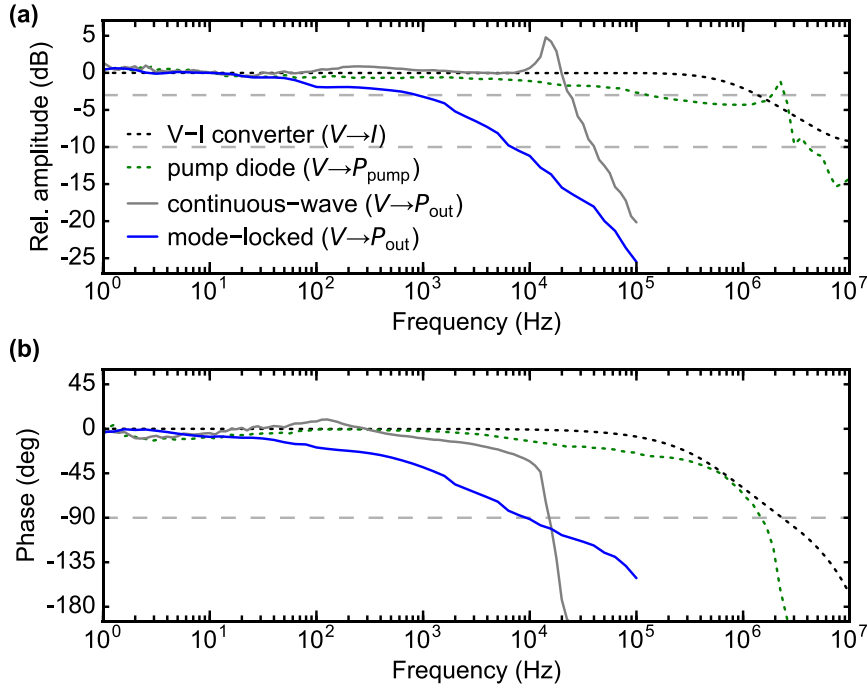


Fig. 3. Transfer functions for the modulation of the input voltage (V) of the voltage-to-current (V - I) converter. (a) Relative amplitude and (b) phase are shown in dotted lines for the resulting modulation of the pump current (I) and diode pump power (P_{pump}), and in solid lines for the output power (P_{out}) in continuous-wave and mode-locked operation. Gray dashed lines highlight a 3-dB and 10-dB drop in the relative amplitude and a -90° phase shift.

The transfer function of the laser output power in the strongly SPM-broadened regime was similarly measured at an operation current of 16 A. It is to be noted that in this case, the pump current can be varied in a range of ~ 400 mA equivalent to a change of 4 W in pump power without destabilizing the mode-locking. In this condition, the laser operated stably for hours. A 3-dB drop in the relative amplitude is reached at a frequency of around 1 kHz, while the -90° phase shift occurs near 10 kHz (Fig. 3). The amplitude response drops by an order of magnitude up to this point. The transfer function corresponds roughly to a second-order lowpass filter, which is characteristic of a laser operating in a strongly damped regime [24,25]. The frequency response and modulation bandwidth are comparable to TDL oscillators that have been successfully f_{CEO} -stabilized via pump power modulation [16,26]. Based on previous studies of Yb-DPSSL bulk [13] and TDL [16] oscillators, a similar behavior can be considered for the transfer function of the f_{CEO} . Therefore, the cavity dynamics of our KLM TDL limit the pump-current-to- f_{CEO} modulation bandwidth for CEO beat stabilization to about 10 kHz.

3.2.4 CEO beat detection and stabilization

An octave-spanning supercontinuum spectrum was generated in a photonic crystal fiber (PCF) using a small fraction of 3% of the laser output power directly from the oscillator and without the need of an additional pulse compression stage [Fig. 2(b)]. The major part of the laser output power remained accessible for applications. A variable attenuator enabled fine adjustment of the average power launched into the 2-m-long collapse-cleaved PCF (NKT Photonics, SC-3.7-975). The fiber has a core diameter of 3.7 μm , a cut-off wavelength of 975 nm and a nonlinear coefficient of γ 18 W⁻¹km⁻¹ (at 1060 nm). The coupling efficiency into the PCF was approximately 67%. From around 63 mW of launched average power, an octave-spanning supercontinuum spectrum was generated, ranging from 680 nm to 1360 nm. It was then launched into a standard quasi-common-path f -to- $2f$ interferometer for CEO-beat detection [27]. An MgO-doped periodically-poled lithium niobate (MgO:PPLN, 14.00- μm poling period, 3.0-mm length) crystal was used for second harmonic generation of the Raman soliton. The CEO beat was detected at 5 MHz with a signal-to-noise ratio >25 dB at a resolution bandwidth of 10 kHz using a fiber-coupled avalanche photodiode [Fig. 4(a)]. The free-running CEO beat fluctuated in a range of around 200 kHz in a timescale in the order of a few seconds [Fig. 4(b)]. We attribute this fluctuation to power fluctuations of the free-running pump laser. The noise of the pump power has generally the dominant contribution to the CEO frequency noise in TDLs, being pumped by highly transverse-multimode fiber coupled diode modules with power levels of several hundreds of watts [16]. This pump noise also has a significant contribution to the amplitude noise of the oscillator [16]. Therefore, the active stabilization of f_{CEO} by modulation of the pump current results in the simultaneous decrease of the amplitude noise of the oscillator up to a frequency of 10 kHz [Fig. 4(d)]. The increase in amplitude noise observed at higher frequencies of around 20 kHz is attributed to the servo bump of the CEO stabilization loop. A similar correlation between the CEO frequency noise and the amplitude noise of the mode-locked laser was also observed in other types of frequency combs based on diode-pumped solid-state lasers [12] or fiber lasers [28].

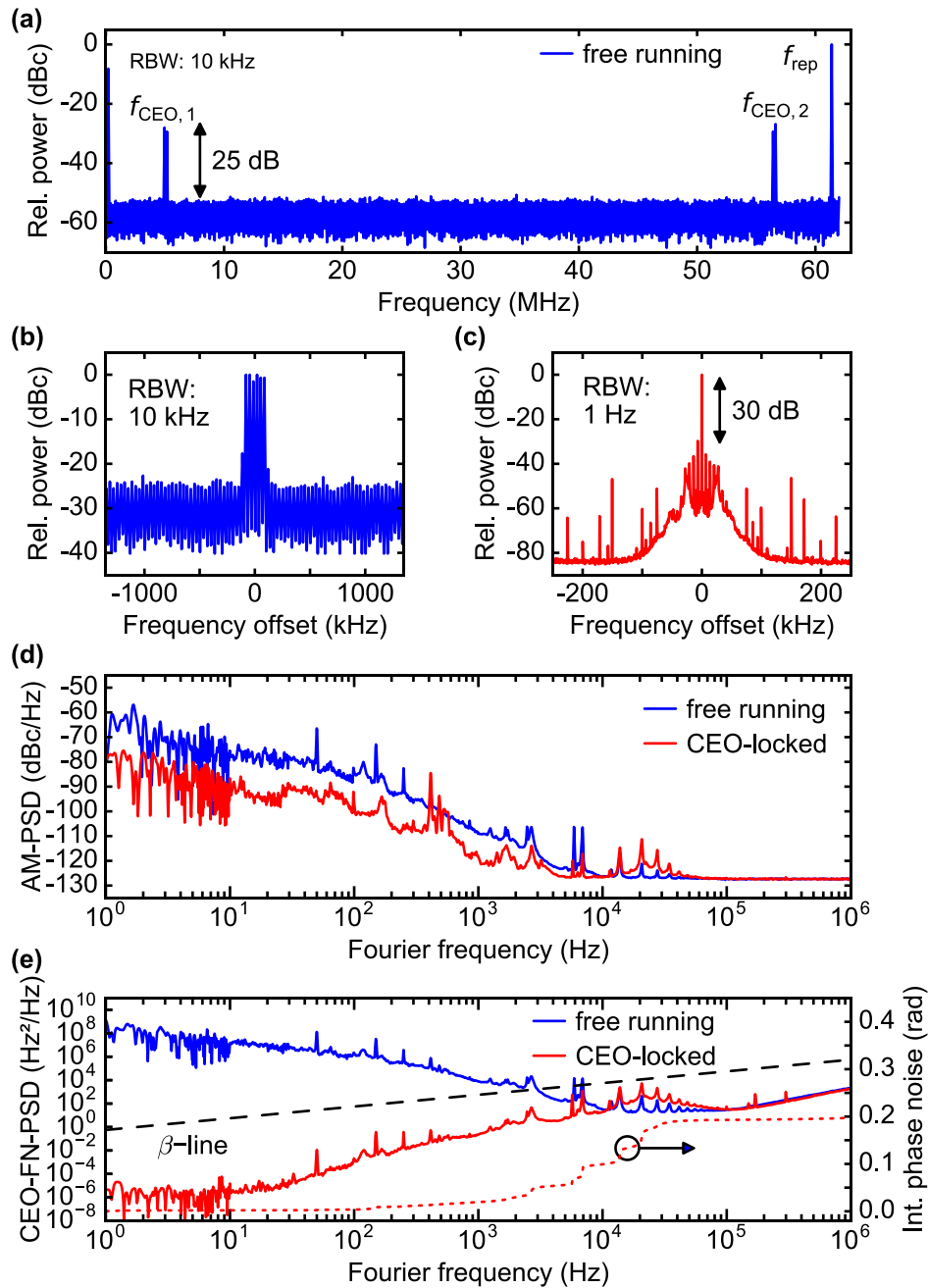


Fig. 4. (a) Radio-frequency spectrum of the free-running carrier-envelope offset (CEO) beat frequency (f_{CEO}). (b) Frequency jitter of the free-running CEO beat in a time scale of seconds and (c) coherent peak of the CEO beat spectrum when phase-locked at a central frequency of 5 MHz. (d) Relative amplitude modulation power spectral density (AM-PSD) of the laser output measured at the fundamental harmonic of the repetition frequency in free-running (blue) and CEO-locked (red) operation. (e) CEO frequency noise power spectral density (CEO-FNPSD) of the free-running (blue) and locked (red) CEO beat (left axis, solid lines) and integrated phase noise as a function of the upper cut-off frequency (right axis, dotted line). f_{rep} : repetition rate frequency; RBW: resolution bandwidth.

The detected CEO beat signal was low-pass filtered, amplified and phase-locked to an external waveform generator that was itself referenced to a hydrogen maser for long-term stable operation [Fig. 2(b)]. The phase error signal was generated using a digital phase detector and was subsequently amplified in a proportional-double-integral-derivative (PI₂D) servo-controller. The feedback signal was applied to the V-I converter to modulate the pump current. The frequency noise power spectral density (FN-PSD) of the free-running and stabilized CEO beat was directly measured from the photodiode signal with a phase-noise analyzer (Rohde-Schwarz FSWP26) [Fig. 4(e)]. From the crossing-point of the FN-PSD of the free-running CEO beat with the β -separation line [29], a feedback bandwidth in the order of 3 kHz is estimated to be necessary to achieve a tight phase lock of the f_{CEO} . When the f_{CEO} stabilization loop was activated, the noise was reduced up to a frequency of ~ 10 kHz, which is in good agreement with the -90° phase-shift bandwidth retrieved from the transfer function in mode-locked operation [Fig. 3(b)]. The servo bump appears at around 20 kHz. The residual in-loop integrated phase noise was 197 mrad (integrated from 1 Hz to 1 MHz) and is comparable to previously reported TDL oscillator results [15,26,30]. Residual spikes at 50 Hz and its harmonics as well as at 6-8 kHz and at around 20 kHz are attributed to the noise of the pump diode [16]. A tight phase-lock of the CEO beat was achieved as shown by the coherent peak with a signal-to-noise ratio of >30 dB in the radio-frequency spectrum, measured with a resolution bandwidth of 1 Hz [Fig. 4(c)]. An out-of-loop measurement of the CEO noise has not been performed since no second f -to- $2f$ interferometer was available at the time of the experiments.

3.2.5 Conclusion and outlook

In conclusion, we demonstrated the first f_{CEO} stabilization of an Yb-DPSSL oscillator operating in the strongly SPM-broadened regime. This is also the first time that a f_{CEO} stabilization is demonstrated for the gain material Yb:Lu₂O₃. The KLM Yb:Lu₂O₃ TDL oscillator generates 50-fs pulses at an average power of 4.4 W. This is to the best of our knowledge the shortest pulse duration and the highest average power that has been CEO-stabilized from an Yb-DPSSL oscillator without the need for additional amplification or pulse compression. We investigated the transfer functions of the laser output power by modulating the pump power in cw and mode-locked operation. The cavity dynamics in mode-locked operation limit the CEO modulation bandwidth to

~10 kHz. A tight phase-lock of the CEO beat has been achieved with a residual in-loop integrated phase noise of 197 mrad (integrated from 1 Hz to 1 MHz). As a next step, we will investigate the long-term stability of the CEO lock and simultaneously stabilize the repetition rate frequency for a fully-stabilized OFC. Additionally, we will investigate other f_{CEO} -stabilization techniques to increase the locking bandwidth, e.g., by implementing an optical-to-optical modulator inside the oscillator [31].

We believe that Yb-DPSSL frequency combs will benefit from the power scalability of KLM TDL oscillators [32]. The strongly SPM-broadened regime will soon enable OFCs based on Yb-DPSSL oscillators to operate directly with several tens of watts and sub-100-fs pulse durations [20]. Such systems are highly attractive as compact sources for the generation of extreme ultraviolet OFCs via high harmonics generation in gases directly driven by the oscillator [33–35].

Funding

H2020 European Research Council (ERC) (279505); National Center of Competence in Research for Molecular Ultrafast Science and Technology (NCCR-MUST); Swiss National Science Foundation (SNSF) (200020_179146 and 200021_159931).

Acknowledgments

Experimental results presented in this work are open-access available under DOI: <http://doi.org/10.23728/b2share.35123c2043e9405d9a2891f368dbec4e>

References

1. D. J. Jones, S. A. Diddams, J. K. Ranka, A. Stentz, R. S. Windeler, J. L. Hall, and S. T. Cundiff, "Carrier-Envelope Phase Control of Femtosecond Mode-Locked Lasers and Direct Optical Frequency Synthesis," *Science* **288**(5466), 635–639 (2000).
2. A. Apolonski, A. Poppe, G. Tempea, C. Spielmann, T. Udem, R. Holzwarth, T. W. Hänsch, and F. Krausz, "Controlling the Phase Evolution of Few-Cycle Light Pulses," *Phys. Rev. Lett.* **85**(4), 740–743 (2000).
3. A. Schliesser, N. Picqué, and T. W. Hänsch, "Mid-infrared frequency combs," *Nat. Photonics* **6**(7), 440–449 (2012).
4. S. A. Diddams, "The evolving optical frequency comb [Invited]," *J. Opt. Soc. Am. B* **27**(11), B51–B62 (2010).
5. K. Gürel, V. J. Wittwer, S. Hakobyan, S. Schilt, and T. Südmeyer, "Carrier envelope offset frequency detection and stabilization of a diode-pumped mode-locked Ti:sapphire laser," *Opt. Lett.* **42**(6), 1035–1038 (2017).
6. M. E. Fermann and I. Hartl, "Ultrafast Fiber Laser Technology," *IEEE J. Sel. Top. Quantum Electron.* **15**(1), 191–206 (2009).

7. S. A. Meyer, J. A. Squier, and S. A. Diddams, "Diode-pumped Yb:KYW femtosecond laser frequency comb with stabilized carrier-envelope offset frequency," *Eur. Phys. J. D* **48**(1), 19–26 (2008).
8. S. Schilt and T. Südmeyer, "Carrier-Envelope Offset Stabilized Ultrafast Diode-Pumped Solid-State Lasers," *Appl. Sci.* **5**(4), 787–816 (2015).
9. D. T. Reid, C. M. Heyl, R. R. Thomson, R. Trebino, G. Steinmeyer, H. H. Fielding, R. Holzwarth, Z. Zhang, P. Del'Haye, T. Südmeyer, G. Mourou, T. Tajima, D. Faccio, F. J. M. Harren, and G. Cerullo, "Roadmap on ultrafast optics," *J. Opt.* **18**(9), 093006 (2016).
10. R. J. Jones, K. D. Moll, M. J. Thorpe, and J. Ye, "Phase-Coherent Frequency Combs in the Vacuum Ultraviolet via High-Harmonic Generation inside a Femtosecond Enhancement Cavity," *Phys. Rev. Lett.* **94**(19), 193201 (2005).
11. A. K. Mills, T. J. Hammond, M. H. C. Lam, and D. J. Jones, "XUV frequency combs via femtosecond enhancement cavities," *J. Phys. B At. Mol. Opt. Phys.* **45**(14), 142001 (2012).
12. A. Klenner, S. Schilt, T. Südmeyer, and U. Keller, "Gigahertz frequency comb from a diode-pumped solid-state laser," *Opt. Express* **22**(25), 31008–31019 (2014).
13. S. Hakobyan, V. J. Wittwer, P. Brochard, K. Gürel, S. Schilt, A. S. Mayer, U. Keller, and T. Südmeyer, "Full stabilization and characterization of an optical frequency comb from a diode-pumped solid-state laser with GHz repetition rate," *Opt. Express* **25**(17), 20437–20453 (2017).
14. Z. Yu, H. Han, Y. Xie, Y. Peng, X. Xu, and Z. Wei, "CEO stabilized frequency comb from a 1- μm Kerr-lens mode-locked bulk Yb:CYA laser," *Opt. Express* **24**(3), 3103–3111 (2016).
15. A. Klenner, F. Emaury, C. Schriber, A. Diebold, C. J. Saraceno, S. Schilt, U. Keller, and T. Südmeyer, "Phase-stabilization of the carrier-envelope-offset frequency of a SESAM modelocked thin disk laser," *Opt. Express* **21**(21), 24770–24780 (2013).
16. F. Emaury, A. Diebold, A. Klenner, C. J. Saraceno, S. Schilt, T. Südmeyer, and U. Keller, "Frequency comb offset dynamics of SESAM modelocked thin disk lasers," *Opt. Express* **23**(17), 21836–21856 (2015).
17. S. Gröbmeyer, J. Brons, M. Seidel, and O. Pronin, "100 W-level carrier-envelope-phase stable thin-disk oscillator," in 8th EPS-QEOD Europhoton conference, (2018), paper FrM2.2.
18. C. Kränkel, "Rare-earth-doped sesquioxides for diode-pumped high-power lasers in the 1-, 2-, and 3- μm spectral range," *IEEE J. Sel. Top. Quantum Electron.* **21**(1), 250–262 (2015).
19. J. Zhang, J. Brons, M. Seidel, V. Pervak, V. Kalashnikov, Z. Wei, A. Apolonski, F. Krausz, and O. Pronin, "49-fs Yb:YAG thin-disk oscillator with distributed Kerr-lens mode-locking," in European Quantum Electronics Conference (Optical Society of America, 2015), paper PD_A_1.
20. C. Paradis, N. Modsching, V. J. Wittwer, B. Deppe, C. Kränkel, and T. Südmeyer, "Generation of 35-fs pulses from a Kerr lens mode-locked Yb:Lu₂O₃ thin-disk laser," *Opt. Express* **25**(13), 14918–14925 (2017).
21. N. Bucalovic, V. Dolgovskiy, M. C. Stumpf, C. Schori, G. Di Domenico, U. Keller, S. Schilt, and T. Südmeyer, "Effect of the carrier-envelope-offset dynamics on the stabilization of a diode-pumped solid-state frequency comb," *Opt. Lett.* **37**(21), 4428–4430 (2012).
22. T. Südmeyer, C. Kränkel, C. R. E. Baer, O. H. Heckl, C. J. Saraceno, M. Golling, R. Peters, K. Petermann, G. Huber, and U. Keller, "High-power ultrafast thin disk laser oscillators and their potential for sub-100-femtosecond pulse generation," *Appl. Phys. B* **97**(2), 281–295 (2009).
23. A. E. Siegman, *Lasers* (Univ. Science Books, 1986).
24. A. Schlatter, S. C. Zeller, R. Grange, R. Paschotta, and U. Keller, "Pulse-energy dynamics of passively mode-locked solid-state lasers above the Q-switching threshold," *JOSA B* **21**(8), 1469–1478 (2004).
25. L. Matos, O. D. Mücke, J. Chen, and F. X. Kärtner, "Carrier-envelope phase dynamics and noise analysis in octave-spanning Ti: sapphire lasers," *Opt. Express* **14**(6), 2497–2511 (2006).
26. M. Seidel, J. Brons, F. Lücking, V. Pervak, A. Apolonski, T. Udem, and O. Pronin, "Carrier-envelope-phase stabilization via dual wavelength pumping," *Opt. Lett.* **41**(8), 1853 (2016).

27. H. R. Telle, G. Steinmeyer, A. E. Dunlop, J. Stenger, D. H. Sutter, and U. Keller, "Carrier-envelope offset phase control: A novel concept for absolute optical frequency measurement and ultrashort pulse generation," *Appl. Phys. B* **69**(4), 327–332 (1999).
28. C. Benko, A. Ruehl, M. J. Martin, K. S. E. Eikema, M. E. Fermann, I. Hartl, and J. Ye, "Full phase stabilization of a Yb:fiber femtosecond frequency comb via high-bandwidth transducers," *Opt. Lett.* **37**(12), 2196–2198 (2012).
29. G. Di Domenico, S. Schilt, and P. Thomann, "Simple approach to the relation between laser frequency noise and laser line shape," *Appl. Opt.* **49**(25), 4801–4807 (2010).
30. O. Pronin, M. Seidel, F. Lücking, J. Brons, E. Fedulova, M. Trubetskov, V. Pervak, A. Apolonski, T. Udem, and F. Krausz, "High-power multi-megahertz source of waveform-stabilized few-cycle light," *Nat. Commun.* **6**, 6988 (2015).
31. K. Gürel, S. Hakobyan, V. J. Wittwer, S. Schilt, and T. Südmeyer, "Frequency Comb Stabilization of Ultrafast Lasers by Opto-Optical Modulation of Semiconductors," *IEEE J. Sel. Top. Quantum Electron.* **24**(5), 1–9 (2018).
32. J. Brons, V. Pervak, E. Fedulova, D. Bauer, D. Sutter, V. Kalashnikov, A. Apolonskiy, O. Pronin, and F. Krausz, "Energy scaling of Kerr-lens mode-locked thin-disk oscillators," *Opt. Lett.* **39**(22), 6442–6445 (2014).
33. F. Emaury, A. Diebold, C. J. Saraceno, and U. Keller, "Compact extreme ultraviolet source at megahertz pulse repetition rate with a low-noise ultrafast thin-disk laser oscillator," *Optica* **2**(11), 980–984 (2015).
34. F. Labaye, M. Gaponenko, V. J. Wittwer, A. Diebold, C. Paradis, N. Modsching, L. Merceron, F. Emaury, I. J. Graumann, C. R. Phillips, C. J. Saraceno, C. Kränkel, U. Keller, and T. Südmeyer, "Extreme ultraviolet light source at a megahertz repetition rate based on high-harmonic generation inside a mode-locked thin-disk laser oscillator," *Opt. Lett.* **42**(24), 5170–5173 (2017).
35. M. Gaponenko, F. Labaye, P. Brochard, N. Modsching, K. Gürel, V. J. Wittwer, C. Paradis, C. Kränkel, S. Schilt, and T. Südmeyer, "CEO frequency stabilization of a thin disk laser with intracavity high harmonic generation," in 8th EPS-QEOD Europhoton conference, (2018), paper FrM2.6.

3.3 Towards TDL-based frequency combs

This preliminary study investigates the simultaneous stabilization of the f_{CEO} and the f_{rep} . The f_{CEO} stabilization was already discussed in detail in section 3.2. The extended schematic of the experimental setup for full frequency comb stabilization is shown in Fig. 1. The repetition rate was detected on a photodiode with sufficient bandwidth. The signal was filtered and mixed with a referenced waveform generator. The resulting error signal was low-pass filtered and send to a proportional-integral (PI) servo controller. The output of the PI servo controller was amplified to high voltage and applied to the piezoelectric transducer (PZT). The PZT controlled the position of a cavity-folding mirror for stabilization of the f_{rep} .

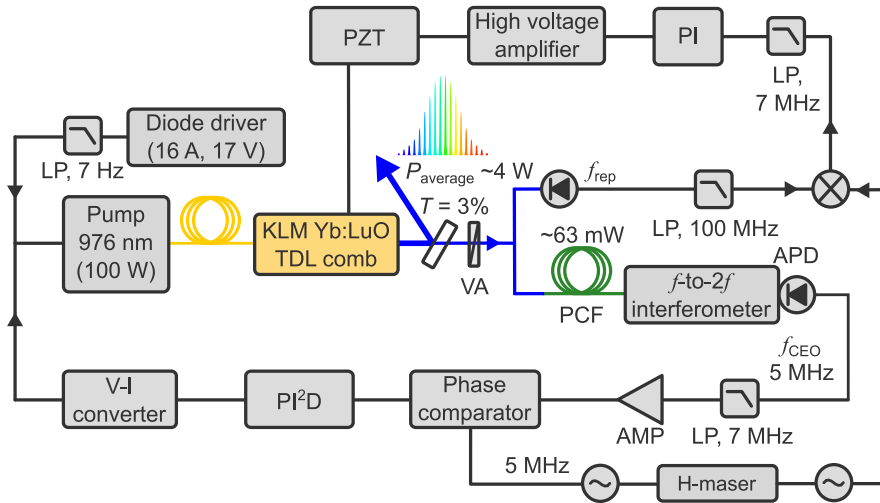


Fig. 1. Schematic of the experimental setup for f_{CEO} and f_{rep} detection and stabilization of the KLM Yb:Lu₂O₃ TDL oscillator. Electrical connections are highlighted as black lines. Blue lines indicate free space beam propagation. AMP: amplifier; APD: avalanche photodiode; LP: low-pass filter; P_{average} : average power; PCF: photonic crystal fiber; T : transmission; VA, variable attenuator; V-I converter: voltage-to-current converter; PI²D: proportional-double-integral-derivative servo controller; PI: proportional-integral servo controller; PZT: piezoelectric transducer; \sim : signal generator.

The transfer function of the PZT onto the f_{rep} shows a -90° shift in the phase / 3-dB bandwidth at around 3 kHz (Fig. 2). The bandwidth is attributed to the mass of mirror that was mounted onto the PZT ($\frac{1}{2}$ inch diameter, 6 mm thick). During the presented investigation the f_{CEO} was locked first and a tight-lock was assured by measuring its frequency noise power spectral density. Then, the f_{rep} -stabilization loop was activated

as second. Cross-talking between both stabilization loops was observed. A too high response in the PI controller of the f_{rep} -stabilization loop resulted repeatably in the loss of the f_{CEO} stabilization. As such, the response of the PI controller was decreased until both stabilization loops stayed locked simultaneously.

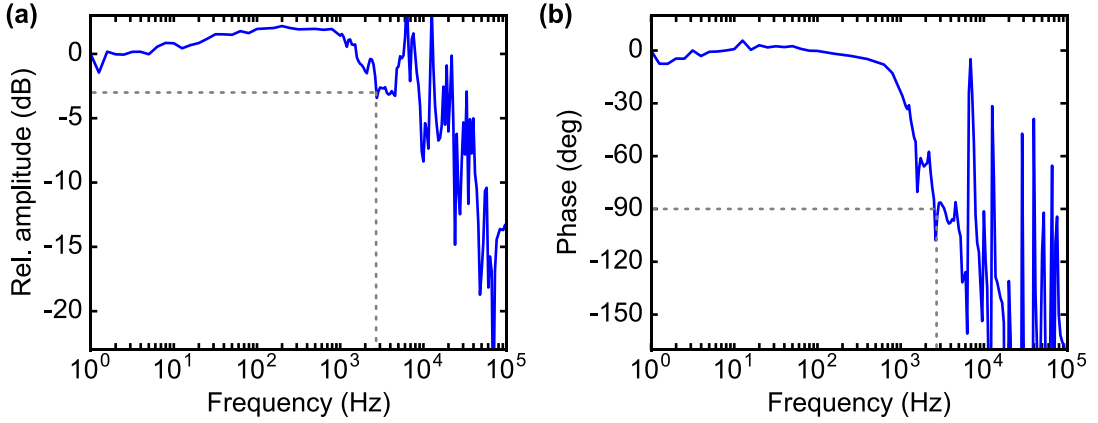


Fig. 2. Transfer function modulating the piezoelectric transducer voltage onto the f_{rep} for the (a) normalized amplitude and (b) phase. The dashed lines represent a 3-dB drop in relative amplitude and a -90° phase shift.

The resulting f_{rep} stabilization shows a decrease in the frequency noise up to a bandwidth of ~ 35 Hz [Fig. 3(a)]. This value is well below the 3 kHz bandwidth determined by the transfer-function. It is attributed to the reduced response of the PI servo controller. The f_{rep} stabilization decreased the timing jitter by about an order of magnitude from 60 ps to 7 ps (integrated from 1 Hz to 1 MHz). Cross-talking between both stabilization loops resulted in an increased f_{CEO} noise, mainly at around 20 kHz [Fig. 3(b)]. This range is surprisingly well beyond the 3 kHz transfer-function bandwidth of the PZT. At the same time increased cross-talking the integrated phase noise from 197 mrad to 745 mrad. This observation explains the previous mentioned loss of the f_{CEO} lock with too high gain in the f_{rep} -stabilization loop. Potential origins could be piezo resonances or issues in the electronics, i.e. electromagnetic coupling between the high voltage amplifier and other devices. Cross-talking increased as well the f_{CEO} noise negligibly up to the bandwidth of the f_{rep} stabilization at ~ 35 Hz [Fig. 3(b)]. Both stabilization loops could be kept simultaneously locked in the range of minutes. The limited travel range of the PZT was not able to compensate for the long-term f_{rep} drift of the meter-long cavity length.

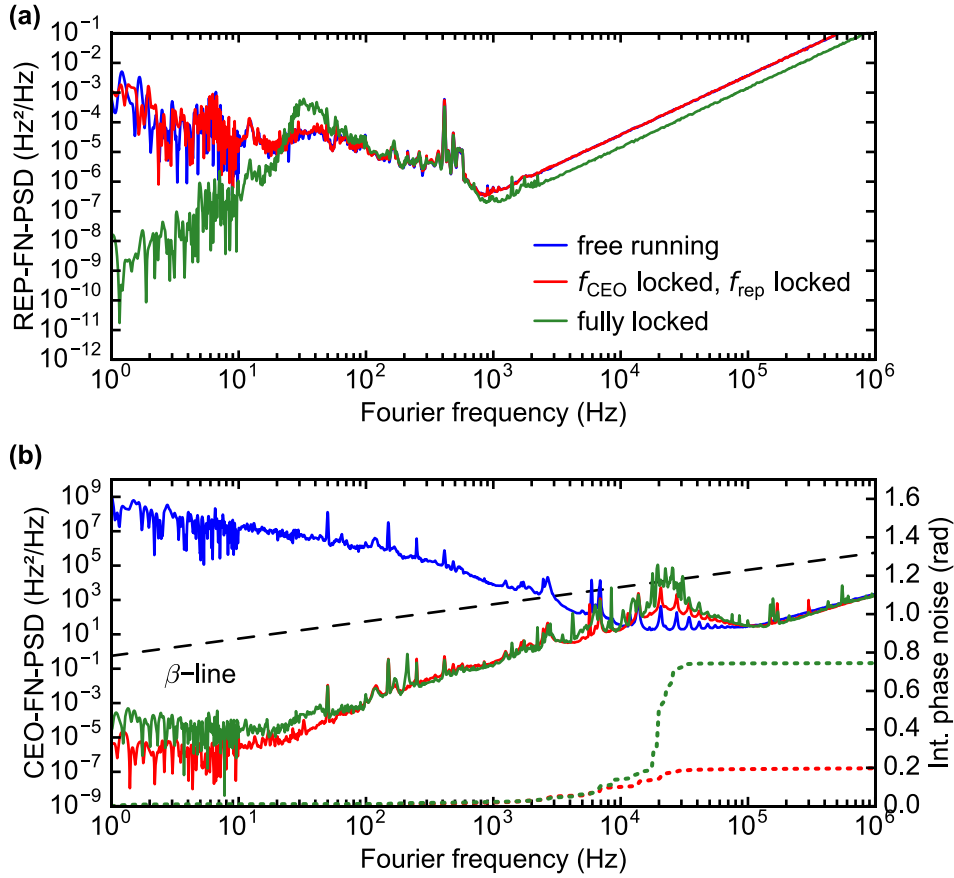


Fig. 3. Noise performance of the sub-100-fs KLM TDL oscillator of different configuration of the stabilization (a) f_{rep} frequency noise power spectral density (REP-FN-PSD); (b) f_{CEO} frequency noise power spectral density (CEO-FN-PSD); (right-axis) corresponding integrated phase noise as a function of the upper cut-off frequency.

This preliminary investigation demonstrates that full frequency comb stabilization of sub-100-fs KLM TDL oscillators operating in the SPM-broadened regime is possible. Yet, further investigations need to determine the cross-talking between both stabilization loops. In this particular study, the origin of the introduced noise at around 20 kHz is of high interest. Once this noise source has been eliminated, f_{rep} stabilization with larger bandwidth and reduced timing jitter can be expected while the tight lock of the f_{CEO} should be maintained. For long-term f_{rep} stabilization a combination of two PZT is suggested. A slow PZT for the correction of the long-term drift with sufficient travel range and a PZT optimized for response at higher frequencies. Additionally, the reduction of the mirror mass that is attached to the PZT is recommended for a larger f_{rep} -stabilization bandwidth.

Chapter 4

THz generation driven by sub-100-fs thin-disk laser oscillators

This chapter presents the application of the developed sub-100-fs KLM Yb:Lu₂O₃ TDL oscillators (chapter 2) for the generation and detection of quasi single-cycle broadband THz pulses at MHz repetition rates.

4.1 Powerful Yb-based lasers for THz generation

Table-top broadband THz sources operating at MHz repetition rates are of interest for various spectroscopic and imaging applications [1]. Among several techniques, optical rectification (OR) of sub-100-fs pulses in $X^{(2)}$ nonlinear crystals has become a suitable approach for the generation of broadband THz pulses at high repetition rates [1,2]. However, conversion efficiencies in the order of 10^{-2} to 10^{-5} limit currently the available THz average power [3,4]. As such, THz sources for hands-on applications would strongly benefit to be driven by simple yet powerful ultrafast laser systems.

Ultrafast laser systems based on Ti:sapphire benefit from the available broad gain bandwidth for the direct generation of sub-100-fs pulse durations. However, thermal effects in the gain medium limit their average power to several watts [5]. In contrast, ultrafast Yb-based laser systems utilizing gain geometries for optimized heat dissipation (fiber, slab, thin disk) can operate at the kW-level of average power [6-8]. But, these systems rely often on multiple amplification stages and the limited gain

bandwidth of Yb-based gain materials requires typically a nonlinear pulse compression to reach sub-100-fs pulse durations.

The developed sub-100-fs KLM Yb:Lu₂O₃ TDL oscillators (chapter 2) possess suitable properties as single-stage driving laser for THz generation. Sub-100-fs pulses allow for the direct generation and detection of broadband THz radiation from the output of the oscillator, circumventing the need for amplification and nonlinear pulse compression.

In the framework of this thesis THz generation via OR in gallium phosphide (GaP) was investigated in the 1- μ m wavelength range. GaP is a semiconductor material which phase velocity in the THz range matches the group velocity of the driving pulse in the 1- μ m range. This makes GaP suitable for THz generation driven by Yb-based laser systems [9–12]. GaP offers a large rectification bandwidth of up to 40 THz, but possess a transverse optical phonon resonance at 11 THz [13]. Although OR in GaP has been intensively studied at the 800-nm range of Ti:Sapphire lasers [14,15], the 1- μ m range of Yb-based laser systems remained still less explored.

Section 4.2 presents broadband THz generation and detection directly driven by the developed sub-100-fs KLM Yb:Lu₂O₃ TDL oscillator (section 2.2). In this investigation the oscillator generated 50-fs pulses at 4 W of average power and 61 MHz of repetition rate. Key messages of the investigation are:

- First demonstration of THz generation driven by a TDL oscillator
- Generation of a THz spectrum extending up to 7 THz; gaps in the THz spectrum are attributed to the phase mismatch in GaP
- Spectroscopic characterization of GaP in the THz range; resulting phase matching calculations are in good agreement with the observed features in the THz spectra
- Benchmark measurement for applications in linear THz time-domain spectroscopy by measuring the absorption spectrum of water vapor in the range of 1 to 5 THz

Section 4.3 presents a more detailed investigation of the impact of the GaP crystal thickness and driving pulse duration at 1- μ m onto the generated THz spectrum. In the first part of the experiment, the generated THz spectrum was investigated for three different GaP crystal thicknesses using a 50-fs configuration of the driving KLM

Yb:Lu₂O₃ TDL oscillator (section 2.2). In a second part of the experiment, the driving pulse duration was varied by adjusting the amount of introduced group delay dispersion, output coupler transmission and hard aperture diameter of the TDL oscillator. This enabled high-fidelity measurements with almost transform-limited solution pulses at discrete pulse durations ranging between 50 fs and 220 fs. Based on the experimental results a procedure is presented allowing to estimate the THz spectrum via multiplicative factors in the frequency domain. Power-scaling of the sub-100-fs KLM Yb:Lu₂O₃ TDL oscillator (section 2.3) allowed driving OR in GaP with 95-fs pulses at 20 W of average power and 48 MHz of repetition rate. The key results of this investigation are:

- Experimental investigation of the THz spectrum achievable by OR at the 1- μ m range in GaP in function of the GaP crystal thickness and the driving pulse duration
- A simple procedure is presented to estimate the THz spectrum generated by OR at 1- μ m in GaP in dependence of the crystal thickness and driving pulse duration
- Generation of a gap-less THz spectrum extending up to 7 THz
- Generation of 0.3 mW of THz average power in a THz spectrum extending to nearly 5 THz.

References

1. P. U. Jepsen, D. G. Cooke, and M. Koch, "Terahertz spectroscopy and imaging - Modern techniques and applications," *Laser Photonics Rev.* **5**(1), 124–166 (2011).
2. C. J. Saraceno, "Mode-locked thin-disk lasers and their potential application for high-power terahertz generation," *J. Opt.* **20**(4), 044010 (2018).
3. K. Reimann, "Table-top sources of ultrashort THz pulses," *Rep. Prog. Phys.* **70**(10), 1597 (2007).
4. J. A. Fülöp, L. Pálfalvi, G. Almási, and J. Hebling, "Design of high-energy terahertz sources based on optical rectification," *Opt. Express* **18**(12), 12311 (2010).
5. S. Dewald, T. Lang, C. D. Schröter, R. Moshhammer, J. Ullrich, M. Siegel, and U. Morgner, "Ionization of noble gases with pulses directly from a laser oscillator," *Opt. Lett.* **31**(13), 2072–2074 (2006).
6. P. Russbueldt, T. Mans, J. Weitenberg, H. D. Hoffmann, and R. Poprawe, "Compact diode-pumped 1.1 kW Yb:YAG Innoslab femtosecond amplifier," *Opt. Lett.* **35**(24), 4169–4171 (2010).
7. J.-P. Negel, A. Loescher, A. Voss, D. Bauer, D. Sutter, A. Killi, M. A. Ahmed, and T. Graf, "Ultrafast thin-disk multipass laser amplifier delivering 1.4 kW (47 mJ, 1030 nm) average power converted to 820 W at 515 nm and 234 W at 343 nm," *Opt. Express* **23**(16), 21064 (2015).
8. M. Müller, A. Klenke, A. Steinkopff, H. Stark, A. Tünnermann, and J. Limpert, "3.5 kW coherently combined ultrafast fiber laser," *Opt. Lett.* **43**(24), 6037–6040 (2018).

9. J. Li, L. Chai, J. Shi, F. Liu, B. Liu, B. Xu, M. Hu, Y. Li, Q. Xing, C. Wang, A. B. Fedotov, and A. M. Zheltikov, "Generation of 0.3 mW high-power broadband terahertz pulses from GaP crystal pumped by negatively chirped femtosecond laser pulses," *Laser Phys. Lett.* **10**(12), 125404 (2013).
10. J. Hamazaki, K. Furusawa, N. Sekine, A. Kasamatsu, and I. Hosako, "Effects of chirp of pump pulses on broadband terahertz pulse spectra generated by optical rectification," *Jpn. J. Appl. Phys.* **55**(11), 110305 (2016).
11. J. Xu, B. Globisch, C. Hofer, N. Lilienfein, T. Butler, N. Karpowicz, and I. Pupeza, "Three-octave terahertz pulses from optical rectification of 20-fs, 1- μ m, 78-MHz pulses in GaP," *J. Phys. B At. Mol. Opt. Phys.* **51**(15), 154002 (2018).
12. G. Chang, C. J. Divin, C.-H. Liu, S. L. Williamson, A. Galvanauskas, and T. B. Norris, "Power scalable compact THz system based on an ultrafast Yb-doped fiber amplifier," *Opt. Express* **14**(17), 7909-7913 (2006).
13. A. Leitenstorfer, S. Hunsche, J. Shah, M. C. Nuss, and W. H. Knox, "Detectors and sources for ultrabroadband electro-optic sampling: experiment and theory," *Appl. Phys. Lett.* **74**(11), 1516 (1999).
14. Q. Wu and X.-C. Zhang, "7 terahertz broadband GaP electro-optic sensor," *Appl. Phys. Lett.* **70**(14), 1784-1786 (1997).
15. K. Aoki, J. Savolainen, and M. Havenith, "Broadband terahertz pulse generation by optical rectification in GaP crystals," *Appl. Phys. Lett.* **110**(20), 201103 (2017).

4.2 Broadband terahertz pulse generation driven by an ultrafast thin-disk laser oscillator

Clément Paradis,^{1,*} Jakub Drs,¹ Norbert Modsching,¹ Olga Razskazovskaya,¹ Frank Meyer,² Christian Kränkel,³ Clara J. Saraceno,² Valentin J. Wittwer,¹ and Thomas Südmeyer¹

¹*Laboratoire Temps-Fréquence, Institut de Physique, Université de Neuchâtel, Avenue de Bellevaux 51, 2000 Neuchâtel, Switzerland*

²*Photonics and Ultrafast Laser Science, Ruhr Universität Bochum, 44801 Bochum, Germany*

³*Center for Laser Materials, Leibniz-Institut für Kristallzüchtung, Max-Born-Str. 2, 12489 Berlin, Germany*

We demonstrate broadband THz generation driven by an ultrafast thin-disk laser (TDL) oscillator. By optical rectification of 50-fs pulses at 61 MHz repetition rate in a collinear geometry in crystalline GaP, THz radiation with a central frequency at around 3.4 THz and a spectrum extending from below 1 THz to nearly 7 THz are generated. We realized a spectroscopic characterization of a GaP crystal and a benchmark measurement of the water-vapor absorption spectrum in the THz range. Sub-50-GHz resolution is achieved within a 5 THz bandwidth. Our experiments show the potential of ultrafast TDL oscillators for driving MHz-repetition-rate broadband THz systems.

4.2.1 Introduction

THz time-domain spectroscopy (THz-TDS) is a powerful tool to explore material properties and the dynamics of complex molecular systems through static and time-resolved investigations [1–5]. The employed THz source must fulfill a set of requirements including a spectral coverage in agreement with the studied system and a sufficient signal-to-noise ratio. Additionally, a compact system and a short acquisition time are often preferable. These criteria result in the demand for table-top high-power high-repetition-rate broadband THz sources.

Amongst other techniques, optical rectification of femtosecond pulses is a well-suited approach to produce high-power broadband THz radiation [6,7]. The

development of THz sources based on optical rectification has been closely linked to the advances of sub-100-fs Ti:sapphire laser systems, which contributed to tremendous progress in this area. The efficiency of the optical rectification process is typically in the order of 10^{-7} to 10^{-2} [6,7]. Therefore, THz systems would benefit from power scalable laser technology. Recently developed diode-pumped ultrafast Yb-based lasers emitting at $\sim 1 \mu\text{m}$ central wavelength demonstrated operation at average powers up to the kW level and high repetition rates with hundreds of femtosecond pulse duration [8–11]. In these lasers, detrimental thermal effects are significantly reduced due to alternative gain medium geometries (fibre, slab, thin disk) which allow for an efficient heat dissipation.

Most commonly, high-power ultrafast lasers rely on amplifier schemes based on complex multi-stage architecture (typically a seeding master oscillator, pulse stretching, multiple amplification stages and compression). In contrast, ultrafast thin-disk laser (TDL) oscillators offer a one-box solution for delivering nearly-ideal sech^2 -shaped femtosecond pulses at MHz repetition rates, high average powers in diffraction-limited Gaussian beams. Nearly 300 W of average power have been achieved [12,13], but TDL oscillators typically operate at pulse durations longer than 100 fs [14]. However, sub-100-fs TDL oscillators based on broadband gain materials were recently demonstrated, albeit at moderate average power [15].

Despite appropriate laser parameters, Yb-based laser technology remains widely unexplored for THz generation [16]. Only few results have been reported attempting to use Yb-based lasers to produce THz radiation. A high average power of 4 mW with a spectrum extending up to 1.2 THz has been demonstrated using tilted pulse front optical rectification in LiNbO_3 from 7 W average pump power and 1.3 ps pulse duration delivered by a 1 kHz repetition rate regenerative amplifier based on an Yb:YAG thin-disk crystal [17]. Compared to LiNbO_3 , broader spectra are achieved in semiconductors such as ZnTe and GaP due to a broad collinear phase matching in the near infrared [18–20]. GaP has a large rectification bandwidth up to 40 THz, although it possesses a transverse optical phonon resonance at 11 THz [19]. Despite the associated dispersion, collinear phase matching up to 8 THz is achievable using crystal thicknesses in the order of hundreds of microns [21]. In 2006, the first experiments of optical rectification in GaP conducted with an Yb-based ultrafast pump laser yielded $6.5 \mu\text{W}$ THz average power from a 10-W 210-fs fiber amplifier operating at 120 MHz

[22]. Later in 2013, 300 μW THz average power has been obtained with frequency content up to 2 THz using an Yb-doped fibre amplifier delivering 21 W of average power in 52-fs pulses at a repetition rate of 42 MHz [23]. Broad spectra with frequency content up to 5 THz have been achieved both from a 3-W, 120-fs, 100-MHz Yb-doped fibre laser amplifier [24] and a 5-W, 20-fs, 78-MHz Yb-doped fibre laser amplifier [25]. Here, we report on MHz-repetition-rate broadband THz generation using the output of a mode-locked TDL. The 50-fs oscillator allows for a pulse-compression-free generation and detection of THz radiation up to 7 THz via optical rectification and electro-optic sampling (EOS) in crystalline GaP in a simple collinear geometry. Employing this THz source, we refine the Sellmeier coefficients of GaP in the THz range, enabling accurate phase matching calculations. Additionally, we benchmarked our system via THz spectroscopy of water vapor. Due to their power scalability and the high temporal resolution provided by sub-100-fs pump pulses, we believe that this result confirms the potential of ultrafast TDL oscillators to drive high-power broadband THz sources for static and time-resolved THz-TDS.

4.2.2 *Broadband THz generation and detection*

The experimental setup is depicted in Fig. 1. The driving laser source (described in [26]) is a Kerr lens mode-locked TDL oscillator based on the gain material Yb:Lu₂O₃ [27]. It delivers a diffraction limited beam ($M^2 = 1$) with 4 W of average power in 50-fs sech²-shaped pulses at 61 MHz repetition rate. This leads to >60 nJ pulse energy and >1 MW peak power available directly at the output of the laser oscillator. The optical spectrum is centered at around 1031 nm with a FWHM of 20 nm (corresponding to 5 THz). THz radiation is generated via optical rectification of the femtosecond near-infrared pulses in a <110>-cut GaP crystal. The pump pulses are pre-chirped by three dispersive mirrors accounting for -1500 fs² of group delay dispersion to compensate for the propagation through the focusing lens and crystal. The pump beam is focused into the crystal to a 45 μm $1/e^2$ beam radius. Accounting for the 20% Fresnel reflection at the front interface of the uncoated GaP crystal, the peak intensity inside the crystal is estimated to be 27 GW/cm² and the fluence 1.7 mJ/cm². These values remain below the damage threshold of the material which has been measured to be 4.3 mJ/cm² (corresponding to 60 GW/cm² peak power) at 1040 nm with 61 fs pulses [28]. We used a ~5 mm diameter mirror to deflect the unconverted pump light. Due to the stronger divergence, only a small fraction of the THz radiation

is reflected. An optical chopper running at 2.5 kHz modulates the pump beam for phase sensitive detection using a lock-in amplifier. The THz signal is then characterized via field-resolved detection using EOS in a second <110>-cut GaP [29,30]. The 50 fs gating probe pulses offer sufficient temporal resolution and do not require any additional temporal compression for a distortion-free broadband EOS measurement. The system is operated at room temperature ($\sim 22^\circ\text{C}$) in a purged atmosphere with $\sim 9\%$ relative humidity.

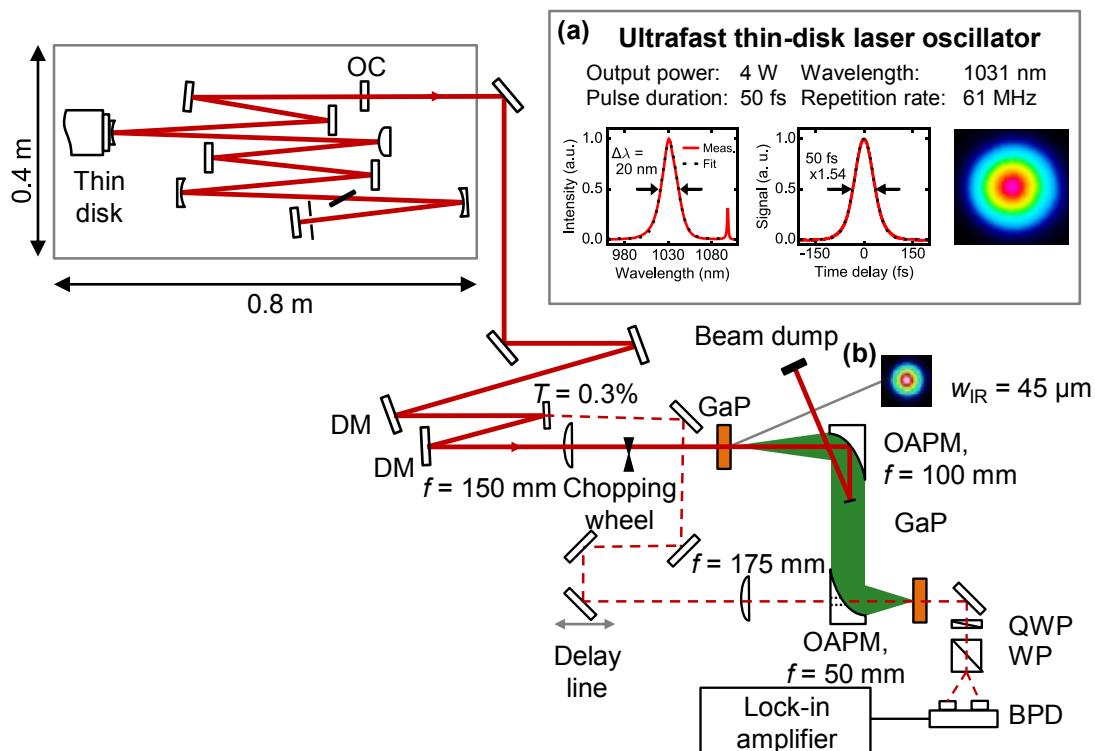


Fig. 1. Experimental setup for THz generation driven by the output of an ultrafast thin-disk laser oscillator. The inset (a) shows (from left to right) the optical spectrum, the autocorrelation trace and the output beam profile of the laser; the inset (b) shows the beam profile of the near-infrared laser at the focus. BPD: balanced photo-detector; DM: dispersive mirror; OAPM: off-axis parabolic mirror; OC: output coupler; QWP: quarter-wave plate; T: transmission; WP, Wollaston prism; w_{IR} : infrared beam radius.

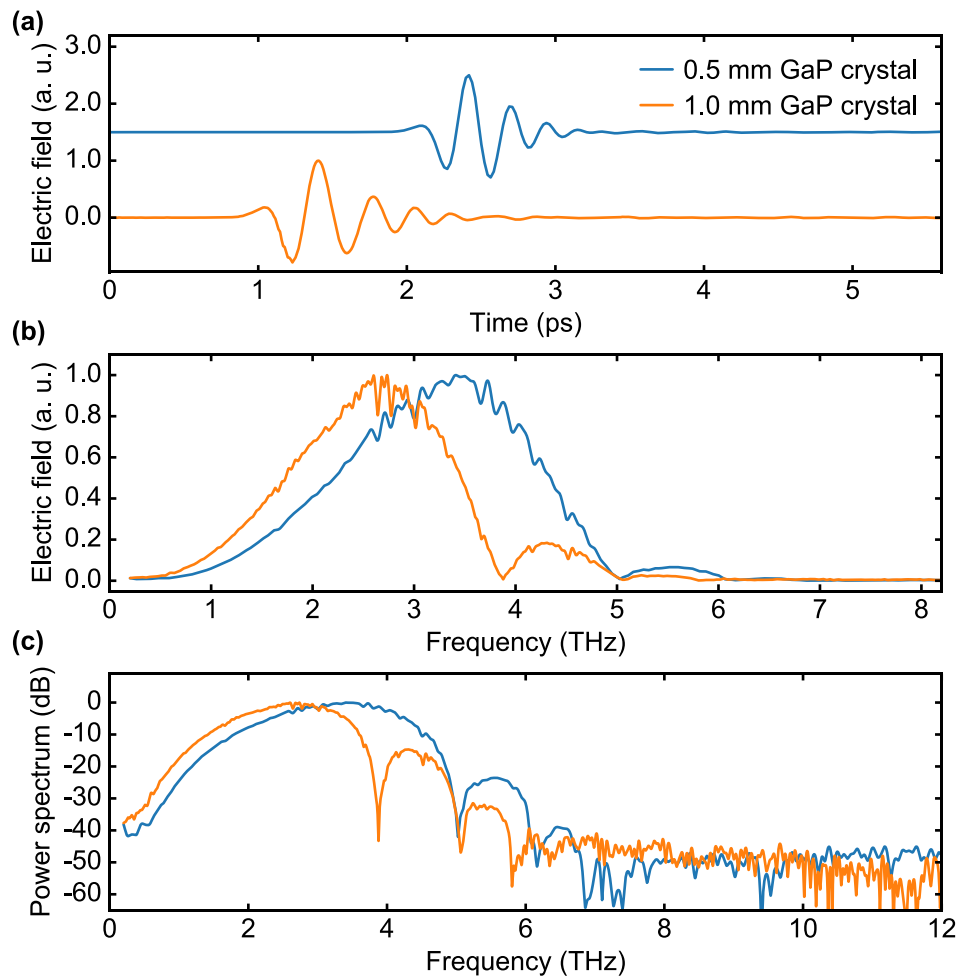


Fig. 2. (a) Time-resolved THz signals generated and detected in 0.5 mm (blue) and 1.0 mm (orange) thick GaP crystals (an offset in time and electric field has been added for better visibility) and (b) corresponding spectra of the electric field amplitude after Fourier transformation. (c) Corresponding power spectrum represented in logarithmic scale.

Quasi-single-cycle THz pulses were produced via optical rectification in 0.5 mm and 1.0 mm GaP crystals. The THz waveforms acquired in single scans with 30 ms and 10 ms integration constant, respectively, are shown in Fig. 2(a). They are detected via EOS using crystals with the same thicknesses as the rectification crystals. The corresponding THz spectra obtained by Fourier transformation of the waveforms have a central frequency at around 3.4 THz and 2.7 THz and extend up to nearly 6 THz and 7 THz, respectively [Fig. 2(b)]. The noise-like features in the spectrum are caused by residual water absorption. For both measurements, a dynamic range greater than 40 dB is achieved [Fig. 2(c)].

We evaluated the THz average power produced in the configuration with 1.0 mm GaP crystal using a calibrated pyroelectric photodetector (Ophir, RM9-THz) placed at the position of the detection crystal. The total path length from crystal to the detector is ~ 50 cm. Two filters made of black paper and fabric are used to block residual pump light. At a relative humidity level of $\sim 25\%$, we measured an average power of $0.2 \mu\text{W}$. We calibrated the measurement by characterizing the filters spectral transmission using the EOS setup. They exhibit a 2% total transmission for our spectrum. Thus the estimated THz average power is in the order of $10 \mu\text{W}$, implying a conversion efficiency in the order of 10^{-6} , which is in a reasonable agreement with results obtained with similar laser parameters [22,23,25].

4.2.3 Spectroscopic characterization of GaP

Prompted by the discrepancies among the published data [31,32], we performed an independent measurement of the refractive index of GaP in the THz region via THz-TDS [3,4]. For this, we inserted a 1.0 mm $\langle 110 \rangle$ -cut GaP test-crystal into the collimated THz beam between two 0.5 mm GaP rectification and detection crystals. Comparing the spectral phase of this measurement to a reference measurement without the test-crystal allows to extract the refractive index of GaP [4]. Our data shown in Fig. 3 are consistent with [31] but disagree with more recent work [32]. Using our data in the range 1-6 THz and the data from [33] in the near infrared, the refractive index n is fitted to the Sellmeier equation given by

$$n^2 = 1 + \frac{B_1 \lambda^2}{\lambda^2 - \lambda_1^2} + \frac{B_2 \lambda^2}{\lambda^2 - \lambda_2^2} \quad (1)$$

with $B_1 = 2.064$, $\lambda_1 = 27.284 \mu\text{m}$, $B_2 = 8.089$ and $\lambda_2 = 0.2707 \mu\text{m}$ and λ the wavelength in μm .

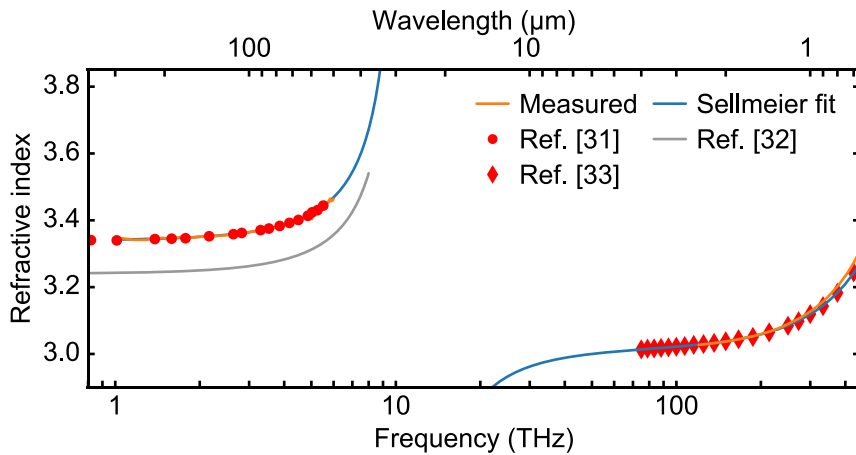


Fig. 3. Refractive index of GaP. In the THz region, it is retrieved from a THz time-domain spectroscopy measurement and compared to values taken from [31,32]. In the near-infrared range, it is measured by spectroscopic ellipsometry combined with transmission data and compared to [33].

The origin of the pronounced modulations in the THz spectra, e.g. at 5 THz, can be explained by phase matching. It accounts for the difference between the group velocity of GaP in the near-infrared and its phase velocity in the THz domain. The curves presented in Fig. 4 are calculated using the model introduced in [18] taking into consideration both generation and detection processes. In the calculation, we used a value of 3.31 for the optical group index of GaP at 1031 nm [33] and the refractive index in the THz range given by Eq. (1). Our calculated spectra are in a reasonable agreement with the measured ones in the range from 2 to 5 THz. In comparison, the refractive index given in [32] would yield a much broader phase matching for our system. The low-frequency behavior is not explained by this simple calculation because it does not include the influence of the pump pulse shape and propagation effects. The discrepancies in the amplitude at frequencies above 5 THz are due to the linear absorption in GaP and vanishing nonlinear constant [32]. Based on phase matching considerations, we estimate an optimal crystal thickness to be 150 μm for producing a gapless spectrum spanning up to 7 THz using an Yb-based driving laser source.

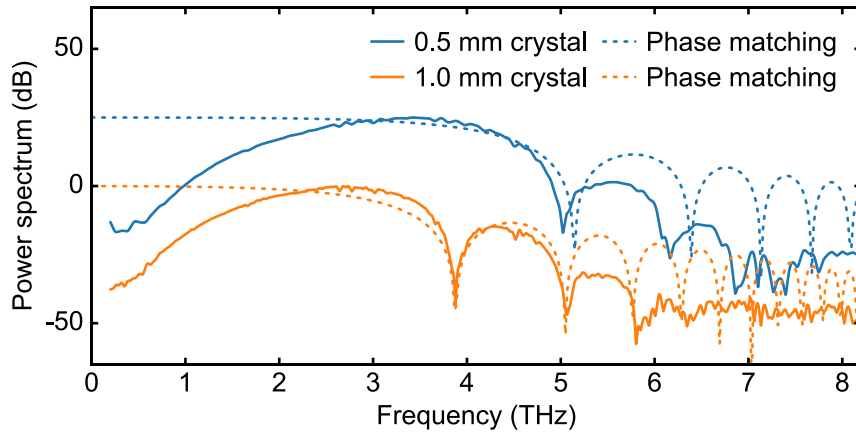


Fig. 4. THz spectra generated in 0.5 mm and 1.0 mm thick GaP crystals (solid lines). The corresponding phase matching curves (dashed lines) are calculated following the model presented in [18], using a value of 3.31 for the optical group index of GaP at 1031 nm and the refractive index in the THz domain given by (1).

4.2.4 THz spectroscopy of water vapor

To confirm the suitability of the system for broadband THz-TDS, we performed a benchmarking spectroscopic measurement of water vapor absorption [2] [Fig. 5]. For this, we compared the THz spectra acquired at two humidity levels (23% and 9% relative humidity) in a setup using 1.0 mm GaP crystals for generation and detection. Each data set is acquired in a single scan with 10 ms integration constant. The water vapor absorption coefficient is given by the logarithm of the ratio of the two amplitude spectra as a function of the frequency. The resulting water vapor absorption spectrum is compared to the one reported in [34]. Water vapor lines are reliably detected with a sub-50-GHz resolution up to 5 THz. A better reliability in the 5-6 THz range could be obtained by averaging over multiple scans or by increasing the integration time constant. A finer spectral resolution is achievable by acquiring longer temporal scans including the echo pulses from the reflections inside the crystals, which would not affect the data analysis as they divide out in the frequency domain [2].

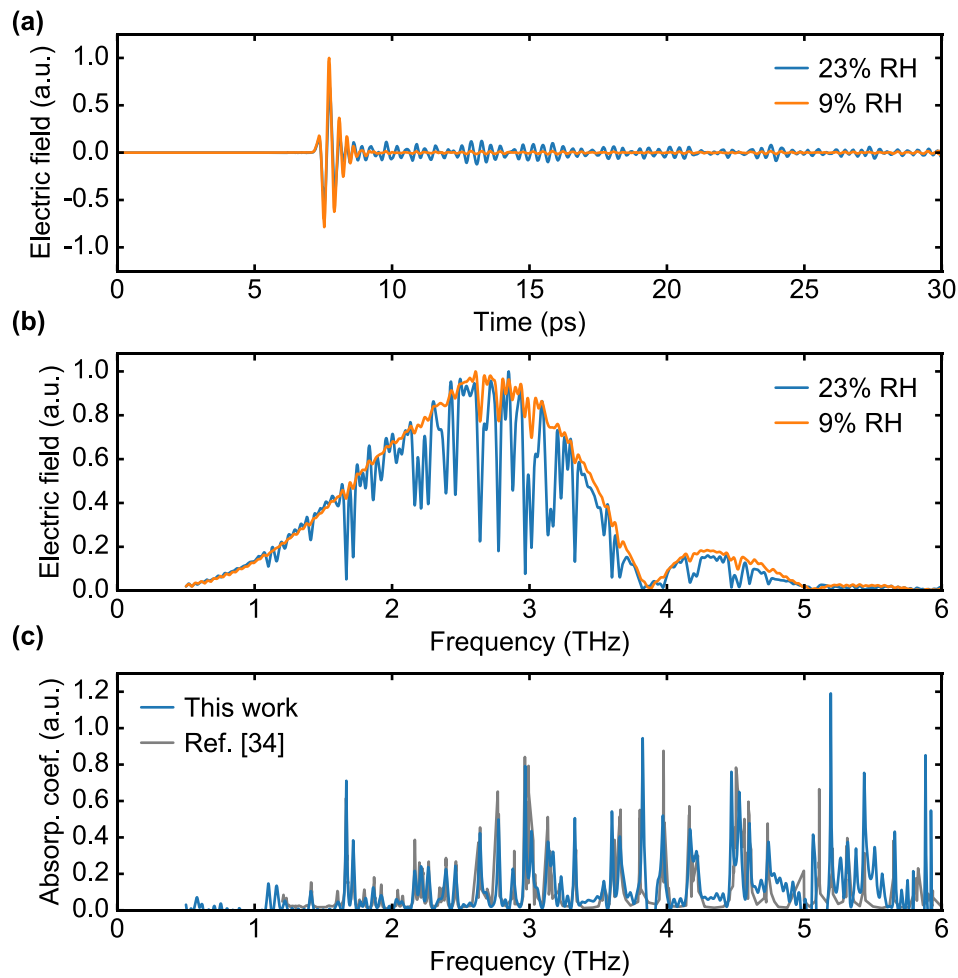


Fig. 5. (a) THz time-domain waveforms and (b) THz power spectra generated in a 1.0 mm GaP crystal at different relative humidity (RH) levels. (c) Frequency-dependent absorption coefficient of the water vapor, compared to the data taken from [34].

4.2.5 Conclusion and outlook

In conclusion, we have demonstrated broadband THz generation at MHz repetition rate using an ultrafast TDL oscillator as pump source. This simple single-stage laser source enabled the generation and detection of spectra with frequency content extending up to nearly 7 THz. We performed a spectroscopic measurement of GaP and refined its Sellmeier equation in the THz range. It is used for phase matching calculations, which are consistent with the acquired THz spectra. We conducted benchmarking linear THz-TDS experiment, measuring water vapor absorption

spectrum with a sub-50-GHz resolution achieved in a frequency range between 0.5 and 5 THz.

We believe that higher THz frequencies are within reach by using thinner GaP crystals for improved phase matching or different types of emitters [35] such as ZnTe [20], nonlinear organic crystals [36], plasma [37] or metallic spintronic emitters [38]. On the other hand, higher THz average power should be achievable by using thicker crystals, albeit at the expense of a reduced bandwidth. A compromise fulfilling the demands of a particular experiment is certainly possible. Similar to the case of THz generation in LiNbO₃ [7], our preliminary calculations indicate that a pump pulse duration of 50 fs is not optimal for efficient THz generation with a targeted bandwidth of 7 THz. As a next step, we will investigate the influence of the pulse duration on the THz generation in GaP crystals. TDL oscillators delivering more than 10 W of average power with 90 fs pulses at 61 MHz repetition rate have been as well recently demonstrated [26]. We expect that such parameters would allow increasing the THz average power due to the availability of higher pump power and longer pulses offering an adequate spectral bandwidth for efficient conversion. Therefore, we believe that TDL oscillators are a promising technology for scaling up the average power of broadband THz radiation. We expect that such compact sources of broadband THz pulses based on thin-disk laser oscillators will be beneficial for linear static THz-TDS and time-resolved THz spectroscopy.

Funding

German Ministry of Education and Research (BMBF) (FKZ 13N14192); Alexander von Humboldt Foundation and the Cluster of Excellence RESOLV (EXC 1069); National Center of Competence in Research for Molecular Ultrafast Science and Technology (NCCR-MUST) and the Swiss National Science Foundation (SNF) (200021_159931; 200020_179146).

Acknowledgements

We thank Gregory Gäumann, Yannik Wäber, Prof. Thomas Feurer (IAP, Bern) and Prof. J. P. Wolf (GAP, Geneva) for scientific discussions on terahertz generation and for the contributed equipment. We are grateful to Dr. Nicholas Karpowicz (MPQ, Garching, Germany) for fruitful personal scientific communication.

C. K. acknowledges financial support by the German Ministry of Education and Research (BMBF) (FKZ 13N14192). C. J. S. acknowledges financial support by the Alexander von Humboldt Foundation and the Cluster of Excellence RESOLV (EXC 1069). T. S. acknowledges financial support by the National Center of Competence in Research for Molecular Ultrafast Science and Technology (NCCR-MUST) and the Swiss National Science Foundation (SNF) (200021_159931; 200020_179146).

References

1. K. P. Cheung and D. H. Auston, "A novel technique for measuring far-infrared absorption and dispersion," *Infrared Phys.* **26**(1), 23–27 (1986).
2. M. van Exter, C. Fattinger, and D. Grischkowsky, "Terahertz time-domain spectroscopy of water vapor," *Opt. Lett.* **14**(20), 1128 (1989).
3. D. Grischkowsky, S. Keiding, M. van Exter, and C. Fattinger, "Far-infrared time-domain spectroscopy with terahertz beams of dielectrics and semiconductors," *JOSA B* **7**(10), 2006–2015 (1990).
4. P. U. Jepsen, D. G. Cooke, and M. Koch, "Terahertz spectroscopy and imaging – Modern techniques and applications," *Laser Photonics Rev.* **5**(1), 124–166 (2011).
5. T. A. A. Oliver, "Recent advances in multidimensional ultrafast spectroscopy," *R. Soc. Open Sci.* **5**(1), 171425 (2018).
6. K. Reimann, "Table-top sources of ultrashort THz pulses," *Rep. Prog. Phys.* **70**(10), 1597 (2007).
7. J. A. Fülöp, L. Pálfalvi, G. Almási, and J. Hebling, "Design of high-energy terahertz sources based on optical rectification," *Opt. Express* **18**(12), 12311 (2010).
8. P. Russbueldt, T. Mans, J. Weitenberg, H. D. Hoffmann, and R. Poprawe, "Compact diode-pumped 1.1 kW Yb:YAG Innoslab femtosecond amplifier," *Opt. Lett.* **35**(24), 4169–4171 (2010).
9. J.-P. Negel, A. Loescher, A. Voss, D. Bauer, D. Sutter, A. Killi, M. A. Ahmed, and T. Graf, "Ultrafast thin-disk multipass laser amplifier delivering 1.4 kW (47 mJ, 1030 nm) average power converted to 820 W at 515 nm and 234 W at 343 nm," *Opt. Express* **23**(16), 21064 (2015).
10. T. Nubbemeyer, M. Kaumanns, M. Ueffing, M. Gorjan, A. Alismail, H. Fattahi, J. Brons, O. Pronin, H. G. Barros, Z. Major, T. Metzger, D. Sutter, and F. Krausz, "1 kW, 200 mJ picosecond thin-disk laser system," *Opt. Lett.* **42**(7), 1381 (2017).
11. M. Müller, M. Kienel, A. Klenke, T. Gottschall, E. Shestaev, M. Plötner, J. Limpert, and A. Tünnermann, "1 kW 1 mJ eight-channel ultrafast fiber laser," *Opt. Lett.* **41**(15), 3439 (2016).
12. C. J. Saraceno, F. Emaury, O. H. Heckl, C. R. E. Baer, M. Hoffmann, C. Schriber, M. Golling, T. Südmeyer, and U. Keller, "275 W average output power from a femtosecond thin disk oscillator operated in a vacuum environment," *Opt. Express* **20**(21), 23535–23541 (2012).
13. J. Brons, V. Pervak, E. Fedulova, D. Bauer, D. Sutter, V. Kalashnikov, A. Apolonskiy, O. Pronin, and F. Krausz, "Energy scaling of Kerr-lens mode-locked thin-disk oscillators," *Opt. Lett.* **39**(22), 6442–6445 (2014).
14. C. J. Saraceno, F. Emaury, C. Schriber, A. Diebold, M. Hoffmann, M. Golling, T. Südmeyer, and U. Keller, "Toward millijoule-level high-power ultrafast thin-disk oscillators," *IEEE J. Sel. Top. Quantum Electron.* **21**(1), 106–123 (2015).
15. C. J. Saraceno, O. H. Heckl, C. R. E. Baer, C. Schriber, M. Golling, K. Beil, C. Kränkel, T. Südmeyer, G. Huber, and U. Keller, "Sub-100 femtosecond pulses from a SESAM modelocked thin disk laser," *Appl. Phys. B* **106**(3), 559–562 (2012).
16. C. J. Saraceno, "Mode-locked thin-disk lasers and their potential application for high-power terahertz generation," *J. Opt.* **20**(4), 044010 (2018).

17. Y. Ochi, K. Nagashima, M. Maruyama, M. Tsubouchi, F. Yoshida, N. Kohno, M. Mori, and A. Sugiyama, "Yb:YAG thin-disk chirped pulse amplification laser system for intense terahertz pulse generation," *Opt. Express* **23**(11), 15057 (2015).
18. Q. Wu and X.-C. Zhang, "7 terahertz broadband GaP electro-optic sensor," *Appl. Phys. Lett.* **70**(14), 1784–1786 (1997).
19. A. Leitenstorfer, S. Hunsche, J. Shah, M. C. Nuss, and W. H. Knox, "Detectors and sources for ultrabroadband electro-optic sampling: experiment and theory," *Appl. Phys. Lett.* **74**(11), 1516 (1999).
20. Q. Wu and X.-C. Zhang, "Free-space electro-optics sampling of mid-infrared pulses," *Appl. Phys. Lett.* **71**(10), 1285–1286 (1997).
21. I. D. Vugmeyster, J. F. Whitaker, and R. Merlin, "GaP based terahertz time-domain spectrometer optimized for the 5-8 THz range," *Appl. Phys. Lett.* **101**(18), 181101 (2012).
22. G. Chang, C. J. Divin, C.-H. Liu, S. L. Williamson, A. Galvanauskas, and T. B. Norris, "Power scalable compact THz system based on an ultrafast Yb-doped fiber amplifier," *Opt. Express* **14**(17), 7909–7913 (2006).
23. J. Li, L. Chai, J. Shi, F. Liu, B. Liu, B. Xu, M. Hu, Y. Li, Q. Xing, C. Wang, A. B. Fedotov, and A. M. Zheltikov, "Generation of 0.3 mW high-power broadband terahertz pulses from GaP crystal pumped by negatively chirped femtosecond laser pulses," *Laser Phys. Lett.* **10**(12), 125404 (2013).
24. J. Hamazaki, K. Furusawa, N. Sekine, A. Kasamatsu, and I. Hosako, "Effects of chirp of pump pulses on broadband terahertz pulse spectra generated by optical rectification," *Jpn. J. Appl. Phys.* **55**(11), 110305 (2016).
25. J. Xu, B. Globisch, C. Hofer, N. Lilienfein, T. Butler, N. Karpowicz, and I. Pupeza, "Three-octave terahertz pulses from optical rectification of 20-fs, 1- μ m, 78-MHz pulses in GaP," *J. Phys. B At. Mol. Opt. Phys.* **51**(15), 154002 (2018).
26. C. Paradis, N. Modsching, V. J. Wittwer, B. Deppe, C. Kränkel, and T. Südmeyer, "Generation of 35-fs pulses from a Kerr lens mode-locked Yb:Lu₂O₃ thin-disk laser," *Opt. Express* **25**(13), 14918–14925 (2017).
27. C. Kränkel, "Rare-earth-doped sesquioxides for diode-pumped high-power lasers in the 1-, 2-, and 3- μ m spectral range," *IEEE J. Sel. Top. Quantum Electron.* **21**(1), 250–262 (2015).
28. Y. Li, F. Liu, Y. Li, L. Chai, Q. Xing, M. Hu, and C. Wang, "Experimental study on GaP surface damage threshold induced by a high repetition rate femtosecond laser," *Appl. Opt.* **50**(13), 1958–1962 (2011).
29. Q. Wu and X.-C. Zhang, "Free-space electro-optic sampling of terahertz beams," *Appl. Phys. Lett.* **67**(24), 3523–3525 (1995).
30. A. Nahata, D. H. Auston, T. F. Heinz, and C. Wu, "Coherent detection of freely propagating terahertz radiation by electro-optic sampling," *Appl. Phys. Lett.* **68**(2), 150–152 (1996).
31. D. F. Parsons and P. D. Coleman, "Far infrared optical constants of gallium phosphide," *Appl. Opt.* **10**(7), 1683_1 (1971).
32. S. Casalbuoni, H. Schlarb, B. Schmidt, P. Schmäser, B. Steffen, and A. Winter, "Numerical studies on the electro-optic detection of femtosecond electron bunches," *Phys. Rev. Spec. Top. - Accel. Beams* **11**(7), 072802 (2008).
33. W. L. Bond, "Measurement of the refractive indices of several crystals," *J. Appl. Phys.* **36**(5), 1674–1677 (1965).
34. B. Clough, J. Dai, and X.-C. Zhang, "Laser air photonics: beyond the terahertz gap," *Mater. Today* **15**(1), 50–58 (2012).
35. B. Ferguson and X.-C. Zhang, "Materials for terahertz science and technology," *Nat. Mater.* **1**(1), 26–33 (2002).
36. X.-C. Zhang, X. F. Ma, Y. Jin, T.-M. Lu, E. P. Boden, P. D. Phelps, K. R. Stewart, and C. P. Yakymyshyn, "Terahertz optical rectification from a nonlinear organic crystal," *Appl. Phys. Lett.* **61**(26), 3080–3082 (1992).

37. K. Y. Kim, J. H. Glowia, A. J. Taylor, and G. Rodriguez, "Terahertz emission from ultrafast ionizing air in symmetry-broken laser fields," *Opt. Express* **15**(8), 4577–4584 (2007).
38. T. Seifert, S. Jaiswal, U. Martens, J. Hannegan, L. Braun, P. Maldonado, F. Freimuth, A. Kronenberg, J. Henrizi, I. Radu, E. Beaurepaire, Y. Mokrousov, P. M. Oppeneer, M. Jourdan, G. Jakob, D. Turchinovich, L. M. Hayden, M. Wolf, M. Münzenberg, M. Kläui, and T. Kampfrath, "Efficient metallic spintronic emitters of ultrabroadband terahertz radiation," *Nat. Photonics* **10**(7), 483–488 (2016).

4.3 Optical rectification of ultrafast Yb-lasers: Pushing power and bandwidth of THz generation in GaP

Jakub Drs,^{1,*} Norbert Modsching,¹ Clément Paradis,¹ Christian Kränkel,³
Valentin J. Wittwer,¹ Olga Razskazovskaya,¹ and Thomas Südmeyer¹

¹*Laboratoire Temps-Fréquence, Institut de Physique, Université de Neuchâtel, Avenue de Bellevaux 51, 2000 Neuchâtel, Switzerland*

²*Center for Laser Materials, Leibniz-Institut für Kristallzüchtung, Max-Born-Str. 2, 12489 Berlin, Germany*

We demonstrate broadband high-power THz generation at MHz repetition rates by optical rectification in GaP driven by an ultrafast Yb-based thin-disk laser oscillator. We investigate the influence of pulse duration in the range of 50 fs to 220 fs and thickness of the GaP crystal on the THz generation. Optimization of these parameters with respect to the broadest spectral bandwidth yields a gap-less THz spectrum extending to nearly 7 THz. We further tailor the driving laser and the THz generation parameters for the highest average power, demonstrating 0.3 mW THz radiation with a spectrum extending to 5 THz. This was achieved using a 0.5 mm thick GaP crystal pumped with a 95 fs, 20 W thin disk laser, operating at 48 MHz repetition rate. We also provide a comprehensive method to estimate the THz spectrum, which can be used for design and optimization of similar THz systems.

4.3.1 Introduction

Increasing both the average power and the repetition rate of broadband THz sources is of high interest for various spectroscopic and imaging THz applications [1]. So far, tabletop high-power broadband THz sources have been mostly driven by high energy laser amplifier systems, typically based on Ti:sapphire gain material, operating at kHz repetition rates and modest average powers of several watts.

In the last years Yb-based directly diode-pumped solid-state lasers have become a promising alternative to Ti:sapphire systems. The higher Stokes efficiency of the Yb-doped gain medium together with the direct diode pumping scheme allows for substantial increase in average power, albeit at the expense of longer pulse durations

due to the narrower gain bandwidth of Yb-doped media. Several studies investigated the potential of Yb-based amplifier systems for high-power THz generation. A chirped pulse thin-disk laser amplifier has been used to generate 4 mW of THz average power in LiNbO₃ with a spectrum extending to 1 THz [2]. Li *et al.* demonstrated generation of 0.3 mW THz radiation with a spectrum extending to 2 THz by optical rectification in GaP driven by a 21 W, 52 fs fiber amplifier [3]. More recently, broadband THz systems with spectra extending to 5 and 6 THz have been demonstrated, however, yet in a few- μ W average power range [4,5].

Ultrafast Yb-based thin-disk laser (TDL) oscillators operating at MHz repetition rates reach high output powers directly out of the oscillator circumventing the necessity for amplification stages. They usually emit transform-limited soliton pulses without pre- or post-pulses in a TEM₀₀ beam. Nearly 300 W have been obtained from TDL oscillators with several hundred fs pulse durations [6,7]. In the last years, there was also a large progress in the development of ultrafast thin-disk lasers operating directly in the sub-100-fs regime [8–13]. The shortest pulse durations of ultrafast thin-disk lasers have been reduced to 30 fs [14], and power levels up to 20 W have been achieved in 95-fs pulses [15], making TDL oscillators very attractive sources to drive broadband high-power THz generation [16].

Recently, we demonstrated the generation of broadband THz radiation with a gap-less spectrum extending to 5 THz at a few μ W of average power [17]. This was achieved by optical rectification in GaP of 50-fs pulses, delivered by a 4-W TDL oscillator. Shortly after, Meyer *et al.* demonstrated the potential for increasing the available THz power by using a high-power TDL oscillator as a driving source [18]. They showed that 100 W of average laser power with 580 fs pulse duration could be optically rectified in GaP, yielding 80 μ W of average THz power with a spectrum extending up to 1.6 THz.

In this study, we show that optical rectification in GaP allows for high average THz powers approaching the mW range also with broadband spectra. We investigate the influence of the pulse duration of the driving laser and the thickness of the GaP crystal on the THz generation. Optimization of these parameters with respect to spectral bandwidth allowed us to generate THz radiation with a spectrum extending to nearly 7 THz. This is to our knowledge the broadest gap-less THz spectrum obtained from an Yb-based laser driven system. Optimization with respect to average power yielded

0.3 mW of THz radiation with a spectrum extending to nearly 5 THz. We further provide a comprehensive guideline to estimate the generated THz spectrum based on pulse duration and thickness of the crystal, which we believe can be a very useful tool for the optimization of similar THz systems.

4.3.2 Experimental setup

The driving laser of our setup described in [13] is a Kerr lens mode-locked TDL oscillator (Fig. 1) based on the gain material Yb:Lu₂O₃ [19] emitting at a center wavelength of 1.03 μm . It generates transform limited soliton pulses at 60 MHz repetition rate with pulse durations between 50 and 220 fs at typical average powers of several watts and diffraction limited beam quality ($M^2 < 1.05$). Pulse duration and average power of the laser oscillator can be modified by changing the intra-cavity dispersion (replacing dispersive mirrors), the output-coupling rate and by variation of the hard aperture size (elements shown in blue in Fig. 1). This approach is limited to discrete operation parameters and does not allow for a large continuous tuning range; however, it ensures maintaining transform-limited soliton pulses and TEM₀₀ beam profile at all the accessible pulse durations. This allowed us to perform high-fidelity measurements of the influence of pulse duration on the THz generation. In the second part of the study, focused on optimization of the THz average power, we utilized a power-scaled version of the driving TDL oscillator, delivering a higher average power of 20 W at 95 fs pulse duration.

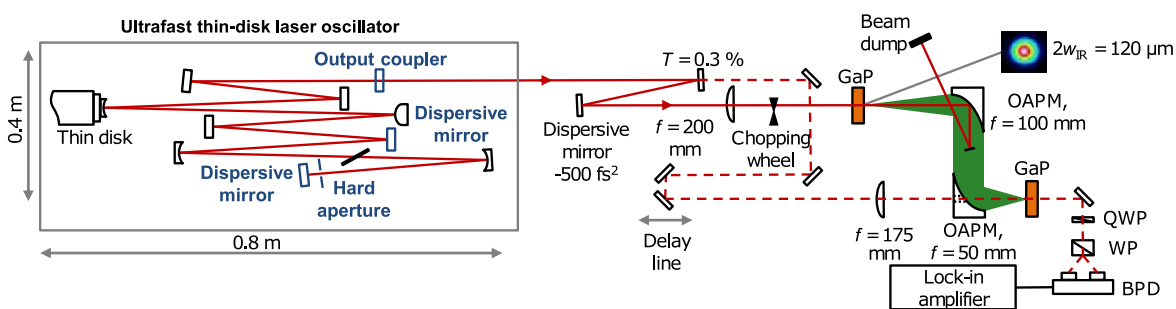


Fig. 1. Experimental setup for THz generation via optical rectification and detection by electro-optic sampling driven by an ultrafast TDL oscillator. Pulse duration and average power of the driving laser can be modified by replacing the cavity elements highlighted in blue. OAPM: off-axis parabolic mirror; QWP: quarter-wave plate; WP: Wollaston prism; BPD: balanced photo-detector; T: output coupler; w_{1R} : beam radius at $1/e^2$.

The THz radiation is generated via optical rectification in uncoated <110>-cut GaP crystals of different thickness. The pump pulses are pre-chirped by -500 fs^2 to compensate for the focusing lens and crystal dispersion. The beam is chopped at a frequency of 2.5 kHz for lock-in detection and focused into the crystal at a $1/e^2$ beam diameter of 120 μm . The unconverted infrared (IR) light is separated from the THz radiation by a 5-mm diameter mirror placed on the optical axis. Due to the much stronger divergence of the THz radiation, this does not create significant losses for the THz beam.

The generated THz radiation is detected by electro-optic sampling (EOS) in a second <110>-cut uncoated GaP crystal. The EOS signal is sent to the lock-in amplifier with a typical time constant of 30 ms. The delay line is moved by fixed steps and remains on the spot during each measured point. This avoids vibrations and eliminates dependence on stage speed and lock-in time constant. The system is operated at room temperature in a dry air purged environment with residual relative humidity of $\sim 7\%$.

4.3.3 Influence of pulse duration and crystal thickness on the THz spectrum

The THz spectrum generated by optical rectification in GaP is mainly determined by the pulse duration of the driving laser and the thickness of the nonlinear crystal. While the corresponding parameters are well investigated for Ti:sapphire lasers emitting at 800 nm, their influence in the emission wavelength range of Yb-based lasers around 1 μm remains relatively less explored, which motivated our investigations.

In a first experiment, we investigated the influence of the GaP crystal thickness on the THz spectrum. We used 50-fs pulses and measured the THz spectra for three different crystal thicknesses (see Fig. 2 a). The experiment demonstrates how the thickness of the GaP crystals limits the THz spectrum due to the mismatch between the group velocity of the IR pulse and the phase velocity of the THz radiation [20]. The theoretical phase matching curves are plotted as dashed lines for reference. The solid blue and orange curves depict spectra for crystals thicker than optimum for the generation of broadest spectra, which show frequency cut-offs at 4 and 5 THz, respectively. The green curve demonstrates the results with a thinner crystal, where the phase mismatch frequency cut-off at 7.3 THz is not anymore the main limiting factor and the THz spectrum is mostly limited by the pulse duration of the driving

laser. The phase matching conditions between the IR and THz pulse in GaP were calculated according to [20] based on a Sellmeier fit of the THz refractive indices presented in [17] and a group refractive index for the IR pulse $n_g = 3.31$ calculated from [21] (see Tab. 1 in the appendix).

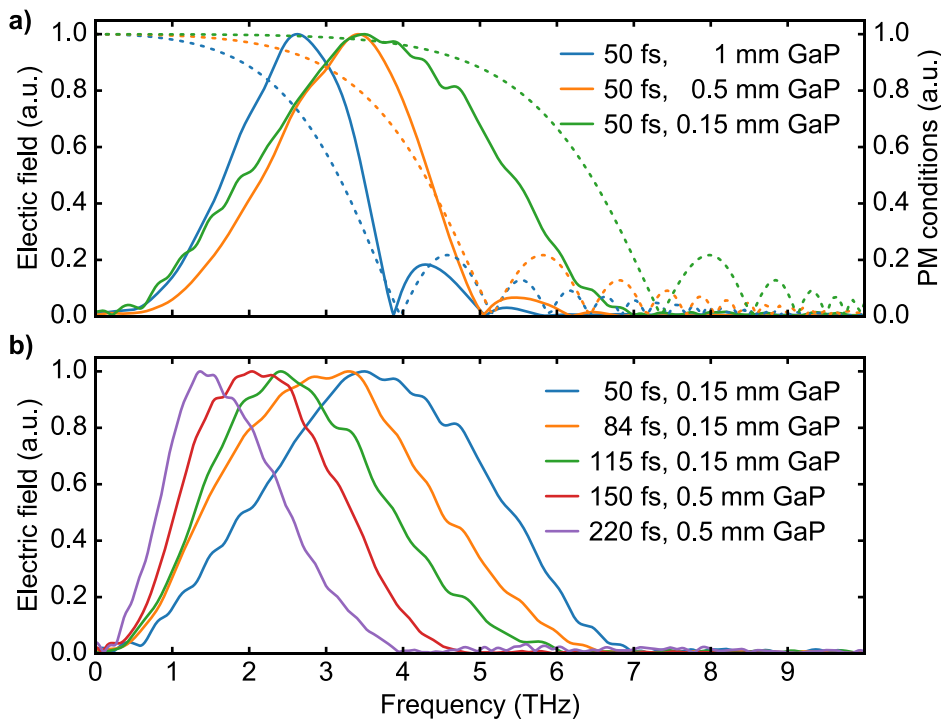


Fig. 2 a) THz spectra generated by optical rectification of 50 fs pulses in GaP crystals of different thicknesses. The use of thick crystals (blue and orange) poses a frequency cut-off on the measured THz spectrum due to the phase mismatch between the IR and THz pulses. The theoretical phase matching curves are plotted by dashed lines for reference. The green curve shows a spectrum for a crystal thin enough to prevent phase mismatch being the most limiting factor. b) Experimental measurement of the achievable THz spectra for different pulse durations of the driving laser. The thickness of the crystal is adapted to the respective pulse duration in order to maximize the signal, while avoiding the phase mismatch frequency cut-off.

In a second experiment, we studied the influence of the pulse duration of the driving laser. The experiment was designed to assess the maximum spectral bandwidth at each pulse duration. To this end, we adapted the crystal thickness to maximize the THz signal, while avoiding the phase mismatch frequency cut-off in the THz spectrum. Five different configurations of the driving laser were chosen for the experiment with pulse durations between 50 and 220 fs at average powers of 3 to 7 W.

Despite the different average power levels obtained at different pulse durations, we did not observe any significant dependence of the THz spectral shape on the driving laser average power in our experiments. We therefore used the full available power of each configuration to drive the THz generation.

The THz spectra measured for different pulse durations are shown in Fig. 2 b). The central frequency shifts from 1.5 THz for 220-fs pulses to 3.5 THz for the 50-fs configuration. The broadest THz spectrum acquired in the 50-fs configuration extends to nearly 7 THz.

We further verify the THz spectral bandwidth of our system by performing a THz time domain spectroscopy measurement of water vapor shown in the appendix of this study in Fig 5. The measurement was taken using 84 fs pulse duration (orange curve in Fig. 2b) and shows a good agreement with the theoretical absorption of water vapor obtained from the HITRAN database [22] in a frequency range between 1 and 6 THz with < 20 GHz spectral resolution.

4.3.4 Estimation of the THz spectrum

Understanding of the underlying mechanisms of the THz generation and detection is a key requirement for optimization of THz systems. Although solving a nonlinear coupled wave equation is generally required to fully describe the THz generation process [23,24], according to our measurements, the THz spectrum can be reasonably approximated by decoupled multiplicative factors in the frequency domain. This approach provides a comprehensive tool to isolate the influence of different parameters and determine the key limitations. The considered frequency factors and their parameters are shown in Eq. (1) and depicted graphically in Fig. 3. For the convenience of the reader, we also include all the formulas in Table 1 in the appendix.

$$\begin{aligned}
 E_{\text{THz}}(\omega) \approx & E_{0\text{ THz}}(\omega, \tau_{\text{laser}}) \cdot \text{PM}_{\text{Gen}}(\omega, n_g, d_{\text{crystal}}) \cdot \text{EOS}(\omega, \tau_{\text{laser}}) \\
 & \cdot \text{PM}_{\text{Det}}(\omega, n_g, d_{\text{crystal}}) \cdot r_{41}(\omega) \cdot t_{\text{GaP}}(\omega, d_{\text{crystal}})
 \end{aligned} \tag{1}$$

The maximum bandwidth of the THz field $E_{0\text{ THz}}$ generated by optical rectification in $\chi^{(2)}$ nonlinearity (shown in blue in Fig. 3) can be approximated by the 2nd derivative of the IR pulse intensity envelope with respect to time [25]. Both the generation and the detection of the THz radiation are affected by the phase matching (PM) condition

between the phase velocity of the THz radiation and the group velocity of the IR pulse in the nonlinear crystal. The factor $PM_{\text{Gen}} \cdot PM_{\text{Det}}$ (red curve in Fig. 3) is strongly dependent on the thickness of the GaP crystal d_{crystal} and the center wavelength of the driving laser through the group refractive index n_g . The response of the EOS detection can be described as a cross correlation between the THz field and the intensity envelope of the IR probing pulse as derived in [26], i.e., multiplication with the IR pulse intensity spectrum (depicted in orange in Fig. 3) in the frequency domain. The THz radiation is further affected by an electro-optic coefficient r_{41} (purple curve in Fig. 3) and the THz transmission t_{GaP} of the GaP crystal (gray curve in Fig. 3), determined by Fresnel reflection and material absorption. Both curves are based on Lorentzian fits to third party experimental data obtained from [27]. The fits might have significant uncertainties; however, they do not have a major influence on most of our data compared to the phase matching condition.

We present three example spectral estimates for pulse durations of 220 fs, 95 fs, and 50 fs and different crystal thicknesses. In the case of longest pulse duration (Fig. 3a), the THz spectrum is mostly limited by the EOS detection. The phase matching condition for the 0.5 mm thick GaP crystal does not strongly influence the THz spectrum at such long pulse durations. For sub-100-fs pulses, the thickness of the crystal starts to play an important role. Due to the indirect phonon resonance of GaP at 11 THz [28], higher THz frequencies are getting rapidly phase mismatched with the driving IR pulse. Thus, the use of thin crystals is required in order to support the highest spectral bandwidth. Fig. 3b) shows that the phase mismatch in the 0.5 mm thick GaP crystal already slightly limits the THz spectrum for a 95-fs driving laser (see the dip at 5 THz). The shortest pulses of 50 fs duration (Fig. 3c) finally require a more than three times thinner crystal to support the THz spectrum extending to 7 THz.

The described method slightly overestimates the spectral bandwidth, as it does not take into account processes like dispersion and self-focusing of the IR pulses in GaP or the coupled nonlinear propagation of IR and THz pulses. It predicts that THz frequencies beyond 7 THz are within reach for pulse durations shorter than 50 fs and crystal thickness below 0.15 mm. The credibility of the prediction for these higher THz frequencies, approaching the phonon resonance of GaP, is however further reduced by the uncertainties of the used material properties. Nevertheless, according to our

measurements, the model provides valid estimates for pulse durations in excess of 50 fs.

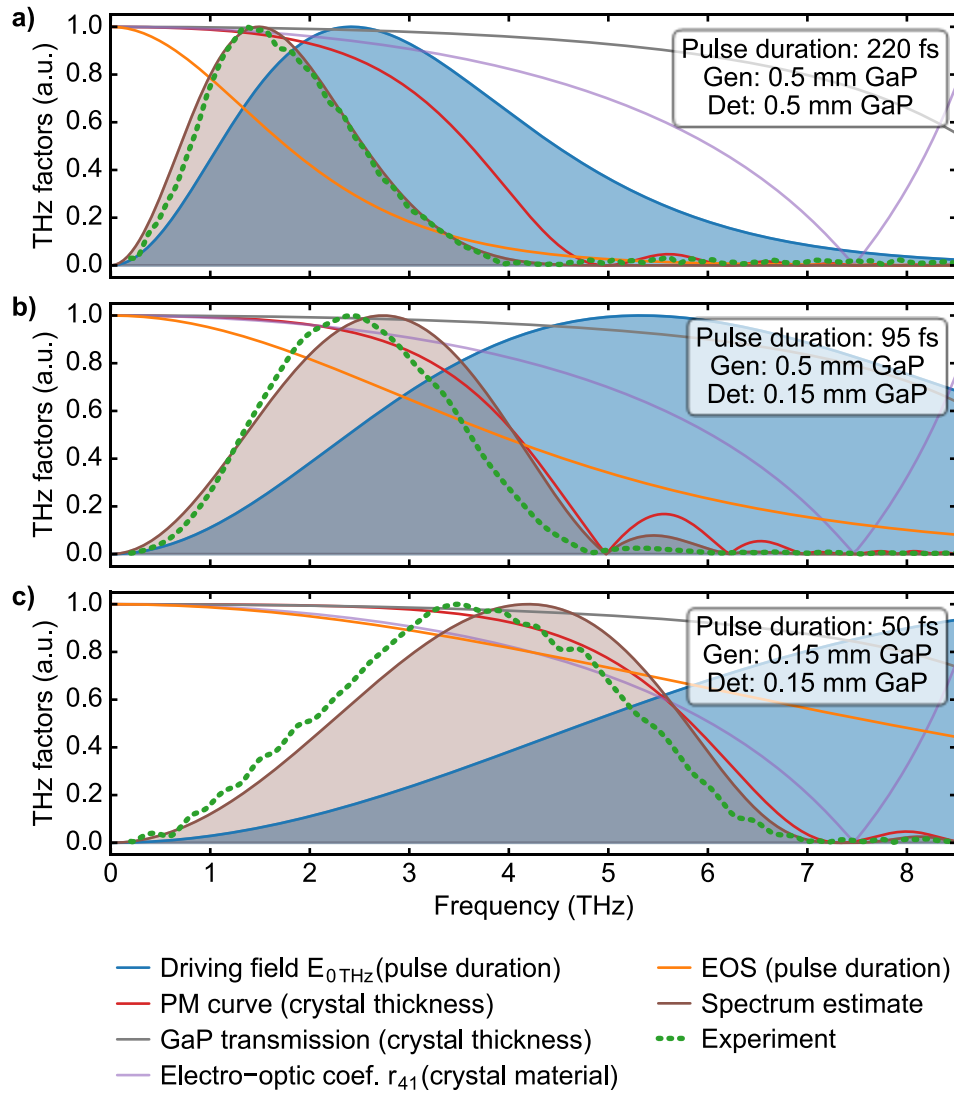


Fig. 3. Estimate of the THz spectra considering multiplicative factors in frequency domain. The blue curve depicts the maximum bandwidth of the driving THz field $E_{0\text{THz}}$. The red curve shows the phase matching condition for 1 μm IR pulse and THz radiation considering both the detection and the generation GaP crystal. The orange curve determines the EOS corresponding to the probing pulse intensity spectrum. Violet and gray curves depict GaP transmission and electro-optic coefficient r_{41} . The overall spectral estimate E_{THz} calculated according to Eq. 1 is shown by the brown filled curve, the corresponding experimental data are shown in dashed green.

4.3.5 *Toward high THz powers*

In order to investigate the achievable power levels of our THz system, we utilized a power-scaled version of our TDL oscillator optimized for high output power in the sub-100-fs regime as a compromise between achievable average power and shortest pulse duration. This laser configuration, described in detail in [15], delivers 95-fs transform limited soliton pulses at 20 W average power and 48 MHz repetition rate, which corresponds to 3.9 MW peak power and 0.4 μ J pulse energy. The laser beam is focused into the generation crystal by a 200 mm focusing lens. The THz average power is measured by an Ophir pyroelectric THz power detector. Corresponding THz spectra are measured by EOS in a 0.15 mm thick GaP crystal. In order to prevent all unconverted IR light from reaching the pyroelectric detector and influencing the power measurement we use a small mirror centered on the optical axis deflecting the main beam into a beam block combined with two layers of black plastic foil to block the residual IR light scattered from the crystal. The THz transmission of one layer of the plastic foil was determined to be 46% and the presented average THz power was corrected accordingly.

We first investigated the influence of the driving field peak intensity in the crystal by performing a 1 cm z-scan of the focusing lens. The spot size diameter in the crystal was varied between 200 and 370 μ m. We limited ourselves to peak intensities of 20 GW/cm² to avoid damage of the crystals. The result of the experiment for 0.5 and 0.15 mm thick crystals is shown in Fig. 4a). Although the $\chi^{(2)}$ origin of the optical rectification suggests quadratic dependence of the THz power on the peak intensity, our result already shows an onset of saturation. The highest driving peak intensity of 20 GW/cm² thus seems to be close to the maximum efficiency at this pulse duration. It yields an average THz power of 65 μ W for the 0.15 mm thick crystal and 0.3 mW for 0.5 mm thickness, corresponding to an optical-to-optical efficiency of $3.2 \cdot 10^{-6}$ and $1.5 \cdot 10^{-5}$, respectively, for the 20-W driving laser.

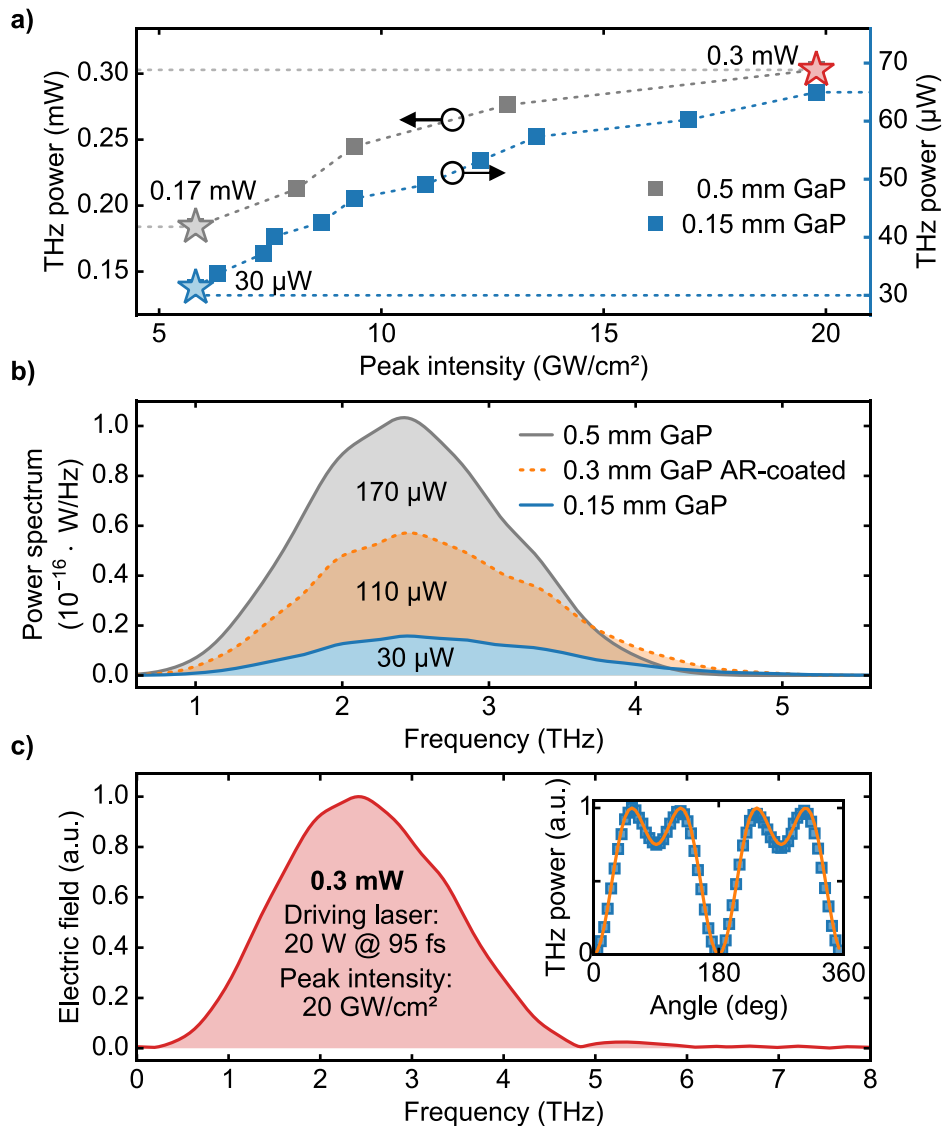


Fig. 4 a) Z-scan experiment showing the dependence of the THz power on the peak intensity in the crystal. The curves for 0.5 mm and 0.15 mm thick crystals are plotted on two different power scales (left and right axis) sharing same zero. The stars in the graph correspond to the same colored spectra shown below. b) THz spectral power density for different crystal thicknesses measured with a $1/e^2$ focus diameter of $370 \mu\text{m}$, corresponding to peak intensities of 5.8 GW/cm^2 for the 0.5 mm and 0.15 mm crystals and 7.2 GW/cm^2 for the AR-coated 0.3 mm crystal (dashed orange line). c) The electric field spectrum at maximum THz average power generated in a 0.5 mm GaP crystal at $200 \mu\text{m}$ spot size diameter (20 GW/cm^2 peak intensity). The blue markers in the inset graph show the measured dependence of the THz power on the crystal orientation compared with a theoretical curve in orange, proving the $\chi^{(2)}$ origin of the THz generation.

In the second part of the experiment, we investigated the influence of the GaP crystal thickness on the THz power. We used three crystal thicknesses of 0.5, 0.3 and 0.15 mm, with a modest focusing spot size diameter of 370 μm measured at $1/e^2$. The corresponding spectral power densities are depicted in Fig. 4b). Accounting for 20% Fresnel reflection for the uncoated crystals, the used spot size corresponds to peak intensities of 5.8 GW/cm^2 and amounts to 7.2 GW/cm^2 for the 0.3 mm crystal, which is AR coated and thus plotted by dashed line.

Fig. 4c) finally shows the electric field amplitude spectrum of the highest generated THz average power. The 0.5 mm GaP crystal already slightly limits the spectral bandwidth. The spectra shown in Fig. 4b) and c) correspond to the data points marked with same color stars in Fig. 4a).

We further validated the $\chi^{(2)}$ nonlinear origin of the THz radiation by measuring the THz power as a function of the crystal orientation, comparing it with the theoretical values [25] for the $\langle 110 \rangle$ -cut zincblende structure of the GaP crystal. The experiment, shown in the inset of Fig. 4c), agrees very well with the theoretical curve.

4.3.6 Conclusion

We have demonstrated that broadband high-power THz radiation approaching mW power levels can be efficiently generated in a simple collinear phase matching scheme in GaP driven by a sub- μJ -pulse-energy MHz-repetition-rate Yb-based TDL oscillator. We generated 0.3 mW of THz power with a spectrum extending to nearly 5 THz in a 0.5 mm GaP crystal using a 20 W, 95 fs driving laser operating at 48 MHz repetition rate.

Benefiting from the excellent beam quality and transform-limited soliton pulses of our driving laser, we provide high-fidelity measurements of the influence of the pulse duration, the peak intensity, and the crystal thickness on both the THz average power and the THz spectral bandwidth for the less-investigated 1 μm emission range of Yb-lasers. Optimization of these parameters allowed us to extend the THz spectrum to nearly 7 THz, which is to our knowledge the broadest gap-less THz spectrum generated by an Yb-based laser.

We further show that the measured THz spectrum can be reasonably approximated by considering decoupled multiplicative factors in the frequency

domain, providing a simple and comprehensive method for the design and optimization of similar THz systems.

In agreement with [18], we thus conclude that optical rectification in GaP is highly suitable for broadband THz generation driven by high-power Yb-based lasers. Further power scalability has been recently confirmed by Meyer et al. utilizing a high power TDL oscillator combined with an external pulse compression delivering 88-fs pulses at 112 W of average power as a driving source. This yielded 1.35 mW THz radiation with a spectrum extending to 4 THz [29]. Since further improvements in the area of ultrafast TDL are expected, we believe that broadband THz sources delivering tens of mW of average power at MHz repetition rates are soon within reach.

Funding

Swiss National Science Foundation (SNSF) (179146, 170772, 144970); German Ministry of Education and Research (BMBF) (13N14192).

4.3.7 Appendix

In order to verify the usable spectral range of our system we performed a simple THz-TDS measurement of water vapor as depicted in Fig. 5. The measurement was taken using 84 fs pulse duration and shows a good agreement with the reference HITRAN database [22] water absorption spectrum in the frequency range between 1 and 6 THz with < 20 GHz resolution.

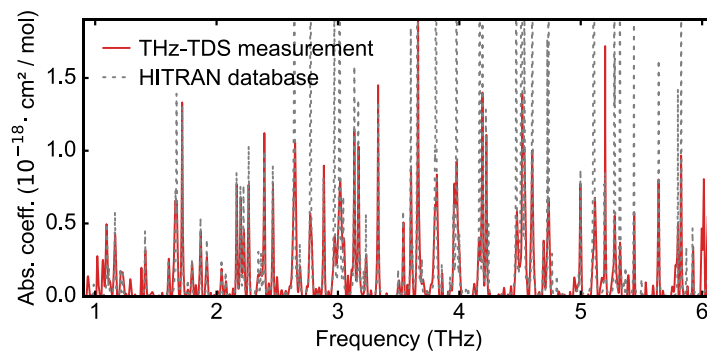


Fig. 5. THz-TDS measurement of water vapor absorption obtained by comparing two 40 ps THz scans at 40% and 10% relative humidity, respectively. The measurement is compared with the absorption spectrum from the HITRAN database [22].

Table 1. Equation for estimation of the THz spectrum.^a

Process	Equation	Ref.
IR sech ² pulse intensity envelope, where $\tau_{\text{laser}} \cdot 1.76$ corresponds to the FWHM pulse duration	$I_{\text{IR}}(t) = \text{sech}^2\left(\frac{t}{\tau_{\text{laser}}}\right)$	
Driving THz field, defined by second derivative of the driving pulse intensity envelope I_{IR} with respect to time	$E_{0\text{THz}}(\omega) = \mathcal{F}\left(\frac{d^2 I_{\text{IR}}(t)}{dt^2}\right)(\omega)$	[25]
Sellmeier equation for refractive index of GaP	$n_{\text{THz}}^2 = 1 + \frac{B_1 \lambda^2}{\lambda^2 - \lambda_1^2} + \frac{B_2 \lambda^2}{\lambda^2 - \lambda_2^2},$ $B_1 = 2.064, \lambda_1 = 27.284 \mu\text{m},$ $B_2 = 8.089, \lambda_2 = 0.2707 \mu\text{m}$	[17]
Phase matching condition for group velocity of the IR pulse and THz radiation phase velocity, where d_{crystal} determines thickness of the GaP crystal	$\text{PM}(\omega) = \frac{e^{i\omega\delta(\omega)} - 1}{i\omega\delta(\omega)},$ $\delta(\omega) = \frac{n_g(\lambda_0) - n_{\text{THz}}(\omega)}{c_{\text{light}}} d_{\text{crystal}},$ $n_g(1.03 \mu\text{m}) = 3.31$	[20]
EOS response, determined by intensity envelope spectrum of the probing IR pulse	$\text{EOS}(\omega) = \mathcal{F}(I_{\text{IR}}(t))(\omega)$	[26]
GaP absorption coefficient	$k(\omega) = \text{Im}\left(\varepsilon_{\text{el}} + \frac{S_0 \omega_0^2}{\omega_0^2 - \omega^2 - i\Lambda_0 \omega}\right),$ $\varepsilon_{\text{el}} = 8.7, S_0 = 1.8,$ $\Lambda_0 = 0.126 \cdot 10^{12} \text{ rad/s},$ $\omega_0 = 69 \cdot 10^{12} \text{ rad/s}$	[27]
GaP transmission, based on Fresnel reflection and material absorption, where d_{crystal} determines thickness of the GaP crystal	$t_{\text{GaP}}(\omega) = \frac{2}{n_{\text{THz}}(\omega) + 1} \cdot e^{-k \frac{\omega \cdot d_{\text{crystal}}}{c_{\text{light}}}}$	

Electro-optic coefficient r_{41} of GaP	$r_{41}(\omega) = d_E \left(1 + \frac{C_0 \omega_0^2}{\omega_0^2 - \omega^2 - i\Lambda_0 \omega} \right),$ $d_E = 10^{-12} \text{ m/V}, C_0 = -0.53,$ $\Lambda_0 = 0.126 \cdot 10^{12} \text{ rad/s},$ $\omega_0 = 69 \cdot 10^{12} \text{ rad/s}$	[27]
Overall THz field estimate	$E_{\text{THz}} = E_{0 \text{ THz}} \cdot \text{PM}_{\text{Det}} \cdot \text{PM}_{\text{Gen}} \cdot \text{EOS}$ $\cdot t_{\text{GaP}} \cdot r_{41}$	
Dependence of THz average power on angle θ of <110>-cut GaP crystal with respect to laser polarization	$P(\theta) \propto \sin^2(2\theta) + \sin^4(\theta)$	[25]

^a $I_{\text{IR}}(t)$: soliton pulse intensity envelope; t : time (s); τ_{laser} : 1.76: FWHM pulse duration (s); $E_{0 \text{ THz}}$: driving THz field; ω : angular frequency of the THz radiation (rad/s); n_{THz} : refractive index for THz frequencies; PM: Phase matching condition; λ_0 : laser central wavelength; n_g : group refractive index; EOS: electro-optic sampling; k : absorption coefficient; t_{GaP} : GaP transmission; d_{crystal} : thickness of the GaP crystal; c_{light} : speed of light (m/s); r_{41} : electro-optic coefficient of GaP (m/V); E_{THz} : estimate of THz spectrum; $P(\theta)$: THz power (W)

References

1. P. U. Jepsen, D. G. Cooke, and M. Koch, "Terahertz spectroscopy and imaging - Modern techniques and applications," *Laser & Photon. Rev.* **5**(1), 124-166 (2011).
2. Y. Ochi, K. Nagashima, M. Maruyama, M. Tsubouchi, F. Yoshida, N. Kohno, M. Mori, and A. Sugiyama, "Yb:YAG thin-disk chirped pulse amplification laser system for intense terahertz pulse generation," *Opt. Express* **23**(11), 15057-15064 (2015).
3. J. Li, L. Chai, J. Shi, F. Liu, B. Liu, B. Xu, M. Hu, Y. Li, Q. Xing, C. Wang, A. B. Fedotov, and A. M. Zheltikov, "Generation of 0.3 mW high-power broadband terahertz pulses from GaP crystal pumped by negatively chirped femtosecond laser pulses," *Laser Phys. Lett.* **10**(12), 125404 (2013).
4. J. Xu, B. Globisch, C. Hofer, N. Lilienfein, T. Butler, N. Karpowicz, and I. Pupeza, "Three-octave terahertz pulses from optical rectification of 20-fs, 1- μm , 78-MHz pulses in GaP," *J. Phys. B: At. Mol. Opt. Phys.* **51**(15), 154002 (2018).
5. W. Cui, A. W. Schiff-Kearn, E. Zhang, N. Couture, F. Tani, D. Novoa, P. St. J. Russell, and J.-M. Ménard, "Broadband and tunable time-resolved THz system using argon-filled hollow-core photonic crystal fiber," *APL Photonics* **3**(11), 111301 (2018).
6. C. J. Saraceno, F. Emaury, O. H. Heckl, C. R. E. Baer, M. Hoffmann, C. Schriber, M. Golling, T. Südmeyer, and U. Keller, "275 W average output power from a femtosecond thin disk oscillator operated in a vacuum environment," *Opt. Express* **20**(21), 23535-23541 (2012).
7. J. Brons, V. Pervak, E. Fedulova, D. Bauer, D. Sutter, V. Kalashnikov, A. Apolonskiy, O. Pronin, and F. Krausz, "Energy scaling of Kerr-lens mode-locked thin-disk oscillators," *Opt. Lett.* **39**(22), 6442-6445 (2014).
8. T. Südmeyer, C. Kränkel, C. R. E. Baer, O. H. Heckl, C. J. Saraceno, M. Golling, R. Peters, K. Petermann, G. Huber, and U. Keller, "High-power ultrafast thin disk laser oscillators and their potential for sub-100-femtosecond pulse generation," *Appl. Phys. B* **97**(2), 281-295 (2009).
9. C. J. Saraceno, O. H. Heckl, C. R. E. Baer, C. Schriber, M. Golling, K. Beil, C. Kränkel, T. Südmeyer, G. Huber, and U. Keller, "Sub-100 femtosecond pulses from a SESAM modelocked thin disk laser," *Appl. Phys. B* **106**(3), 559-562 (2012).

10. A. Diebold, F. Emaury, C. Schriber, M. Golling, C. J. Saraceno, T. Südmeyer, and U. Keller, "SESAM mode-locked Yb:CaGdAlO₄ thin disk laser with 62 fs pulse generation," *Opt. Lett.* **38**(19), 3842–3845 (2013).
11. C. Schriber, L. Merceron, A. Diebold, F. Emaury, M. Golling, K. Beil, C. Kränkel, C. J. Saraceno, T. Südmeyer, and U. Keller, "Pushing SESAM modelocked thin-disk lasers to shortest pulse durations," in *Advanced Solid State Lasers* (Optical Society of America, 2014), paper AF1A.4.
12. J. Zhang, J. Brons, M. Seidel, V. Pervak, V. Kalashnikov, Z. Wei, A. Apolonski, F. Krausz, and O. Pronin, "49-fs Yb:YAG thin-disk oscillator with distributed Kerr-lens mode-locking," in *European Quantum Electronics Conference* (Optical Society of America, 2015), paper PD_A_1.
13. C. Paradis, N. Modsching, V. J. Wittwer, B. Deppe, C. Kränkel, and T. Südmeyer, "Generation of 35-fs pulses from a Kerr lens mode-locked Yb:Lu₂O₃ thin-disk laser," *Opt. Express* **25**(13), 14918–14925 (2017).
14. N. Modsching, C. Paradis, F. Labaye, M. Gaponenko, I. J. Graumann, A. Diebold, F. Emaury, V. J. Wittwer, and T. Südmeyer, "Kerr lens mode-locked Yb:CALGO thin-disk laser," *Opt. Lett.* **43**(4), 879–882 (2018).
15. N. Modsching, J. Drs, J. Fischer, C. Paradis, F. Labaye, M. Gaponenko, C. Kränkel, V. J. Wittwer, and T. Südmeyer, "Sub-100-fs Kerr lens mode-locked Yb:Lu₂O₃ thin-disk laser oscillator operating at 21 W average power," *Opt. Express* **27**(11), 16111–16120 (2019).
16. C. J. Saraceno, "Mode-locked thin-disk lasers and their potential application for high-power terahertz generation," *J. Opt.* **20**(4), 044010 (2018).
17. C. Paradis, J. Drs, N. Modsching, O. Razskazovskaya, F. Meyer, C. Kränkel, C. J. Saraceno, V. J. Wittwer, and T. Südmeyer, "Broadband terahertz pulse generation driven by an ultrafast thin-disk laser oscillator," *Opt. Express* **26**(20), 26377–26384 (2018).
18. F. Meyer, N. Hekmat, S. Mansourzadeh, F. Fobbe, F. Aslani, M. Hoffmann, and C. J. Saraceno, "Optical rectification of a 100 W average power mode-locked thin-disk oscillator," *Opt. Lett.* **43**(24), 5909–5912 (2018).
19. C. Kränkel, "Rare-earth-doped sesquioxides for diode-pumped high-power lasers in the 1-, 2-, and 3- μ m spectral range," *IEEE J. Sel. Top. Quantum Electron.* **21**(1), 250–262 (2015).
20. Q. Wu and X.-C. Zhang, "7 terahertz broadband GaP electro-optic sensor," *Appl. Phys. Lett.* **70**(14), 1784–1786 (1997).
21. W. L. Bond, "Measurement of the refractive indices of several crystals," *J. Appl. Phys.* **36**(5), 1674–1677 (1965).
22. contact: HITRAN online, <https://hitran.org/>.
23. T. Hattori and K. Takeuchi, "Simulation study on cascaded terahertz pulse generation in electro-optic crystals," *Opt. Express* **15**(13), 8076–8093 (2007).
24. K. Aoki, J. Savolainen, and M. Havenith, "Broadband terahertz pulse generation by optical rectification in GaP crystals," *Appl. Phys. Lett.* **110**(20), 201103 (2017).
25. Y.-S. Lee, *Principles of Terahertz Science and Technology* (Springer US, 2009).
26. G. Gallot and D. Grischkowsky, "Electro-optic detection of terahertz radiation," *J. Opt. Soc. Am. B* **16**(8), 1204–1212 (1999).
27. S. Casalbuoni, H. Schlarb, B. Schmidt, P. Schmüser, B. Steffen, and A. Winter, "Numerical studies on the electro-optic detection of femtosecond electron bunches," *Phys. Rev. ST Accel. Beams* **11**(7), 072802 (2008).
28. E. D. Palik, *Handbook of Optical Constants of Solids* (Academic Press, 1997).
29. F. Meyer, N. Hekmat, T. Vogel, A. Omar, S. Mansourzadeh, F. Fobbe, M. Hoffmann, Y. Wang, and C. J. Saraceno, "1.35 mW, MHz-Repetition-Rate Broadband THz Source Driven by a 112 W, 88 fs Thin-Disk Laser," in *Conference on Lasers and Electro-Optics* (Optical Society of America, 2019), paper JTh5A.3.

Chapter 5

Thin-disk laser driven intra-oscillator high harmonic generation

This chapter presents the first high harmonic generation (HHG) driven inside the cavity of a mode-locked TDL oscillator. Section 5.1 motivates different approaches for HHG in gas jets. Section 5.2 presents the experimental setup and obtained results of this proof-of-principle demonstration. This result opens the path for a novel class of single-stage extreme ultraviolet (XUV) light sources operating at MHz repetition rates.

5.1 High-harmonic generation in gas jets

HHG in gases is, besides in solids and liquids, the most common approach for the generation of coherent XUV light from table-top laser sources [1-3]. Coherent XUV sources possess a great potential for a large number of applications in science and technology [4,5]. The generation of XUV light at MHz repetition rates (MHz-XUV) has gained additional attention as it can result in strongly decreased experimental measurement times, improved signal-to-noise ratios and enable XUV frequency comb applications [6,7]. For hands on application, MHz-XUV sources would benefit to be driven by simple and powerful ultrafast laser systems.

The extreme nonlinear process of HHG occurs in noble gases at high intensities well above 10^{13} W/cm² [8]. In order to reach those high intensities usually femtosecond pulses with high peak power (> 100 MW) have to be focused down to spot diameters

of 20-30 μm . The reabsorption of the generated XUV light in ambient atmosphere requires HHG to be driven in a vacuum environment. The dumping of the gas is required to maintain the vacuum environment during the interaction. Very low conversion efficiencies below 7.5×10^{-5} for a single harmonic [9] make the development of MHz-XUV sources with high photon flux challenging and require the driving ultrafast laser system to operate at high average powers. Nowadays standard HHG systems are driven by Ti:sapphire laser amplifier systems which are limited to a few watts of average power and operate typically at kHz repetition rates. The tremendous effort in power-scaling of the Yb-based laser systems over the last decade and the development of novel approaches enabled to drive MHz-XUV sources at orders of magnitude higher average powers [10–12]. An overview about the achieved performance of MHz-XUV sources based on different approaches is given in Fig. 1. Yet, the generation of higher photon energies at increased average power per harmonic would be of interest. Advantages and challenges of the three approaches enabling MHz-XUV sources will be discussed in the following.

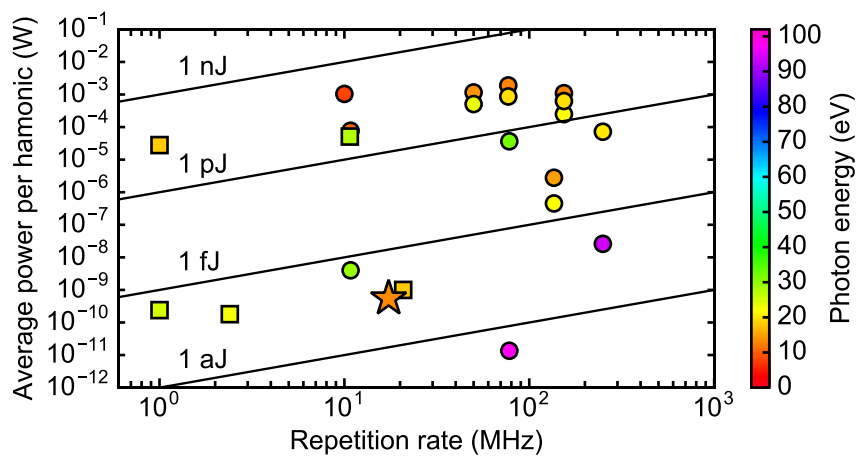


Fig. 1. Overview of XUV light sources based on HHG in gas jets operating at MHz repetition rates. Symbols represent the applied approach (single-pass in squares, intra-cavity in circles, and intra-oscillator with a star). If the generated power was not reported by the authors, it was estimated using known extraction coefficients. (Figure taken and adapted from [13])

HHG based on the single-pass geometry [1,10,12,14] is the most straight forward experimental approach [Fig. 2(a)]. After focusing the driving laser pulse into the gas target, the infrared pulse is separated from the copropagating XUV light by spatial separation or spectral filtering. Higher XUV photon flux can be achieved by further power-scaling of the driving laser system. Typically, single-pass XUV sources rely on

complex multi-stage amplifier system and require additional nonlinear pulse compression before interaction [10,15]. High-power TDL oscillator are an amplification-stage free alternative for MHz-XUV generation, but nonlinear pulse compression remains still required [11]. The dumping of the driving infrared laser pulse after the interaction with the gas target is a limiting factor for the overall conversion efficiency.

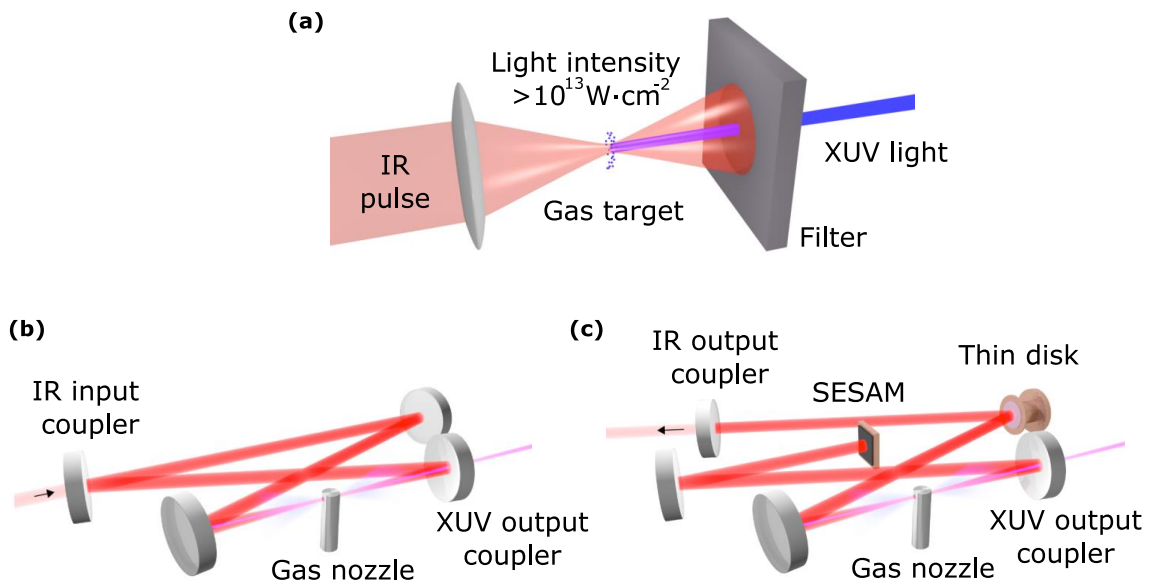


Fig. 2. Different approaches for HHG in gas jets at MHz repetition rates. (a) Single-pass HHG, (b) intra-cavity HHG based on a passive enhancement cavity, (c) intra-oscillator HHG inside a mode-locked thin-disk laser oscillator. The figures are courtesy of Martin Saraceno [16].

Intra-cavity HHG [17–20] is an alternative approach to increase the XUV photon flux and the overall conversion efficiency with respect to the driving laser source [Fig. 2(b)]. Here, consecutive infrared pulses are coupled coherently into a passive enhancement cavity. The coherent superposition enables a several times enhanced intra-cavity performance compared to the driving laser system. In contrast to the single-pass geometry, the driving laser pulse is reused after the interaction with the gas target and XUV light is generated once during each cavity round-trip. As such, this approach relaxes the requirement on the average power of the driving laser system. Intra-cavity HHG enabled so far XUV sources to operate at the highest repetition rate and average power per harmonic (Fig. 1). However, coupling of femtosecond pulses into an enhancement cavity is experimentally challenging. Active stabilization of the

driving laser source and the enhancement cavity is necessary to achieve efficient coherent coupling. As the enhancement depends strongly on the cavity finesse, this approach is as well sensitive to the overall cavity losses. Also, plasma induced instabilities by the HHG can affect and limit the performance [21]. An additional challenge of this approach arises from the output coupling of the XUV light. Different XUV output coupling methods have been successfully demonstrated by placing sapphire plates under Brewster's angle for the driving laser pulse into the cavity [17,18], the use of optical gratings [19,22,23] or pierced mirrors [24,25].

Intra-oscillator HHG overcomes the requirement of coherent coupling [Fig. 2(c)]. In this single-stage approach, HHG is driven directly inside the laser cavity of a mode-locked oscillator [26]. The circulating pulse can adapt to the nonlinearities and the dispersion induced by the HHG process. Laser gain during each cavity round-trip makes this approach less sensitive to the total cavity losses. The generated XUV light has to be coupled out of the cavity by use of the same methods as applied for intra-cavity HHG. However, the strongest challenge of this approach relies in the cavity design of the oscillator. Stable mode-locked operation with femtosecond pulses at high intracavity peak powers has to be achieved in combination with a tight focus for HHG in a high vacuum environment.

The next section describes the first experimental realization of intra-oscillator HHG inside the cavity of a mode-locked TDL oscillator. This proof-of-principle result shows that the addressed challenges in the cavity design can be successfully overcome. As such, TDL oscillators have a high potential as single-stage MHz-XUV source. For a more detailed discussion about the current status and future prospects of intra-oscillator HHG the reader is already referred to [13] (the manuscript is currently under review).

References

1. M. Ferray, A. L'Huillier, X. F. Li, L. A. Lompré, G. Mainfray, and C. Manus, "Multiple-harmonic conversion of 1064 nm radiation in rare gases," *J. Phys. B At. Mol. Opt. Phys.* **21**, L31-L35 (1988).
2. S. Ghimire, A. D. DiChiara, E. Sistrunk, P. Agostini, L. F. DiMauro, and D. A. Reis, "Observation of high-order harmonic generation in a bulk crystal," *Nat. Phys.* **7**(2), 138-141 (2011).
3. T. T. Luu, Z. Yin, A. Jain, T. Gaumnitz, Y. Pertot, J. Ma, and H. J. Wörner, "Extreme-ultraviolet high-harmonic generation in liquids," *Nat. Commun.* **9**(1)(2018).
4. T. Popmintchev, M.-C. Chen, P. Arpin, M. M. Murnane, and H. C. Kapteyn, "The attosecond nonlinear optics of bright coherent X-ray generation," *Nat. Photonics* **4**(12), 822-832 (2010).
5. F. Krausz and M. Ivanov, "Attosecond physics," *Rev. Mod. Phys.* **81**(1), 163-234 (2009).

6. G. K. Tadesse, R. Klas, S. Demmler, S. Hädrich, I. Wahyutama, M. Steinert, C. Spielmann, M. Zürch, T. Pertsch, A. Tünnermann, J. Limpert, and J. Rothhardt, "High speed and high resolution table-top nanoscale imaging," *Opt. Lett.* **41**(22), 5170–5173 (2016).
7. T. Südmeyer, S. V. Marchese, S. Hashimoto, C. R. E. Baer, G. Gingras, B. Witzel, and U. Keller, "Femtosecond laser oscillators for high-field science," *Nat. Photonics* **2**(10), 599–604 (2008).
8. P. B. Corkum, "Plasma perspective on strong field multiphoton ionization," *Phys. Rev. Lett.* **71**(13), 1994–1997 (1993).
9. R. Klas, S. Demmler, M. Tschernajew, S. Hädrich, Y. Shamir, A. Tünnermann, J. Rothhardt, and J. Limpert, "Table-top milliwatt-class extreme ultraviolet high harmonic light source," *Optica* **3**(11), 1167–1170 (2016).
10. J. Bouillet, Y. Zaouter, J. Limpert, S. Petit, Y. Mairesse, B. Fabre, J. Higuët, E. Mével, E. Constant, and E. Cormier, "High-order harmonic generation at a megahertz-level repetition rate directly driven by an ytterbium-doped-fiber chirped-pulse amplification system," *Opt. Lett.* **34**(9), 1489–1491 (2009).
11. F. Emaury, A. Diebold, C. J. Saraceno, and U. Keller, "Compact extreme ultraviolet source at megahertz pulse repetition rate with a low-noise ultrafast thin-disk laser oscillator," *Optica* **2**(11), 980–984 (2015).
12. S. Hädrich, M. Krebs, A. Hoffmann, A. Klenke, J. Rothhardt, J. Limpert, and A. Tünnermann, "Exploring new avenues in high repetition rate table-top coherent extreme ultraviolet sources," *Light Sci. Appl.* **4**(8), e320 (2015).
13. F. Labaye, M. Gaponenko, N. Modsching, B. Pierre, C. Paradis, S. Schilt, V. J. Wittwer, and T. Südmeyer, "XUV sources based on intra-oscillator high harmonic generation with thin-disk lasers: current status and prospects," *IEEE J. Sel. Top. Quantum Electron.* **submitted** (2018).
14. A. McPherson, G. Gibson, H. Jara, U. Johann, T. S. Luk, I. A. McIntyre, K. Boyer, and C. K. Rhodes, "Studies of multiphoton production of vacuum-ultraviolet radiation in the rare gases," *J. Opt. Soc. Am B* **4**(4), 595–601 (1987).
15. A. Vernaleken, J. Weitenberg, T. Sartorius, P. Russbuedt, W. Schneider, S. L. Stebbings, M. F. Kling, P. Hommelhoff, H.-D. Hoffmann, R. Poprawe, and others, "Single-pass high-harmonic generation at 20.8 MHz repetition rate," *Opt. Lett.* **36**(17), 3428–3430 (2011).
16. M. Saraceno, martin@saraceno.info.
17. C. Gohle, T. Udem, M. Herrmann, J. Rauschenberger, R. Holzwarth, H. A. Schuessler, F. Krausz, and T. W. Hänsch, "A frequency comb in the extreme ultraviolet," *Nature* **436**(7048), 234–237 (2005).
18. R. J. Jones, K. D. Moll, M. J. Thorpe, and J. Ye, "Phase-Coherent Frequency Combs in the Vacuum Ultraviolet via High-Harmonic Generation inside a Femtosecond Enhancement Cavity," *Phys. Rev. Lett.* **94**(19), 193201 (2005).
19. A. Cingöz, D. C. Yost, T. K. Allison, A. Ruehl, M. E. Fermann, I. Hartl, and J. Ye, "Direct frequency comb spectroscopy in the extreme ultraviolet," *Nature* **482**(7383), 68–71 (2012).
20. D. C. Yost, A. Cingöz, T. K. Allison, A. Ruehl, M. E. Fermann, I. Hartl, and J. Ye, "Power optimization of XUV frequency combs for spectroscopy applications [Invited]," *Opt. Express* **19**(23), 23483–23493 (2011).
21. J. Lee, D. R. Carlson, and R. J. Jones, "Optimizing intracavity high harmonic generation for XUV fs frequency combs," *Opt. Express* **19**(23), 23315–23326 (2011).
22. A. Ozawa, Z. Zhao, M. Kuwata-Gonokami, and Y. Kobayashi, "High average power coherent vuv generation at 10 MHz repetition frequency by intracavity high harmonic generation," *Opt. Express* **23**(12), 15107–15118 (2015).
23. G. Porat, C. M. Heyl, S. B. Schoun, C. Benko, N. Dörre, K. L. Corwin, and J. Ye, "Phase-matched extreme-ultraviolet frequency-comb generation," *Nat. Photonics* **12**(7), 387–391 (2018).
24. I. Pupeza, S. Holzberger, T. Eidam, H. Carstens, D. Esser, J. Weitenberg, P. Rußbüldt, J. Rauschenberger, J. Limpert, T. Udem, A. Tünnermann, T. W. Hänsch, A. Apolonski, F. Krausz,

- and E. Fill, "Compact high-repetition-rate source of coherent 100 eV radiation," *Nat. Photonics* **7**(8), 608–612 (2013).
25. H. Carstens, M. Högner, T. Saule, S. Holzberger, N. Lilienfein, A. Guggenmos, C. Jocher, T. Eidam, D. Esser, V. Tosa, V. Pervak, J. Limpert, A. Tünnermann, U. Kleineberg, F. Krausz, and I. Pupeza, "High-harmonic generation at 250 MHz with photon energies exceeding 100 eV," *Optica* **3**(4), 366–369 (2016).
 26. E. Seres, J. Seres, and C. Spielmann, "Extreme ultraviolet light source based on intracavity high harmonic generation in a mode locked Ti:sapphire oscillator with 9.4 MHz repetition rate," *Opt. Express* **20**(6), 6185–6190 (2012).

5.2 Extreme ultraviolet light source at a megahertz repetition rate based on high-harmonic generation inside a mode-locked thin-disk laser oscillator

François Labaye,^{1,*} Maxim Gaponenko,¹ Valentin J. Wittwer,¹ Andreas Diebold,² Clément Paradis,¹ Norbert Modsching,¹ Loïc Merceron,¹ Florian Emaury,² Ivan J. Graumann,² Chris R. Phillips,² Clara J. Saraceno,³ Christian Kränkel,^{4,5} Ursula Keller,² and Thomas Südmeyer¹

¹Laboratoire Temps-Fréquence, Institut de Physique, Université de Neuchâtel, Avenue de Bellevaux 51, 2000 Neuchâtel, Switzerland

²Ultrafast Laser Physics, Institute for Quantum Electronics, ETH Zurich, Auguste-Piccard-Hof 1, 8093 Zurich, Switzerland

³Photonics and Ultrafast Laser Science, Ruhr-Universität Bochum, Universitätsstraße 150, 44801 Bochum, Germany

⁴Institut für Laser-Physik, Universität Hamburg, Luruper Chaussee 149, 22761 Hamburg, Germany

⁵Center for Laser Materials, Leibniz Institute for Crystal Growth, Max-Born-Str. 2, 12489 Berlin, Germany

We demonstrate a compact extreme ultraviolet (XUV) source based on high-harmonic generation (HHG) driven directly inside the cavity of a mode-locked thin-disk laser oscillator. The laser is directly diode-pumped at a power of only 51W and operates at a wavelength of 1034 nm and a 17.35 MHz repetition rate. We drive HHG in a high-pressure xenon gas jet with an intracavity peak intensity of 2.8×10^{13} W/cm² and 320 W of intracavity average power. Despite the high-pressure gas jet, the laser operates at high stability. We detect harmonics up to the 17th order (60.8 nm, 20.4 eV) and estimate a flux of 2.6×10^8 photons/s for the 11th harmonic (94 nm, 13.2 eV). Due to the power scalability of the thin-disk concept, this class of compact XUV sources has the potential to become a versatile tool for areas such as attosecond science, XUV spectroscopy, and high-resolution imaging.

5.2.1 Introduction

Focusing intense femtosecond pulses into a gas target enables the generation of higher harmonics of the fundamental laser frequency [1]. To drive this highly nonlinear process, the femtosecond laser has to deliver peak intensities above 10^{13} W/cm². Standard HHG systems typically rely on Ti:sapphire chirped pulse amplifiers, which usually operate at kilohertz repetition rates and average powers of a few watts. The conversion efficiency to the high-harmonic radiation being very low [2,3] (below 7.5×10^{-5} for a single harmonic [4]); this results in very low average power of the generated extreme ultraviolet (XUV) radiation. This is an issue for applications such as high-resolution imaging, because it strongly affects measurement speed and resolution [5]. Furthermore, the low repetition rate is a challenge for many measurements, for example, experiments in which the energy or momentum of photoelectrons has to be precisely measured. Increasing the repetition rate from kilohertz to megahertz can avoid space charge effects and strongly decrease measurement time [6]. Moreover, XUV sources operating at kilohertz repetition rates are not suitable for direct frequency comb spectroscopy. Due to this large scientific potential, the last years have seen a tremendous increase in research efforts targeting HHG with high photon flux at a megahertz repetition rate. So far, two main directions have been investigated. The most obvious one is to increase both the average power and the repetition rate of the driving laser system, so that sufficiently high peak intensities can be obtained to drive single-pass HHG at megahertz repetition rates. This was demonstrated for the first time in 2009 with a high-power fiber chirped-pulse-amplifier (FCPA) system as the driving laser [7]. Record-high megahertz HHG power levels have recently been achieved using coherently combined FCPAs, in combination with temporal pulse compression in gas-filled hollow-core fibers [8]. Ultrafast high-power slab amplifiers also enabled HHG at a megahertz repetition rate, however, so far at significantly lower XUV power levels [9]. An alternative to amplifier-based systems is single-pass HHG driven by ultrafast thin-disk laser (TDL) oscillators [6,10] which was demonstrated in 2015 [11]. The second direction is based on enhancement cavities for ultrashort pulses, which enabled HHG at megahertz repetition rates already in 2005 [12,13]. The development of powerful FCPA-based frequency combs [14] pushed this technique further, which has resulted in the generation of an XUV photon flux up to several hundred microwatts in a given harmonic [15] and allowed, e.g., the generation of

photon energies exceeding 100 eV at a repetition rate of 250 MHz [16]. However, its experimental realization is highly complex. Stable coupling of femtosecond pulses from an amplified frequency comb into a high-finesse resonator containing the HHG interaction is challenging. In addition, the requirements on the phase stability of the driving laser system are very demanding.

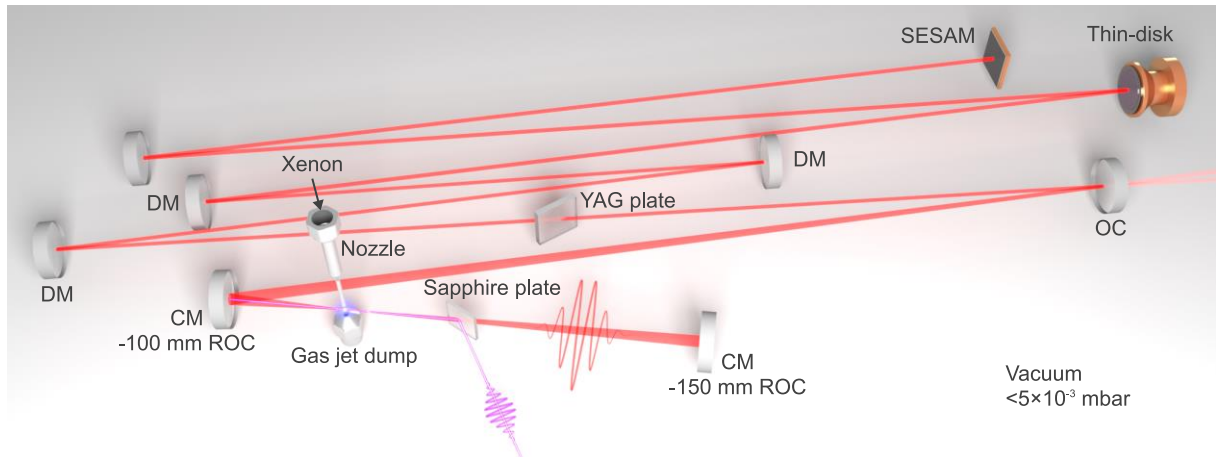


Fig. 1 Illustration of the experiment's principle (DM, dispersive mirror; CM, concave mirror; ROC, radius of curvature; OC, output coupler).

Placing the HHG interaction directly inside a mode-locked oscillator is a simpler approach that does not require any input matching of ultrashort pulses. Instead, the circulating femtosecond pulse can adapt to the present cavity nonlinearities and the dispersion. In 2012, the feasibility of this concept was demonstrated using a Ti:sapphire laser oscillator [17], but only at an intracavity average power of 10 W. Due to thermal effects and nonlinearities, ultrafast lasers using bulk crystals, such as Ti:sapphire, are severely limited in average power. This is not the case for ultrafast TDL oscillators. Here the gain medium has the shape of a thin disk which is mounted onto a heat sink and used in reflection with a large beam diameter [10,18]. The thin-disk geometry enables efficient cooling, thus limiting thermal aberrations, and strongly reduces nonlinearities in the gain element. Ultrafast TDL oscillators achieve the highest average power and pulse energy of any mode-locked laser oscillator technology, both intra- and extra-cavity [19–21]. Recently, ultrafast TDL oscillators based on Yb-doped gain materials achieved pulse durations as short as 30 fs directly emitted from the oscillator [22,23]. Furthermore, they can operate with low noise, and carrier-envelope offset (CEO) frequency stabilization has been achieved [24,25], showing their suitability for frequency comb applications.

In this Letter, we report on the first HHG inside an ultrafast TDL oscillator. Our system is based on a diode-pumped Yb:Lu₂O₃ thin disk, and mode-locked with a semiconductor saturable absorber mirror (SESAM) [26]. We evaluate the laser noise properties and compare operation with and without HHG process. Even though we inject xenon gas at high backing pressure into an intracavity focus, we do not observe any instabilities of the mode-locked laser. Our experiment shows that ultrafast TDL oscillators are well suited for extreme intracavity nonlinear optics experiments such as HHG.

5.2.2 *Experimental setup*

The resonator, TDL head, and gas target are placed in a compact vacuum chamber with dimensions of 80 × 160 cm². An illustration of the experimental setup is shown in Fig. 1. The vacuum chamber is evacuated to a pressure of ~10⁻⁴ mbar with two turbomolecular pumps. As a gain element, we use a wedged 200 μm thick Yb:Lu₂O₃ disk that is mounted onto a water-cooled diamond heat sink. The disk is pumped by a fiber-coupled diode at the zero-phonon line at 976 nm. It is used as a folding mirror in the standing-wave cavity. A SESAM inserted as an end mirror enables mode locking. It has 1.6% modulation depth, 0.3% nonsaturable losses, and a saturation fluence of 47.5 μJ/cm². The beam radii on the SESAM and on the disk are 0.95 and 1.15 mm, respectively. A 4 mm thick YAG plate is placed at a Brewster's angle for enforcing linear p-polarization and introduces sufficient self-phase modulation (SPM) for soliton mode locking. The SPM is balanced by three dispersive mirrors (DMs). The total intracavity group delay dispersion is -3000 fs² per roundtrip. An output coupler (OC) with a transmission of 0.7% is used as a folding mirror. A 12 μm radius intracavity focus is created between two concave mirrors (CMs) with 100 and 150 mm radii of curvature (ROC), the latter one being used as an end mirror. To extract the generated XUV light, we placed a sapphire plate with a thickness of 250 μm at a Brewster's angle for the laser wavelength 2 cm behind the focus. This outcoupling method has been extensively used in cavity-enhanced HHG [12,13]. Without gas, the laser generates 264 fs pulses at a repetition rate of 17.35 MHz with an intracavity average power of 320 W at a pump power of 49 W. Its intracavity peak power of 62 MW leads to a peak intensity of ~2.7 × 10¹³ W/cm² at the focus. The corresponding intensity autocorrelation trace, optical spectrum, and radio frequency (RF) spectrum

are shown in Figs. 2(a)–2(c). At higher pump power levels without the HHG process, we observed mode locking instabilities, most likely due to operation close to the roll-over of the SESAM reflectivity, in combination with the finite gain bandwidth of the gain material [27].

5.2.3 *Experimental results*

We use a quartz nozzle with a ~ 100 μm opening diameter for gas delivery into the intracavity focus. In order to keep the chamber pressure below 5×10^{-3} mbar while a high-pressure gas jet is used, a gas jet dump is placed below the nozzle [28]. When the xenon gas jet is emitted into the focus, HHG is observed and detected with a channel electron multiplier (CEM, Photonis Magnum 5900). The XUV light is directed by an unprotected gold mirror to a wavelength calibrated monochromator (Acton VM-502) equipped with a 1200 g/mm iridium-coated grating. The slits' width was set for a 3.4 nm spectral resolution. We acquired the XUV spectra with and without a 0.2 μm thick aluminum filter to check the validity of our measurement.

We use 3.4 bar of backing pressure in the nozzle which leads to a pressure at the laser focus estimated to ~ 400 mbar. At this gas pressure, the average output power of the laser drops slightly, and we increase the pump power from 49 to 51 W to achieve the same intracavity average power of 320 W as without gas jet. The TDL oscillator with HHG operates with slightly shorter 255 fs pulses. Its intracavity peak power is 64 MW, which leads to a peak intensity of $\sim 2.8 \times 10^{13}$ W/cm² at the focus. The corresponding intensity autocorrelation trace, optical spectrum, and RF spectrum are shown in Figs. 2(d)–2(f). High harmonics with orders up to the 17th (60.8 nm, 20.4 eV) are detected, in accordance with predictions from the cutoff formula [29]. The acquired spectra are shown in Fig. 3. Harmonics below the 11th order (94 nm, 13.2 eV) were not detected, most likely due to reabsorption in xenon for the 9th harmonic and the low quantum efficiency of our detector in the spectral range corresponding to the 7th harmonic and above it. Using the measured spectra and an additional measurement of the XUV flux with the CEM in all the detected harmonics before the monochromator without an aluminum filter, we estimate the average power and photon flux generated at the focus for the 11th harmonic with a similar method as the one described in Ref. [11]. A very conservative estimation results in a generated flux $\gtrsim 2.6 \times 10^8$ photons/s. This corresponds to an average power $\gtrsim 0.55$ nW and a conversion efficiency \gtrsim

1.7×10^{-12} with respect to the intracavity average power and $\gtrsim 1.1 \times 10^{-11}$ with respect to the diode pump power.

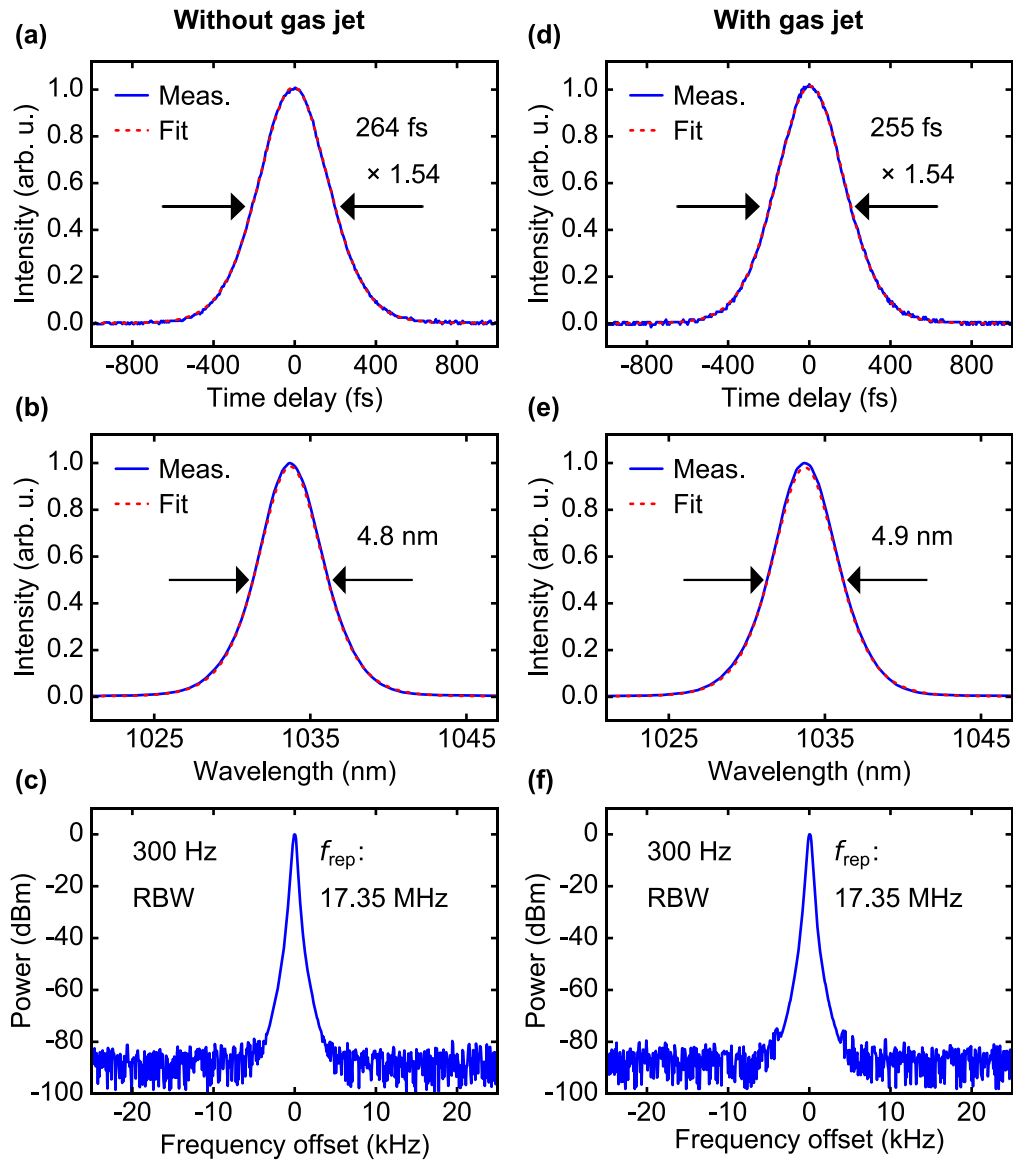


Fig. 2. Comparison of the TDL oscillator output parameters (a)–(c) without a high-pressure gas jet and (d)–(f) with a high-pressure gas jet. (a), (d) Intensity autocorrelation traces; (b), (e) optical spectra, and (c), (f) RF spectra.

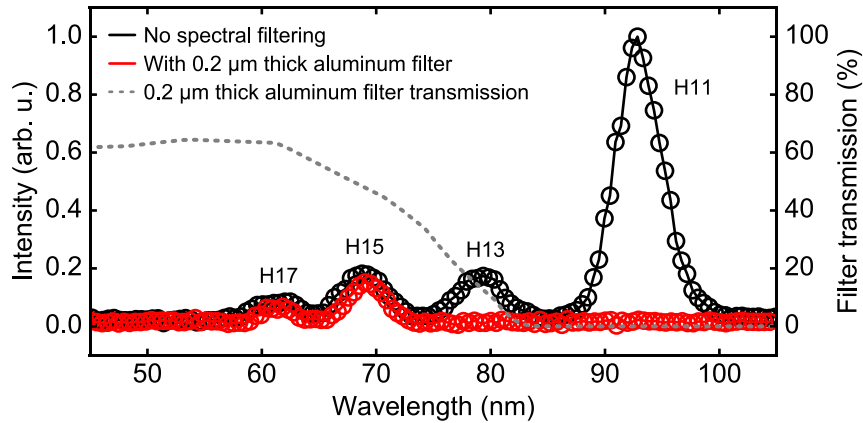


Fig. 3. Measured spectra of the generated XUV light. The full spectrum is plotted in black, while the spectrum filtered by a 0.2 μm thick aluminum foil is plotted in red. The theoretical transmission of the aluminum filter is shown for reference and plotted as a gray dashed line.

To evaluate if there is any laser perturbation induced by the plasma generated during the HHG process, we compare the transverse beam quality and laser noise with and without HHG. The laser operates in both cases in a fundamental transverse TEM_{00} mode with an M^2 factor < 1.02 . The noise of the TDL oscillator output was measured in free-running operation on the passively filtered 4th harmonic of the repetition rate using a phase noise analyzer (Rohde & Schwarz FSWP). The measured power spectral densities of the amplitude and phase noises are shown in Fig. 4. Although our vacuum chamber is connected to two turbomolecular pumps and we did not optimize our opto-mechanical components for high stability, we achieve an integrated relative intensity noise over a large frequency range (1 Hz–1 MHz) of only 0.78% and 0.76% with and without gas, respectively. The phase noise integrated in the same frequency range amounts to 1.33 and 1.25 mrad at 17.35 MHz with and without gas, respectively. Both turbomolecular pumps were running at their maximum speeds during these measurements, and the nozzle's backing pressure during the measurement with gas was 3.4 bar as during the XUV light spectra acquisition. Our laser noise is comparable to the typical values of free-running ultrafast TDL oscillators [11,30]. We therefore expect that CEO stabilization of a TDL oscillator can also be achieved with an intracavity HHG process.

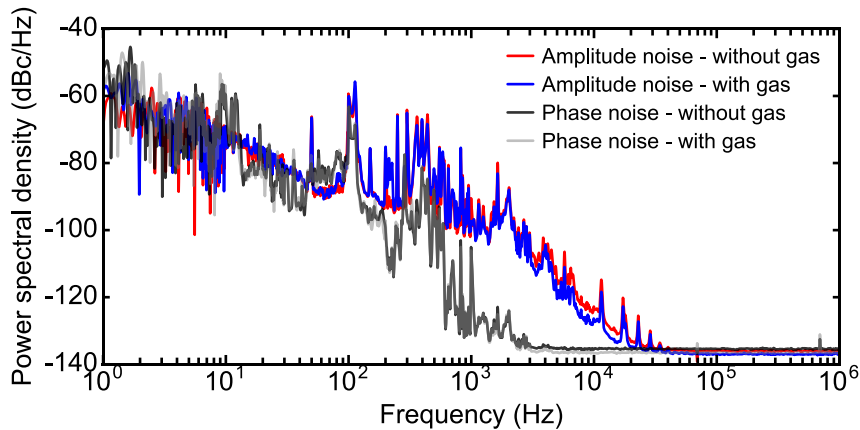


Fig. 4. Amplitude and phase noise measurements of the mode-locked TDL oscillator output in free-running operation with and without gas.

5.2.4 Conclusion

In conclusion, we have reported the first intracavity HHG inside a mode-locked TDL oscillator, generating XUV light down to a wavelength of 60.8 nm (17th harmonic, 20.4 eV) at a repetition rate of 17.35 MHz. The conversion efficiency and flux of this proof-of-principle experiment are limited by the long pulse duration and the moderate peak power. However, TDL oscillators are power-scalable and have already been operated at 10 times higher intracavity peak power [31]. Moreover, we recently generated 35 fs pulses with 73 MW intracavity peak power from a Yb:Lu₂O₃ Kerr lens mode-locked TDL oscillator operating in air [23]. The corresponding optical spectrum was three times larger than the gain spectrum. We expect that by using materials with a broader gain bandwidth such as Yb:CALGO [22], substantially shorter pulse durations should be within reach of ultrafast TDL oscillators. Therefore, further optimization of laser parameters to reach performance similar to state-of-the-art HHG systems at the megahertz repetition rate [8,16] appears feasible. In combination with phase-matching optimization of the HHG process [3,32], this should significantly increase the conversion efficiency and allow for generating higher-energy photons. Furthermore, more efficient extraction schemes [33–35] should significantly increase the XUV flux available in future experiments. Our approach of HHG inside a TDL oscillator can lead to a novel class of coherent XUV light sources, which combines efficient megahertz repetition rate operation at a high XUV flux with a compact and portable design. Such systems will be highly attractive for driving a large number of

applications ranging from high-resolution imaging to XUV spectroscopy and attosecond science.

Funding

Seventh Framework Programme (FP7); H2020 European Research Council (ERC) "Efficient megahertz XUV light source" (279545), Starting Grant 2011; National Center of Competence in Research for Molecular Ultrafast Science and Technology (NCCR-MUST); Swiss National Science Foundation (SNSF) (206021_144970, 200021_159931, 200020_172644); Deutsche Forschungsgemeinschaft (DFG) (EXC 1074, EXC 1069).

Acknowledgments

The authors thank John W. G. Tisch for helpful discussions and the loan of the XUV monochromator. C. J. Saraceno acknowledges the support of the Alexander von Humboldt foundation.

References

1. M. Ferray, A. L'Huillier, X. F. Li, L. A. Lompré, G. Mainfray, and C. Manus, "Multiple-harmonic conversion of 1064 nm radiation in rare gases," *J. Phys. B At. Mol. Opt. Phys.* **21**, L31–L35 (1988).
2. E. Constant, D. Garzella, P. Breger, E. Mével, C. Dorrer, C. Le Blanc, F. Salin, and P. Agostini, "Optimizing high harmonic generation in absorbing gases: Model and experiment," *Phys. Rev. Lett.* **82**, 1668 (1999).
3. J. Rothhardt, M. Krebs, S. Hädrich, S. Demmler, J. Limpert, and A. Tünnermann, "Absorption-limited and phase-matched high harmonic generation in the tight focusing regime," *New J. Phys.* **16**, 033022 (2014).
4. R. Klas, S. Demmler, M. Tschernajew, S. Hädrich, Y. Shamir, A. Tünnermann, J. Rothhardt, and J. Limpert, "Table-top milliwatt-class extreme ultraviolet high harmonic light source," *Optica* **3**, 1167–1170 (2016).
5. G. K. Tadesse, R. Klas, S. Demmler, S. Hädrich, I. Wahyutama, M. Steinert, C. Spielmann, M. Zürich, T. Pertsch, A. Tünnermann, J. Limpert, and J. Rothhardt, "High speed and high resolution table-top nanoscale imaging," *Opt. Lett.* **41**, 5170–5173 (2016).
6. T. Südmeyer, S. V. Marchese, S. Hashimoto, C. R. E. Baer, G. Gingras, B. Witzel, and U. Keller, "Femtosecond laser oscillators for high-field science," *Nat. Photonics* **2**, 599–604 (2008).
7. J. Bouillet, Y. Zaouter, J. Limpert, S. Petit, Y. Mairesse, B. Fabre, J. Higué, E. Mével, E. Constant, and E. Cormier, "High-order harmonic generation at a megahertz-level repetition rate directly driven by an ytterbium-doped-fiber chirped-pulse amplification system," *Opt. Lett.* **34**, 1489–1491 (2009).
8. S. Hädrich, M. Krebs, A. Hoffmann, A. Klenke, J. Rothhardt, J. Limpert, and A. Tünnermann, "Exploring new avenues in high repetition rate table-top coherent extreme ultraviolet sources," *Light Sci. Appl.* **4**, e320 (2015).
9. A. Vernaleken, J. Weitenberg, T. Sartorius, P. Russbueldt, W. Schneider, S. L. Stebbings, M. F. Kling, P. Hommelhoff, H.-D. Hoffmann, R. Poprawe, and others, "Single-pass high-harmonic generation at 20.8 MHz repetition rate," *Opt. Lett.* **36**, 3428–3430 (2011).

10. J. A. der Au, G. J. Spühler, T. Südmeyer, R. Paschotta, R. Hövel, M. Moser, S. Erhard, M. Karszewski, A. Giesen, and U. Keller, "16.2-W average power from a diode-pumped femtosecond Yb:YAG thin disk laser," *Opt. Lett.* **25**, 859–861 (2000).
11. F. Emaury, A. Diebold, C. J. Saraceno, and U. Keller, "Compact extreme ultraviolet source at megahertz pulse repetition rate with a low-noise ultrafast thin-disk laser oscillator," *Optica* **2**, 980–984 (2015).
12. R. J. Jones, K. D. Moll, M. J. Thorpe, and J. Ye, "Phase-Coherent Frequency Combs in the Vacuum Ultraviolet via High-Harmonic Generation inside a Femtosecond Enhancement Cavity," *Phys. Rev. Lett.* **94**, 193201 (2005).
13. C. Gohle, T. Udem, M. Herrmann, J. Rauschenberger, R. Holzwarth, H. A. Schuessler, F. Krausz, and T. W. Hänsch, "A frequency comb in the extreme ultraviolet," *Nature* **436**, 234–237 (2005).
14. A. Ruehl, A. Marcinkevicius, M. E. Fermann, and I. Hartl, "80 W, 120 fs Yb-fiber frequency comb," *Opt. Lett.* **35**, 3015–3017 (2010).
15. J. Lee, D. R. Carlson, and R. J. Jones, "Optimizing intracavity high harmonic generation for XUV fs frequency combs," *Opt. Express* **19**, 23315–23326 (2011).
16. H. Carstens, M. Högner, T. Saule, S. Holzberger, N. Lilienfein, A. Guggenmos, C. Jocher, T. Eidam, D. Esser, V. Tosa, V. Pervak, J. Limpert, A. Tünnermann, U. Kleineberg, F. Krausz, and I. Pupeza, "High-harmonic generation at 250 MHz with photon energies exceeding 100 eV," *Optica* **3**, 366–369 (2016).
17. E. Seres, J. Seres, and C. Spielmann, "Extreme ultraviolet light source based on intracavity high harmonic generation in a mode locked Ti:sapphire oscillator with 9.4 MHz repetition rate," *Opt. Express* **20**, 6185–6190 (2012).
18. A. Giesen, H. Hügel, A. Voss, K. Wittig, U. Brauch, and H. Opower, "Scalable concept for diode-pumped high-power solid-state lasers," *Appl. Phys. B Lasers Opt.* **58**, 365–372 (1994).
19. C. J. Saraceno, F. Emaury, O. H. Heckl, C. R. E. Baer, M. Hoffmann, C. Schriber, M. Golling, T. Südmeyer, and U. Keller, "275 W average output power from a femtosecond thin disk oscillator operated in a vacuum environment," *Opt. Express* **20**, 23535–23541 (2012).
20. C. J. Saraceno, F. Emaury, C. Schriber, M. Hoffmann, M. Golling, T. Südmeyer, and U. Keller, "Ultrafast thin-disk laser with 80 μ J pulse energy and 242 W of average power," *Opt. Lett.* **39**, 9–12 (2014).
21. J. Brons, V. Pervak, E. Fedulova, D. Bauer, D. Sutter, V. Kalashnikov, A. Apolonskiy, O. Pronin, and F. Krausz, "Energy scaling of Kerr-lens mode-locked thin-disk oscillators," *Opt. Lett.* **39**, 6442–6445 (2014).
22. C. Paradis, N. Modsching, M. Gaponenko, F. Labaye, F. Emaury, A. Diebold, I. Graumann, B. Deppe, C. Kränkel, V. J. Wittwer, and T. Südmeyer, "Sub-50-fs Kerr Lens Mode-Locked Thin-Disk Lasers," in *CLEO Europe - EQEC 2017* (Optical Society of America, 2017), p. PD-1.4.
23. C. Paradis, N. Modsching, V. J. Wittwer, B. Deppe, C. Kränkel, and T. Südmeyer, "Generation of 35-fs pulses from a Kerr lens mode-locked Yb:Lu₂O₃ thin-disk laser," *Opt. Express* **25**, 14918–14925 (2017).
24. A. Klenner, F. Emaury, C. Schriber, A. Diebold, C. J. Saraceno, S. Schilt, U. Keller, and T. Südmeyer, "Phase-stabilization of the carrier-envelope-offset frequency of a SESAM modelocked thin disk laser," *Opt. Express* **21**, 24770–24780 (2013).
25. O. Pronin, M. Seidel, J. Brons, F. Lücking, V. Pervak, A. Apolonski, T. Udem, and F. Krausz, "Carrier-envelope phase stabilized thin-disk oscillator," in *Advanced Solid-State Lasers Congress (2013), Paper AF3A.5* (Optical Society of America, 2013), p. AF3A.5.
26. U. Keller, K. J. Weingarten, F. X. Kärtner, D. Kopf, B. Braun, I. D. Jung, R. Fluck, C. Hönninger, N. Matuschek, and J. Aus der Au, "Semiconductor Saturable Absorber Mirrors (SESAM's) for Femtosecond to Nanosecond Pulse Generation in Solid-State Lasers," *IEEE J. Sel. Top. Quantum Electron.* **2**, 435–453 (1996).

27. C. J. Saraceno, C. Schriber, F. Emaury, O. H. Heckl, C. R. E. Baer, M. Hoffmann, K. Beil, C. Kränkel, M. Golling, T. Südmeyer, and U. Keller, "Cutting-Edge High-Power Ultrafast Thin Disk Oscillators," *Appl. Sci.* **3**, 355–395 (2013).
28. D. C. Yost, "Development of an Extreme Ultraviolet Frequency Comb for Precision Spectroscopy," PhD Thesis, University of Colorado (2011).
29. J. L. Krause, K. J. Schafer, and K. C. Kulander, "High-order harmonic generation from atoms and ions in the high intensity regime," *Phys. Rev. Lett.* **68**, 3535 (1992).
30. F. Emaury, A. Diebold, A. Klenner, C. J. Saraceno, S. Schilt, T. Südmeyer, and U. Keller, "Frequency comb offset dynamics of SESAM modelocked thin disk lasers," *Opt. Express* **23**, 21836 (2015).
31. N. Kanda, A. A. Eilanlou, T. Imahoko, T. Sumiyoshi, Y. Nabekawa, M. Kuwata-Gonokami, and K. Midorikawa, "High-Pulse-Energy Yb: YAG Thin Disk Mode-Locked Oscillator for Intra-Cavity High Harmonic Generation," in *Advanced Solid State Lasers* (Optical Society of America, 2013), p. AF3A-8.
32. C. M. Heyl, C. L. Arnold, A. Couairon, and A. L'Huillier, "Introduction to macroscopic power scaling principles for high-order harmonic generation," *J. Phys. B At. Mol. Opt. Phys.* **50**, 013001 (2017).
33. K. D. Moll, R. J. Jones, and J. Ye, "Output coupling methods for cavity-based high-harmonic generation," *Opt. Express* **14**, 8189–8197 (2006).
34. I. Pupeza, S. Holzberger, T. Eidam, H. Carstens, D. Esser, J. Weitenberg, P. Rußbüldt, J. Rauschenberger, J. Limpert, T. Udem, A. Tünnermann, T. W. Hänsch, A. Apolonski, F. Krausz, and E. Fill, "Compact high-repetition-rate source of coherent 100 eV radiation," *Nat. Photonics* **7**, 608–612 (2013).
35. O. Pronin, V. Pervak, E. Fill, J. Rauschenberger, F. Krausz, and A. Apolonski, "Ultrabroadband efficient intracavity XUV output coupler," *Opt. Express* **19**, 10232–10240 (2011).

Chapter 6

Conclusion and outlook

This thesis presented new frontiers of ultrafast TDL oscillators operating in the sub-100-fs pulse duration regime. The developed single-stage ultrafast laser sources possess a high potential to directly drive applications in industry and science without the need for additional amplification or nonlinear pulse compression. The combination of excellent spatiotemporal beam properties, sub-100-fs pulse durations and laser operation at tens of watt of average power at MHz repetition rates offers versatile advantages to perform measurements at higher signal-to-noise ratios and shorter acquisition times. In the framework of this thesis the potential of sub-100-fs TDL oscillators for applications in metrology and THz time-domain spectroscopy has been investigated. Additionally, a novel class of single-stage extreme ultraviolet (XUV) light sources was demonstrated by driving high harmonic generation (HHG) directly inside the cavity of an ultrafast TDL oscillator. Yet, further performance improvement is required to unleash the full potential of this promising ultrafast laser technology.

The key ingredient for pushing the performance of sub-100-fs TDL oscillators was the combination of Yb-doped gain materials with broader gain bandwidth and the Kerr lens mode-locking scheme. The gain material Yb:Lu₂O₃ possesses a gain bandwidth which is beneficial for the generation of sub-100-fs pulse durations. Its thermal conductivity remains excellent even at high doping concentrations. Operating the developed Kerr lens mode-locked (KLM) Yb:Lu₂O₃ TDL oscillator in the regime of strong intracavity self-phase modulation (SPM) enabled the generation of shorter pulse durations than supported by the spectral gain bandwidth. Record average powers of TDL oscillators were achieved in the sub-100-fs and sub-50-fs pulse duration

regime. The experimental optimization of this systems for laser operation with sub-100-fs pulses has been discussed in more detail in this thesis. In an initial configuration the laser cavity was folded once on the disk. Laser operation at 10.7 W of average power with 88-fs pulses and 4.5 W with 49-fs pulses was demonstrated, albeit at moderate optical-to-optical efficiencies below 6%. In the extreme case, laser operation in the strongly SPM-broadened regime enabled the generation of pulse durations as short as 35 fs at 1.6 W of average power. Further optimization targeted an increased round-trip gain by folding the laser cavity a second time on the disk. In this configuration 95-fs pulses were generated at 21 W of average power while featuring an almost three times higher optical-to-optical efficiency of 16%. This is the highest average power so far demonstrated by a sub-100-fs oscillator [1] and a four times higher value than achieved by sub-100-fs TDL oscillators prior to this thesis [2,3]. The result shows that TDL oscillators are capable of operating in the sub-100-fs pulse duration regime at optical-to-optical efficiencies comparable to the one of sub-100-fs Yb-based bulk oscillators [1]. The average power of Yb:Lu₂O₃ TDL oscillators mode-locked with saturable absorber mirrors (SESAMs) has been scaled to 141 W at somewhat longer pulse durations of several hundred femtoseconds [4]. It can be anticipated that similar power-scaling should be feasible for sub-100-fs Yb:Lu₂O₃ KLM TDL oscillators. Further improvement of the performance should be possible by:

- **Increasing the beam radius in the Kerr medium** [5] to scale the intracavity peak power. An experimental investigation whether this approach results in improved output performance can be realized straightforward by increasing the radius of curvature of the concave mirrors that form the intracavity focus together with according adjustment of the cavity lengths.
- **Increasing the pump spot diameter** [6]. The cavity design needs to be adjusted for laser operation with increased beam diameter on the disk. The challenge of this approach lies in optimization of the laser performance at a reduced width of the stability zone with respect to thermal lensing.
- **Folding the cavity multiple times on the disk** [7]. By applying a multi-pass scheme higher round-trip gain enables laser operation at an increased output coupler transmission. As demonstrated in this thesis, assuming constant intracavity performance, even higher average powers can be expected. However, higher round-trip gain also causes stronger gain narrowing. An

according increase of the SPM in the cavity is required for the generation of sub-100-fs pulses. It is suggested to decouple the Kerr lens mode-locking mechanism and the generation of SPM for more freedom in the cavity optimization. Decoupling can be achieved i.e. by placing additional Brewster plates in the cavity at positions where a Kerr lens has minor effect on the cavity dynamics [8]. The multi-pass cavity design should be as well robust against thermal lensing of the disk. Even minor thermal lensing can be strongly promoted by folding the cavity several times on the disk. Also, soft-aperture effects of the Kerr lens mode-locking scheme have to be considered for an optimized pump spot overlap.

- **Implementing multiple disks in the cavity** [9]. Combined with multiple passes on each disk the total round-trip gain can be further increased. This approach enables as well to split the generated heat load onto multiple disks which can suppress effects of thermal lensing further. However, implementing multiple thin-disk heads with individual pump sources, cooling and electronics is rather costly and adds more complexity into the full system.
- **Laser operation in vacuum/ controlled atmosphere** [10,11]. Air inside the laser cavity leads to the accumulation of parasitic nonlinearities for laser operation at high intracavity peak powers. Laser operation in vacuum or a controlled atmosphere (i.e. purged with helium) suppresses parasitic nonlinearities and enables further increase of the intracavity peak power which can result in improved output performance [10]. Placing the TDL oscillator in a controlled environment requires engineering efforts and automatization, i.e. the usage of motorized translation stages for the optimization of the system.

Laser operation of the KLM Yb:Lu₂O₃ TDL oscillators in the strongly SPM-broadened regime enabled the generation of 35-fs pulses. In this thesis even shorter pulse durations of 30 fs were generated by the first KLM Yb:CALGO TDL oscillator. This is the shortest pulse duration so far achieved by a TDL oscillator. At that time, this pulse duration was equal to the shortest one generated by Yb-based bulk oscillators [12]. The very broad gain bandwidth of Yb:CALGO is attractive as it supports the generation of sub-20-fs pulse durations. Yet, the full gain bandwidth of Yb:CALGO has not been exploited and by laser operation in the SPM-broadened regime even much shorter

pulse durations are feasible. Further progress in the growing technology should enable improved Yb:CALGO crystal qualities. It can be anticipated that improved Yb:CALGO disks will enable the development of sub-30-fs TDL oscillators operating at the watt level of average power.

The development of the 35-fs KLM Yb:Lu₂O₃ TDL oscillator and the 30-fs KLM Yb:CALGO TDL oscillator demonstrated that the thin-disk geometry is suitable for the generation of shortest pulse durations. Compared to standard end-pumped bulk oscillators, the thin-disk concept features a design advantage for the generation of the short pulse durations. In standard end-pumped bulk oscillators pump and laser beam co-propagate in the gain medium for improved overlap. Co-propagation is achieved by launching the pump beam from outside into the bulk gain medium via a dichroic cavity mirror. While being transmissive for the pump beam, the dichroic mirror limits the supported spectral bandwidth for lasing at the shorter wavelength side. In contrast, in the thin-disk geometry, pump and laser beam are folded in reflection over the disk. As such, the spectral limitation to shorter wavelengths does not exist. This allows the optimization of optical coatings for a broader spectral range, extended towards shorter wavelengths. In the presented results the optical spectra of the shortest pulses generated expands towards the shorter wavelength range well below the corresponding pump wavelength. In comparison, standard Yb-based bulk oscillators generating similar short pulse durations require a shift to longer central wavelengths. This shift reduces the overlap with the gain spectrum which can cause losses in efficiency. In the thin-disk geometry such a shift is not required. However, reabsorption effects of the broad spectra in the gain medium still need to be further investigated. It can be anticipated that the thin-disk geometry will profit from further optimization of broadband optical coatings.

The potential of the developed sub-100-fs Yb:Lu₂O₃ TDL oscillators for applications in metrology was demonstrated by detecting and stabilizing the carrier envelope offset (CEO) frequency (f_{CEO}). Prior to this work it was uncertain whether f_{CEO} stabilization could be achieved for oscillators operating in the SPM-broadened regime. Although their laser parameters appear suitable, cavity and f_{CEO} dynamics could prevent a stabilization [13,14].

In the presented configuration the TDL oscillator generated 50-fs pulses at 4.5 W of average power and 61 MHz of repetition rate. Self-referenced f_{CEO} detection was realized by the use of a standard nonlinear f -to- $2f$ interferometer. The short pulse duration enabled the generation of the required coherent super continuum by launching only few mW of the available average power into a photonic crystal fiber. A preceding nonlinear pulse compression was not needed. Thus, almost the full laser output remained available for applications. The f_{CEO} was stabilized up to a bandwidth of 10 kHz to an external radio-frequency reference by applying an active feedback to the current of the pump diode. A tight phase lock was achieved with a residual in-loop integrated phase noise of 197 mrad (integrated from 1 Hz to 1 MHz).

A preliminary study investigated the potential for full frequency comb stabilization by simultaneously stabilizing the f_{CEO} and the repetition rate (f_{rep}). Stabilization of the f_{rep} to an external reference was enabled by mounting a cavity folding mirror onto a controlled piezoelectric transducer (PZT). Simultaneous stabilization of f_{CEO} and f_{rep} was achieved in the range of minutes. Long-term stabilization was limited by the travel range of the PZT that could not compensate for the drift of the cavity length. Cross-talking between both stabilization loops required to limit the f_{rep} stabilization bandwidth in order not to lose the f_{CEO} lock. As such, the f_{rep} -stabilization bandwidth was only 35 Hz with a residual timing jitter of 7 ps (integrated from 1 Hz to 1 MHz). When both stabilization loops were locked, the integrated phase noise of f_{CEO} increased to 745 mrad. Further investigations need to determine the origin of the introduced noise at ~ 20 kHz into f_{CEO} by the f_{rep} stabilization. Once this noise source is determined and eliminated a f_{rep} stabilization with larger bandwidth and reduced timing jitter can be expected while the tight lock of the f_{CEO} should be maintained.

For long-term f_{rep} stabilization a combination of two PZTs is suggested. A slow PZT corrects the long-term drift with larger travel range and a fast PZT is optimized for response at higher frequencies. A reduction of the mass of the mounted mirror should be considered for larger f_{rep} -stabilization bandwidth. Investigations utilizing f_{CEO} -stabilization techniques can enable locking with larger bandwidth, e.g., by placing an optical-to-optical modulator inside the oscillator [15]. It is anticipated that by further power-scaling frequency combs based on sub-100-fs TDL oscillators will

operate in the near future at tens of watt. Furthermore, this study is of particular interest for the generation of XUV frequency combs via intra-oscillator HHG.

Another promising application of the developed sub-100-fs KLM Yb:Lu₂O₃ TDL oscillator is the generation of broadband THz radiation at MHz repetition rates. In the performed studies optical rectification (OR) in gallium phosphide (GaP) was driven in a simple collinear geometry. Sub-100-fs pulses emitted by the oscillator enabled the direct generation and detection of THz radiation without need for amplification or nonlinear pulse compression. In our experimental results we confirm that OR of 1- μ m pulses in GaP is suitable for the generation THz radiation with spectra expanding to about 7 THz and demonstrate 0.3 mW of THz average power in a spectrum expanding to 5 THz. As such, sub-100-fs KLM TDL oscillators are suitable as single-stage driving laser system for linear THz time-domain spectroscopy.

In an initial study the laser generated 50-fs pulses at 4 W of average power and 61 MHz of repetition rate. Quasi single-cycle broadband THz pulses were generated in 0.5 mm thick GaP, albeit only at a few μ W of THz average power. The THz spectrum was centered at around 3.4 THz and extended from 1 THz to nearly 7 THz. A spectroscopic characterization of GaP in the THz and infrared range was performed. Corresponding calculations attributed the origin of the observed dips in the measured THz spectra to not-optimized phase matching. As benchmark application of the developed source for THz time-domain spectroscopy the absorption spectrum of water vapor was measured in a range of up to 5 THz with a sub-50-GHz resolution.

A second study investigated the impact of the GaP crystal thickness and driving pulse duration on the generated THz spectrum in more detail. Different pulse durations were realized by adapting the KLM Yb:Lu₂O₃ TDL oscillator of the initial study. The pulse duration was varied between 50 fs and 220 fs by adjusting the introduced group delay dispersion, output coupler transmission and hard aperture diameter. This allowed for high-fidelity measurements with almost time-bandwidth product limited soliton pulses at discrete operation parameters. Although the average power varied for laser operation at different pulse durations between 3 W and 7 W average power, a significant impact of the driving laser average power onto the shape of the THz spectrum was not observed. Based on the experimental results a simple method has been presented to estimate the THz spectrum in dependence of the driving

pulse duration and GaP crystal thickness. In a power-scaled version of the KLM Yb:Lu₂O₃ TDL oscillators OR in a 0.5-mm thick GaP crystal was driven with 95-fs pulses at 20 W of average power and 48 MHz of repetition rate. Increasing the peak intensity in the GaP crystal up to 20 GW/cm² showed the onset of saturation effects. At the highest peak intensity 0.3 mW of THz average power were obtained in a spectrum extending up to 5 THz. This corresponds to a conversion efficiency of $1.5 \cdot 10^{-5}$.

Broadband THz radiation at several mW of THz average power is within reach via OR in GaP by further scaling of the average power of the driving sub-100-fs KLM TDL oscillator. Already up to 100 W average power have been optically rectified in GaP, albeit at a moderate THz average power of 80 μ W [16]. Further optimization of the driving KLM TDL oscillators in the sub-50-fs regime would enable to exploit the supported THz bandwidth of GaP up to 7 THz at high THz average powers.

Additionally, in a proof-of-principle demonstration HHG was driven inside the cavity of a mode-locked TDL oscillator. This approach benefits from the up to orders of magnitude higher intra-cavity peak and average powers that can be achieved inside a TDL oscillator cavity. Compared to intra-cavity HHG driven in passive enhancement cavities, coherent coupling is not required. The oscillating pulse can instead adapt to changes in the nonlinearity caused by the interaction with the gas jet. Gain during the cavity round-trip makes this approach less sensitive to losses.

The driving SESAM mode-locked Yb:Lu₂O₃ TDL oscillator generated 250-fs pulses at 1034 nm of central wavelength and 17.3 MHz of repetition rate at an evacuated environment with a pressure of 10^{-4} mbar. The laser operated at 320 W of intracavity average power and 64 MW of intracavity peak power. HHG was driven at an intracavity peak intensity of $2.8 \cdot 10^{13}$ W/cm² inside a high-pressure xenon gas jet. XUV light was extracted by placing a sapphire plate under Brewster's angle for the driving laser wavelength in the vicinity of the intracavity focus. Harmonics up to the 17th order (60.8 nm, 20.4 eV) of the driving laser wavelength have been detected. The photon flux of the 11th harmonic (94 nm, 13.2 eV) was estimated to be $2.6 \cdot 10^8$ photons/s. Launching of the gas jet into the intracavity focus of the oscillator showed only a minor influence on the driving pulse duration. Amplitude and phase noise remained unaffected.

The second generation of intra-oscillator HHG targets higher photon fluxes and photon energies. This requires the improvement of the driving intracavity laser performance. Compared to the initially applied SESAM mode-locking scheme, Kerr lens mode-locking offers promising advantages for achieving shorter pulse durations [17]. Laser operation in the strongly SPM-broadened regime enables even the generation of shorter pulses than actually supported by the gain bandwidth of gain materials [8,18]. The developed KLM Yb:Lu₂O₃ TDL oscillator in this thesis operated with 35-fs pulses at 70 MW of intracavity peak power in ambient air. Following the proposed scaling law of the intracavity peak power several hundred MW should be feasible with sub-100-fs pulse durations in a vacuum environment [5]. The demonstration of HHG inside a multi-port ring-cavity based on a KLM Yb:YAG TDL oscillator demonstrated already that all challenges in the cavity design of can be successfully overcome [19].

As HHG is a coherent process an XUV frequency comb can be obtained by stabilizing the f_{CEO} and the f_{rep} of the driving laser. The preliminary study presented in this thesis demonstrated that full frequency comb stabilization for laser operation in the SPM-broadened regime is feasible. As such, the combination of Kerr lens mode-locking, frequency-comb stabilization and intra-oscillator HHG in one TDL oscillator would result in a novel class of single-stage XUV frequency combs operating at MHz repetition rates. Such devices would be highly attractive for hands on applications in research fields like high-precision spectroscopy or high-resolution imaging.

In conclusion, this thesis presented record performance of sub-100-fs laser oscillators by the combination of the thin-disk geometry, Yb-doped gain materials and the Kerr lens mode-locking scheme. Laser operation in the SPM-broadened regime overcomes the bandwidth limitation of most Yb-doped gain materials. This enables the generation of sub-100-fs pulses directly from the oscillator at high average power and comparably good optical-to-optical efficiency. Powerful sub-100-fs TDL oscillators overcome the need for amplification and nonlinear pulse compression. As such, these single-stage laser systems are highly attractive to drive directly many applications with almost transform limited pulses at MHz repetition rates. Their potential for application in metrology as frequency comb and for linear THz time-domain spectroscopy has been demonstrated. By further improvement it can be expected that sub-100-fs TDL oscillators will soon operate at the excess of hundred watt of average power.

Furthermore, the extreme nonlinear process of HHG was driven for the first time inside the cavity of a SESAM mode-locked TDL oscillator. Further optimization utilizing the Kerr lens mode-locking scheme and laser operation in the SPM-broadened regime will enable to generate higher XUV photon energies and photon flux. Together with f_{rep} and f_{CEO} stabilization, this opens the path for the development of single-stage XUV frequency combs in the near future.

References

1. A. Greborio, A. Guandalini, and J. Aus der Au, "Sub-100 fs pulses with 12.5-W from Yb:CALGO based oscillators," in Proc. SPIE, (2012), paper 823511.
2. C. J. Saraceno, O. H. Heckl, C. R. E. Baer, C. Schriber, M. Golling, K. Beil, C. Kränkel, T. Südmeyer, G. Huber, and U. Keller, "Sub-100 femtosecond pulses from a SESAM modelocked thin disk laser," Appl. Phys. B **106**(3), 559–562 (2012).
3. A. Diebold, F. Emaury, C. Schriber, M. Golling, C. J. Saraceno, T. Südmeyer, and U. Keller, "SESAM mode-locked Yb:CaGdAlO₄ thin disk laser with 62 fs pulse generation," Opt. Lett. **38**(19), 3842–3845 (2013).
4. S. V. Marchese, C. R. E. Baer, R. Peters, C. Kränkel, A. G. Engqvist, M. Golling, D. J. H. C. Maas, K. Petermann, T. Südmeyer, G. Huber, and U. Keller, "Efficient femtosecond high power Yb:Lu₂O₃ thin disk laser," Opt. Express **15**(25), 16966 (2007).
5. J. Brons, V. Pervak, E. Fedulova, D. Bauer, D. Sutter, V. Kalashnikov, A. Apolonskiy, O. Pronin, and F. Krausz, "Energy scaling of Kerr-lens mode-locked thin-disk oscillators," Opt. Lett. **39**(22), 6442–6445 (2014).
6. A. Giesen, H. Hügel, A. Voss, K. Wittig, U. Brauch, and H. Opower, "Scalable concept for diode-pumped high-power solid-state lasers," Appl. Phys. B Lasers Opt. **58**(5), 365–372 (1994).
7. J. Neuhaus, J. Kleinbauer, A. Killi, S. Weiler, D. Sutter, and T. Dekorsy, "Passively mode-locked Yb:YAG thin-disk laser with pulse energies exceeding 13 uJ by use of an active multipass geometry," Opt. Lett. **33**(7), 726–728 (2008).
8. J. Zhang, J. Brons, M. Seidel, V. Pervak, V. Kalashnikov, Z. Wei, A. Apolonski, F. Krausz, and O. Pronin, "49-fs Yb: YAG thin-disk oscillator with distributed Kerr-lens mode-locking," in European Quantum Electronics Conference (Optical Society of America, 2015), paper PD_A_1.
9. C. Schriber, F. Emaury, A. Diebold, S. Link, M. Golling, K. Beil, C. Kränkel, C. J. Saraceno, T. Südmeyer, and U. Keller, "Dual-gain SESAM modelocked thin disk laser based on Yb:Lu₂O₃ and Yb:Sc₂O₃," Opt. Express **22**(16), 18979–18986 (2014).
10. C. J. Saraceno, F. Emaury, O. H. Heckl, C. R. E. Baer, M. Hoffmann, C. Schriber, M. Golling, T. Südmeyer, and U. Keller, "275 W average output power from a femtosecond thin disk oscillator operated in a vacuum environment," Opt. Express **20**(21), 23535–23541 (2012).
11. S. V. Marchese, T. Südmeyer, M. Golling, R. Grange, and U. Keller, "Pulse energy scaling to 5 uJ from a femtosecond thin disk laser," Opt Lett **31**(18), 2728–2730 (2006).
12. J. Ma, H. Huang, K. Ning, X. Xu, G. Xie, L. Qian, K. P. Loh, and D. Tang, "Generation of 30 fs pulses from a diode-pumped graphene mode-locked Yb:CaYAlO₄ laser," Opt. Lett. **41**(5), 890–893 (2016).
13. F. Emaury, A. Diebold, A. Klenner, C. J. Saraceno, S. Schilt, T. Südmeyer, and U. Keller, "Frequency comb offset dynamics of SESAM modelocked thin disk lasers," Opt. Express **23**(17), 21836–21856 (2015).

14. N. Bucalovic, V. Dolgovskiy, M. C. Stumpf, C. Schori, G. Di Domenico, U. Keller, S. Schilt, and T. Südmeyer, "Effect of the carrier-envelope-offset dynamics on the stabilization of a diode-pumped solid-state frequency comb," *Opt. Lett.* **37**(21), 4428–4430 (2012).
15. K. Gürel, S. Hakobyan, V. J. Wittwer, S. Schilt, and T. Südmeyer, "Frequency Comb Stabilization of Ultrafast Lasers by Opto-Optical Modulation of Semiconductors," *IEEE J. Sel. Top. Quantum Electron.* **24**(5), 1–9 (2018).
16. F. Meyer, N. Hekmat, S. Mansourzadeh, F. Fobbe, F. Aslani, M. Hoffmann, and C. J. Saraceno, "Optical rectification of a 100 W average power mode-locked thin-disk oscillator," *Opt. Lett.* **43**(24), 5909–5912 (2018).
17. O. Pronin, J. Brons, C. Grasse, V. Pervak, G. Boehm, M.-C. Amann, V. L. Kalashnikov, A. Apolonski, and F. Krausz, "High-power 200 fs Kerr-lens mode-locked Yb:YAG thin-disk oscillator," *Opt. Lett.* **36**(24), 4746–4748 (2011).
18. C. Paradis, N. Modsching, V. J. Wittwer, B. Deppe, C. Kränkel, and T. Südmeyer, "Generation of 35-fs pulses from a Kerr lens mode-locked Yb:Lu₂O₃ thin-disk laser," *Opt. Express* **25**(13), 14918–14925 (2017).
19. N. Kanda, N. Kanda, T. Imahoko, K. Yoshida, A. A. Eilanlou, Y. Nabekawa, T. Sumiyoshi, M. Kuwata-Gonokami, M. Kuwata-Gonokami, K. Midorikawa, and K. Midorikawa, "Multi-port Intra-Cavity High Harmonic Generation in a Yb:YAG Thin Disk Mode-Locked Oscillator with MHz Repetition Rate," in *Frontiers in Optics 2017* (Optical Society of America, 2017), paper LW5F.4.

Curriculum Vitae



Name: Norbert Paul Modsching
Date of Birth: 17. December 1986
Citizenship: German

Education

05/2015 – **University of Neuchâtel (CH), Laboratoire Temps-Fréquence**
present Doctoral researcher
10/2011 – **Friedrich-Schiller Universität Jena (Germany)**
07/2014 Master of Science in Photonics
10/2006 – **University of Applied Sciences Zwickau (Germany)**
03/2011 Bachelor of Engineering in Microtechnology (dual)

Professional Experience

05/2015 **Doctoral researcher at the Laboratoire Temps-Fréquence**
4 years **(Neuchâtel, CH)**
Development of ultrafast thin-disk laser oscillators for applications in metrology and the generation of THz and XUV radiation; research group of Prof. Thomas Südmeyer

12/2013 **Master's thesis at the Institute of Applied Physics (Jena, Germany)**
9 months
Development of an ultrafast fiber oscillator for the investigation of the wavelength dependence of mode-instabilities in Yb-doped fiber amplifiers; research group of Prof. Jens Limpert

04/2011 **Research internship as laser engineer at the Laser Towns Institute**
6 months **(Orlando, USA)**
Development and characterization of a Tm-doped photonic crystal fiber laser in continuous-wave and Q-switched operation; research group of Prof. Martin Richardson

08/2008 **Trainee and Bachelor's thesis at Infineon Technologies (Dresden, Germany)**
2.5 years
Electrical wafer test, clean room experience, handling, monitoring and adjustment of prober and probe-cards for electrical wafer inspection

Awards and Publications

- 2018 Best student paper award in the area “Optical Combs” at the 32nd *European Frequency and Time Forum* (Torino, Italy)
- 2017 Outstanding student poster presentation award at the *Advanced Solid State Laser Conference 2017* (Nagoya, Japan)
- 2012/2013 Awarded two times in the row with the “German Scholarship” for excellent performance during the Master’s studies
- 2011 - 2018 More than 10 journal publications in *Optics Letters*, *Optics Express* and *Advanced Optical Technologies* (4× 1st authorship)

Extra activities

- 2011 - 2014 Research experiences abroad, each supported by German government scholarships (6 months USA, 2 months Taiwan, 5 months Argentina)

Acknowledgements

I want to thank Prof. Thomas Südmeyer for the opportunity to perform my PhD studies at the Laboratoire temps-fréquence in Neuchâtel. I appreciated a lot this friendly and constructive research environment, especially the freedom to develop, discuss and realize new ideas. Working in such a well-equipped lab with coworker of high expertise enabled me to learn a lot and develop many new skills.

My thank goes as well to Valentin. Independent of how much workload you had, you always found the time to support even until late night and on the weekends. I learned a lot from you, may it be the setting up of equipment, automated device readout or all the fun one can have by trying to get things finally running in python. Your support in the development and the fabrication of optical coatings was crucial to push the performance of our systems. With your experimental expertise you improved the quality of all our measurements. Thank you as well for the great time in the office and the gym.

I want to say a special thanks to Clément for the support during my first steps in the development of thin-disk laser oscillators. His demonstration of the first Kerr lens mode-locking in our lab and the common optimization of this laser system was the crucial first step enabling most of the presented results in this thesis. Thank your for your support during the nightshifts and in writing the manuscripts.

I would like to thank Jakub and Olga for the experimental realization of the THz experiment as well as Stephane, Pierre, Nayara and Kutan for their support and knowledge transfer during the f_{CEO} -stabilization experiment. Furthermore, I want to thank François and Maxim for the scientific discussions and all the members of the LTF for the great time in such a constructive working environment.

Without the people working in the background and the organization of the institute our work would not be possible. A big thank you for this to our team assistants Natacha, Joelle, Séverine and Patricia as well as to our engineers and technicians Marc, Patrick, Christian, Isidro, André, Thierry, Daniel and Dominique.

Furthermore, I would like to thank Christian Kränkel for the fabrication of the Yb:Lu₂O₃ disks and the high quality of his comments during internal review rounds before submission.

Living here in Neuchâtel for 4 years allowed me to meet many great people. Especially I would like to thank my dear friends Vanessa, Andrea and Paulo as well as my roommates Valentin, Germain, Sven, Peter and Quentin for making the time here so unique. Thanks for all the great moments we shared.

Mein abschließendes und herzlichstes Danke gilt meinen Eltern, meinen Geschwistern und meinen Nichten Annika und Heidi. Trotz der Weite habt ihr mich jederzeit mit allen Kräften unterstützt. Ich habe mich jedes Mal gefreut zu Euch in die Heimat zurück zu kehren und so herzlich empfangen zu werden. Danke das ihr mir diese große Stütze seid und mir ein zu Hause gebt.

Norbert

Declaration

I hereby certify that this thesis has been made by myself independently and without use of other than the stated sources and aids. All contained references to external sources have been identified as such.

Date: 26. April 2019

Signature:

A handwritten signature in blue ink, appearing to be 'M. J.', written in a cursive style.

This work discusses the development of high-power ultrafast laser oscillators based on the thin-disk geometry. The combination of the Kerr lens mode-locking scheme with gain materials of broader gain emission bandwidth (Yb:Lu₂O₃ and Yb:CALGO) enabled pushing the laser performance in the sub-100-fs pulse duration regime. Thin-disk laser (TDL) oscillators operating at 21 W of average power in 95-fs pulses and 4.5 W in 49-fs pulses are presented, which are the highest average powers so far achieved by a sub-100-fs and sub-50-fs laser oscillator, correspondingly. In addition, the generation of pulse durations as short as 30-fs is achieved, which is the shortest pulse duration so far directly emitted by an ultrafast TDL oscillator.

The potential of the developed laser sources for applications in metrology is investigated by detecting and stabilizing carrier-envelope offset frequency. A preliminary study discusses further steps towards full TDL-based frequency combs by parallel stabilization of the repetition rate. In addition, the TDL oscillators were used to drive the generation of broadband THz radiation via optical rectification in gallium phosphide (GaP). A THz average power of 0.3 mW was obtained in a spectrum ranging up to nearly 5 THz. Further optimization of the experimental parameters resulted in the generation of a continuous THz spectrum ranging up to 7 THz. Finally, a proof-of-principle realization of intra-cavity high harmonic generation (HHG) inside a SESAM mode-locked TDL as single-stage XUV source is reported.

The presented results confirm the potential to ultrafast TDL oscillators together with further power-scaling as single-stage laser sources for driving an extensive range of applications free of additional amplification and nonlinear pulse compression.

About the author:

Norbert Modsching received his Master of Science in Photonics degree from the Friedrich-Schiller-Universität Jena, Germany, in 2014. He joined the Laboratoire Temps-Fréquence (LTF), Université de Neuchâtel, Switzerland, for his PhD studies in 2015. His research interests focus on the development of ultrafast thin-disk laser oscillators operating in the sub-100-fs pulse duration regime and their subsequent application for the generation of THz and XUV radiation. He has written or co-authored more than 10 journal publications and more than 40 conference contributions. He got awarded two times for his student-paper contributions on international conferences.